AWARD NUMBER: **W81XWH-12-1-0139**

TITLE: Loss of PEDF: A Novel Mechanism of Antihormone Resistance in Breast Cancer

PRINCIPAL INVESTIGATOR: Dr. Joan Lewis-Wambi

CONTRACTING ORGANIZATION: University of Kansas Medical Center Research Institute, Inc.
Kansas City, KS 66103-2937

REPORT DATE: Oct 2015

TYPE OF REPORT: Final

PREPARED FOR: U.S. Army Medical Research and Materiel Command
Fort Detrick, Maryland 21702-5012

REPORT DOCUMENTATION PAGE

Form Approved
OMB No. 0704-0188

1. REPORT DATE	**2. REPORT TYPE**	**3. DATES COVERED**
October 2015	Final Report	8/1/2012 – 7/31/2015

4. TITLE AND SUBTITLE
Loss of PEDF: A Novel Mechanism of Antihormone Resistance in Breast Cancer

5a. CONTRACT NUMBER

5b. GRANT NUMBER
W81XWH-12-1-0139

5c. PROGRAM ELEMENT NUMBER

6. AUTHOR(S)
Joan Lewis-Wambi, PhD

E-Mail: jlewis-wambi@kumc.edu

5d. PROJECT NUMBER

5e. TASK NUMBER

5f. WORK UNIT NUMBER

7. PERFORMING ORGANIZATION NAME(S) AND ADDRESS(ES)

University of Kansas Medical Center
Research Institute, Inc.
3901 Rainbow Blvd Msn 1039
Kansas City, KS 66103-2937

8. PERFORMING ORGANIZATION REPORT NUMBER

9. SPONSORING / MONITORING AGENCY NAME(S) AND ADDRESS(ES)

U.S. Army Medical Research and Materiel Command
Fort Detrick, Maryland 21702-5012

10. SPONSOR/MONITOR'S ACRONYM(S)

11. SPONSOR/MONITOR'S REPORT NUMBER(S)

12. DISTRIBUTION / AVAILABILITY STATEMENT

Approved for Public Release; Distribution Unlimited

13. SUPPLEMENTARY NOTES

14. ABSTRACT: Our laboratory has identified a novel protein called pigment epithelium derived factor (PEDF) that appears to be suppressed in endocrine resistant breast cancer. Specifically, we have found that PEDF protein and mRNA expression is dramatically reduced in endocrine-resistant breast cancer cells and endocrine-resistant tumors. PEDF is a secreted glycoprotein that has potent antiangiogenic activity and has recently been shown to have antitumor properties. However, its role in endocrine resistance has never been studied. The objective of our proposed study was to characterize the role of PEDF in endocrine resistance and elucidate its mechanism of action *in vitro* and *in vivo*. We hypothesized that loss of PEDF expression in breast cancer is a novel mechanism for the development of endocrine resistance and that estrogen receptor alpha (ERα) plays a critical role in suppressing PEDF expression in resistant cells. To test our hypothesis, we proposed three Specific Aims: 1) To elucidate the mechanism(s) by which loss of PEDF confers resistance to endocrine therapy and its reexpression resensitizes resistant cells to the inhibitory effects of antihormones; 2) To study the role of ERα in PEDF regulation in endocrine sensitive and endocrine resistant breast cancer cells; and 3) To determine the effect of PEDF overexpression on tumor growth in athymic mice and elucidate PEDF mechanism of action *in vivo*. Our findings indicate that genetic manipulation of PEDF expression in breast cancer cells alter their sensitivity to tamoxifen and aromatase inhibitors *in vitro* and *in vivo* and that crosstalk between ERα, RET, and AP2 (i.e. AP2A and AP2C) suppress PEDF expression in endocrine resistant cells. Additionally, DNA pull-down and chromatin immunoprecipitation assays have confirmed that ERα, AP2, and the corepressor NCoR1 are constitutively bound to the PEDF promoter in the endocrine resistant MCF-7:5C and BT474 cells and disruption of ERα and AP2 binding to the PEDF promoter markedly increases PEDF expression in the resistant cells. Overall, these findings highlight the clinical potential of using PEDF expression as an additional marker of endocrine responsiveness in breast cancer and its therapeutic potential as an alternative treatment option for patients with endocrine resistant disease.

15. SUBJECT TERMS

Nothing listed

16. SECURITY CLASSIFICATION OF:			**17. LIMITATION OF ABSTRACT**	**18. NUMBER OF PAGES**	**19a. NAME OF RESPONSIBLE PERSON**
					USAMRMC
a. REPORT	**b. ABSTRACT**	**c. THIS PAGE**			**19b. TELEPHONE NUMBER** *(include area code)*
Unclassified	Unclassified	Unclassified	Unclassified	88	

ABSTRACT: Our laboratory has identified a novel protein called pigment epithelium derived factor (PEDF) that appears to be suppressed in endocrine resistant breast cancer. Specifically, we have found that PEDF protein and mRNA expression is dramatically reduced in endocrine-resistant breast cancer cells and endocrine-resistant tumors. PEDF is a secreted glycoprotein that has potent antiangiogenic activity and has recently been shown to have antitumor properties. However, its role in endocrine resistance has never been studied. The objective of our proposed study was to characterize the role of PEDF in endocrine resistance and elucidate its mechanism of action in vitro and in vivo. We hypothesized that loss of PEDF expression in breast cancer is a novel mechanism for the development of endocrine resistance and that estrogen receptor alpha (ERα) plays a critical role in suppressing PEDF expression in resistant cells. To test our hypothesis, we proposed three Specific Aims: 1) To elucidate the mechanism(s) by which loss of PEDF confers resistance to endocrine therapy and its reexpression resensitizes resistant cells to the inhibitory effects of antihormones; 2) To study the role of ERα in PEDF regulation in endocrine sensitive and endocrine resistant breast cancer cells; and 3) To determine the effect of PEDF overexpression on tumor growth in athymic mice and elucidate PEDF mechanism of action in vivo. Our findings indicate that genetic manipulation of PEDF expression in breast cancer cells alter their sensitivity to tamoxifen and aromatase inhibitors *in vitro* and *in vivo* and that crosstalk between ERα, RET, and AP-2 (i.e. AP-2A and AP-2C) suppress PEDF expression in endocrine resistant cells. Additionally, DNA pull-down and chromatin immunoprecipitation assays have confirmed that ERα, AP-2, and the corepressor NCoR1 are constitutively bound to the PEDF promoter in the endocrine resistant MCF-7:5C cells and that disruption of ERα and AP-2 binding to the PEDF promoter markedly increases PEDF expression in the resistant cells. **Overall, these findings highlight the clinical potential of using PEDF expression as an additional marker of endocrine responsiveness in breast cancer and its therapeutic potential as an alternative treatment option for patients with endocrine resistant disease**.

Table of Contents

INTRODUCTION: Resistance to endocrine therapy such as tamoxifen or aromatase inhibitors is a major clinical obstacle to the effective treatment and cure of women with estrogen receptor (ERα)-positive breast cancer. It is estimated that ~40% of breast cancer patients will develop endocrine-resistant disease following long-term treatment. The possibility of identifying new targets for therapy in resistant disease, or patients, who may benefit from additional treatment with existing therapies, provides a strong impetus to identify markers and mediators of therapeutic resistance. Our laboratory has identified a novel protein called pigment epithelium derived factor (PEDF) that appears to be suppressed/silenced in endocrine resistant breast cancer. Specifically, we have found that PEDF protein and mRNA expression is dramatically reduced in endocrine-resistant breast cancer cells and endocrine-resistant/recurrence tumors. PEDF is a multifunctional glycoprotein that is known to have potent antiangiogenic activities and has recently been shown to have antitumor properties. However, its role in endocrine resistance has never been studied. The objective of our proposed study was to characterize the role of PEDF in endocrine resistance and elucidate its mechanism of action *in vitro* and *in vivo*. We hypothesized that loss of PEDF expression in breast cancer is a novel mechanism for the development of endocrine resistance and that overexpression of estrogen receptor alpha (ERα) plays a critical role in suppressing PEDF expression in resistant cells. To test our hypothesis, we proposed the following **Specific Aims**: **1**) To elucidate the mechanism(s) by which loss of PEDF confers resistance to endocrine therapy and its reexpression resensitizes resistant cells to the inhibitory effects of antihormones; **2**) To study the role of ERα in PEDF regulation in endocrine sensitive and endocrine resistant breast cancer cells; and **3**) To determine the effect of PEDF overexpression on endocrine resistant breast cancer cell growth in athymic mice and elucidate its mechanism of action *in vivo*. In Aim 1, we developed a tetracycline-inducible lentivirus vector system to overexpress the PEDF gene in endocrine resistant breast cancer cell lines (MCF-7:5C and BT474) and we measured tamoxifen sensitivity in the PEDF-overexpressing cells (5C-PEDF-LV and BT474-PEDF-LV). For comparison, small interfering RNA (siRNA) was used to suppress PEDF expression in endocrine-sensitive MCF-7 and T47D breast cancer cells and tamoxifen sensitivity was also assessed in these cells. In Aim 2, mechanistic studies were performed to determine how loss of PEDF leads to resistance and the role that ERα plays in regulating PEDF expression in the endocrine resistant breast cancer cells. Finally, in Aim 3, we performed *in vivo* studies in athymic mice to assess the tumorigenic potential of PEDF-overexpressing versus PEDF-knockdown breast cancer cells. Specifically, the PEDF-lentivirus overexpressing cell lines (5C-PEDF-LV and BT474-PEDF-LV) and the PEDF-knockdown cell lines (MCF7/PEDF-KD and T47D/PEDF-KD) were orthotopically injected into the mammary fat pads of athymic mice and tumor growth and response to endocrine therapy (i.e. tamoxifen) was assessed over a 6 weeks' time period. At the end of our *in vivo* studies, tumors were removed from mice and analyzed for various biological markers. Our *in vitro* studies revealed that genetic manipulation of PEDF expression in breast cancer cells alters their response to tamoxifen and aromatase inhibitors and that crosstalk between ERα and several signaling proteins including RET and AP2 (i.e. AP2A and AP2C) plays a critical role in suppressing PEDF expression in endocrine resistant cells. In addition, DNA pull-down and chromatin immunoprecipitation assays confirm that ERα, AP2, and the corepressor NCoR1 are constitutively bound to the PEDF promoter in the endocrine resistant MCF-7:5C and BT474 cells, however, in endocrine-sensitive MCF-7 and T47D cells these factors are not bound to the PEDF promoter. Our *in vivo* studies revealed that knockdown of PEDF in endocrine-sensitive MCF-7 and T47D cells significantly enhanced tumor growth and reduced tamoxifen sensitivity whereas overexpression of PEDF in endocrine-resistant MCF-7:5C and BT474 cells reduced tumor growth and resensitize the tumors to tamoxifen treatment. Immunohistochemistry and Western blot analysis of the tumors isolated from the PEDF-overexpressing mice indicated that total ER, phosphor-ER (Ser167), phosphor-RET, AP2A, and AP2C were markedly reduced compared to tumors isolated from the PEDF-negative mice. **Impact**: Our findings highlight the clinical potential of using PEDF expression as an additional marker of endocrine responsiveness in breast cancer and they provide the opportunity to evaluate the therapeutic benefits of recombinant PEDF for treating endocrine resistant disease.

KEYWORDS: Breast cancer, endocrine resistance, PEDF, tamoxifen, aromatase inhibitors, estrogen receptor, RET, AP2, athymic mice, lentivirus

BODY: This is a final report for grant number W81XWH-12-1-0139 which covers the funding period from August 1st 2012 to July 31st, 2015. **Please note** that this grant was initially awarded to me (August 1st, 2012) when I was a faculty member at Fox Chase Cancer Center (Philadelphia, PA), however, due to family reasons, I left Fox Chase Cancer Center on December 31st 2012 and accepted a faculty position at the University of Kansas Medical Center on January 1st 2013. I was granted permission in September 2013 to transfer my grant from Fox Chase Cancer Center to the University of Kansas Medical Center and I was also granted a 1 year no-cost extension on my grant due to my relocation. To date, I have completed all of the proposed experiments/Tasks as described in my SOW without modification and the results are summarized and shown below.

Summary of Results for Task 1: In Task 1a, we used siRNA knockdown to suppress PEDF expression in tamoxifen sensitive MCF-7 and T47D breast cancer cells to ask the question whether the presence of PEDF is important for sensitizing breast cancer cells to the anti-proliferative effects of tamoxifen. Based on the results shown in **Figure 1a)**, we found that suppression of PEDF mRNA and protein expression in endocrine sensitive MCF-7 and T47D breast cancer cells significantly reduced their sensitivity to tamoxifen. Specifically, we found that the ability of tamoxifen to reduce the proliferation of MCF-7 and T47D cells was reduced by 40-50% compared to the control cells, thus suggesting that the presence of PEDF in breast cancer cells sensitizes them to the inhibitory effect of tamoxifen. We further confirmed the importance of PEDF in tamoxifen sensitivity by developing a tetracycline inducible lentivirus system that allowed us to conditionally overexpresses PEDF in two resistant breast cancer cell lines (MCF-7:5C and BT474) in the presence of doxycycline. **Figure 1b** shows that reexpression of PEDF in the resistant cells almost completely reversed tamoxifen resistance in these cells. Specifically, we found that tamoxifen reduced the growth of 5C-PEDF-LV and BT474-PEDF-LV breast cancer cells by 70% and 50%, respectively, whereas it had no inhibitory effect on resistant MCF-7:5C and BT474 cells which lack PEDF, thus confirming its role in tamoxifen sensitivity. We also investigated the mechanism by which PEDF reverses tamoxifen resistance in our endocrine resistant breast cancer cells and we found that the presence of PEDF blocked the ability of the receptor tyrosine kinase RET to phosphorylate and activate the estrogen receptor protein. PEDF also suppressed AKT and mTOR activation in the resistant cells (**Figure 2a & 2b**). We have previously published these findings in *Breast Cancer Research* (reference Jan et al. 2012; 14(6):R146; please see appendices for a copy).

Task 1: **Elucidate the mechanism(s) by which loss of PEDF confers resistance to endocrine therapy and its reexpression resensitizes resistant cells to the inhibitory effects of antihormones. (Months 0-8)**

Task 1-1*) Determine whether PEDF silencing or its overexpression alters tamoxifen sensitivity in breast cancer cells.* (Months 0-12)

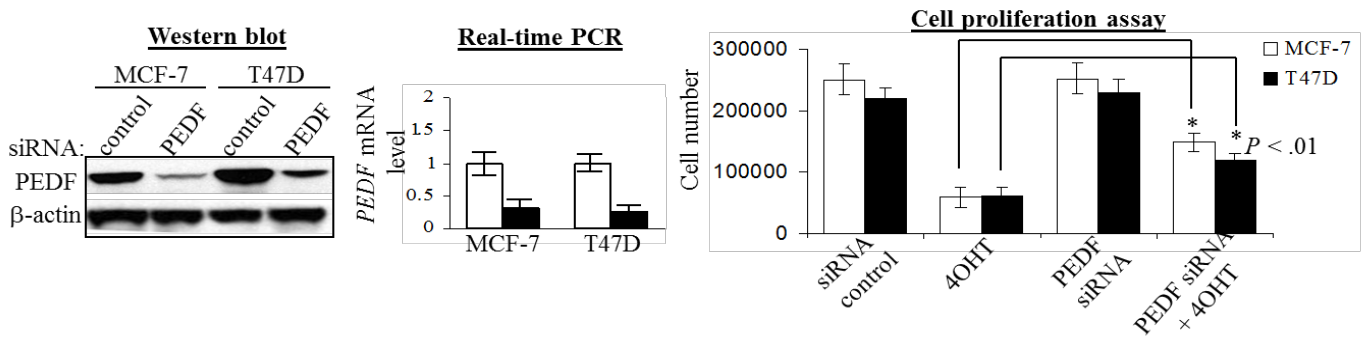

Figure 1: Knockdown of pigment epithelium-derived factor expression by siRNA reduces tamoxifen sensitivity in breast cancer cells. (**a**) MCF-7 and T47D cells were transfected with PEDF or control siRNA for 72 hours and PEDF protein and mRNA levels were determined by western blot analysis. Transfected cells were also treated with 1 μM TAM for 72 hours and cell proliferation was determined by cell counting. (**b**) MCF-7:5C and BT474 breast cancer cells were transfected with a doxycycline-inducible lentivirus vector encoding the human PEDF cDNA and Western blot analysis was used to confirm PEDF overexpression. The lentivirus-transduced 5C-PEDF-LV and BT474-PEDF-LV cells were then treated TAM and cell proliferation was determined by cell counting.

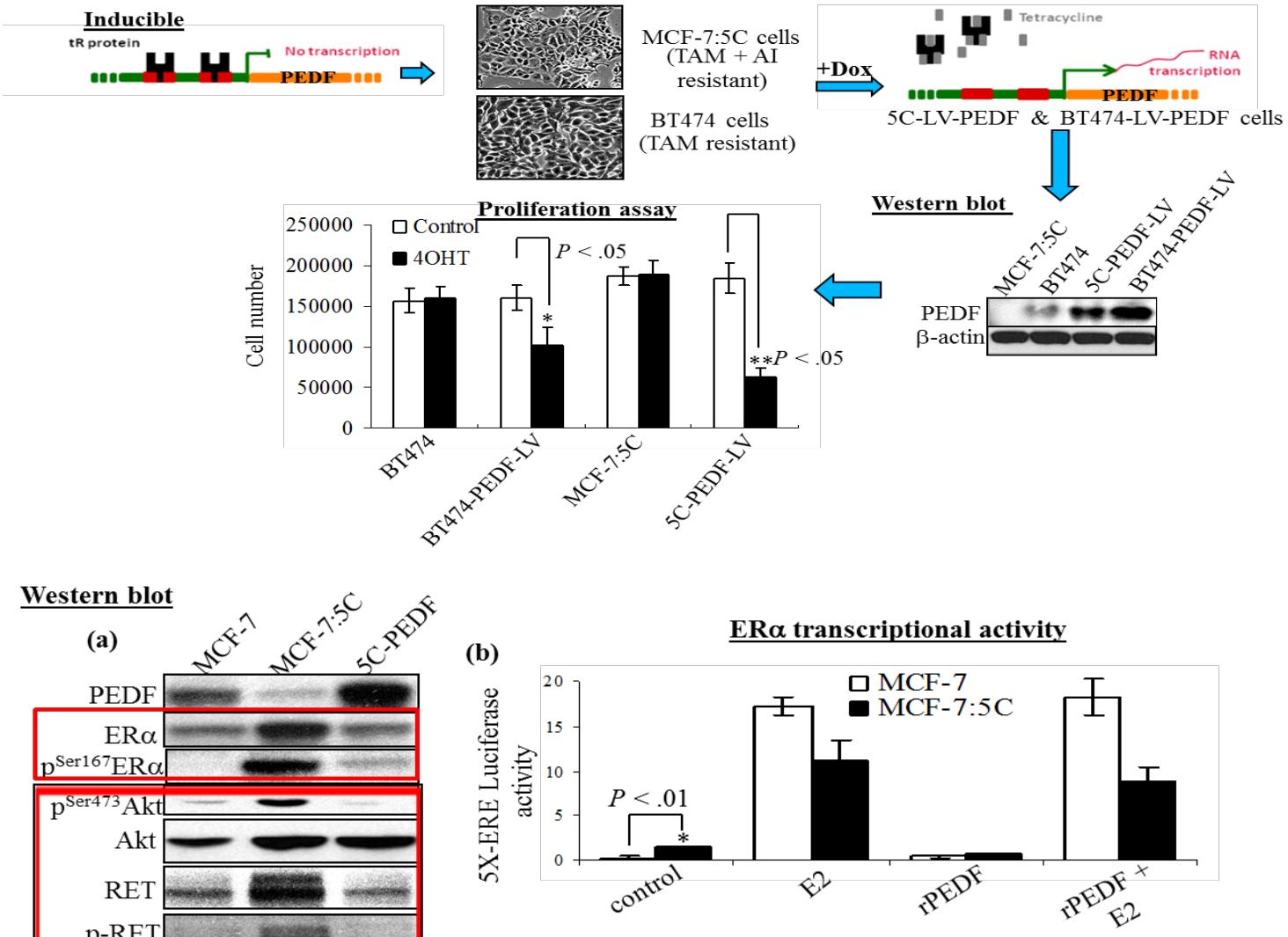

Figure 2: Reexpression of PEDF in endocrine resistant breast cancer cells inhibits the estrogen receptor (ER) signaling pathway. (**a**) Western blot analysis of protein lysates isolated from MCF-7, MCF-7:5C, and 5C-PEDF-LV cells to assess PEDF, total and phosphorylated ERα, RET, and other downstream kinases. (**b**) ERα transcriptional activity as determined by estrogen response element (ERE) luciferase assay.

Summary of Results for Task 2: In Task #2, we performed experiments to assess the role of the estrogen receptor (ER alpha) in regulating PEDF expression in endocrine resistant MCF-7:5C and BT474 breast cancer cells with parental MCF-7 cells. We hypothesized that ERα suppresses PEDF expression in endocrine resistant MCF-7:5C and BT474 breast cancer cells by binding to the PEDF promoter and recruiting additional proteins to the protein that function to repress PEDF expression. To address our hypothesis, we first performed siRNA knockdown of ERα to see whether suppressing ER has a direct impact on PEDF expression in endocrine resistant MCF-7:5C breast cancer cells. Our results shown in **Figure 3** demonstrated that knockdown of ERα in MCF-7:5C cells markedly increased PEDF protein (**Figure 3a**) and PEDF mRNA expression (**Figure 3b**) in these cells, however, in parental MCF-7 cells knockdown of ERα increased PEDF expression. Additionally, we found that estradiol treatment also increased PEDF expression in endocrine resistant MCF-7:5C cells however it did not increase PEDF in MCF-7 cells. We should note that knockdown of ERα in HER2-overexpressing BT474 breast cancer cells did not alter PEDF expression in these cells (data not shown) thus suggesting that the resistant phenotype of these cells is driven more by HER2-

overexpression rather than loss of PEDF. Notably, we also discovered another protein called activator protein 2 (AP-2) that appears to be an important regulator of both ERα and PEDF. AP-2 is a family of cell type-specific developmentally regulated transcription factors that have been implicated as critical regulators of gene expression during vertebrate development, embryogenesis, and transformation. There are four known members of the AP-2 gene family: AP-2A/α, AP-2B/β, AP-2C/γ, and AP-2D/δ, each encoded by a separate gene (Schorle et al. 1996; Hilger-Eversheim, 2000). Several genes with a variety of functions like cell growth, cell morphology, and cell communication have been shown to possess sequences similar to the AP-2 binding sequence (5'-GCCN3GGC-3') in their promoter regions or be regulated by AP-2 (Zeng et al. 1997; Somasundaram et al. 1996; Mitchell et al. 1987). We found that AP-2A and AP-2C were highly expressed at the protein and mRNA level in endocrine resistant MCF-7:5C cells compared to parental MCF-7 cells (**Figure 4a and 4b**) and that siRNA knockdown of AP-2A and AP-2C markedly increased PEDF protein and mRNA expression in MCF-7:5C cells which was associated with a reduction in ERα expression in these cells (**Figure 4c**). Further analysis revealed that AP-2A expression was regulated by ERα and that loss of ERα decreased AP-2A protein, however, AP-2A mRNA level was dramatically increased in endocrine-resistant MCF-7:5C cells. Similar experiments performed in endocrine-sensitive MCF-7 cells revealed that AP-2A and AP-2C levels were not significantly altered by loss of ERα, thus confirming an important link between ERα and AP-2 in endocrine resistant MCF-7:5C cells but not the parental MCF-7 cells. We should note that evidence from many laboratories suggests that AP-2A is a tumor suppressor gene and that reduced expression or loss of expression of AP-2A is found to be associated with breast cancer and colon carcinoma (Gee et al. 1999; Karjalainen et al. 1998). Furthermore, dominant negative mutant of AP-2A has been shown to increase its invasiveness and tumorigenicity and its overexpression has been shown to induce p21 and inhibit cellular DNA synthesis and colony formation (Karjalainen et al. 1998). However, our data suggest that AP-2A has a tumor promoting effect in MCF-7:5C cells possibly due to its ability to interact with ERα and suppress PEDF expression in these cells. We have previously shown that endocrine-resistant MCF-7:5C cells are highly aggressive, migratory, and invasive and these cells are capable of forming tumors when injected into athymic mice (Lewis et al. 2005; please see appendices for a copy), hence, it is possible that elevated level of AP-2A combined with loss of PEDF enhances tumor growth and contributes to the development of endocrine resistance in this particular model system.

Task 2: Study the role of ERα in PEDF regulation in endocrine sensitive and endocrine resistant breast cancer cells (Months 12-24).

Task 2-1) Determine whether PEDF protein and mRNA levels are differentially regulated by estrogen and antiestrogens in endocrine resistant and endocrine sensitive breast cancer cells and whether ERa plays a direct role in regulating PEDF expression.

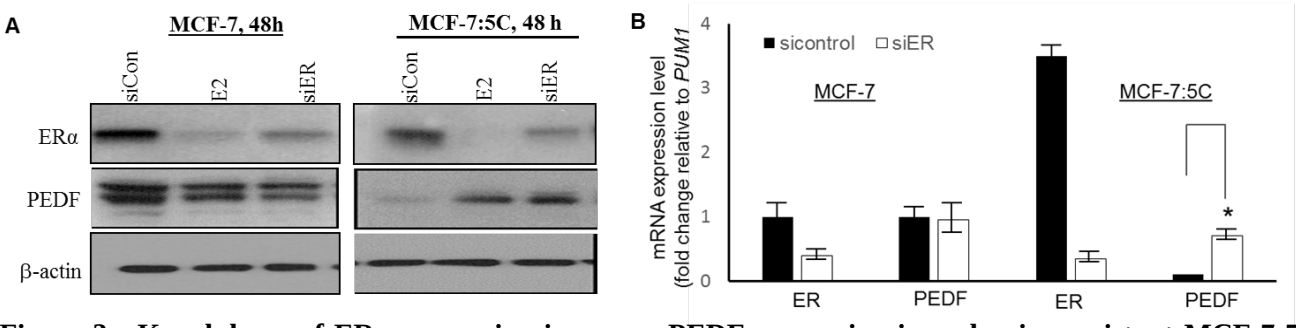

Figure 3: Knockdown of ERα expression increases PEDF expression in endocrine resistant MCF-7:5C cells. (**a**) Endocrine-sensitive MCF-7 cells and endocrine-resistant MCF-7:5C cells were transfected with control siRNA (siCon) or ERα siRNA (siERα) and after 24 h cells were treated with E2 (1 nM) for an additional 48 h. (**a**) Western blot analysis were performed on MCF-7 and MCF-7:5C cells following siRNA knockdown of ERα and total ERα and PEDF protein expression were measured with β-actin as a positive loading control. (**b**) Effect of ERα knockdown on PEDF mRNA expression was confirmed by quantitative real-time PCR analysis with PUM1 used as an internal control. Data shown is representative of three separate experiments yielding similar results. Error bars correspond to mean ± SD. *P <0.01 as compared with sicontrol group.

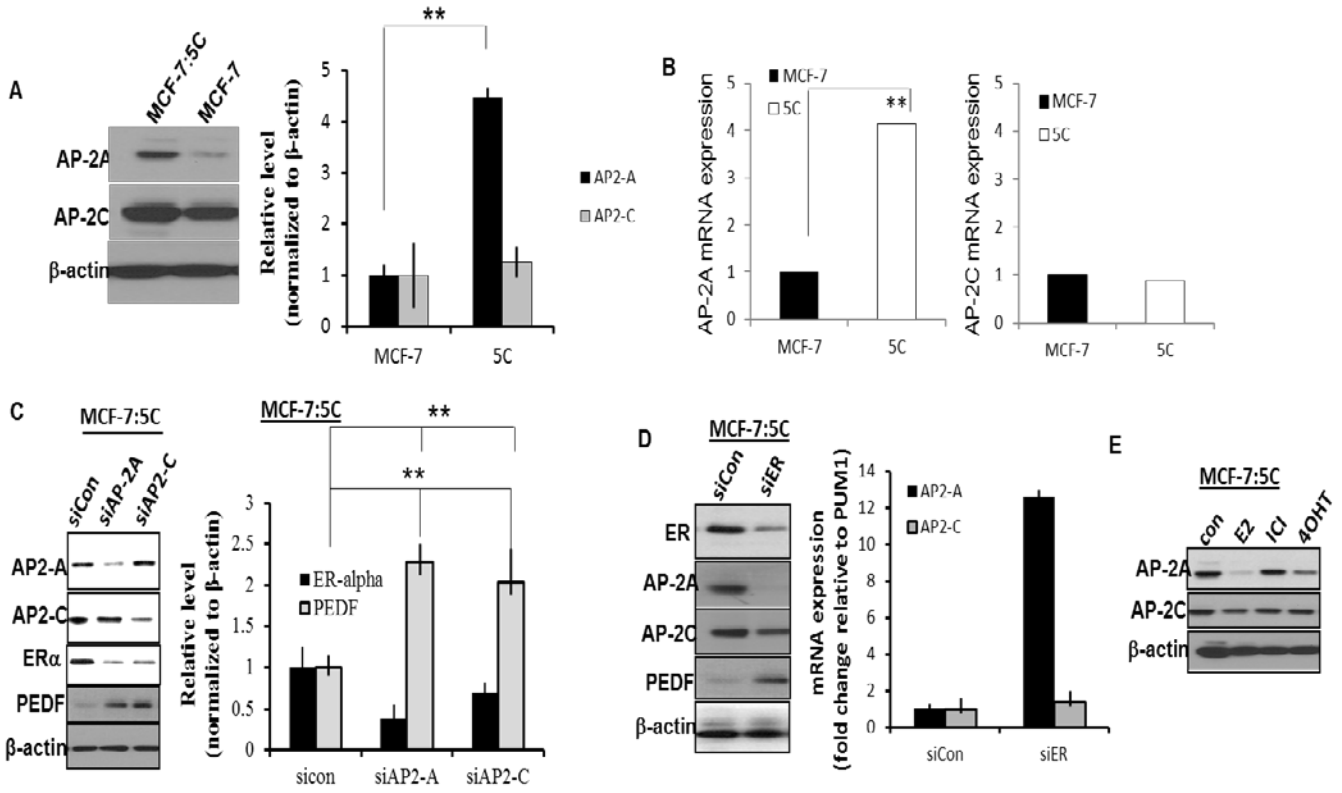

Figure 4: AP-2A and AP-2C expression in endocrine resistant MCF-7:5C cells (**a**) AP-2A and AP-2C protein expression in endocrine-resistant MCF-7:5C cells and endocrine sensitive MCF-7 cells as assessed by Western blot analysis. Relative levels of AP-2A or AP-2C in MCF-7:5C and MCF-7 cells were quantified using the ImageJ software (downloaded from the NIH website) and normalized to β-actin. Each value is a mean ± SD from three experiments. (**b**) AP-2A and AP-2C mRNA expression in MCF-7 and MCF-7:5C (5C) cells as determined by quantitation real-time PCR. (**c**) Effect of AP-2A and AP-2C knockdown on ERα and PEDF protein and mRNA expression in MCF-7:5C cells. For experiments, MCF-7:5C cells were transfected with control siRNA (siCon), siAP-2A, or siAP-2C and after 48 hours the cells were harvested and protein lysates collected and analyzed by Western blot. AP-2A, AP-2C, ERα, and PEDF protein levels are shown following knockdown experiments with β-actin used as a loading control. (**d**) Effect of ERα knockdown on AP-2A, AP-2C, and PEDF expression in MCF-7:5C cells. For experiment, cells were transfected with control siRNA (siCon) or ERα siRNA (siERα) (100 ng) and after 24 h cells were harvested and processed for Western blot (left panel) and RT-PCR (right panel) analyses. Knockdown of ERα mRNA expression was confirmed by quantitative RT-PCR analysis. Standard deviations are shown. **P < 0.01. (**e**) Hormonal regulation of AP-2A and AP-2C in MCF-7:5C cells. To assess whether AP-2 proteins are hormonally regulated, MCF-7:5C cells were treated with E2 (1 nM), ICI (1 μM), and 4OHT (1 μM) for 48 h. Cell extracts were subject to Western blotting analysis to assess AP2-A and AP2-C protein expression.

Task 2-2) Investigate the regulation of PEDF promoter activity by ERα using transient transfection luciferase assays

ERα is known to regulate target genes through a regulatory mechanism involving its direct binding to estrogen response elements (EREs) with the sequence AGGTCAxxxTGACCT or by tethering to other response elements through protein-protein interactions with other DNA-bound transcription factors such as SP1 and AP1. The 5'-flanking region of the PEDF promoter is dominated by a dense cluster of Alu repeats in which are embedded several promoter consensus sequences including an estrogen response element (ERE) located within 200 bps of the translational start site. Since PEDF expression is loss/suppressed in endocrine resistant MCF-7:5C cells, we hypothesize that loss of PEDF is due to constitutive binding of ERα, AP-2, and

the co-repressor NCoR to the PEDF promoter which function to suppress PEDF expression. Indeed, luciferase reporter assay using different PEDF promoter constructs (**Figure 5a**) showed very low PEDF promoter activity in endocrine resistant MCF-7:5C cells with the different PEDF constructs (**Figure 5b, left panel**), however, when PEDF was re-expressed in the resistant cells, its promoter activity was significantly elevated with all of the constructs with the full length promoter construct (pGL3-PEDF-1310/+27) showing the most robust response (**Figure 5b, right panel**). Notably, knockdown of ERα significantly reduced the promoter activity of the PEDF constructs containing the ERE sequences (**Figure 5d**, **right panel**).

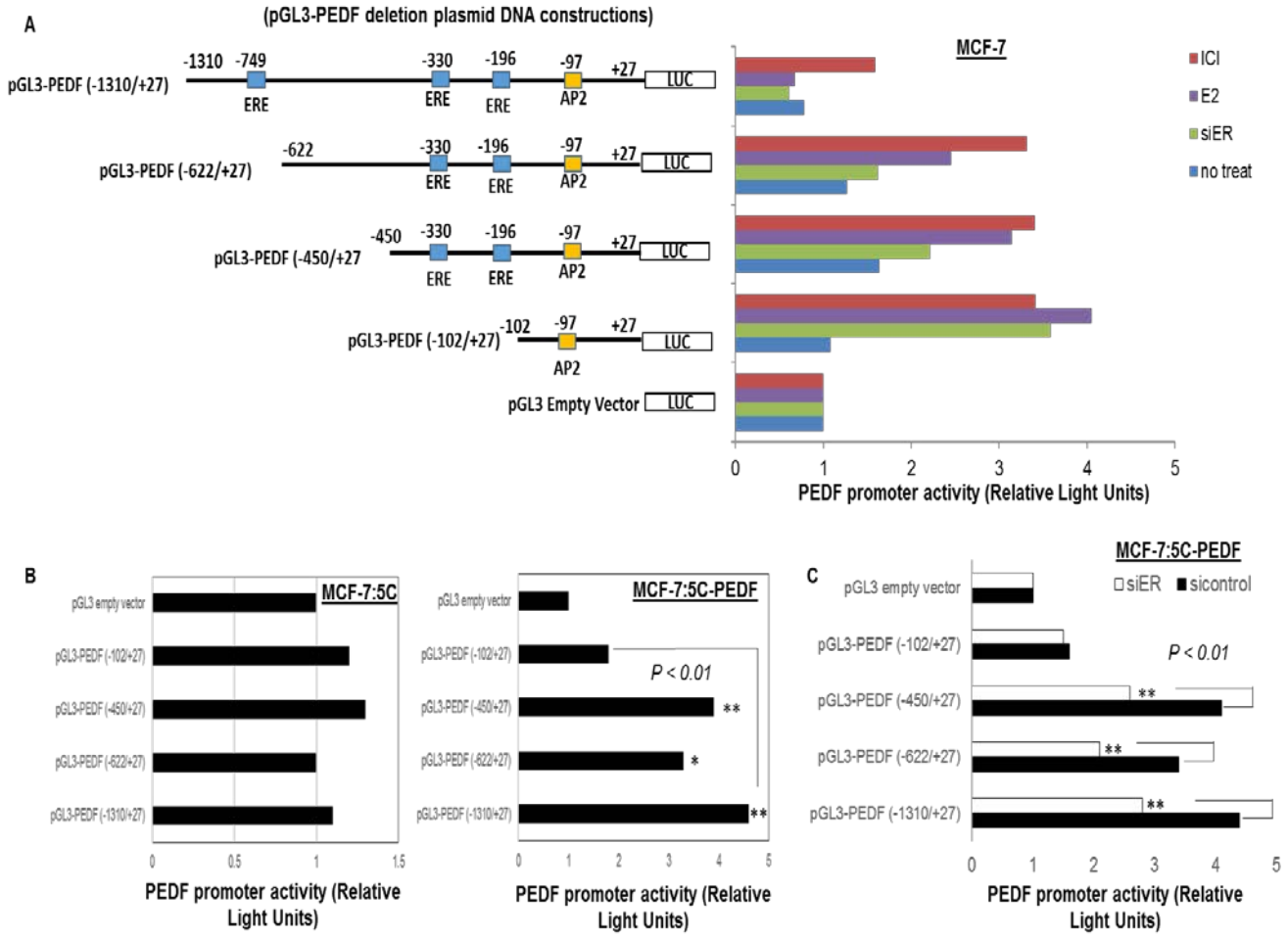

Figure 5: PEDF promoter cloning and luciferase activity. (a) Full-length and fragments of the human *PEDF* promoter were cloned from human genomic DNA (Promega) by PCR using the primers 5′-gtagactcatttacagatagaaggcaag-3′ (forward) and 5′-gtaagtcagccaggcagccggtcactg-3′ (reverse), yielding a fragment spanning from −1310 to +27 of the promoter sequence (GenBank™ accession number M76979.1). Nucleotide numbers indicated for the human PEDF promoter relates to the transcriptional initiation site. After the fragments were subcloned into the pSC-A vector, sequences were checked and then cloned into the SmaI site of the pGL3-Basic vector (Promega) to produce the pGL3-PEDF plasmid. The PvuII restriction site at nucleotide −622 and the NdeI restriction site at nucleotide −450 and -102 were used to generate the hPEDF-Luc deletion constructs. The resulting products were blunt cloned into the SmaI site of the pGL3-Basic vector, creating the reporter vectors PEDF-1-Luc and PEDF-2-Luc. pGL3-PEDF-mutants were generated from pGL3-PEDF-wild-type by site-directed mutagenesis (QuikChange™ mutagenesis kit; Stratagene, La Jolla, CA) using primer 5′-GAGAAAAACCACATATGGAACATTCAGGTC-3′ (GT to CA mutation underlined). The presence of the mutations was confirmed by sequencing. (**b**) PEDF luciferase promoter activity in endocrine sensitive MCF-7, endocrine-resistant MCF-7:5C cells, and PEDF-overexpressing MCF-7:5C cells. For experiment, cells were transiently transfected with either full-length PEDF promoter fragment or PEDF-deletion mutants and luciferase activity was measured. (**c**) Effect of ERα knockdown on PEDF promoter activity in MCF-7:5C-PEDF-overexpressing cells.

Task 2-3) Determine whether ERα binds directly to ERE sequences in the PEDF promoter to regulate its activity. ERα is known to regulate target genes through a regulatory mechanism involving its direct binding to estrogen response elements (EREs) with the sequence AGGTCAxxxTGACCT or by tethering to other response elements through protein-protein interactions with other DNA-bound transcription factors such as SP1 and AP1. Studies have shown that the PEDF promoter contains an ERE sequence that is embedded within an Alu repeat located within 200 bps (-210 bps) of the translation start site, however, the functional significance of this sequence is not known. In this task, we investigated whether ERα directly binds to the PEDF promoter and regulate its expression in the resistant MCF-7:5C cells. Specifically, we tested whether ERα binds directly to the ERE-like element on the PEDF promoter in MCF-7, MCF-7:5C, MCF-7:5C-PEDF, and BT474 cells using biotin-labelled streptavidin-agarose DNA pull-down assays using the PEDF-probe shown in **Figure 6a**. Our DNA pulldown data shown in **Figure 6b** revealed that ERα and several other proteins including AP-2A, AP-2C, and the corepressor NCoR (nuclear receptor corepressor) were constitutively bound to the full-length PEDF promoter in the resistant MCF-7:5C cells but they were not bound in endocrine-sensitive MCF-7 cells. Notably, we detected marginal ERα binding to the PEDF promoter in BT474 cells; however, the binding was markedly less than that observed in MCF-7:5C cells (data not shown). Additional studies performed with three different PEDF promoter fragments (Figure 7A) indicated robust binding of ERα, AP-2A, and AP-2C to probe A (-450 to +27) and probe B (-102 to +27) but very little binding to probe C (-62 to +27) which lacks the ERE and AP-2 binding sites (**Figure 7b**), thus confirming the importance of these two sites in the regulation of PEDF by ERα and AP-2. To confirm that the ERE-like element at -210 bp of the PEDF promoter conferred the responsiveness to ERα, we introduced point mutations using site-directed mutagenesis by base-substitution in both arms of the ERE-like palindrome of the PEDFm2 (300 bp) truncation. For comparison, a single point mutation that did not grossly disrupt the ERE-consensus was also introduced in one arm of the ERE-like element in mERE1. We found that the mERE-1-luc construct (which had the intact ERE) showed similar responsiveness to ERα comparable to the wild-type PEDFm2-luc whereas mERE3-luc and mERE4-luc mutants, which had a disrupted ERE loop, lost their sensitivity to ER (data not shown). Lastly, we confirmed the specificity of ERα binding to the ERE-like element of the PEDF promoter by performing the DNA pull-down assays with a wild-type ERE fragment (PEDFm2) (5'-GTTCCGTCACGTGACCTTAA-3') and a mutant ERE fragment (mERE3) (5'-GTTCCGTAACGTTACGTTAA-3'). We found that ERα bound to the 210 bp wild-type PEDF fragment (PEDFm2) in both MCF-7 and MCF-7:5C cells but not the mutant PEDF fragment (mERE3), thus confirming the importance of the ERE sequence in the mechanistic action of ERα in PEDF regulation (**Figure 8**).

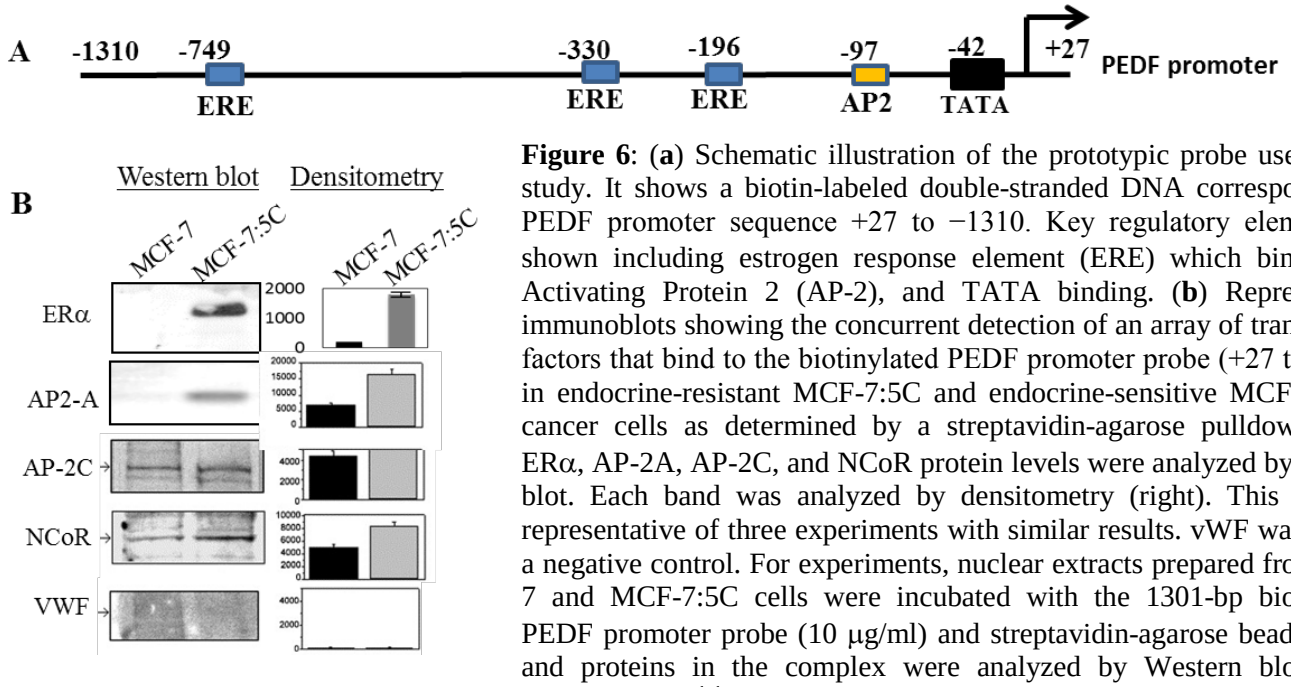

Figure 6: (**a**) Schematic illustration of the prototypic probe used in this study. It shows a biotin-labeled double-stranded DNA corresponding to PEDF promoter sequence +27 to −1310. Key regulatory elements are shown including estrogen response element (ERE) which binds ERα, Activating Protein 2 (AP-2), and TATA binding. (**b**) Representative immunoblots showing the concurrent detection of an array of transcription factors that bind to the biotinylated PEDF promoter probe (+27 to −1310) in endocrine-resistant MCF-7:5C and endocrine-sensitive MCF-7 breast cancer cells as determined by a streptavidin-agarose pulldown assay. ERα, AP-2A, AP-2C, and NCoR protein levels were analyzed by Western blot. Each band was analyzed by densitometry (right). This figure is representative of three experiments with similar results. vWF was used as a negative control. For experiments, nuclear extracts prepared from MCF-7 and MCF-7:5C cells were incubated with the 1301-bp biotinylated PEDF promoter probe (10 μg/ml) and streptavidin-agarose beads for 1 h and proteins in the complex were analyzed by Western blots. Each densitometry bar denotes mean ± SE of three experiments.

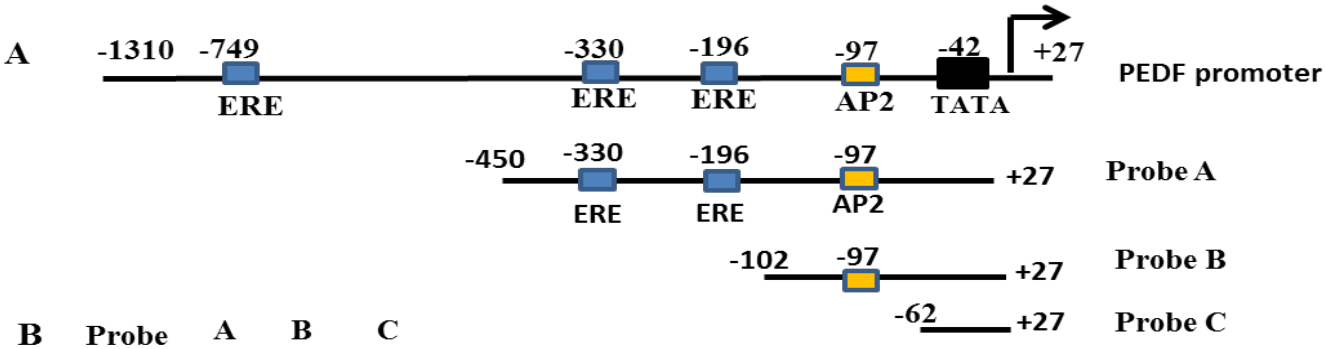

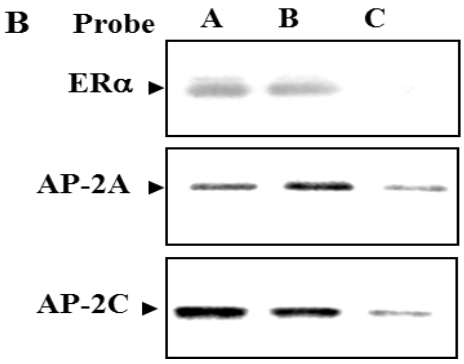

Figure 7: Influence of promoter fragment length on ERα, AP-2A, and AP-2C binding to PEDF promoter. (**a**) Schematic illustration of the size of the three probes (A, B, C) used in the assay. (**b**) Level of ERα, AP-2A, and AP-2C binding to the three DNA probes in endocrine-resistant MCF-7:5C cells. The concentration of each probe was 10 μg/ml (36 nM for the +27/−450 probe, 126 nM for the +27/−102 probe, and 720 nM for the +27/−62 probe). The Western blot is representative of three experiments and the densitometry figure shows mean ± SE. Binding of the transcription factors to the biotinylated DNA probe was assessed by streptavidin-agarose pulldown assay.

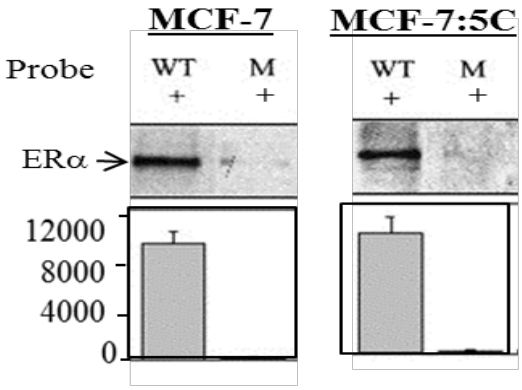

Figure 8: Specificity of binding of ERα to the 210-bp PEDF promoter probe. ERα binding to PEDF probe at basal state detected with wild-type (WT) ERE probe or ERE-mutated (M) probe. Data shows that ERα binding was undetectable in both MCF-7 and MCF-7:5C cells when the probe with ERE mutation was used as a probe. Each bar denotes mean ± SE of three experiments.

Summary of Results for Task 3:

PEDF is a potent antiangiogenic factor that has been shown to inhibit tumor growth and progression. We previously showed that PEDF expression is loss in endocrine resistant breast cancer cells and that lentivirus-mediated PEDF gene transfer in endocrine-resistant MCF-7:5C and BT474 breast cancer cells resensitize them to the inhibitory effects of tamoxifen *in vitro* (**Figure. 2B**). Furthermore, we previously showed that administration of recombinant PEDF is capable of reducing the growth of endocrine resistant breast cancer cells in athymic (nude) mice which was due in part to inhibition of angiogenesis (Jan et al.2012; please see appendices for copy). In the 3rd Aim of this grant proposal, we examined the effect of PEDF overexpression on endocrine resistant tumor growth and tamoxifen sensitivity in athymic mice. Furthermore, we tested whether the inhibitory effect of PEDF in vivo was mediated by inhibition of angiogenesis or through suppression/disruption of ERα crosstalk with upstream kinase signaling pathways. For our studies, we used ovariectomized outbred athymic/nude mice (4- to 6-week-old) from Taconic (Hudson, NY). For in vivo studies, athymic mice were bilaterally injected with MCF-7:5C-PEDF-LV or BT474-PEDF-LV cells into the mammary fat pads and tumor growth was monitored over a 4 week period. As shown in **Figure 8a**, the tumor size in the lentivirus-5C-PEDF-treated group was significantly smaller (~40% reduction) in comparison with the control group (no PEDF/-doxycycline) on day 21 after cell inoculation. Analysis of the 5C-PEDF-LV tumors confirmed PEDF overexpression in that group and it revealed that the presence of

PEDF dramatically reduced phosphorylation of ERα (Serine 167), RET, and AKT in the 5C-PEDF-LV (**Figure 8b**). These findings are consistent with our in vitro data which revealed similar results. We should also note that sections of tumor xenografts were stained for CD31 to measure the microvascular density (MVD). Notably, we found that the MVD of tumor tissues was dramatically decreased in lenti-PEDF-treated group compared with that of control group (**Figure 8c**), thus confirming the antiangiogenic effect of PEDF in the resistant cells. Lastly, we found that mice inoculated with 5C-PEDF-LV cells showed a marked decrease in tumor size when they were treated with tamoxifen (20 mg/kg body weight) or the aromatase inhibitor letrozole (20 mg/kg) and this inhibitory effect was almost comparable to that seen with recombinant PEDF (data not show).

Task 3. Determine the effect of PEDF overexpression on endocrine resistant breast cancer cell growth in animals (xenograft) and elucidate the mechanism of action of PEDF in vivo. (Months 18-36)

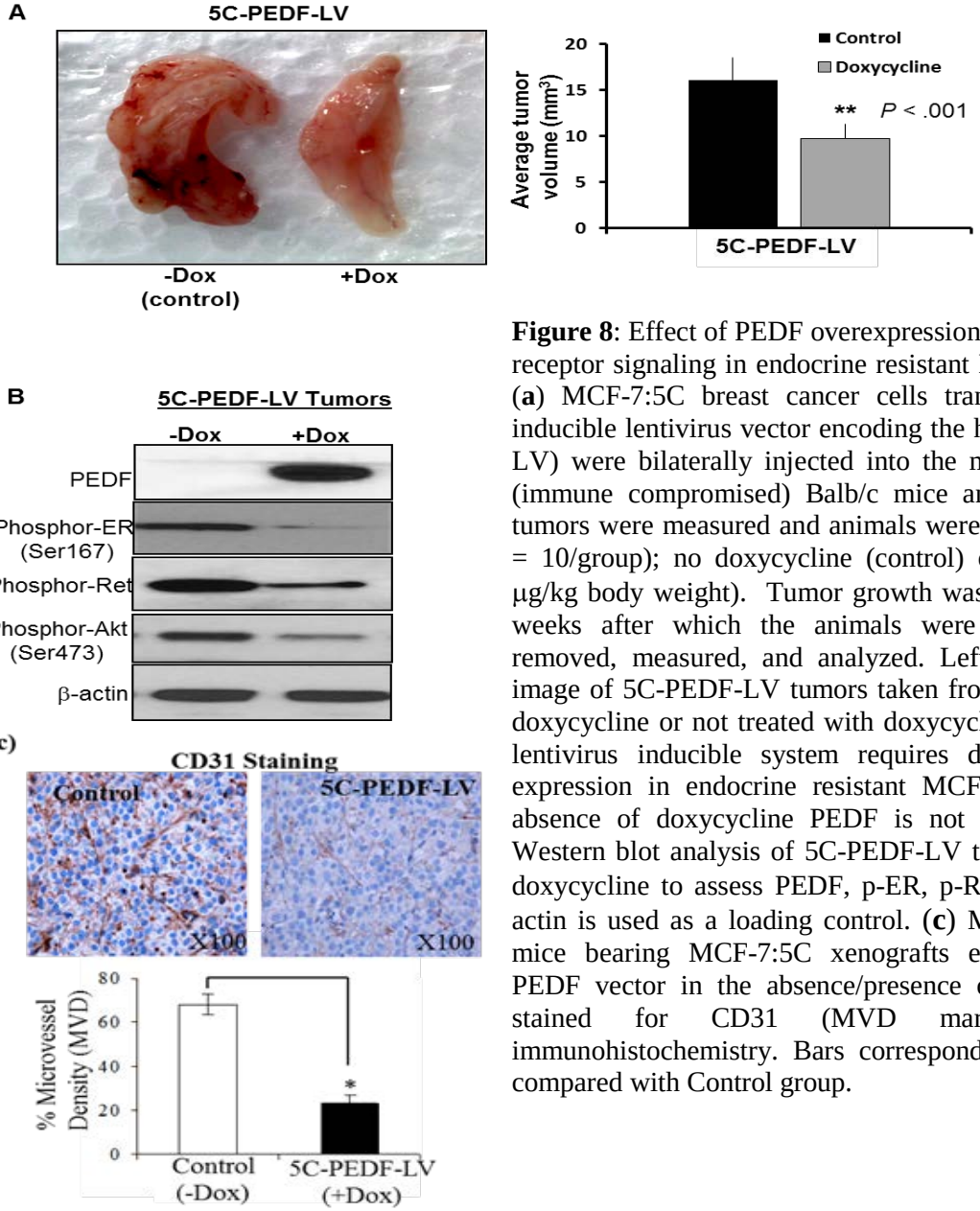

Figure 8: Effect of PEDF overexpression on tumor growth and estrogen receptor signaling in endocrine resistant MCF-7:5C breast cancer cells. (**a**) MCF-7:5C breast cancer cells transfected with a doxycycline-inducible lentivirus vector encoding the human PEDF gene (5C-PEDF-LV) were bilaterally injected into the mammary fat pads of athymic (immune compromised) Balb/c mice and after two weeks, palpable tumors were measured and animals were randomized to two groups (N = 10/group); no doxycycline (control) or + doxycycline (Dox at 50 μg/kg body weight). Tumor growth was measured for an additional 2 weeks after which the animals were euthanized and the tumors removed, measured, and analyzed. Left panel shows a side-by-side image of 5C-PEDF-LV tumors taken from mice that were treated with doxycycline or not treated with doxycycline (control). Please note that lentivirus inducible system requires doxycycline to induce PEDF expression in endocrine resistant MCF-7:5C cells, however, in the absence of doxycycline PEDF is not expressed in these cells. (**b**) Western blot analysis of 5C-PEDF-LV tumors treated with or without doxycycline to assess PEDF, p-ER, p-RET, and p-Akt expression. β-actin is used as a loading control. (**c**) Microvessel density (MVD) of mice bearing MCF-7:5C xenografts expressing lentivirus-inducible PEDF vector in the absence/presence of doxycycline. Tissues were stained for CD31 (MVD marker) and analyzed by immunohistochemistry. Bars correspond to mean ± SD. *P<0.01 as compared with Control group.

RESEARCH ACCOMPLISHMENTS:

- **Cell lines developed**: Our laboratory has developed two unique human breast cancer cell lines (MCF-7:5C-PEDF-LV and BT474-PEDF-LV) that stably overexpress the pigment epithelium derived factor (PEDF) gene. We have also developed MCF-7:5C-AP2A-KD and MCF-7:5C-AP2C-KD breast cancer cell lines.

- **Xenograft mouse models of endocrine resistance (**5C-PEDF-LV and BT474-PEDF-LV)

- **Research opportunities**: I am currently collaborating with my colleague Dr. Fariba Behbod at the University of Kansas Medical Center to study whether PEDF expression is capable of blocking the conversion of ductal carcinoma in situ (DCIS) to invasive breast cancer and whether it can block the development of tumors derived from BRCA-1 mutation/knockout. I am also collaborating with Dr. Patricia Baccerra at the National Eye Institute at NIH (Bethesda, MD) to develop PEDF peptides to better understand the functional domains of the protein and to assess their therapeutic potential in cancer as well as other diseases (diabetes).

REPORTABLE OUTCOMES: Our laboratory has developed an inducible lentivirus expression system that allows us to reexpress the antitumor gene PEDF in endocrine resistant breast cancer cells and to use these genetically modified cell lines to generate clinically relevant mouse models to study the evolution of endocrine resistance *in vivo.* With the development of our genetically modified PEDF-inducible cell lines and xenograft mouse models were have been able to fully investigate the role of PEDF in the development of endocrine resistance. The development of drug resistance to endocrine therapies such as tamoxifen and aromatase inhibitors is a major clinical problem for 40-50% of breast cancer patients. With these animal models, we were able to study how endocrine resistance develops and what role PEDF plays in the process. Additionally, we were able to assess the therapeutic effects of recombinant PEDF in vivo and in vitro and to gain greater insight into the mechanism of action of PEDF in endocrine resistant cells. During the course of our study, we identified novel interactions between the ERα signaling pathway and several other proteins including RET (receptor tyrosine kinase) and the transcription factor AP-2. Overall, our data demonstrate the importance of PEDF in sensitizing breast cancer cells to endocrine therapy and they highlight the consequences of PEDF loss in breast cancer as it relates to disease progression and response to endocrine therapy. It is possible that PEDF loss, combined with ERα status, might be used a potential marker of response to endocrine therapy. Furthermore, we have discovered a novel link between PEDF loss and an increase in inflammatory and interferon response signaling in endocrine resistant breast cancers. This unique interaction has important clinical implications for patients especially since increased interferon signaling has been linked to disease progression and poor prognosis. In particular, we have found that endocrine resistant breast cancer cells and recurrence tumors constitutively overexpress several type 1 interferon-stimulated genes including; IFITM1, STAT1, STAT2, IFIT1, IFI27, OAS1, MX1, PLSCR1, IRF-7, IFNα/β, and IRF-9 and that the overexpression of these genes enhances cell proliferation and survival and leads to drug resistance (Choi et al. 2015; please see appendices for copy). Our goal is to further characterize the link between PEDF signaling, immune response, and inflammatory signaling in different subtypes of breast cancer. We recently submitted a R21 grant application that focuses on understanding the role of interferon signaling in inflammatory breast cancer (IBC) and the potential therapeutic benefits of PEDF in treating IBC disease. This grant has received an impact score of 30 and percentile of 16% and we are waiting to hear whether it will be funded this cycle.

. **Publications**:

1. Jan R, Brewer C, Huang M**, Lewis-Wambi JS**. Loss of pigment epithelium-derived factor: A novel mechanism for the development of endocrine resistance in breast cancer. *Breast Cancer Res* 2012; 14(6):R146. PMID: 23151593.

2. Choi HJ, Lui A, Ogony J, Jan R, Sims P, **Lewis-Wambi JS**. Targeting interferon signaling pathway sensitizes aromatase inhibitor resistant breast cancer cells to estrogen-induced cell death. Breast Cancer Research 2015; 17:6 PMCID: PMC4336497

3. Hayes EL, **Lewis-Wambi JS**. Mechanisms of endocrine resistance in breast cancer: an overview of the proposed roles of noncoding RNA. Breast Cancer Res. 2015; 17:40. PMCID: PMC4362832

Published Abstracts:

1. Rifat Jan, Min Huang, **Joan Lewis-Wambi**. Loss of PEDF expression: A novel mechanism for the development of endocrine resistance. AACR Meeting, April 2012; 2010:687. Chicago, IL

2. Asona Lui, Hye Joung Choi, **Joan Lewis-Wambi**. 2015. Overexpression of interferon stimulated genes is critical for the survival of aromatase inhibitor-resistant breast cancer cells. Proceedings of the American Association for Cancer Research. Abstract #766. Philadelphia, PA

3. Hye Joung Choi and **Joan Lewis-Wambi**. 2015. Loss of interferon-induced transmembrane protein 1 enhances estrogen-induced cell death in AI-resistant breast cancer cells. Proceedings of the American Association for Cancer Research. Abstract #25. Philadelphia, PA

4. Erin L. Hayes, Jennifer Knapp, **Joan Lewis-Wambi**. 2015. MicroRNA analysis of aromatase inhibitor-resistant breast cancer cells reveals a unique miRNA cluster on chromosome 14. Proceedings of the American Association for Cancer Research. Abstract #2556. Philadelphia, PA

. **Invited Lectures**:

"The role of pigment epithelium derived factor (PEDF) in endocrine resistance". City College of New York (CCNY), Department of Pharmacology, New York City, NY, August 26th, 2012.

"A novel approach to treat endocrine resistant breast cancer". University of Kansas Medical Center (KUMC). Department of Cancer Biology. Kansas City, KS, December 15th, 2012.

Targeting RET oncogene using PEDF: A novel strategy to reverse endocrine resistance. University of Missouri, Department of Pharmacology, Kansas City, MO, March 2013.

Endocrine resistance and breast cancer: A novel approach for treatment. University of Mississippi Medical Center, Department of Pathology Seminar Series, Jackson, MS, October 2014.

Exploiting Vulnerabilities in Endocrine Resistant Breast Cancer Cells using PEDF: A new therapeutic approach. University of Kansas, Department of Biosciences, Lawrence, KS, June 6th, 2014.

A novel role for PEDF in breast cancer. National Institutes of Health-National Eye Institute (NIH/NEI). Bethesda, MD, Sept 10th, 2014.

Impact: Resistance to endocrine therapy such as tamoxifen or aromatase inhibitors is a major clinical obstacle to the effective treatment and cure of women with estrogen receptor alpha (ERα)-positive breast cancer. The possibility of identifying new targets for therapy in resistant disease, or patients, who may benefit from additional treatment with existing therapies, provides a strong impetus to identify markers and mediators of therapeutic resistance. Our preliminary data indicates that PEDF, a naturally occurring glycoprotein that has potent antiangiogenic activity, is suppressed in endocrine resistant breast cancer cells and tumors and that reexpression of PEDF in resistant cells resensitizes them to the inhibitory effects of tamoxifen. Our findings have important clinical implications for breast cancer patients who have developed resistant to tamoxifen and aromatase inhibitors because they suggest that PEDF expression can be used as a potential marker of endocrine responsiveness in breast cancer and that it can potentially be used to treat patients with resistant disease. The fact that PEDF is a naturally occurring protein that is present at relatively high concentration (up to 100 nM) in the serum of healthy individuals suggests that can be tolerated at high concentrations without significant side effects and can potentially be used as a therapeutic. Our proposed animal studies with recombinant PEDF will help to provide additional information regarding the bioavailability of PEDF, its safety profile, and its efficacy at reversing tamoxifen resistance in vivo. We also plan to study whether PEDF is capable of blocking the transition of ductal carcinoma in situ (DCIS) to invasive breast cancer using the DCIS animal model which is available at KUMC.

Changes/Problems: The only change that was made to this grant application was a change in institution. I was awarded this grant in August 2012 when I was an Assistant Professor at Fox Chase Cancer Center (FCCC) (Philadelphia, PA). I accepted a faculty position at my current institution, the University of Kansas Medical Center (KUMC), in January 2013 and I requested to transfer my grant from FCCC to KUMC upon my relocation. My request to transfer my grant was approved in Sept 2013 and I was granted a 1 year no-cost extension to complete the proposed work.

REFERENCES:

Jan R, Brewer C, Huang M, **Lewis-Wambi JS**. Loss of pigment epithelium derived factor: A novel mechanism for the development of endocrine resistance in breast cancer. *Breast Cancer Res* 2012; 14(6):R146. PMID: 23151593.

Schorle H, Meier P, Buchert M, Jaenisch R, Mitchell PJ. Transcription factor AP-2 essential for cranial closure and craniofacial development. Nature. 1996; 381(6579):235-8.

Hilger-Eversheim K, Moser M, Schorle H, Buettner R. Regulatory roles of AP-2 transcription factors in vertebrate development, apoptosis and cell-cycle control. Gene. 2000; 2 60(1-2):1-12.

Zeng YX, Somasundaram K, el-Deiry WS. AP2 inhibits cancer cell growth and activates p21WAF1/CIP1 expression. Nat Genet. 1997; 15(1):78-82.

Somasundaram K, Jayaraman G, Williams T, Moran E, Frisch S, Thimmapaya B. Repression of a matrix metalloprotease gene by E1A correlates with its ability to bind to cell type-specific transcription factor AP-2. Proc Natl Acad Sci U S A. 1996; 93(7):3088-93.

Mitchell PJ, Wang C, Tjian R. Positive and negative regulation of transcription in vitro: enhancer-binding protein AP-2 is inhibited by SV40 T antigen. Cell. 1987; 50(6):847-61.

Gee JM, Robertson JF, Ellis IO, Nicholson RI, Hurst HC. Immunohistochemical analysis reveals a tumour suppressor-like role for the transcription factor AP-2 in invasive breast cancer. J Pathol. 1999; 189(4):514-20.

Karjalainen JM, Kellokoski JK, Eskelinen MJ, Alhava EM, Kosma VM. Downregulation of transcription factor AP-2 predicts poor survival in stage I cutaneous malignant melanoma. J Clin Oncol. 1998; 16(11):3584-91.

Lewis JS, Meeke K, Osipo C, Ross EA, Kidawi N, Li T, Bell E, Chandel NS, Jordan VC. Intrinsic mechanism of estradiol-induced apoptosis in breast cancer cells resistant to estrogen deprivation. J Natl Cancer Inst. 2005; 97(23):1746-59.

APPENDICES:

Please see attachments.

Breast Cancer RESEARCH

RESEARCH ARTICLE Open Access

Loss of pigment epithelium-derived factor: a novel mechanism for the development of endocrine resistance in breast cancer

Rifat Jan[1], Min Huang[2] and Joan Lewis-Wambi[1*]

Abstract

Introduction: Despite the benefits of endocrine therapies such as tamoxifen and aromatase inhibitors in treating estrogen receptor (ER) alpha-positive breast cancer, many tumors eventually become resistant. The molecular mechanisms governing resistance remain largely unknown. Pigment epithelium-derived factor (PEDF) is a multifunctional secreted glycoprotein that displays broad anti-tumor activity based on dual targeting of the tumor microenvironment (anti-angiogenic action) and the tumor cells (direct anti-tumor action). Recent studies indicate that PEDF expression is significantly reduced in several tumor types, including breast cancer, and that its reduction is associated with disease progression and poor patient outcome. In the current study, we investigated the role of PEDF in the development of endocrine resistance in breast cancer.

Methods: PEDF mRNA and protein levels were measured in several endocrine-resistant breast cancer cell lines including MCF-7:5C, MCF-7:2A, and BT474 and in endocrine-sensitive cell lines MCF-7, T47D, and ZR-75-1 using real-time PCR and western blot analyses. Tissue microarray analysis and immunohistochemistry were used to assess the PEDF protein level in tamoxifen-resistant breast tumors versus primary tumors. Lentiviruses were used to stably express PEDF in endocrine-resistant breast cancer cell lines to determine their sensitivity to tamoxifen following PEDF re-expression.

Results: We found that PEDF mRNA and protein levels were dramatically reduced in endocrine-resistant MCF-7:5C, MCF-7:2A, and BT474 breast cancer cells compared with endocrine-sensitive MCF-7, T47D, and ZR-75-1 cells, and that loss of PEDF was associated with enhanced expression of $p^{Ser167}ER\alpha$ and the receptor tyrosine kinase rearranged during transfection (RET). Importantly, we found that silencing endogenous PEDF in tamoxifen-sensitive MCF-7 and T47D breast cancer cells conferred tamoxifen resistance whereas re-expression of PEDF in endocrine-resistant MCF-7:5C and MCF-7:2A cells restored their sensitivity to tamoxifen *in vitro* and *in vivo* through suppression of RET. Lastly, tissue microarray studies revealed that PEDF protein was reduced in ~52.4% of recurrence tumors (31 out of 59 samples) and loss of PEDF was associated with disease progression and poor patient outcome.

Conclusion: Overall, these findings suggest that PEDF silencing might be a novel mechanism for the development of endocrine resistance in breast cancer and that PEDF expression might be a predictive marker of endocrine sensitivity.

Introduction

The female hormone estrogen has long been recognized as being important for stimulating the growth of a large proportion of breast cancers. Estrogen action is mediated by two receptors; estrogen receptor (ER) alpha and ER beta. Approximately 70% of breast cancers express ERα [1,2], and its presence in breast tumors is routinely used to predict a response to endocrine therapy such as tamoxifen - an anti-estrogen that blocks estrogen-stimulated breast cancer cell growth - or aromatase inhibitors (AIs) - agents that suppress estrogen synthesis in the body. These agents are highly effective and are less toxic compared with chemotherapy, and are often offered to ER-positive breast cancer patients to sustain a better quality of life [3,4]. Despite the clinical benefits of tamoxifen and AIs, however, a large number of breast cancer

* Correspondence: joan.lewis@fccc.edu
[1]Cancer Biology Program, The Research Institute of Fox Chase Cancer Center, 333 Cottman Avenue, Philadelphia, PA 19111, USA
Full list of author information is available at the end of the article

patients develop drug resistance. It is estimated that ~40% of patients with early ER-positive breast cancer relapse within 15 years after adjuvant therapy with tamoxifen and 15% of patients treated with an AI relapse within 9 years [5-7]. These resistant tumors are usually more aggressive and are more likely to metastasize, which is often the leading cause of breast cancer-related death. There is strong evidence that endocrine resistance is associated with cross-talk between upstream kinases and ERα, resulting in estrogen-independent activation of the ERα; however, the exact mechanism by which breast cancer cells develop resistance to endocrine therapy is still not fully understood.

Pigment epithelium-derived factor (PEDF) is a 50 kDa glycoprotein that belongs to the non-inhibitory serine protease inhibitor superfamily but it does not inhibit proteases [8,9]. PEDF was first discovered as a factor secreted by retinal pigment epithelial cells [10], but was later found to be expressed in several tissues including the brain, spinal cord, eye, plasma, bone, prostate, pancreas, heart and lung [11]. PEDF is present in human blood at a concentration of approximately 100 nM (5 μg/ml) or twice the level required to inhibit aberrant blood-vessel growth in the eye [10]. PEDF possesses potent anti-angiogenic activity, far greater than any other known anti-angiogenic factor [12], and it has anti-tumor properties including the ability to promote tumor differentiation and initiate apoptosis [13-16]. In endothelial cells, PEDF has been shown to induce apoptosis by activating the Fas/Fas-L caspase-8 apoptotic pathway [17,18] and there is evidence that the p38 mitogen-activated protein kinase (MAPK) pathway is involved in the anti-angiogenic activity of PEDF [19]. More recently, a number of studies have reported that PEDF expression is significantly reduced in several tumor types, including prostate adenocarcinoma [20], pancreatic adenocarcinoma [21], glioblastoma [22], ovarian carcinoma [23], and breast cancer [24]. With regards to breast cancer, PEDF expression has been shown to be markedly reduced in breast tumors compared with normal tissue and this reduction is associated with disease progression and poor patient outcome [24,25]. At present, however, it is not known whether PEDF plays a role in the development of endocrine resistance.

In this study, we examined the role of PEDF in the development of endocrine resistance using several breast cancer cell lines. Specifically, we evaluated PEDF expression in endocrine-resistant MCF-7:5C, MCF-7:2A, and BT474 breast cancer cells versus endocrine-sensitive MCF-7, T47D, and ZR-75-1 cells and found that PEDF mRNA and protein levels were dramatically reduced in the endocrine-resistant breast cancer cell lines compared with the endocrine-sensitive cell lines. In addition, tissue microarray studies revealed that PEDF protein was significantly reduced in tamoxifen-resistant/recurrence tumors compared with primary tumors. We also found that re-expression of PEDF in endocrine-resistant MCF-7:5C and BT474 cells restored their sensitivity to tamoxifen, whereas siRNA knockdown of PEDF in MCF-7 and T47D cells markedly reduced their sensitivity to tamoxifen. Notably, re-expression of PEDF in endocrine-resistant MCF-7:5C cells resulted in a significant reduction in the level of p-ERα, p-AKT, and rearranged during transfection (RET) proteins, which were constitutively overexpressed in these cells. Lastly, we found that recombinant PEDF (rPEDF) dramatically reduced the tumor growth of MCF-7:5C xenographs in athymic mice and that re-expression of PEDF in MCF-7:5C cells partially restored tamoxifen sensitivity *in vivo*. Taken together, these findings suggest that PEDF silencing might be a novel mechanism for the development of endocrine resistance in breast cancer.

Materials and methods

Cell lines and culture conditions

The MCF-7 cells used in this study [26] were cloned from ERα-positive human MCF-7 breast cancer cells originally obtained from the American Type Culture Collection (Manassas, VA, USA). MCF-7 cells were maintained in full serum medium composed of RPMI-1640 medium, 10% fetal bovine serum, 2 mM glutamine, penicillin at 100 U/ml, streptomycin at 100 μg/ml, 1× nonessential amino acids (Invitrogen, Grand Island, NY, USA), and bovine insulin at 6 ng/ml (Sigma-Aldrich, St Louis, MO, USA). ER-positive MCF-7:5C [27,28] and MCF-7:2A [29,30] breast cancer cells were cloned from MCF-7 cells following long-term (> 12 months) culture in estrogen-free medium composed of phenol red-free RPMI, 10% fetal bovine serum treated three times with dextran-coated charcoal, 2 mM glutamine, bovine insulin at 6 ng/ml, penicillin at 100 U/ml, streptomycin at 100 μg/ml, and 1× nonessential amino acids. MCF-7:5C cells are resistant to AIs (that is, hormone independent) and tamoxifen, but these cells undergo apoptosis in the presence of physiologic concentrations of 17β-estradiol (E2), as previously reported [28]. MCF-7:2A cells are also resistant to AIs but only partially sensitive to tamoxifen, and these cells undergo apoptosis in the presence of E2 [29,31].

The human breast cancer cell line T47D:A18, referred to as T47D in this study, is a hormone-responsive clone of wild-type T47D that has been described previously [32]. These cells were maintained in phenol red-containing RPMI medium supplemented with 10% fetal bovine serum (FBS), bovine insulin (6 ng/ml), and antibiotics. ER-positive ZR-75-1 and BT474 breast cancer cells were obtained from the American Type Culture Collection and were maintained in phenol red-containing RPMI medium supplemented with 10% FBS, bovine insulin (6 ng/ml), and antibiotics. The BT474 cell line was isolated by Lasfargues

and Coutinho from a solid, invasive ductal carcinoma of the breast [33]. ER-negative MDA-MB-231 breast cancer cells were obtained from the American Type Culture Collection and were cultured in DMEM medium supplemented with 10% FBS and antibiotics.

MCF-7:5C cells stably expressing PEDF (5C-PEDF) were grown in phenol red-free RPMI 1640 medium supplemented with 10% phenol red-free RPMI, 10% fetal bovine serum treated three times with dextran-coated charcoal and 4 μg/ml blasticidin (InvivoGen, San Diego, CA, USA), and BT474 cells stably expressing PEDF (BT474-PEDF) were grown in RPMI medium supplemented with 10% FBS and 4 μg/ml blasticidin (InvivoGen, San Diego, CA, USA).

Cell proliferation assay

This procedure has been described previously [28,29,34]. Briefly, MCF-7 and T47D cells were grown in fully estrogenized medium. Cells were seeded in 24-well plates (30,000/well) and after overnight incubation were transfected with either control (nontarget) or PEDF siRNA. Transfected cells were treated with 10^{-6} M 4-hydroxytamoxifen (4OHT) after 48 hours, and then cells were harvested after 72 hours and total DNA was determined using a Fluorescent DNA Quantitation kit (Bio-Rad Laboratories, Hercules, CA, USA), as previously described [28]. Cell proliferation was also determined by cell counting using the trypan blue exclusion assay. MCF-7 and T47D cells were seeded in six-well plates (1×10^5/well) and then treated with 10^{-6} M 4OHT for 72 hours. The 4OHT used in the cell proliferation studies was purchased from Sigma-Aldrich.

We also performed proliferation studies using MCF-7:5C, BT474, 5C-PEDF, and BT474-PEDF cells. MCF-7:5C and 5C-PEDF cells were grown in non-estrogenized media, and BT474 and BT474-PEDF cells were grown in fully estrogenized media. For the DNA proliferation assay, cells were seeded at a density of 30,000/well in 24-well plates and after overnight incubation were treated with 10^{-12} M to 10^{-6} M 4OHT for 7 days with retreatment on alternate days. Cells were then harvested and total DNA quantitated using a Fluorescent DNA kit as described previously [28]. For cell counting, cells were seeded at 75,000/well in six-well plates and after overnight incubation were treated with 10^{-6} M 4OHT for 72 hours. Cells were then harvested and counted using trypan blue exclusion.

Western blot analysis

Immunoblotting was performed using 30 μg protein per well as described previously [28,35]. Membranes were probed with primary antibodies against PEDF (Chemicon Inc., Temecula, CA., USA), against ERα and phospho-Ser167-ERα (Santa Cruz Biotechnology, Inc., Santa Cruz, CA, USA), against RET, p-RET (Y1062), mammalian target of rapamycin (mTOR), p-mTOR and AKT, and against pAKT, MAPK, pMAPK and p70S6K (Cell Signaling Technology Inc., Danvers, MA, USA), and against β-actin (Sigma Chemical Co., St Louis, MO, USA). The appropriate secondary antibody conjugated to horseradish peroxidase (Santa Cruz Biotechnology) was used to visualize the stained bands with an enhanced chemiluminescence visualization kit (Amersham, Arlington Heights, IL, USA). Bands were quantitated by densitometry using the Molecular Dynamics Software ImageQuant (GE Healthcare Life Sciences, Piscataway, NJ, USA) and densitometric values were corrected for loading control.

Knockdown of PEDF and RET with small interference RNA

For the iRNA silencing experiments, PEDF, RET, and nontarget control siRNAs were purchased from Dharmacon Inc (Pittsburg, PA, USA). For transfection, 100 nM siRNAs were combined with siRNA transfection reagent according to the manufacturer's instructions. Cells were seeded in 24-well plates at a density of 0.5×10^5 cells/well in antibiotics-free medium 12 hours before the transfection. One and a half microliters of the siRNA (20 μM) were mixed with 1 μl transfection reagent in 50 μl serum-free RPMI-1640 medium and were incubated at room temperature for 25 minutes to form a complex. After washing cells with PBS, the 50 μl transfection mixtures were added to each well with 450 μl RPMI-1640 medium containing 10% FBS at a final concentration of 100 nM siRNA. Twenty-four hours after the transfection, the medium was replaced with fresh 500 μl RPMI-1640 medium containing 10% FBS. Transfected cells were then harvested for western blotting and RT-PCR or subsequently treated with 10^{-9} M to 10^{-6} M 4OHT for 3 days to determine cell growth.

RNA isolation and RT-PCR analysis

Total RNA was isolated from cultured cells using the TRIzol reagent (Invitrogen) according to the manufacturer's procedure. First-strand cDNA synthesis was performed from 2.5 μg total RNA using Super-Script Reverse Transcriptase (Invitrogen). cDNA was amplified in a 15-μl PCR mixture containing 1 mm dNTPs, 1× PCR buffer, 2.5 mm $MgCl_2$, and 1 U DNA *Taq* polymerase (Promega, Madison, WI, USA) with 25 pmol of primers specific for human *PEDF* (sense, 5'-CATTCACCGGGCTCTCTAC-3'; antisense, 5'-GGCAGCTGGGCAATCTTGCA-3') and human *RET* (sense, 5'-GGATTTCGGCTTGTCCCGAG-3'; antisense, 5'-CCATGTGGAAGG GAGGGCTC-3'). The conditions in the logarithmic phase of PCR amplification were as follows: 5 minutes initial denaturation at 94°C, 1 minute denaturation at 94°C, 35 seconds annealing at 67°C, and 1.5 minute extension at 72°C for 30 cycles. The number of amplification cycles during which PCR product formation was limited by the template concentration

was determined in pilot experiments. *PUM1* was used as the internal control (sense, 5'-TCACCGAGGCCCCTCT-GAACCCTA-3'; antisense, 5'-GGCAGTAATC TCCTTCT GCATCCT-3').

The reproducibility of the quantitative measurements was evaluated by three independent cDNA syntheses and PCR amplification from each preparation of RNA. Densitometric analysis was performed using Scion Image software (Scion Corp., Frederick, MD, USA), and the relative *PEDF* or *RET* mRNA expression levels were determined as the ratio of the signal intensity of PEDF to that of *PUM1*.

Estrogen response element luciferase assay

To determine ERα transcriptional activity, cells were transfected with an estrogen response element (ERE)-regulated (pERE(5×)TA-ffLuc plus pTA-srLuc) dual-luciferase reporter gene set. pERE(5×)-ffLuc contained five copies of a consensus ERE and a TATA-box driving firefly luciferase; pTATA-srLuc contained a TATA-box element driving renilla luciferase. Cells were grown in the estrogen-free medium containing no exogenous compounds for 2 days before transfection. All transfection experiments were carried-out using LT1 (Mirus Bio LLC, Madison, WI, USA) at a 1:3 ratio of micrograms of plasmid to micoliters of LT1. In the ERE reporter gene experiment, the cells were treated as indicated 24 hours following the transfection. Forty-eight hours following the ERE transfection, the cells were harvested and processed for dual-luciferase reporter activity (Promega, Madison, WI, USA), in which the firefly luciferase activity was normalized by renilla luciferase activity.

Breast cancer tissue microarray and immunohistochemistry

Paraffin-embedded de-identified human breast cancer tissue samples were collected from the Tumor Bank facility at the Fox Chase Cancer Center and the protocols were reviewed and approved by the Institutional Review Board at our institution. The archived tumor samples were obtained from patients who were initially treated with tamoxifen and either responded (n = 150) or responded but then developed recurrence disease (n = 59) with an average time to disease progression of 93 months. Patients provided written informed consent for the use of their tumor samples.

Tissue microarray slides were constructed from 59 matching primary and recurrence tumors using duplicate cores of 0.6 mm per tumor sample. Tissue microarray slides were also created using endocrine-responsive tumors. For PEDF and ERα immunohistochemistry, sections were incubated at room temperature for 20 minutes with anti-PEDF or anti-ERα antibody (Chemicon Inc.) applied at 1:100 dilution in antibody diluent (Dako USA, Carpinteria, CA, USA). A secondary anti-mouse antibody polymer conjugated with horseradish peroxidase (Dako USA) was applied for 30 minutes and 3,3'-diaminobenzidine was used to produce visible, localized staining viewable with light microscopy. Sections without primary antibody served as negative controls. Normal breast tissue from archival specimens was used as positive controls for PEDF and ERα expression. A semi-automated quantitative image analysis system (ACIS II; ChromaVision Medical Systems, Inc., San Juan Capistrano, CA, USA) was used to quantitate the staining of the tissue microarray slides. For immunohistochemical analysis, the brown stain intensity of the chromogen was compared with the blue counterstain used as background. Staining for PEDF was quantified as an intensity score (scale 0 to 255) and staining for ERα was graded as follows: 0, negative (no cells stained); 1, weakly positive (< 10% of cells stained); 2, moderately positive (10 to 50% of cells stained); or 3, strongly positive (> 50% cells stained).

TUNEL staining for apoptosis

Apoptosis was determined by the terminal deoxynucleotidyl transferase-mediated dUTP nick end-labeling (TUNEL) assay using an *in situ* cell death detection kit (POD; Roche Molecular Biochemicals, Branchburg, NJ, USA), according to the manufacturer's instructions. Briefly, fixed cells were washed, permeabilized, and then incubated with 50 μl terminal deoxynucleotidyl transferase end-labeling cocktail for 60 minutes at 37°C in a humidified atmosphere in the dark. For signal conversion, slides were incubated with 50 μl converter-POD (anti-fluorescein antibody conjugated with horseradish peroxidase) for 30 minutes at 37°C, rinsed with PBS, and then incubated with 50 μl of 3,3'-diaminobenzidine substrate solution for 10 minutes at 25°C. The slides were then rinsed with PBS, mounted under glass coverslips, and analyzed under a light microscope (Inverted Nikon TE300; Melville, NY, USA).

Lentiviral vector design, production, and transduction

For PEDF overexpression, we generated a lentiviral construct encoding the full-length human PEDF cDNA inserted between *Xba*I and *Bam*HI sites of the prrl.CMV.EGFP.wpre.SIN lentiviral vector. Briefly, PEDF cDNA was amplified by PCR from pCEP4-PEDF plasmid (a gift from Dr Bouck, Northwestern University, Chicago, IL, USA); *Xba*I and *Xba*I + *Eco*RV sites were added to the 5' and 3' ends, respectively, using primers 5'-CTAGTCTAGAG GCCCCAGGATGCAGGC CCTG-3' and 5'-GGCCTC TAGATATCTTAGGGGCCCCTGGGGTCCAG-3'. This fragment was then subcloned into TA cloning vector (Invitrogen, San Diego, CA, USA), digested with *Eco*RV and *Xba*I and re-cloned in the prrl.CMV.EGFP.wpre.SIN plasmid digested with *Xba*I and *Bam*HI. To produce

lentiviral stock, 293FT cells (Invitrogen) were plated in 10-cm tissue culture plates. When the cells were 90 to 95% confluent, the complete culture medium was removed and the cells were exposed to 5 ml medium (Opti-MEM I; Invitrogen) with complexes (DNA-Lipofectamine 2000; Invitrogen) containing 9 μg packaging mix (ViralPower; Invitrogen), 3 μg expression plasmid DNA (prrl.CMV.EGFP.wpre.SIN/PEDF), or control plasmid DNA (prrl.CMV.EGFP.wpre.SIN/LacZ) with lipofectamine (Lipofectamine 2000; Invitrogen). Hexadimethrine bromide (Polybrene; Sigma-Aldrich) was added at the final concentration of 10 μg/ml. After incubation for 24 hours, the infection medium was replaced with complete culture medium. Lentivirus-containing supernatants were harvested 72 hours after transfection. The supernatants were centrifuged to remove pellet debris and stored at -80°C.

For lentiviral vector transduction, MCF-7:5C and BT474 cells were plated in six-well plates. When the cells reached 30 to 50% confluence, media were changed to either phenol red-free RPMI medium with 10% charcoal-stripped FBS without antibiotic (MCF-7:5C cells) or complete growth medium without antibiotic (BT474 cells) with the lentiviral stock, and 10 μg/ml hexadimethrine bromide (Polybrene; Sigma-Aldrich) was added to improve lentiviral vector transduction. Lentiviral vector expressing lacZ served as a positive control. After overnight incubation at 37°C in 5% CO_2, the media-containing virus was removed and replaced with 2 ml complete culture media. After incubation overnight at 37°C in 5% CO_2, media were changed to phenol red-free RPMI medium with 10% charcoal-stripped FBS without antibiotic or respective media with 4 μg/ml blasticidin (InvivoGen). Transduced cell clones were then selected with antibiotic for 2 weeks. PEDF expression was verified by quantitative real-time RT-PCR and western blot analysis in MCF-7:5C and BT474 cells.

Animal studies

The mammary fat pads of 6-week-old to 8-week-old ovariectomized outbred athymic mice (Taconic, Upstate, NY, USA) were bilaterally inoculated with 5×10^6 MCF-7:5C cells suspended in 0.1 ml sterile PBS solution as described previously [28]. When tumors reached a mean cross-sectional area of 0.1 cm^2, the mice were randomized into groups of 10 and were treated with sterile PBS (100 μl) or 4 mg/kg rPEDF that was administered by intraperitoneal injection for a total of 30 days. Mice were injected every 2 days and tumors were measured every 5 days with vernier calipers. The mean cross-sectional tumor area was calculated by multiplying the length (l) by the width (w) by π and dividing the product by four (that is, $lw\pi/4$). The mean cross-sectional tumor area was plotted against time in days to monitor tumor growth. The mice were sacrificed by CO_2 inhalation and cervical dislocation; tumors were excised and immediately fixed in 10% buffered formalin for immunohistochemistry or snap-frozen in liquid nitrogen. Frozen tumor specimens were stored at -80°C for further analysis.

In another experiment, a total of 96 ovariectomized outbred athymic mice, 6 to 8 weeks old, were bilaterally inoculated with 5×10^6 MCF-7, BT474, or MCF-7:5C breast cancer cells suspended in 0.1 ml sterile PBS. Mice injected with MCF-7 (n = 32) or BT474 cells (n = 32) were simultaneously treated with E2 to stimulate tumor growth. E2 was administered via 0.3 cm long silastic capsules (Innovative Research, Sarasota, FL, USA) that were implanted subcutaneously between the scapules. The capsules remained in place for the duration of the study (3 to 6 weeks). Mice injected with MCF-7:5C cells (n = 32), however, did not require treatment with E2 because these cells are estrogen independent and are capable of forming tumors in the absence of E2, as reported previously [28]. When the mean tumor cross-sectional area reached approximately 0.3 cm^2 for MCF-7 and BT474-injected mice and 0.2 cm^2 for MCF-7:5C-injected mice, groups of eight mice were randomly assigned to the following treatments: PBS alone (control), rPEDF, tamoxifen, or tamoxifen plus rPEDF. Tamoxifen was administered orally by gavage at 1.5 mg/day per mouse for 5 days/week for 21 days and rPEDF was administered by intraperitoneal injection at 4 mg/kg every 2 days for 21 days. Tumors were measured weekly with vernier calipers. The mean cross-sectional tumor area was calculated by multiplying the length (l) by the width (w) and by π and dividing by 4 (that is, $lw\pi/4$).

All animal experiments were carried out according to the guidelines of the American Association for Laboratory Animal Science as an approved protocol by the Institutional Animal Care and Use Committee at the Institute for Cancer Research-Fox Chase Cancer Center.

Microvessel density assay

Frozen tissues were cut into 10-μm sections, fixed in acetone at 4°C for 5 minutes, and blocked for endogenous peroxidase. Sections were treated with normal serum for 10 minutes. Tumor sections were incubated with the rat monoclonal antibody against mouse CD34 (BD Pharmingen, San Diego, CA, USA) at 1:100 dilutions at 4°C. After rinsing with PBS, sections were incubated with biotinylated rabbit antigoat immunoglobulins (Dako, Glostrup, Denmark) at 1:1,000 dilutions for 30 minutes at room temperature followed by incubation with horseradish peroxidase-labeled streptavidin-biotin complex for 30 minutes. The peroxidase reaction was visualized using diaminobenzidine. The tumor microvessel density was quantified as tumor vasculature. In negative-control staining, the primary antibodies were omitted.

Statistical analysis

All *in vitro* experiments were repeated at least twice in either duplicate or triplicate with different cell preparations to ensure consistency of the findings. One-factor analysis of variance was used to demonstrate that there were significant differences between conditions when there were more than two conditions, and paired analyses were performed using either Student's *t* test or the Mann-Whitney test (GraphPad Software, San Diego, CA, USA) in order to identify the conditions that were significantly different. For *in vivo* studies, tumor growth curves were analyzed longitudinally using a two-factor analysis of variance comparing tumor cross-sectional areas within treatments in a time-dependent manner. Tumor growth curves represent the mean ± standard error of tumor cross-sectional areas. $P < 0.05$ was considered statistically significant.

Results

PEDF expression is dramatically reduced in endocrine-resistant breast cancer cells

To determine whether there is an association between PEDF expression and endocrine resistance, we first examined PEDF expression in a panel of breast cancer cell lines using western blot and real-time PCR analyses. We found that PEDF protein (Figure 1a) and mRNA (Figure 1b) levels were dramatically reduced in endocrine-resistant MCF-7:5C, MCF-7:2A, and BT474 breast cancer cells compared with endocrine-sensitive MCF-7, T47D, and ZR-75-1 cells with no PEDF observed in ER-negative MDA-MB-231 cells. A similar trend was observed when the media conditioned by these cells were tested for PEDF expression. As shown in Figure 1c, endocrine-sensitive T47D, ZR-75-1 and, to a lesser extent, MCF-7 cells secreted the most PEDF, whereas endocrine-resistant MCF-7:5C, MCF-7:2A, and BT474 cells secreted markedly less to no detectable level of PEDF. Interestingly, we found that tamoxifen-resistant BT474 cells expressed a level of PEDF almost comparable with that of MCF-7 cells whereas AI-resistant MCF-7:5C and MCF-7:2A cells expressed very little to no PEDF. We should note that there are differences between BT474 cells and long-term estrogen-deprived MCF-7:5C and MCF-7:2A cells. Specifically, BT474 cells overexpress HER2 and the ER coactivator AIB1, which contribute to tamoxifen resistance in these cells [36], whereas MCF-7:5C and MCF-7:2A cells express low levels of HER2 and AIB1 but high levels of phospho-Akt and ERα, which are thought to contribute to the AI-resistant and tamoxifen-resistant phenotype of these cells. Tamoxifen resistance has been studied by several groups [37,38] and is believed to be due primarily to crosstalk between ER and HER2. This crosstalk leads to enhanced cell survival pathways via phosphoinositide 3-kinase (PI3K)/AKT activation in addition to activation of various MAPKs that mediate transcriptional effects resulting in cell proliferation. In contrast, studies using long-term estrogen-deprived breast cancer cells have shown that AI resistance is controlled by several signaling pathways including the P13K/AKT pathway, the insulin-like growth factor receptor (IGF-1R) pathway, and the HER2 pathway [39-41]. In addition, we have previously shown that AI-resistant MCF-7:5C and MCF-7:2A cells undergo apoptosis in the presence of physiological concentrations of E2 [28,29,42]. The differences in PEDF expression between BT474, MCF-7:5C, and MCF-7:2A cells might possibly be influenced by the different signaling pathways that control the resistant phenotype of these cells.

The ERα protein level was also examined in the different cell lines to assess whether there was a correlation between ERα status and PEDF expression. Figure 1a showed that ERα protein was expressed in all of the cell lines except for MDA-MB-231 cells, which are ERα-negative; however, ERα was significantly elevated in endocrine-resistant MCF-7:5C, MCF-7:2A, and BT474 cells compared with endocrine-sensitive MCF-7, T47D, and ZR-75-1 cells. In addition, we found that E2 treatment markedly reduced the PEDF protein level in MCF-7 and T47D cells whereas 4OHT, the active metabolite of tamoxifen, significantly increased the PEDF protein level in both cell lines (Figure 1d). A similar trend was observed for ERα regulation by E2 and 4OHT in MCF-7 and T47D cells (Figure 1d). Overall, these data show that PEDF expression is significantly reduced in endocrine-resistant breast cancer cells compared with endocrine-sensitive cells and that its expression is differentially regulated by estrogen and anti-estrogen in hormone-dependent breast cancer cells. No significant correlation, however, was observed between PEDF expression and total ERα status.

PEDF expression is dramatically reduced in endocrine-resistant breast tumors

Since PEDF expression was dramatically reduced in endocrine-resistant breast cancer cells, we next determined whether there was a clinical correlation between PEDF expression and the development of endocrine resistance in breast tumors. PEDF expression was examined in primary versus recurrence tumors. A total of 209 breast cancer patients were initially treated with tamoxifen and responded; however, 59 patients developed recurrence disease with an average time to disease progression of 93 months. Immunohistochemical staining was performed on tissue microarrays constructed using recurrence breast tumor tissues ($n = 59$) versus matched primary breast tumor tissues ($n = 59$). Figure 2a shows that PEDF protein was dramatically reduced in the recurrence breast cancer tissue (right panel) compared with the primary breast cancer tissue (middle panel) and the normal breast tissue

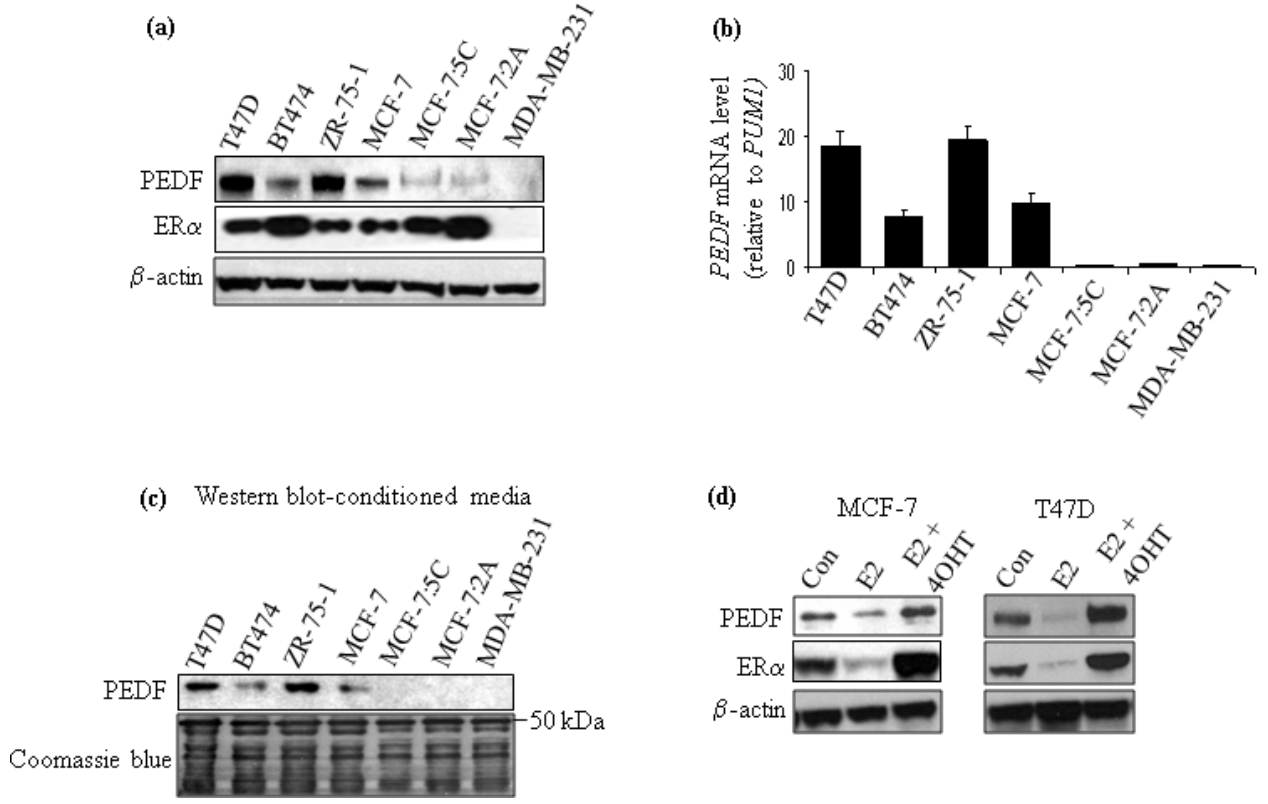

Figure 1 Pigment epithelium-derived factor expression in human breast cancer cell lines. **(a)** Pigment epithelium-derived factor (PEDF) and estrogen receptor alpha (ERα) protein levels were detected by western blot analysis in several human breast cancer cell lines, including hormone-dependent T47D, MCF-7, and ZR-75-1 cells, tamoxifen-resistant BT474 cells, tamoxifen-resistant and aromatase inhibitor-resistant MCF-7:5C and MCF-7:2A cells, and ER-negative MDA-MB-231 cells. **(b)** *PEDF* mRNA expression level in the different breast cancer cell lines was determined by quantitative real-time PCR analysis with *PUM1* used as a normalization control. **(c)** Conditioned media were analyzed by western blot for the presence of PEDF protein in the indicated breast cancer cell lines. Staining of proteins by Coomassie blue included as a loading control. **(d)** Hormonal regulation of PEDF and ERα protein in MCF-7 and T47D breast cancer cells. Cells were incubated in phenol red-free RPMI media supplemented with 10% charcoal-stripped FBS for 72 hours and, subsequently, were treated with vehicle, 1 nM 17β-estradiol (E2), or 1 nM E2 + 1 μM 4-hydroxytamoxifen (4OHT) for 24 hours, and the PEDF and ERα protein level was determined by western blot analysis. β-actin was used as a normalization control. All experiments were performed in triplicate independently.

(left panel). In particular, we found in the normal breast tissue and to a lesser extent in the primary breast cancer tissue that mammary epithelial cells displayed an intense and widespread staining for PEDF. All of the normal breast tissue stained positive for PEDF, whereas 68% of primary tumors were PEDF-positive and 32.2% were PEDF-negative. In contrast, we found that 47.6% of recurrence tumors were PEDF-positive and 52.4% (31 out of 59) of recurrence tumors were PEDF-negative (Table 1). The number of recurrence tumors that were PEDF-negative was statistically significantly different from the number of primary tumors that were PEDF-negative ($P < 0.000001$) (Table 1). We also examined PEDF expression in endocrine-responsive tumors ($n = 150$) to assess whether PEDF expression correlated with response to endocrine therapy. We found that ~83.3% of endocrine-responsive tumors were PEDF-positive and 16.7% were PEDF-negative, which was significantly different from the number of recurrence tumors that were PEDF-negative ($P < 0.000001$) or PEDF-positive ($P < 0.00008$) (Table 1). Overall, these data show that patients who had the worst response to endocrine therapy (defined as progressive disease) had significantly lower PEDF expression than those who had the best response to endocrine therapy (defined as complete response) and that poor clinical response to endocrine therapy is associated with PEDF deficiency in primary breast carcinomas. Notably, Cai and colleagues previously reported that PEDF expression was significantly reduced in breast cancer tissues compared with normal breast tissue [24]; however, these investigators did not examine whether PEDF expression correlated with response to endocrine therapy or acquired resistance.

Since loss of ERα has been shown to be associated with the development of endocrine resistance in breast cancer, we assessed ERα status in the primary tumors versus the recurrence tumors using immunohistochemistry. We

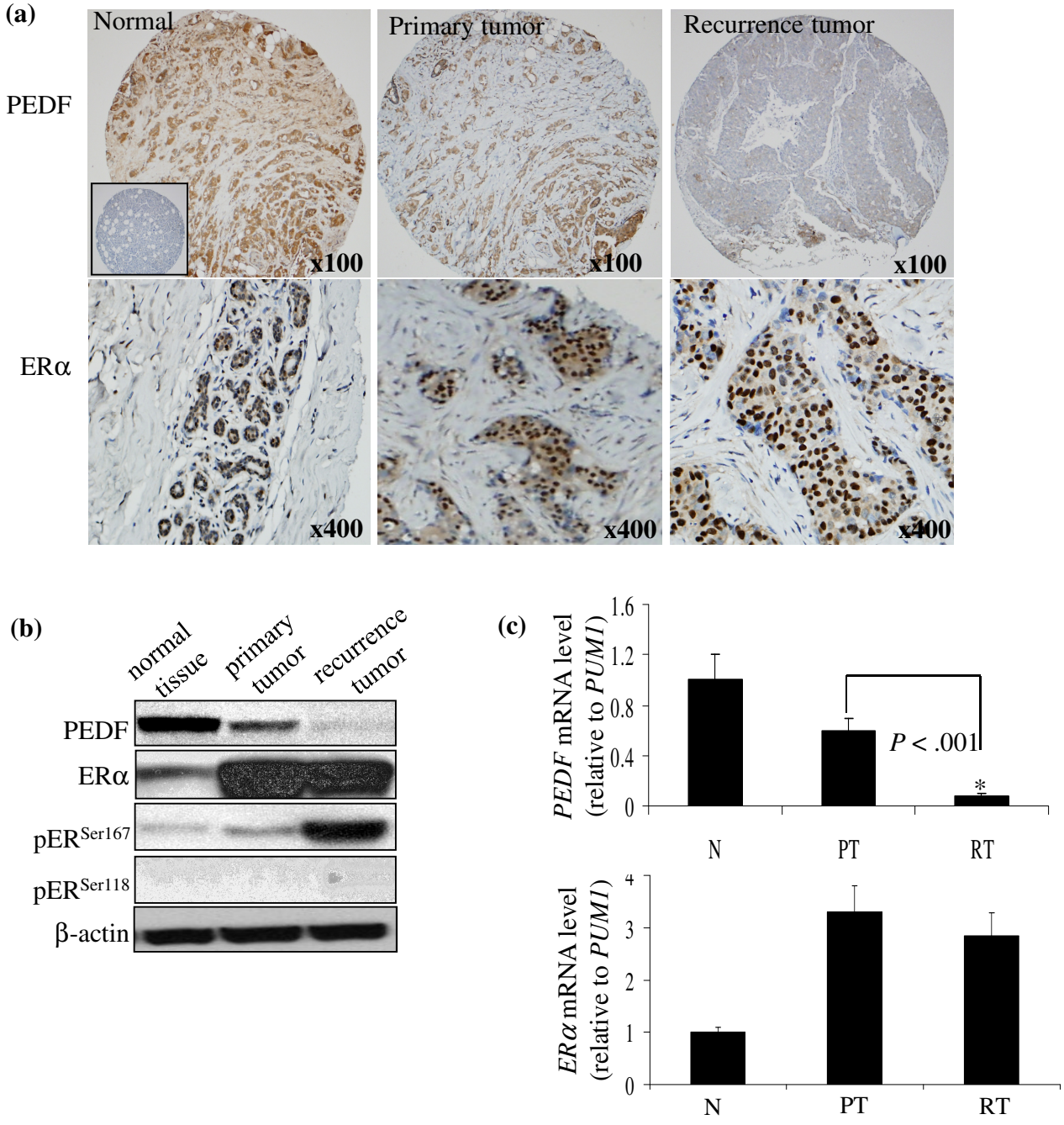

Figure 2 Pigment epithelium-derived factor expression in primary and recurrence breast tumor tissues. **(a)** Immunohistochemistry (IHC) staining for pigment epithelium-derived factor (PEDF) and estrogen receptor alpha (ERα) were performed on tissue microarrays generated from normal breast tissue (left panel), primary breast tumor tissue (n = 59; middle panel), and recurrence breast tumor tissue (n = 59; right panel). Cores used to generate tissue microarrays (TMAs) were 0.6 mm in diameter. Tumor tissues were also stained in the absence of a PEDF antibody to act as a negative control (left panel, inset). PEDF staining was quantified as an intensity score ranging from 0 to 255. A scale of 0 to 3 was used to score staining intensity of ERα. **(b)** Western blot analysis of normal tissue (N), primary breast tumor tissue (PT), or recurrence tumor tissue (RT) to assess PEDF, total ERα, and phosphorylated ERα (Ser118 and Ser167) protein level. β-actin was used as a loading control. **(c)** Representative quantitative real-time PCR analysis of *PEDF* and *ERα* mRNA expression in N, PT, or RT. For experiment, total RNA was extracted from paraffin-embedded tissues using Trizol and analyzed by real-time PCR as described in Materials and methods. *PEDF* and *ERα* mRNA were normalized to the internal control gene *PUM1*. All experiments were performed in triplicate. PEDF mRNA level was statistically significantly lower in the recurrence tumor tissue compared with the primary tumor tissue. *P < 0.001.

Table 1 Pigment epithelium-derived factor expression in normal versus breast tumor tissue samples

Tissue sample	*n*	PEDF status	Intensity score
Recurrence tumors	28 (47.6%)[a]	Positive	> 150
	31 (52.4%)[b]	Negative	≤ 25
Primary tumors	40 (67.8%)[a]	Positive	> 150
	19 (32.2%)[b]	Negative	≤ 25
Endocrine-responsive tumors	125 (83.3%)[c]	Positive	> 150
	25 (16.7%)[d]	Negative	≤ 25
Normal tissue	5 (100%)	Positive	≥ 200
	0 (0%)	Negative	≤ 25

A total of 209 breast cancer patients were initially treated with tamoxifen and 59 patients developed recurrence disease after a mean follow-up of 93 months. Immunohistochemistry (IHC) staining was performed on tissue microarrays (TMAs) constructed from recurrence breast tumors (n = 59) and matched primary breast tumors (n = 59). Normal background breast tissue was also used for comparison. TMAs were also constructed from endocrine-responsive tumor tissues (n = 150). A semi-automated quantitative image analysis system (ACIS II) was used to quantitate the staining of the TMA slides. For IHC analysis, pigment epithelium-derived factor (PEDF) staining was quantified as an intensity score (scale 0 to 255). [a]$P < 0.00003$, number of PEDF-positive recurrence tumors versus PEDF-positive primary tumors. [b]$P < 0.000001$, number of PEDF-negative recurrence tumors versus PEDF-negative primary tumors. [c]$P < 0.00008$, number of PEDF-positive recurrence tumors versus PEDF-positive endocrine-responsive tumors. [d]$P < 0.000001$, number of PEDF-negative recurrence tumors versus PEDF-negative endocrine-responsive tumors.

found that ERα protein was expressed at high levels (+3) in both the primary and the recurrence tumors and that there was no significant difference in ERα expression between the primary versus the recurrence tumors (Figure 2a). Western blot and real-time PCR analyses were also performed on the primary and recurrence breast tumor tissues to determine PEDF and ERα protein and the mRNA status. Figure 2b shows that the PEDF protein level was markedly reduced in the recurrence tumors compared with the primary tumors; however, the total ERα protein level was similar between the two groups with a similar trend observed for PEDF mRNA and ERα mRNA (Figure 2c). We should note that while the total ERα expression level was similar in the primary tumors versus the recurrence tumors, p^{ser167}ER protein was markedly elevated in the recurrence tumors versus the primary tumors.

PEDF silencing confers resistance to tamoxifen in breast cancer cells and its stable expression sensitizes resistant cells to endocrine therapy

To establish a causal connection between PEDF expression and endocrine resistance, we explored the functional consequences of PEDF silencing on tamoxifen sensitivity in endocrine-sensitive MCF-7 and T47D breast cancer cells. Cells were transiently transfected with either PEDF siRNA or nontarget control siRNA for 72 hours and PEDF silencing was quantified by western blot and quantitative RT-PCR analyses. As shown in Figure 3a (top panel), PEDF siRNA dramatically reduced PEDF protein and mRNA levels in both MCF-7 and T47D cells compared with the nontarget control siRNA. PEDF knockdown cells were then treated with 1 μM 4OHT, the active metabolite of tamoxifen, and cell growth was determined after 72 hours using a DNA proliferation assay kit. As shown in Figure 3a (middle panel), PEDF silencing significantly (P < 0.01) reduced the sensitivity of MCF-7 and T47D cells to 4OHT compared with cells transfected with the nontarget control siRNA. Specifically, we found that 1 μM 4OHT inhibited the growth of MCF-7 and T47D cells transfected with the nontarget control siRNA by 92% and 87%, respectively, whereas 4OHT reduced the growth in PEDF-knockdown MCF-7 and T47D cells by 45.6% and 54%, respectively. PEDF-knockdown MCF-7 and T47D cells were also treated with 1 μM 4OHT for 72 hours and cell proliferation was determined by counting viable cells using trypan blue exclusion. Figure 3a (bottom panel) showed that 4OHT reduced the proliferation of MCF-7 and T47D cells transfected with the control siRNA by ~85 to 90%; however, in the PEDF knockdown cells, the ability of 4OHT to inhibit proliferation was significantly reduced compared with 4OHT-treated cells transfected with the control siRNA (P < 0.01).

Since MCF-7:5C and BT474 breast cancer cells are resistant to tamoxifen and they express low levels of PEDF, we next examined whether stable expression of PEDF in these cells would sensitize them to the inhibitory effects of tamoxifen. We used a lentiviral construct encoding the full-length human PEDF cDNA to stably express PEDF in MCF-7:5C and BT474 cells. The efficiency of PEDF lentiviral transduction of MCF-7:5C and BT474 cells was confirmed by western blot analysis. As shown in Figure 3b (top panel), PEDF expression was very high in the lentiviral transduced cells, 5C-PEDF and BT474-PEDF, compared with the untransduced cells, MCF-7:5C and BT474. Following confirmation of PEDF overexpression, transduced 5C-PEDF and BT474-PEDF cells were treated with 10^{-12} to 10^{-6} M of 4OHT for 7 days and cell growth was determined using a DNA quantitation assay. As shown in Figure 3b (middle panel), 4OHT treatment reduced the growth of transduced 5C-PEDF and BT474-PEDF cells in a dose-dependent manner with maximum inhibition at 100 nM compared with

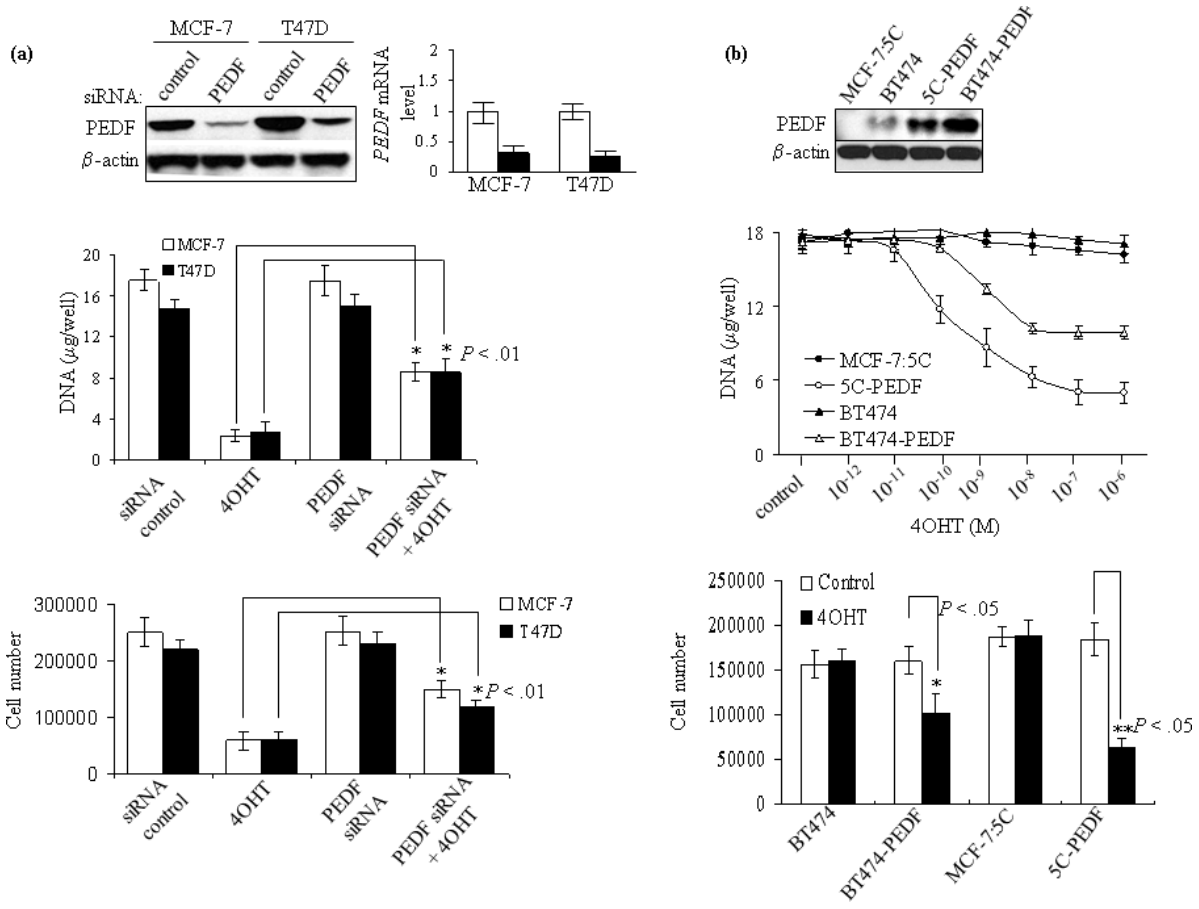

Figure 3 Knockdown of pigment epithelium-derived factor expression by siRNA reduces tamoxifen sensitivity in breast cancer cells. **(a)** siRNA-mediated reduction of pigment epithelium-derived factor (PEDF) expression in MCF-7 and T47D breast cancer cells was performed as described in Materials and methods. Cells were transfected with PEDF or control siRNA for 72 hours and PEDF protein and mRNA levels were determined by western blot and real-time PCR analyses. Transfected cells were also treated with 1 μM 4-hydroxytamoxifen (4OHT) for 72 hours and cell proliferation was determined by DNA quantitation assay and by cell counting using trypan blue exclusion. All experimental points are given as the average of triplicates. **(b)** Stable expression of PEDF in endocrine-resistant MCF-7:5C and BT474 breast cancer cells sensitized them to tamoxifen. A lentiviral construct encoding the human PEDF cDNA was used to stably express PEDF in MCF-7:5C and BT474 cells. Western blot analysis was used to confirm stable expression of PEDF protein in MCF-7:5C and BT474 cells (top panel). To determine the effect of PEDF expression on tamoxifen sensitivity, lentiviral transduced 5C-PEDF and BT474-PEDF cells were treated with 10^{-12} M to 10^{-6} M 4OHT for 72 hours and cell proliferation was determined by DNA quantitation assay (middle panel) and by cell counting using trypan blue exclusion (bottom panel). All experimental points are given as the average of triplicates. Assays were performed twice.

untransduced MCF-7:5C and BT474 cells that showed no response to 4OHT at any of the concentrations tested. We confirmed that the inhibitory effect of 4OHT in 5C-PEDF and BT474-PEDF cells was due to a reduction in cell proliferation/viability as determined by trypan blue exclusion and that the re-expression of PEDF in MCF-7:5C and BT474 cells significantly ($P < 0.05$) enhanced their sensitivity to 4OHT compared with the untransduced cells (Figure 3b, bottom panel).

Effect of PEDF expression on ERα signaling in endocrine-resistant MCF-7:5C cells

Since our tissue microarray data showed increased expression of p^{Ser167}ERα in endocrine-resistant tumors that expressed low levels of PEDF, we examined the effect of PEDF re-expression on ERα signaling in endocrine-resistant MCF-7:5C cells that are PEDF-negative. We found that stable expression of PEDF in MCF-7:5C cells (5C-PEDF) dramatically reduced the protein levels of ERα, p^{Ser167}ERα, pAKT, and the proto-oncogenic receptor tyrosine kinase RET, which were constitutively elevated in the untransduced MCF-7:5C cells but not parental MCF-7 cells (Figure 4a). Furthermore, we found that treatment of MCF-7:5C cells with 100 nM rPEDF markedly reduced the phosphorylation level of ERα and RET protein in these cells (Figure 4b) and it significantly reduced ERα transcriptional activity in these cells (Figure 4c). In particular, we found that basal

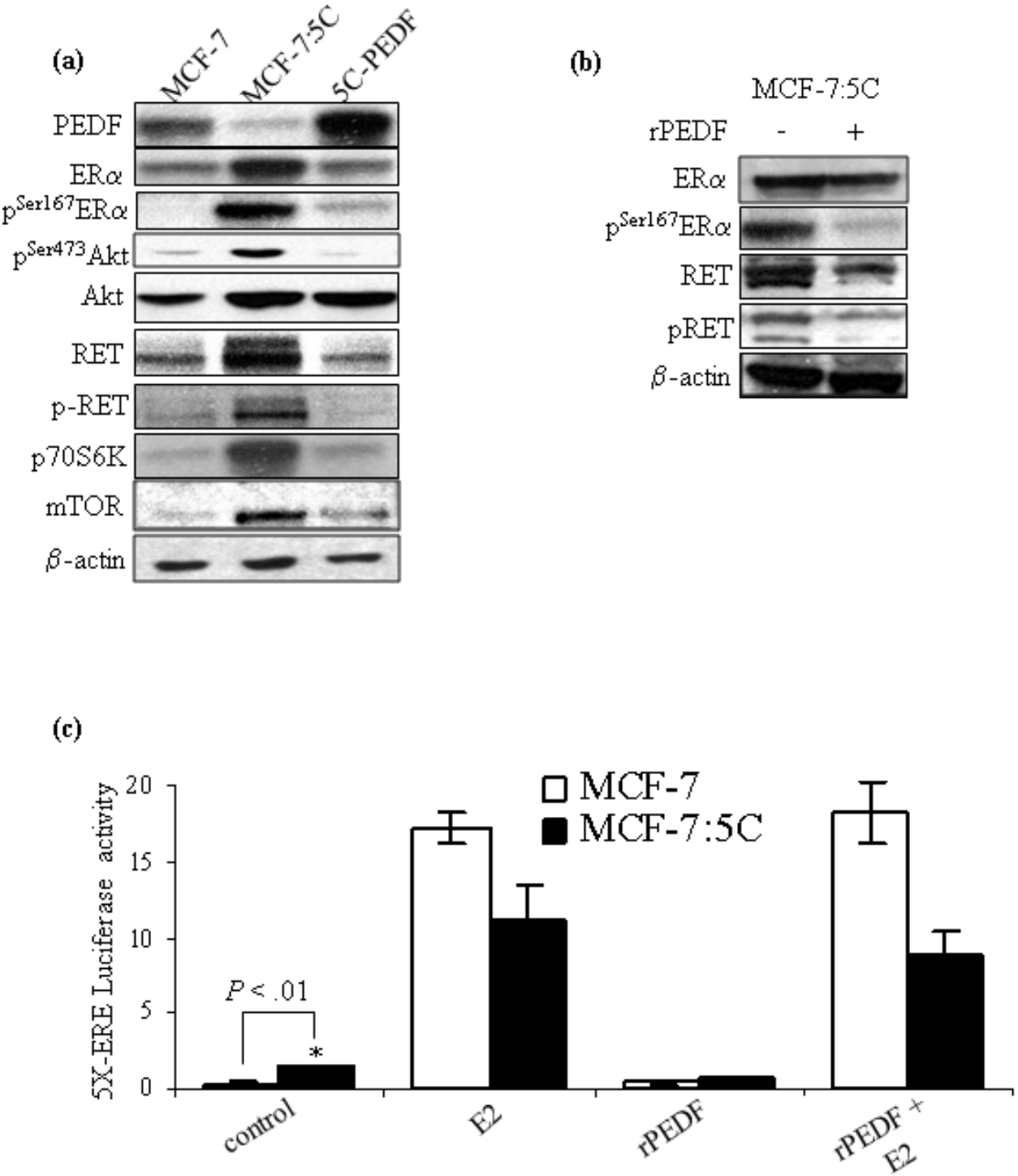

Figure 4 Effect of recombinant pigment epithelium-derived factor on the estrogen receptor alpha signaling pathway. **(a)** Western blot analysis of pigment epithelium-derived factor (PEDF), estrogen receptor alpha (ERα), phospho-ER, phospho-Akt, mitogen-activated protein kinase (MAPK), phospho-MAPK, rearranged during transfection (RET), pRET, p70S6K, and mammalian target of rapamycin (mTOR) protein expression in MCF-7, MCF-7:5C, and 5C-PEDF cells. **(b)** Effect of recombinant PEDF on ERα, pERα, RET, and pRET (Y1062) protein expression in MCF-7:5C cells. Cells were treated with 100 nM recombinant PEDF (rPEDF) protein for 24 hours and cell lysates were analyzed by western blot. β-actin was used as a loading control. **(c)** Effect of rPEDF on estrogen response element (ERE) luciferase activity in MCF-7 and MCF-7:5C cells. MCF-7 and MCF-7:5C cells were grown in estrogen-free RPMI media and then co-transfected with a 5× ERE luciferase plasmid and a renilla reporter plasmid for 24 hours. Following transfection, cells were treated with 1 nM 17β-estradiol (E2), 100 nM rPEDF, or E2 + rPEDF for 24 hours and luciferase activity was measured. Values presented as relative luciferase activity after normalization to *Renilla* luciferase activity. Data expressed as mean ± standard deviation of the results obtained from triplicate experiments. Basal ERE activity was statistically significantly higher in MCF-7:5C cells compared with MCF-7 cells. *$P < 0.01$.

ERE luciferase activity was significantly higher (~3.3-fold) in endocrine-resistant MCF-7:5C cells compared with endocrine-sensitive MCF-7 cells and treatment with rPEDF completely suppressed the basal ERE activity in MCF-7:5C cells and it significantly reduced E2-induced ERE activity in these cells (Figure 4c). Noteworthy is that pAKT and RET are known to enhance phosphorylation of ERα at Ser118 and Ser167, which is associated with increased ERα transcriptional activity and tamoxifen resistance [36]. The fact that stable expression of PEDF and the administration of rPEDF protein in MCF-7:5C cells was able to suppress p^{Ser167}-ERα, p-AKT, and RET expression suggests a potential crosstalk between PEDF, ERα and RET in these cells. This finding highlights a potential mechanism by which silencing/loss of PEDF might contribute to the development of resistance in MCF-7:5C cells. We should note that re-expression of PEDF in BT474 cells did not significantly alter ERα phosphorylation status or RET expression in these cells; however, it did slightly reduce HER2 expression in these cells (data not shown).

Downregulation of RET reverses tamoxifen resistance in MCF-7:5C breast cancer cells

Previous studies have shown that a subset of ERα-positive breast cancers express high levels of mRNA transcripts encoding *RET* and that RET signaling in ERα-positive breast cancer cell lines can result in the activation of MAPK and AKT, which are important regulators of ERα phosphorylation [43,44]. More recently, RET signaling has been implicated in estrogen-independent growth and tamoxifen resistance in breast cancer, potentially through ERα phosphorylation and ligand-independent transcriptional regulation [43-45]. Since our data showed that re-expression of PEDF suppressed RET, ERα and AKT in endocrine-resistant MCF-7:5C cells, we examined the biological effect of RET in endocrine-sensitive MCF-7 breast cancer cells and estrogen-independent and tamoxifen-resistant MCF-7:5C cells. As shown in Figure 5a, RET protein and mRNA levels were markedly increased in endocrine-resistant MCF-7:5C cells compared with MCF-7 cells. Transfection of MCF-7:5C cells with RET siRNA completely downregulated RET protein and mRNA levels (Figure 5b) in these cells. Dose-response survival curves performed over a range of 4OHT concentrations from 10^{-9} to 10^{-6} M confirmed that the untreated and siRNA control-treated MCF-7:5C cells were indeed resistant to 4OHT treatment (Figure 5c). In contrast, RET downregulation resulted in a profound increase in sensitivity to 4OHT (Figure 5c). These results indicate that there might be potential crosstalk between PEDF, RET, and ERα signaling pathways and that RET targeting might be a viable strategy to resensitize resistant breast cancers to endocrine therapy.

PEDF inhibits endocrine-resistant breast cancer cell growth *in vitro* and exhibits anti-tumor activity *in vivo*

Although our studies have shown that PEDF is capable of modulating ERα and RET signaling pathways in endocrine-resistant breast cancer cells, it is worth noting that the most well-known function of PEDF is its ability to inhibit angiogenesis. We therefore examined the effect of rPEDF on the proliferation of endocrine-sensitive MCF-7 and endocrine-resistant MCF-7:5C breast cancer cells. As shown in Figure 6a, rPEDF significantly ($P < 0.001$) reduced the growth of resistant MCF-7:5C cells but had no effect on parental MCF-7 cells. The growth-inhibitory effect of rPEDF was concentration dependent, with maximum inhibition (~90%) observed at 100 nM, and this inhibitory effect of rPEDF was completely blocked by the addition of antibodies specific to PEDF, thus confirming that the effect of PEDF was specific. To determine whether the anti-proliferative effect of rPEDF on MCF-7:5C cells was due to apoptosis, we next performed a TUNEL assay. Figure 6b showed that rPEDF (100 nM) markedly increased apoptosis in MCF-7:5C cells, with 41.8% of cells being TUNEL-positive, compared with the untreated (control) cells that showed very few TUNEL-positive cells. Because rPEDF treatment caused endocrine-resistant MCF-7:5C cells to undergo apoptosis, we also examined whether knockdown of PEDF expression in MCF-7 cells would cause them to undergo apoptosis. We found that PEDF knockdown in MCF-7 cells did not inhibit the growth of these cells or cause them to undergo apoptosis in the presence of rPEDF (data not shown), thus confirming that the ability of rPEDF to induce apoptosis is specific for MCF-7:5C cells.

Since rPEDF was shown to effectively inhibit the growth of endocrine-resistant MCF-7:5C breast cancer cells *in vitro*, we next evaluated the effect of rPEDF on MCF-7:5C tumor growth *in vivo*. Endocrine-resistant MCF-7:5C breast cancer cells were injected subcutaneously into the mammary fat pads of ovariectomized nude mice. When palpable tumors were established (0.1 cm^2), the animals were randomized into two groups and then treated with either rPEDF (4 mg/kg) or PBS vehicle control that was administered every 2 days by intraperitoneal injection. We found that rPEDF reduced the growth of MCF-7:5C tumors at all of the time points examined. The average tumor area was reduced from 0.42 cm^2 in the PBS-treated group to 0.12 cm^2 in the rPEDF-treated group (Figure 6c). The differences between the two groups were statistically significant ($P < 0.001$), as calculated by repeated-measures analysis of variance. We next determined whether the anti-tumor activity of rPEDF *in vivo* was due, in part, to its ability to inhibit angiogenesis. For this purpose, MCF-7:5C xenografts were excised at the end of the experiment (day 30) and were sectioned and analyzed by immunohistochemistry using antibody to CD34, a well-known marker

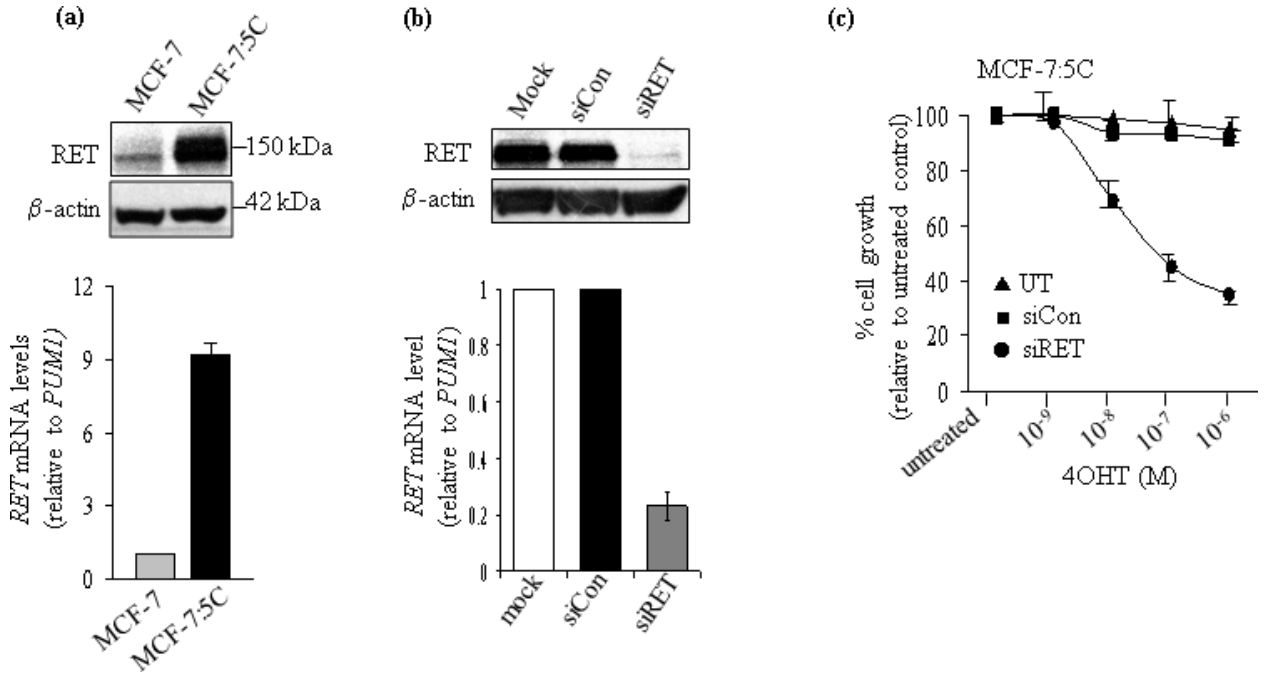

Figure 5 Knockdown of RET mRNA expression sensitizes endocrine-resistant MCF-7:5C breast cancer cells to 4-hydroxytamoxifen. **(a)** Rearranged during transfection (RET) protein and mRNA levels in wild-type MCF-7 cells and endocrine-resistant MCF-7:5C cells as determined by western blot analysis and quantitative real-time PCR, respectively. **(b)** MCF-7:5C cells were transfected with either a RET-targeted siRNA or a nontarget control siRNA for 48 hours and *RET* protein and mRNA expression levels were determined by western blotting and real-time PCR. **(c)** Effect of RET suppression on the proliferation of MCF-7:5C cells. Cells were transfected with a RET-targeted or a nontargeting control siRNA, and after 24 hours cells were seeded into 12-well plates and exposed continuously to the indicated concentrations of 4-hydroxytamoxifen (4OHT) or vehicle for an additional 72 hours. Cell proliferation was determined by cell counting using a hemacytometer. Data shown are representative of three independent experiments. UT, untreated.

for newly formed blood vessels/angiogenesis. As shown in Figure 6d (top), tumors from mice treated with PBS showed intense staining for CD34, indicating the presence of extensive angiogenesis in the tumors, whereas microvessel density in tumors from mice treated with rPEDF was markedly lower. A 48% reduction in microvessel density was observed in the rPEDF-treated group compared with the PBS-treated group ($P < 0.01$; Figure 6d, bottom panel). These data demonstrate that rPEDF is capable of inhibiting the neovascularization of endocrine-resistant breast carcinoma *in vivo*.

PEDF expression sensitizes endocrine-resistant MCF-7:5C tumors to tamoxifen

Since our *in vitro* data showed that stable expression of PEDF in endocrine-resistant MCF-7:5C cells sensitized them to tamoxifen, we examined whether rPEDF is capable of sensitizing endocrine-resistant MCF-7:5C tumors to tamoxifen in athymic mice. Figure 7a shows that the growth of MCF-7:5C tumors was significantly reduced by rPEDF alone ($P < 0.0001$) but not by tamoxifen alone; however, when rPEDF and tamoxifen were combined the growth of MCF-7:5C tumors was significantly reduced compared with rPEDF alone ($P < 0.01$) (Figure 7a). For comparison, we also performed similar experiments using MCF-7 and BT474 tumors. We found that MCF-7 tumor growth was significantly inhibited by tamoxifen ($P < 0.0001$) and rPEDF ($P < 0.01$); however, the combination of tamoxifen and rPEDF did not further reduce the growth of these tumors compared with the individual treatments (Figure 7b). BT474 tumor growth was also significantly inhibited by rPEDF alone ($P < 0.001$) and the combination of rPEDF and tamoxifen ($P < 0.05$), but tamoxifen alone had no effect (Figure 7c). We next investigated whether ERα and other signaling proteins were altered in MCF-7:5C tumors treated with rPEDF, tamoxifen, or rPEDF and tamoxifen. Western blot analysis of MCF-7:5C tumor extracts showed that p^{Ser167}ERα, p-Akt, and p-RET protein were markedly reduced in the rPEDF-treated and rPEDF plus tamoxifen-treated samples compared with control or tamoxifen-treated samples (Figure 7d), which is consistent with our *in vitro* data. Overall, these results suggest that rPEDF is capable of inhibiting the growth of endocrine-sensitive MCF-7 tumors as well as endocrine-resistant MCF-7:5C and BT474 tumors, possibly through its anti-angiogenic activity; however, rPEDF is also capable

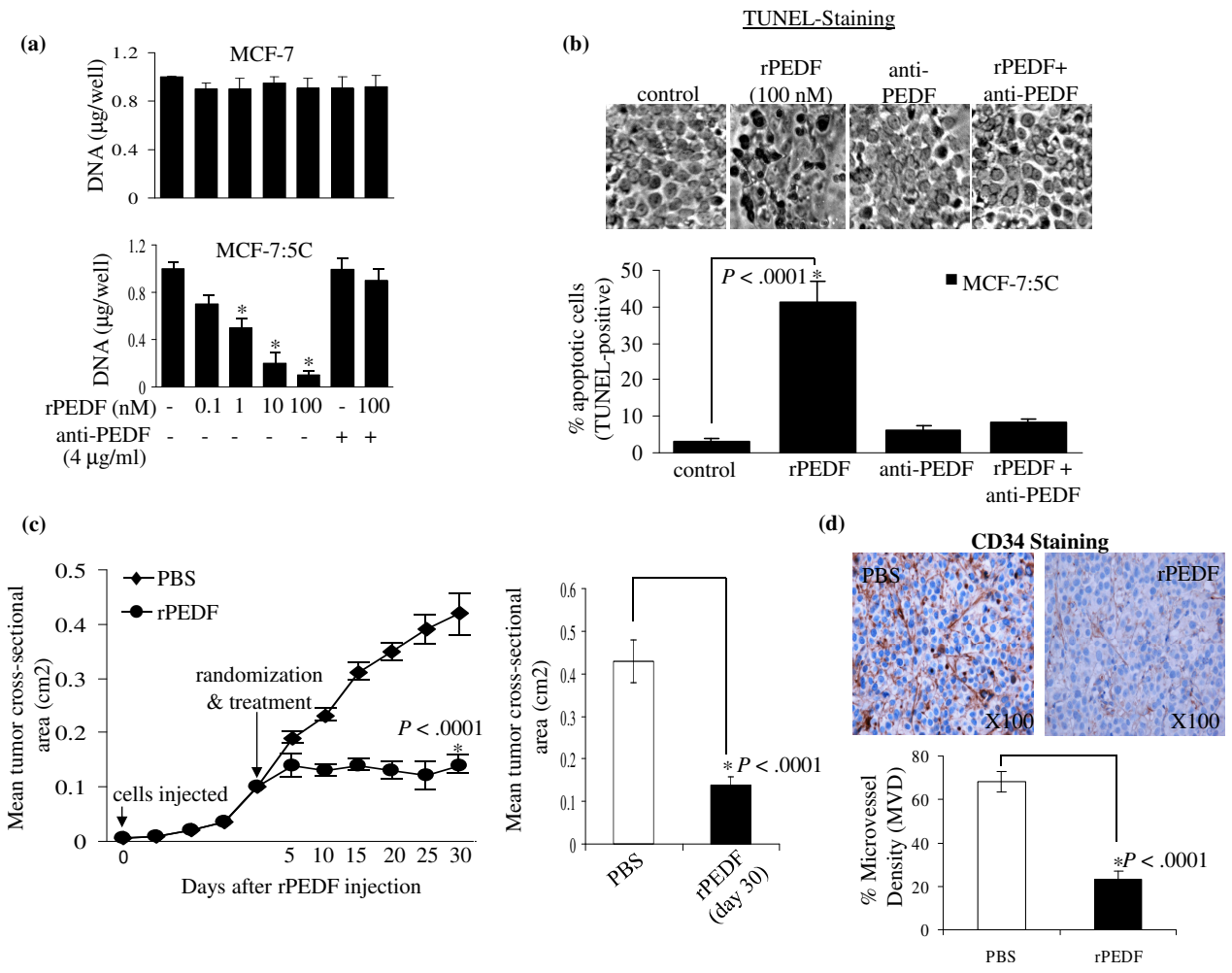

Figure 6 Effect of recombinant pigment epithelium-derived factor (rPEDF) on the growth of endocrine-sensitive MCF-7 and endocrine-resistant MCF-7:5C breast cancer cells *in vitro* and *in vivo*. **(a)** MCF-7 and MCF-7:5C cells were treated with increasing concentrations of rPEDF, rPEDF + anti-PEDF antibody (anti-PEDF), or anti-PEDF antibody for 7 days, and cell proliferation was determined using a DNA quantitation kit as described in Materials and methods. Experiments were repeated three times, and data are shown as mean ± standard deviation (SD). *P < 0.001 compared with untreated controls. **(b)** MCF-7:5C cells were treated with rPEDF, anti-rPEDF, or rPEDF + anti-rPEDF for 72 hours and apoptosis was determined by TUNEL staining. Bar graph: summary of percentage of apoptotic cells counted in five fields from three experiments. Data presented as mean ± SD. **(c)** Effect of rPEDF on the growth of MCF-7:5C cells *in vivo*. MCF-7:5C cells were bilaterally injected into the mammary fat pad of ovariectomized nude mice, and when tumors reached an area of 0.1 cm^2 the mice (n = 15/group) were randomized into two treatment groups: PBS or rPEDF. The mean cross-sectional tumor area was measured up to 30 days. Bar graph: mean cross-sectional tumor area in the control group and the PEDF-treated group. **(d)** Intratumoral microvessel density (MVD) in tumor tissues was determined by immunohistochemical staining by an endothelial-specific antibody CD34; PBS group (×200) and PEDF group (×200). Quantitative analysis of microvessel density is also shown. Data presented as mean ± SD.

of sensitizing MCF-7:5C tumors to tamoxifen, which appears to be associated with its ability to downregulate phosphorylated ERα, Akt, and RET in these tumors.

Discussion

Resistance to endocrine therapy presents a major challenge in the management of ERα-positive breast cancer and is an area under intense investigation. While many studies point towards the cross-talk between ERα and growth factor receptor signaling pathways as the key in the development of resistance [5,6,46,47], the underlying mechanism is still not fully understood and, as a consequence, effective approaches for preventing and overcoming resistance are not yet available. PEDF is a secreted glycoprotein that was first described in the late 1980s after it was identified and isolated from conditioned medium of cultured primary human fetal retinal pigment epithelial cells [8]. PEDF is ubiquitously expressed in many tissues and possesses potent anti-angiogenic activity, being more than twice as potent as

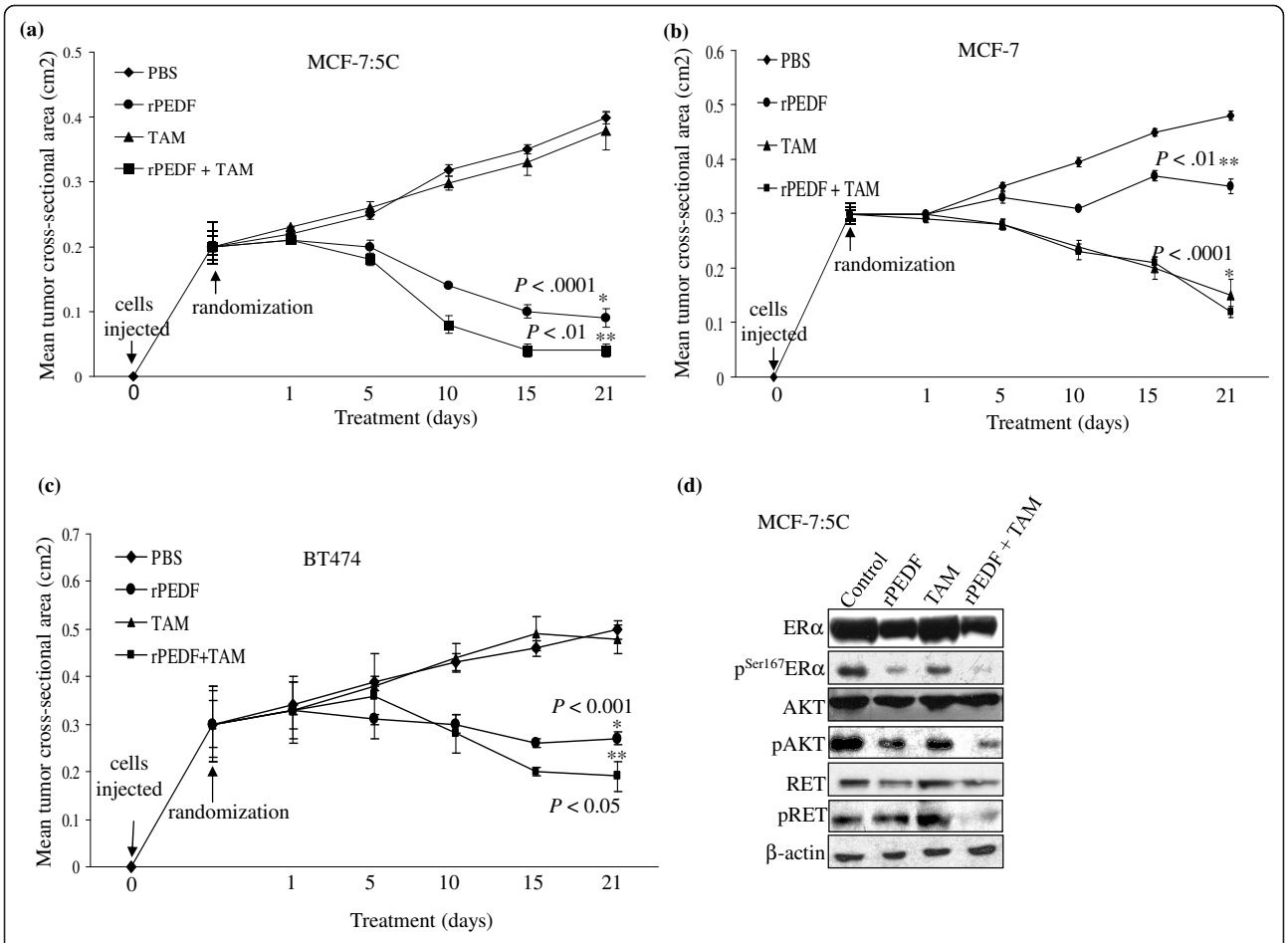

Figure 7 Effect of recombinant pigment epithelium-derived factor on tamoxifen sensitivity in MCF-7:5C, MCF-7, and BT474 xenografts. **(a)** MCF-7:5C cells were bilaterally injected into the mammary fat pads of ovariectomized athymic mice (n = 32), and after tumors reached a mean cross-sectional area of 0.2 cm^2 groups of eight mice were randomly assigned to the following treatments: PBS (control), recombinant pigment epithelium-derived factor (rPEDF), tamoxifen (TAM), or rPEDF + TAM. TAM was given orally by gavage at 1.5 mg/day and rPEDF was given via intraperitoneal injection at 4 mg/kg every other day for 21 days. **(b)** MCF-7 cells were bilaterally injected into the mammary fat pads of ovariectomized mice (n = 32), and after tumors reached a mean cross-sectional area of 0.32 cm^2 groups of eight mice were randomly assigned to the following treatments: PBS (control), rPEDF, TAM, or rPEDF + TAM as described in Materials and methods. **(c)** BT474 cells were bilaterally injected into the mammary fat pads of ovariectomized mice (n = 32), and after tumors reached a mean cross-sectional area of 0.3 cm^2 groups of eight mice were randomly assigned to the following treatments: PBS (control), rPEDF, TAM, or rPEDF + TAM. Mean cross-sectional tumor area was measured every 5 days with vernier calipers. Cross-sectional areas were calculated by multiplying the length (l) by the width (w) and by π and dividing the product by 4 (that is, $lw\pi/4$). **(d)** Western blot analysis of MCF-7:5C tumors following treatment with rPEDF, tamoxifen, or rPEDF and tamoxifen. Tumors were generated as described in 7a and the lysates were preprepared as described in Materials and Methods. Blots were probed with the indicated antibodies.

angiostatin and more than seven times as potent as endostatin [12]. Recent studies indicate that PEDF expression is significantly reduced in a wide range of tumor types and that its re-expression in these tumors delays the onset of primary tumors and decreases metastases [48]. In the present study, we show that loss of PEDF expression in breast cancer is associated with the development of endocrine resistance and that there is functional cross-talk between PEDF and the ERα signaling pathway. Specifically, we found that PEDF protein and mRNA levels were markedly reduced in tamoxifen-resistant breast tumors and in breast cancer cells that are resistant to AIs and/or tamoxifen. We also found that stable re-expression of PEDF in the resistant cells re-sensitized them to the antiproliferative effects of tamoxifen and that re-expression of PEDF dramatically reduced the expression of the receptor tyrosine kinase RET along with p-AKT and $p^{Ser167}ER\alpha$. Furthermore, we found that exogenous administration of rPEDF significantly inhibited the growth of endocrine-resistant breast cancer cells *in vitro* and *in vivo* but had no effect on the growth of endocrine-sensitive breast cancer cells *in vitro* with marginal

effect *in vivo*. While PEDF is known to exert anti-tumor activity by inhibiting angiogenesis [49,50] and inducing apoptosis [17], the present study is the first to demonstrate a link between loss of PEDF expression and the development of endocrine resistance and to show that PEDF re-expression is capable of reversing tamoxifen resistance in breast cancer.

During the past decade, researchers have prepared various forms of PEDF and demonstrated its beneficial effects in several tumor models. Doll and colleagues reported that exogenous rPEDF protein induced tumor epithelial apoptosis in mouse prostate and pancreas [13]. Liu and colleagues showed that a short peptide derived from the parent PEDF molecule was able to inhibit osteosarcoma growth [51]. Hase and colleagues demonstrated that intratumoral injection of a lentivirus vector encoding PEDF resulted in inhibition of human pancreatic cancer in nude mice [52]. Moreover, Wang and colleagues showed that *in vivo* transfer of PEDF mediated by adenoviral vectors exerted a dramatic inhibition of tumor growth in athymic nude mice implanted with the human HCC and in C57BL/6 mice implanted with mouse lung carcinoma [53]. In the present study we showed that exogenous rPEDF preferentially induced apoptosis in endocrine-resistant MCF-7:5C and BT474 breast cancer cells compared with endocrine-sensitive MCF-7 cells and that rPEDF partially reversed the tamoxifen-resistant phenotype of MCF-7:5C and BT474 cells *in vitro* and *in vivo*. Interestingly, we found that lentiviral-mediated re-expression of PEDF in the resistant cells also reversed tamoxifen resistance in these cells. Investigation into the mechanism of action of PEDF in the resistant cells indicated that the anti-tumor activity of PEDF in *vivo* was due, in part, to its ability to inhibit angiogenesis, as was demonstrated by a reduction in microvessel density and an increase in apoptosis. Interestingly, we found that exogenous PEDF failed to induce apoptosis in MCF-7 breast cancer cells *in vitro*; however, it significantly inhibited the growth of MCF-7 tumors in athymic mice, which was due to its anti-angiogenic activity. The anti-tumor activity of PEDF, however, was more pronounced in the endocrine-resistant breast cancer cells compared with the endocrine-sensitive cells. We should note that a similar finding was reported by Konson and coworkers in which they showed that exogenous PEDF preferentially induced apoptosis in endothelial cells compared with MDA-MB-231, HCT116, and U87-MG cancer cells [54,55]; however, PEDF efficiently inhibited the growth rate of xenografts generated from these cancer cells. While the reason for this cell-type specific effect of PEDF is not known, there is evidence for multiple PEDF receptors at the cell surface including the recently identified non-integrin 67/37-kDa laminin receptor [56], extracellular matrix components [57], and a phospholipase-linked membrane protein [58]. Differential expression of these receptors on neuronal, endothelial, and cancer cells may provide a partial explanation for the differential effects on these cell populations. Identification of which of these PEDF receptors are present on cancer cells, as well as further elucidation of signaling downstream of PEDF, could lead to the identification of new pharmacologic targets for both anti-cancer and neuronal survival therapies. We are currently trying to determine whether there is a specific PEDF receptor expressed in breast cancer cells and whether the functional activity of the receptor is altered by the endocrine responsiveness of the cells.

Apart from its ability to inhibit to angiogenesis, we also found that PEDF suppressed RET expression in endocrine-resistant breast cancer cells and that this suppression was associated with the reversal of tamoxifen resistance. Specifically, we found that basal RET, p-RET, ERα, and p^{Ser167}-ERα protein levels were markedly increased in endocrine-resistant MCF-7:5C cells compared with endocrine-sensitive MCF-7 cells and stable expression of PEDF in MCF-7:5C cells or treatment of these cells with rPEDF-suppressed RET, p-RET, and p^{Ser167}-ERα protein in these cells. Furthermore, we found that suppression of RET expression using siRNA knockdown also reversed tamoxifen resistance in MCF-7:5C cells, which suggests a role for RET in tamoxifen resistance. This finding is important because recent studies have indicated that RET is involved in the biology of ERα-positive breast cancers [43,44] and in the response to endocrine treatment [45]. Two independent studies have identified RET overexpression in a subset of ERα-positive breast cancers [43,44], suggesting an important role of RET in this subset. By *in situ* hybridization, in a cohort of 245 invasive breast cancers, RET mRNA was detected in 29.7% of the tumors and preferentially expressed in ER-positive cases. Subsequent studies in the same cohort of patient samples corroborated that increased RET mRNA levels correlated with increased RET protein expression. Similar findings were reported for many breast cancer cell lines where RET expression correlated strongly with ERα expression and/or ErbB2/HER2 overexpression [43].

RET is a receptor tyrosine kinase protein of 150 kDa that is expressed and required during early development for the formation of neural crest-derived lineages, kidney organogenesis, and spermatogenesis [59]. RET is considered the driving oncogene in various neoplasms of the thyroid, where specific mutations lead to defined tumor types [60-62]. The RET protein spans the cell membrane, so that one end of the protein remains inside the cell and the other end projects from the outer surface of the cell. This positioning of the protein allows it to interact with specific factors outside the cell and to receive signals that help the cell respond to its environment. When molecules that stimulate growth and development such as growth factors attach to the RET protein, a complex cascade of

chemical reactions inside the cell is triggered. These reactions instruct the cell to undergo certain changes, such as dividing or maturing to take on specialized functions. RET is the receptor for a family of glial-derived neurotrophic factor (GDNF) ligands, which includes GDNF, artemin, neurturin, and persephin [60,63]. These ligands bind RET in conjunction with glycosylphosphatidylinositol-anchored co-receptors of the GDNF receptor alpha family, and the ligand-co-receptor-RET complex formation results in transient RET dimerization and activation of the RET tyrosine kinase domain. RET protein dimerization results in autophosphorylation of several intracellular RET tyrosine residues, and these autophosphorylation sites serve as binding sites for a variety of docking proteins. In particular, the tyrosine Y1062 has been shown to bind Src homology and collagen, insulin receptor substrate1/2, fibroblast growth factor receptor substrate 2, and protein kinase C alpha. These proteins are able to activate multiple signaling pathways, including MAPK, PI3K/AKT, RAS/extracellular signal-regulated kinase and Rac/c-*jun* NH kinase, which are mediators of cell motility, proliferation, differentiation, and survival [64]. While our present study indicates that PEDF is capable of suppressing RET signaling in endocrine-resistant cells, we do not know the exact mechanism by which this occurs. We should note that RET is the receptor for several ligands including GNDF, which is a potent neurotropic factor similar to PEDF. Like other trophic factors, PEDF is thought to exert its biological effects by specifically binding and activating one or more receptors. While PEDF receptors have not yet been fully characterized, there is a possibility that PEDF, like GDNF, is able to bind to RET and thus regulate its expression and activity in breast cancer cells. This possibility is currently being investigated in our laboratory.

RET and other growth factor receptor tyrosine kinases are known to activate ERα through phosphorylation [36]. The ERα contains two distinct transcription activation domains, AF-1 and AF-2, which can function independently or synergistically. AF-2 is located in the ligand-binding domain region of ERα and its activity is dependent on estrogen binding, whereas AF-1 activity is regulated by phosphorylation that can occur independently of estrogen binding [5]. The extracellular signal-regulated kinase 1/2 pathway phosphorylates ERα directly and/or via p90RSK, whereas AKT phosphorylates ERα directly and/or via mTOR. In contrast, RET increases ERα phosphorylation at Ser118 and Ser167 through activation of the mTOR/p70S6K pathway [43,59,65], which can be independent of the PI3K/AKT pathway. Notably, p70S6K, mTOR, and p-AKT were also constitutively overexpressed in endocrine-resistant MCF-7:5C cells prior to stable expression of PEDF in these cells. In addition, basal ERα transcriptional activity, as determined by ERE luciferase assay, was significantly elevated in MCF-7:5C cells compared with wild-type MCF-7 cells, and treatment of these cells with rPEDF inhibited phosphorylation of ERα and RET and suppressed the basal ERE activity in these cells. Interestingly, we found that suppression of RET expression using siRNA and inhibition of the mTOR pathway using rapamycin was able to reverse tamoxifen resistance in MCF-7:5C cells; however, inhibition of the PI3K/AKT pathway in these cells did not reverse their tamoxifen-resistant phenotype but it did reduce their hormone-independent growth. Notably, crosstalk between RET and ERα has previously been reported by Plaza-Menacho and coworkers, who showed that activation of RET by its ligand GDNF increased ERα phosphorylation on Ser118 and Ser167 and increased estrogen-independent activation of ERα transcriptional activity [45]. Further, they identified mTOR as a key component in this downstream signaling pathway and they showed in tamoxifen-resistant (TAM_R-1) MCF-7 cells that targeting RET restored tamoxifen sensitivity.

Conclusion

In summary, we have found that PEDF expression is markedly reduced in endocrine-resistant breast cancer and that stable expression of PEDF in endocrine-resistant cells restores their sensitivity to tamoxifen by suppressing RET and ERα signaling. The ability of PEDF to suppress RET signaling in endocrine-resistant cells is a newly identified function of PEDF that is independent of its most well-known function as a potent endogenous anti-angiogenic factor. This finding suggests that PEDF expression in breast cancer might be an important marker of endocrine responsiveness and that loss of PEDF might be a potential hallmark for the development of endocrine resistance. The fact that PEDF is endogenously produced and is widely expressed throughout the body reduces the likelihood that it will have adverse side effects like other synthetic agents or develop drug resistance. However, we should caution that relatively little is known of the overall physiologic role of PEDF in the human body; hence, further investigation is required before any clinical trial can be initiated.

Abbreviations

AI: aromatase inhibitor; DMEM: Dulbecco modified eagle's medium; ER: estrogen receptor; ERE: estrogen response element; E2: 17β-estradiol; FBS: fetal bovine serum; GDNF: glial cell-derived neurotrophic factor; 4OHT: 4-hydroxytamoxifen; iRNA: interfering RNA; MAPK: mitogen-activated protein kinase; mTOR: mammalian target of rapamycin; PBS: phosphate-buffered saline; PCR: polymerase chain reaction; PEDF: pigment epithelium-derived factor; PI3K: phosphoinositide 3-kinase; rPEDF: recombinant pigment epithelium-derived factor; RET: rearranged during transfection; RT: reverse transcriptase; siRNA: small interfering RNA; TUNEL: terminal deoxynucleotidyl transferase-mediated dUTP nick end-labeling.

Acknowledgements

This work was supported by grants from the National Institutes of Health National Cancer Institute (K01CA120051 01A2; supporting JL-W), the Department of Defense (W81XWH-12-1-0139; supporting JL-W and RJ) and the Hollenbach Foundation (supporting JL-W and RJ). The authors wish to

acknowledge the Tumor Bank Facility at The Research Institute of Fox Chase Cancer Center for providing the breast tumor tissues for this study and the Laboratory Animal Facility for helping with the care of the animals used in this study. The authors wish to also thank Dr Christel Wambi for his insightful feedback and critical evaluation of this manuscript.

Author details
[1]Cancer Biology Program, The Research Institute of Fox Chase Cancer Center, 333 Cottman Avenue, Philadelphia, PA 19111, USA. [2]Department of Pathology, The Research Institute of Fox Chase Cancer Center, 333 Cottman Avenue, Philadelphia, PA 19111, USA.

Authors' contributions
RJ performed the *in vitro* studies. MH constructed the tissue microarrays and performed all of the immunohistochemistry experiments. JL-W conceived the study, participated in the research design and implementation of the study, analyzed and interpreted the data, and drafted the manuscript. All authors read and approved the final manuscript for publication.

Competing interests
The authors declare that they have no competing interests.

Received: 13 June 2012 Revised: 18 October 2012
Accepted: 9 November 2012 Published: 14 November 2012

References

1. Anderson WF, Chatterjee N, Ershler WB, Brawley OW: **Estrogen receptor breast cancer phenotypes in the Surveillance, Epidemiology, and End Results database.** *Breast Cancer Res Treat* 2002, **76**:27-36.
2. Allred DC, Harvey JM, Berardo M, Clark GM: **Prognostic and predictive factors in breast cancer by immunohistochemical analysis.** *Mod Pathol* 1998, **11**:155-168.
3. **Tamoxifen for early breast cancer: an overview of the randomised trials. Early Breast Cancer Trialists' Collaborative Group.** *Lancet* 1998, **351**:1451-1467.
4. Goss PE, Strasser K: **Aromatase inhibitors in the treatment and prevention of breast cancer.** *J Clin Oncol* 2001, **19**:881-894.
5. Ali S, Coombes RC: **Endocrine-responsive breast cancer and strategies for combating resistance.** *Nat Rev Cancer* 2002, **2**:101-112.
6. Clarke R, Liu MC, Bouker KB, Gu Z, Lee RY, Zhu Y, Skaar TC, Gomez B, O'Brien K, Wang Y, Hilakivi-Clarke LA: **Antiestrogen resistance in breast cancer and the role of estrogen receptor signaling.** *Oncogene* 2003, **22**:7316-7339.
7. Fan P, Yue W, Wang JP, Aiyar S, Li Y, Kim TH, Santen RJ: **Mechanisms of resistance to structurally diverse antiestrogens differ under premenopausal and postmenopausal conditions: evidence from in vitro breast cancer cell models.** *Endocrinology* 2009, **150**:2036-2045.
8. Becerra SP: **Structure-function studies on PEDF. A noninhibitory serpin with neurotrophic activity.** *Adv Exp Med Biol* 1997, **425**:223-237.
9. Becerra SP, Sagasti A, Spinella P, Notario V: **Pigment epithelium-derived factor behaves like a noninhibitory serpin. Neurotrophic activity does not require the serpin reactive loop.** *J Biol Chem* 1995, **270**:25992-25999.
10. Barnstable CJ, Tombran-Tink J: **Neuroprotective and antiangiogenic actions of PEDF in the eye: molecular targets and therapeutic potential.** *Prog Retin Eye Res* 2004, **23**:561-577.
11. Filleur S, Nelius T, de Riese W, Kennedy RC: **Characterization of PEDF: a multi-functional serpin family protein.** *J Cell Biochem* 2009, **106**:769-775.
12. Dawson DW, Volpert OV, Gillis P, Crawford SE, Xu H, Benedict W, Bouck NP: **Pigment epithelium-derived factor: a potent inhibitor of angiogenesis.** *Science* 1999, **285**:245-248.
13. Doll JA, Stellmach VM, Bouck NP, Bergh AR, Lee C, Abramson LP, Cornwell ML, Pins MR, Borensztajn J, Crawford SE: **Pigment epithelium-derived factor regulates the vasculature and mass of the prostate and pancreas.** *Nat Med* 2003, **9**:774-780.
14. Ek ET, Dass CR, Choong PF: **Pigment epithelium-derived factor: a multimodal tumor inhibitor.** *Mol Cancer Ther* 2006, **5**:1641-1646.
15. Ek ET, Dass CR, Choong PF: **PEDF: a potential molecular therapeutic target with multiple anti-cancer activities.** *Trends Mol Med* 2006, **12**:497-502.
16. Fernandez-Garcia NI, Volpert OV, Jimenez B: **Pigment epithelium-derived factor as a multifunctional antitumor factor.** *J Mol Med* 2007, **85**:15-22.
17. Takenaka K, Yamagishi S, Jinnouchi Y, Nakamura K, Matsui T, Imaizumi T: **Pigment epithelium-derived factor (PEDF)-induced apoptosis and inhibition of vascular endothelial growth factor (VEGF) expression in MG63 human osteosarcoma cells.** *Life Sci* 2005, **77**:3231-3241.
18. Volpert OV, Zaichuk T, Zhou W, Reiher F, Ferguson TA, Stuart PM, Amin M, Bouck NP: **Inducer-stimulated Fas targets activated endothelium for destruction by anti-angiogenic thrombospondin-1 and pigment epithelium-derived factor.** *Nat Med* 2002, **8**:349-357.
19. Chen L, Zhang SS, Barnstable CJ, Tombran-Tink J: **PEDF induces apoptosis in human endothelial cells by activating p38 MAP kinase dependent cleavage of multiple caspases.** *Biochem Biophys Res Commun* 2006, **348**:1288-1295.
20. Halin S, Wikstrom P, Rudolfsson SH, Stattin P, Doll JA, Crawford SE, Bergh A: **Decreased pigment epithelium-derived factor is associated with metastatic phenotype in human and rat prostate tumors.** *Cancer Res* 2004, **64**:5664-5671.
21. Uehara H, Miyamoto M, Kato K, Ebihara Y, Kaneko H, Hashimoto H, Murakami Y, Hase R, Takahashi R, Mega S, Shichinohe T, Kawarada Y, Itoh T, Okushiba S, Kondo S, Katoh H: **Expression of pigment epithelium-derived factor decreases liver metastasis and correlates with favorable prognosis for patients with ductal pancreatic adenocarcinoma.** *Cancer Res* 2004, **64**:3533-3537.
22. Guan M, Yam HF, Su B, Chan KP, Pang CP, Liu WW, Zhang WZ, Lu Y: **Loss of pigment epithelium derived factor expression in glioma progression.** *J Clin Pathol* 2003, **56**:277-282.
23. Cheung LW, Au SC, Cheung AN, Ngan HY, Tombran-Tink J, Auersperg N, Wong AS: **Pigment epithelium-derived factor is estrogen sensitive and inhibits the growth of human ovarian cancer and ovarian surface epithelial cells.** *Endocrinology* 2006, **147**:4179-4191.
24. Cai J, Parr C, Watkins G, Jiang WG, Boulton M: **Decreased pigment epithelium-derived factor expression in human breast cancer progression.** *Clin Cancer Res* 2006, **12**:3510-3517.
25. Zhou D, Cheng SQ, Ji HF, Wang JS, Xu HT, Zhang GQ, Pang D: **Evaluation of protein pigment epithelium-derived factor (PEDF) and microvessel density (MVD) as prognostic indicators in breast cancer.** *J Cancer Res Clin Oncol* 2010, **136**:1719-1727.
26. Pink JJ, Jordan VC: **Models of estrogen receptor regulation by estrogens and antiestrogens in breast cancer cell lines.** *Cancer Res* 1996, **56**:2321-2330.
27. Jiang SY, Wolf DM, Yingling JM, Chang C, Jordan VC: **An estrogen receptor positive MCF-7 clone that is resistant to antiestrogens and estradiol.** *Mol Cell Endocrinol* 1992, **90**:77-86.
28. Lewis JS, Meeke K, Osipo C, Ross EA, Kidawi N, Li T, Bell E, Chandel NS, Jordan VC: **Intrinsic mechanism of estradiol-induced apoptosis in breast cancer cells resistant to estrogen deprivation.** *J Natl Cancer Inst* 2005, **97**:1746-1759.
29. Lewis-Wambi JS, Kim HR, Wambi C, Patel R, Pyle JR, Klein-Szanto AJ, Jordan VC: **Buthionine sulfoximine sensitizes antihormone-resistant human breast cancer cells to estrogen-induced apoptosis.** *Breast Cancer Res* 2008, **10**:R104.
30. Pink JJ, Jiang SY, Fritsch M, Jordan VC: **An estrogen-independent MCF-7 breast cancer cell line which contains a novel 80-kilodalton estrogen receptor-related protein.** *Cancer Res* 1995, **55**:2583-2590.
31. Lewis-Wambi JS, Kim H, Curpan R, Grigg R, Sarker MA, Jordan VC: **The selective estrogen receptor modulator bazedoxifene inhibits hormone-independent breast cancer cell growth and down-regulates estrogen receptor alpha and cyclin D_1.** *Mol Pharmacol* 2011, **80**:610-620.
32. Pink JJ, Bilimoria MM, Assikis J, Jordan VC: **Irreversible loss of the oestrogen receptor in T47D breast cancer cells following prolonged oestrogen deprivation.** *Br J Cancer* 1996, **74**:1227-1236.
33. Lasfargues EY, Coutinho WG, Redfield ES: **Isolation of two human tumor epithelial cell lines from solid breast carcinomas.** *J Natl Cancer Inst* 1978, **61**:967-978.
34. Lewis JS, Osipo C, Meeke K, Jordan VC: **Estrogen-induced apoptosis in a breast cancer model resistant to long-term estrogen withdrawal.** *J Steroid Biochem Mol Biol* 2005, **94**:131-141.
35. Lewis-Wambi JS, Cunliffe HE, Kim HR, Willis AL, Jordan VC: **Overexpression of CEACAM6 promotes migration and invasion of oestrogen-deprived breast cancer cells.** *Eur J Cancer* 2008, **44**:1770-1779.
36. Arpino G, Gutierrez C, Weiss H, Rimawi M, Massarweh S, Bharwani L, De Placido S, Osborne CK, Schiff R: **Treatment of human epidermal growth**

factor receptor 2-overexpressing breast cancer xenografts with multiagent HER-targeted therapy. *J Natl Cancer Inst* 2007, **99**:694-705.
37. Gutierrez MC, Detre S, Johnston S, Mohsin SK, Shou J, Allred DC, Schiff R, Osborne CK, Dowsett M: **Molecular changes in tamoxifen-resistant breast cancer: relationship between estrogen receptor, HER-2, and p38 mitogen-activated protein kinase.** *J Clin Oncol* 2005, **23**:2469-2476.
38. Schiff R, Massarweh S, Shou J, Osborne CK: **Breast cancer endocrine resistance: how growth factor signaling and estrogen receptor coregulators modulate response.** *Clin Cancer Res* 2003, **9**:447S-454S.
39. Dowsett M: **Overexpression of HER-2 as a resistance mechanism to hormonal therapy for breast cancer.** *Endocr Relat Cancer* 2001, **8**:191-195.
40. Nicholson RI, Hutcheson IR, Harper ME, Knowlden JM, Barrow D, McClelland RA, Jones HE, Wakeling AE, Gee JM: **Modulation of epidermal growth factor receptor in endocrine-resistant, oestrogen receptor-positive breast cancer.** *Endocr Relat Cancer* 2001, **8**:175-182.
41. Song RX, Mor G, Naftolin F, McPherson RA, Song J, Zhang Z, Yue W, Wang J, Santen RJ: **Effect of long-term estrogen deprivation on apoptotic responses of breast cancer cells to 17beta-estradiol.** *J Natl Cancer Inst* 2001, **93**:1714-1723.
42. Ariazi EA, Cunliffe HE, Lewis-Wambi JS, Slifker MJ, Willis AL, Ramos P, Tapia C, Kim HR, Yerrum S, Sharma CG, Nicolas E, Balagurunathan Y, Ross EA, Jordan VC: **Estrogen induces apoptosis in estrogen deprivation-resistant breast cancer through stress responses as identified by global gene expression across time.** *Proc Natl Acad Sci USA* 2011, **108**:18879-18886.
43. Boulay A, Breuleux M, Stephan C, Fux C, Brisken C, Fiche M, Wartmann M, Stumm M, Lane HA, Hynes NE: **The Ret receptor tyrosine kinase pathway functionally interacts with the ERα pathway in breast cancer.** *Cancer Res* 2008, **68**:3743-3751.
44. Esseghir S, Todd SK, Hunt T, Poulsom R, Plaza-Menacho I, Reis-Filho JS, Isacke CM: **A role for glial cell derived neurotrophic factor induced expression by inflammatory cytokines and RET/GFR alpha 1 receptor up-regulation in breast cancer.** *Cancer Res* 2007, **67**:11732-11741.
45. Plaza-Menacho I, Morandi A, Robertson D, Pancholi S, Drury S, Dowsett M, Martin LA, Isacke CM: **Targeting the receptor tyrosine kinase RET sensitizes breast cancer cells to tamoxifen treatment and reveals a role for RET in endocrine resistance.** *Oncogene* 2010, **29**:4648-4657.
46. Osborne CK, Schiff R: **Mechanisms of endocrine resistance in breast cancer.** *Annu Rev Med* 2011, **62**:233-247.
47. Osborne CK, Shou J, Massarweh S, Schiff R: **Crosstalk between estrogen receptor and growth factor receptor pathways as a cause for endocrine therapy resistance in breast cancer.** *Clin Cancer Res* 2005, **11**:865s-870s.
48. Hoshina D, Abe R, Yamagishi SI, Shimizu H: **The role of PEDF in tumor growth and metastasis.** *Curr Mol Med* 2010, **10**:292-295.
49. Abe R, Fujita Y, Yamagishi S, Shimizu H: **Pigment epithelium-derived factor prevents melanoma growth via angiogenesis inhibition.** *Curr Pharm Des* 2008, **14**:3802-3809.
50. Becerra SP: **Focus on molecules: pigment epithelium-derived factor (PEDF).** *Exp Eye Res* 2006, **82**:739-740.
51. Liu H, Ren JG, Cooper WL, Hawkins CE, Cowan MR, Tong PY: **Identification of the antivasopermeability effect of pigment epithelium-derived factor and its active site.** *Proc Natl Acad Sci USA* 2004, **101**:6605-6610.
52. Hase R, Miyamoto M, Uehara H, Kadoya M, Ebihara Y, Murakami Y, Takahashi R, Mega S, Li L, Shichinohe T, Kawarada Y, Kondo S: **Pigment epithelium-derived factor gene therapy inhibits human pancreatic cancer in mice.** *Clin Cancer Res* 2005, **11**:8737-8744.
53. Wang L, Schmitz V, Perez-Mediavilla A, Izal I, Prieto J, Qian C: **Suppression of angiogenesis and tumor growth by adenoviral-mediated gene transfer of pigment epithelium-derived factor.** *Mol Ther* 2003, **8**:72-79.
54. Konson A, Pradeep S, D'Acunto CW, Seger R: **Pigment epithelium-derived factor and its phosphomimetic mutant induce JNK-dependent apoptosis and p38-mediated migration arrest.** *J Biol Chem* 2011, **286**:3540-3551.
55. Konson A, Pradeep S, Seger R: **Phosphomimetic mutants of pigment epithelium-derived factor with enhanced antiangiogenic activity as potent anticancer agents.** *Cancer Res* 2010, **70**:6247-6257.
56. Bernard A, Gao-Li J, Franco CA, Bouceba T, Huet A, Li Z: **Laminin receptor involvement in the anti-angiogenic activity of pigment epithelium-derived factor.** *J Biol Chem* 2009, **284**:10480-10490.
57. Alberdi E, Hyde CC, Becerra SP: **Pigment epithelium-derived factor (PEDF) binds to glycosaminoglycans: analysis of the binding site.** *Biochemistry* 1998, **37**:10643-10652.
58. Notari L, Baladron V, Aroca-Aguilar JD, Balko N, Heredia R, Meyer C, Notario PM, Saravanamuthu S, Nueda ML, Sanchez-Sanchez F, Escribano J, Laborda J, Becerra SP: **Identification of a lipase-linked cell membrane receptor for pigment epithelium-derived factor.** *J Biol Chem* 2006, **281**:38022-38037.
59. Arighi E, Borrello MG, Sariola H: **RET tyrosine kinase signaling in development and cancer.** *Cytokine Growth Factor Rev* 2005, **16**:441-467.
60. Ichihara M, Murakumo Y, Takahashi M: **RET and neuroendocrine tumors.** *Cancer Lett* 2004, **204**:197-211.
61. Drosten M, Putzer BM: **Mechanisms of disease: cancer targeting and the impact of oncogenic RET for medullary thyroid carcinoma therapy.** *Nat Clin Pract Oncol* 2006, **3**:564-574.
62. Takaya K, Yoshimasa T, Arai H, Tamura N, Miyamoto Y, Itoh H, Nakao K: **Expression of the RET proto-oncogene in normal human tissues, pheochromocytomas, and other tumors of neural crest origin.** *J Mol Med (Berl)* 1996, **74**:617-621.
63. Airaksinen MS, Saarma M: **The GDNF family: signalling, biological functions and therapeutic value.** *Nat Rev Neurosci* 2002, **3**:383-394.
64. Morandi A, Plaza-Menacho I, Isacke CM: **RET in breast cancer: functional and therapeutic implications.** *Trends Mol Med* 2011, **17**:149-157.
65. Boulay A, Rudloff J, Ye J, Zumstein-Mecker S, O'Reilly T, Evans DB, Chen S, Lane HA: **Dual inhibition of mTOR and estrogen receptor signaling in vitro induces cell death in models of breast cancer.** *Clin Cancer Res* 2005, **11**:5319-5328.

doi:10.1186/bcr3356
Cite this article as: Jan *et al.*: Loss of pigment epithelium-derived factor: a novel mechanism for the development of endocrine resistance in breast cancer. *Breast Cancer Research* 2012 **14**:R146.

Choi et al. Breast Cancer Research (2015) 17:6
DOI 10.1186/s13058-014-0506-7

Breast Cancer RESEARCH

RESEARCH ARTICLE Open Access

Targeting interferon response genes sensitizes aromatase inhibitor resistant breast cancer cells to estrogen-induced cell death

Hye Joung Choi[1†], Asona Lui[1,2†], Joshua Ogony[1], Rifat Jan[3], Peter J Sims[4] and Joan Lewis-Wambi[1,2*]

Abstract

Introduction: Estrogen deprivation using aromatase inhibitors (AIs) is currently the standard of care for postmenopausal women with hormone receptor-positive breast cancer. Unfortunately, the majority of patients treated with AIs eventually develop resistance, inevitably resulting in patient relapse and, ultimately, death. The mechanism by which resistance occurs is still not completely known, however, recent studies suggest that impaired/defective interferon signaling might play a role. In the present study, we assessed the functional role of IFITM1 and PLSCR1; two well-known interferon response genes in AI resistance.

Methods: Real-time PCR and Western blot analyses were used to assess mRNA and protein levels of IFITM1, PLSCR1, STAT1, STAT2, and IRF-7 in AI-resistant MCF-7:5C breast cancer cells and AI-sensitive MCF-7 and T47D cells. Immunohistochemistry (IHC) staining was performed on tissue microarrays consisting of normal breast tissues, primary breast tumors, and AI-resistant recurrence tumors. Enzyme-linked immunosorbent assay was used to quantitate intracellular IFNα level. Neutralizing antibody was used to block type 1 interferon receptor IFNAR1 signaling. Small interference RNA (siRNA) was used to knockdown IFITM1, PLSCR1, STAT1, STAT2, IRF-7, and IFNα expression.

Results: We found that IFITM1 and PLSCR1 were constitutively overexpressed in AI-resistant MCF-7:5C breast cancer cells and AI-resistant tumors and that siRNA knockdown of IFITM1 significantly inhibited the ability of the resistant cells to proliferate, migrate, and invade. Interestingly, suppression of IFITM1 significantly enhanced estradiol-induced cell death in AI-resistant MCF-7:5C cells and markedly increased expression of p21, Bax, and Noxa in these cells. Significantly elevated level of IFNα was detected in AI-resistant MCF-7:5C cells compared to parental MCF-7 cells and suppression of IFNα dramatically reduced IFITM1, PLSCR1, p-STAT1, and p-STAT2 expression in the resistant cells. Lastly, neutralizing antibody against IFNAR1/2 and knockdown of STAT1/STAT2 completely suppressed IFITM1, PLSCR1, p-STAT1, and p-STAT2 expression in the resistant cells, thus confirming the involvement of the canonical IFNα signaling pathway in driving the overexpression of IFITM1 and other interferon-stimulated genes (ISGs) in the resistant cells.

Conclusion: Overall, these results demonstrate that constitutive overexpression of ISGs enhances the progression of AI-resistant breast cancer and that suppression of IFITM1 and other ISGs sensitizes AI-resistant cells to estrogen-induced cell death.

* Correspondence: jlewis-wambi@kumc.edu
†Equal contributors
[1]Department of Cancer Biology, University of Kansas Medical Center, Kansas City 66160, KS, USA
[2]Department of Physiology, University of Kansas Medical Center, Kansas City 66160, KS, USA
Full list of author information is available at the end of the article

Introduction

Aromatase inhibitors (AIs) are more effective than the antiestrogen tamoxifen at inhibiting the growth and proliferation of estrogen receptor (ER)-positive breast cancer [1] and these agents are now front-line treatments for postmenopausal women with hormone receptor-positive breast cancer in both the adjuvant and metastatic setting [2,3]. AIs suppress estrogen synthesis in postmenopausal women by inhibiting the aromatase enzyme, which catalyzes the conversion of androgens to estrogens [1,2,4,5]. Unfortunately, the majority of patients treated with AIs eventually develop resistance to these drugs [6] and when resistance occurs it is unclear which endocrine therapy is the most appropriate. Recently, there has been increasing clinical evidence to suggest that 17β-estradiol (E_2) would be an appropriate and effective treatment option for postmenopausal patients with AI-resistant breast cancer [7,8]. Indeed, preclinical studies from our laboratory [9-12] and other investigators [13,14]) have previously shown that long term estrogen deprivation of ER-positive MCF-7 breast cancer cells causes them to lose their dependency on estradiol for proliferation, which recapitulates acquired resistance to aromatase inhibitors in postmenopausal women, and that these AI-resistant breast cancer cells paradoxically undergo apoptosis in the presence of estradiol [10-12,15,16]. The ability of estradiol to induce apoptosis in AI-resistant breast cancer cells was previously shown to be mediated, in part, by the mitochondria death pathway [11]; however, more recent findings suggest that dysregulation of the interferon signaling pathway might also play a role in estradiol-induced cell death [17].

Interferons (IFNs) are a class of glycoproteins known as cytokines that are produced by immune cells of most vertebrates and are secreted in response to viral infections, tumors, and other pathogenic microbial agents [18]. IFNs diffuse to the surrounding cells and bind to high affinity cell surface type I (IFNα/β) and type II (IFNγ) receptors (IFNAR1/2), leading to phosphorylation and activation of JAK1, JAK2 and Tyk2. Activated JAKs phosphorylate and activate STAT1 and STAT2, resulting in the formation of STAT1-STAT1 homodimers and STAT1-STAT2 heterodimers. The dimers are transported to the nucleus by importins and bind to IFN-stimulated response elements (ISREs) to activate the transcription of interferon-stimulated genes (ISGs), such as *IFITM1, PLSCR1, STAT1, IFI27* and *IFIT1* [18-20]. The interferon signaling pathway plays an important role in the proper functioning of the immune system [21] and there is strong evidence that its dysregulation, resulting in constitutive overexpression of ISGs contributes to tumorigenesis [22] and possibly drug resistance [23]. Indeed, our laboratory has previously shown through microarray analysis that immune response and interferon signaling pathways are significantly altered in AI-resistant breast cancer cells and that several interferon response genes including *IFITM1, PLSCR1* and *STAT1* are constitutively overexpressed in AI-resistant breast cancer cells [17,24]. At present, however, the functional significance of the interferon signaling pathway in AI-resistance or its potential involvement in estradiol-induced cell death is not known.

Interferon-inducible transmembrane protein 1 (IFITM1) is a cell surface 17 kDa membrane protein that is a member of the IFN-inducible transmembrane protein family that includes IFITM2, IFITM3 and IFITM5 [25,26]. The IFITM1 gene is located on the short arm of chromosome 11 (11p15.5) and is 3,956 bases in length. IFITM1 expression is highly induced by IFNα and IFNβ to a lesser extent, IFNγ [27]. IFITM1 was initially identified as Leu13, a leukocyte antigen that is part of a membrane complex involved in the transduction of antiproliferative and homotypic adhesion signals in lymphocytes [28,29]. IFITM1 is also known to play a critical role in blocking early stages of viral replication and it potently restricts entry and infections by a number of highly pathogenic viruses, including HIV-1, filovirus, and SARS coronavirus [30]. More recently, there has been increasing evidence to suggest that high expression of IFITM1 plays a role in the progression of several cancers including head and neck cancer, serous ovarian cancer, gastric cancer and colorectal cancer [29,31-33]. However, its role in breast cancer or endocrine resistance is not known.

Phospholipid scramblase 1 (PLSCR1) is a 35 kDa multiply palmitoylated protein that is localized in the cell membrane and is responsible for mediating the translocation of negatively-charged phospholipids from the inner-leaflet of the plasma membrane to the outer-leaflet during cellular injury and apoptosis [34,35]. PLSCR1 is highly induced by type 1 IFNs and it plays an antagonistic role in leukemia [36] and ovarian cancer [37]; however, its role in breast cancer is unknown.

In the present study, we investigated the functional role of IFITM1 and PLSCR1 in AI-resistant breast cancer. We found that IFITM1 and PLSCR1 were constitutively overexpressed in AI-resistant MCF-7:5C breast cancer cells and AI-resistant tumors and that knockdown of IFITM1 significantly reduced their ability to proliferate, invade, and migrate. Most interestingly, we found that suppression of IFITM1 sensitized AI-resistant MCF-7:5C cells to estradiol-induced cell death. Suppression of IFNα level via siRNA knockdown of IRF-7 confirmed that the constitutive overexpression of IFITM1 and PLSCR1 in the resistant cells was driven by increased intracellular levels of IFNα. Further analysis using neutralizing antibody against IFNAR and siRNA knockdown of STAT1 and STAT2 revealed complete suppression of IFITM1, PLSCR1, p-STAT1 and p-STAT2

in the resistant cells, thus confirming a critical role for canonical IFNα signaling in the regulation of IFITM1 and other ISGs in the resistant cells.

Methods

Reagents

RPMI 1640 and fetal bovine serum (FBS) were obtained from Invitrogen Inc. (Grand Island, NY, USA). The antibiotic/antimycotic solution (containing 10,000 U/mL penicillin and 10 mg/mL streptomycin, 25 μg/mL of Fungizone®), NEAA (MEM Non-Essential Amino Acids), L-glutamine, and TrypLE (containing trypsin and ethylenediaminetetraacetic acid (EDTA)) were obtained from Invitrogen. Insulin (bovine pancrease), human recombinant interferon-alpha (IFNα) and 17β-estradiol (E_2) were obtained from Sigma-Aldrich Co. (St. Louis, MO, USA). E_2 was dissolved in ethanol at a stock concentration of 1 μM (10^{-6} M) and stored at −20°C. Anti-PLSCR1, anti-IFITM1, anti-IRF-7, anti-STAT1, anti-Bax, anti-Noxa, anti-PUMA, anti-p53, anti-p21, anti-Lamin B, anti-IFNAR (α – IFNAR), anti-p-STAT2 (Tyr690) and anti-ERα antibodies were purchased from Santa Cruz Technology Inc. (Santa Cruz, CA, USA); anti- poly ADP ribose polymerase (PARP) and anti-p-STAT1 (Y701) were purchased from Cell Signaling Technology (Beverly, MA, USA), and anti-β-actin was purchased from Sigma-Aldrich. PLSCR1 monoclonal antibody 4D2 was a kind gift from Dr. Peter Sims (University of Rochester, NY, USA).

Cell lines and culture conditions

The ER-positive hormone-dependent human breast cancer cell lines, MCF-7 and T47D, were originally obtained from the American Type Culture Collection (Manassas, VA, USA) and were maintained in full serum medium composed of RPMI-1640 medium, 10% FBS, 2 mM glutamine, penicillin at 100 U/mL, streptomycin at 100 μg/mL, 1× NEAA (Invitrogen) and bovine insulin at 6 ng/mL (Sigma-Aldrich). The long term estrogen deprived human breast cancer cell line MCF-7:5C [9,12] was cloned from parental MCF-7 cells following long term (>12 months) culture in estrogen-free medium composed of phenol red-free RPMI-1640, 10% FBS treated three times with dextran-coated charcoal (SFS), 2 mM glutamine, bovine insulin at 6 ng/mL, penicillin at 100 U/mL, streptomycin at 100 μg/mL, and 1× NEAA. The MCF-7:5C cell line was used as a model of AI resistance because it proliferates despite being deprived of estrogen [9,12]. Cells were cultured at 37°C under 5% CO_2 and were subcultured every three to four days.

MTT assay

For determining cell viability, the 3-(4,5-dimethylthiazol-2-Yl)-2,5-diphenyltetrazolium bromide (MTT) assay was used. MCF-7 and MCF-7:5C cells were seeded onto 24-well plates at a density of 5×10^4 cells per well in culture media and incubated until about 60% to 70% confluency, before the start of experimental treatments. The stock solution of E_2 was diluted in the culture medium before addition to each well at desired final concentrations, and the treatments usually lasted 24 hours. Following the treatments as indicated, 50 μl of MTT solution (at 5 mg/mL) was added to each well at a final concentration of 500 μg/mL, and the mixture was further incubated for four hours at 37°C. An aliquot (500 μl) of the solubilizing solution (dimethyl sulfoxide (DMSO):ethanol, 1:1, v:v) was then added to each well, and the absorbance was read with a UV max microplate reader (Molecular Device, Palo Alto, CA, USA) at 560 nm. The relative cell density was expressed as a percentage of the control that was not treated with E_2.

Western blotting

For Western blotting, cells were washed first and then suspended in 100 μL lysis buffer (RIPA buffer, 150 mM NaCl, 1.0% IGEPAL® CA-630, 0.5% sodium deoxycholate, 0.1% SDS, 50 mM Tris, pH 8.0, protease inhibitor cocktail, and phosphatase inhibitor). The amount of proteins was determined using the Bio-Rad protein assay (Bio-Rad, Hercules, CA, USA). An equal amount of proteins was loaded in each lane. The proteins were separated by 4% to 12% SDS–polyacrylamide gel electrophoresis (SDS–PAGE) and electrically transferred to a polyvinylidene difluoride membrane (Bio-Rad). After blocking the membrane using 5% non-fat milk, target proteins were detected using specific antibodies. Thereafter, horseradish peroxidase (HRP)-conjugated anti-rabbit (or anti-mouse) immunoglobulin G (IgG) was applied as the secondary antibody and the positive bands were detected using Amersham ECL Plus Western blotting detection reagents (GE Health Care, Piscataway, NJ, USA).

Nuclear and cytoplasmic fractionation

For protein localization, the nuclear and cytosolic fractions were prepared using the cytosolic/nuclear fractionation kit obtained from Biovision Inc. (Mountain View, CA, USA), by following the instructions of the manufacturer. Briefly, cells were suspended in hypotonic buffer and lysed with the proprietary detergent from the kit. Samples were spun at 800 × *g* for 10 minutes at 4°C. The supernatant was collected, spun five minutes at 16,000 × *g* to remove any remaining nuclei, and then transferred to a new microtube (cytosolic protein fraction). The original pellet was resuspended in the nuclear extraction buffer and then incubated on ice for 40 minutes with occasional vortexing. After salt extraction, the nuclear pellet was centrifuged at 16,000 × *g* for 10 minutes, and the supernatant was saved as the nuclear extract. Extracts were stored in aliquots in −80°C until use.

Annexin V staining for apoptosis

An annexin V–fluorescein isothiocyanate (FITC)-labeled Apoptosis Detection Kit I (Pharmingen, San Diego, CA, USA) was used to detect and quantify apoptosis by flow cytometry according to the manufacturer's instructions. In brief, MCF-7:5C cells (1×10^6 cells/mL) were seeded in 100-mm dishes and cultured overnight in estrogen-free RPMI 1640 medium containing 10% SFS. The next day, cells were treated with <0.1% ethanol vehicle (control) and E_2 (1 nM) for 96 hours and then harvested in cold PBS (Invitrogen) and collected by centrifugation for 10 minutes at 500 × *g*. Cells were then resuspended at a density of 1×10^6 cells/mL in 1 × binding buffer (HEPES buffer, 10 mM, pH 7.4, 150 mM NaCl, 5 mM KCl, 1 mM MgCl2 and 1.8 mM CaCl2) and stained simultaneously with FITC-labeled annexin V (25 ng/mL; green fluorescence) and propidium iodide (PI) (50 ng/mL). PI was provided as a 50 μg/mL stock (Pharmingen) and was used as a cell viability marker. Cells were analyzed using the BD LSR II flow cytometer (BD Bioscience, San Jose, CA, USA), and the data were analyzed with CellQuest software.

Immunofluorescence microscopy

Cells grown on glass coverslips were washed in PBS and fixed with 4% formaldehyde in PBS for 30 minutes. After permeabilization by 0.2% Triton X-100 in PBS for 5 minutes, cells were incubated with 0.1 mg/mL RNAse in 2% whole goat serum/PBS for 30 minutes at 37°C, followed by incubation with PLSCR1 (4D2) or IFITM1 antibody, 5 μg/mL in 2% goat serum/PBS (Jackson Immuno Research Labs Inc., West Grove, PA, USA) for one hour. Cells were stained with FITC-conjugated labeled goat anti-mouse IgG, 4 μg/mL in PBS for one hour, followed by nuclear counterstain with 4′,6-diamidino-2-phenylindole (DAPI) 0.1 μg/mL in PBS for 10 minutes. Coverslips were mounted on glass slides with Vectashield Mounting medium (Vector Laboratories, Burlingame, CA, USA), and samples were analyzed on a Bio-Rad MRC-1024 laser scanning confocal microscope equipped with a Zeiss X60 objective. Images were collected using Bio-Rad's Laser Sharp software. Specificity of staining observed for PLSCR1 mab 4D2 was evaluated by cell staining with the identical concentration of an isotype-matched antibody.

Cell cycle analysis

MCF-7:5C cells were transfected with siCon, siPLSCR1 or siIFITM1 for 72 hours and then harvested by trypsinization and washed once with phosphate-buffered saline (PBS, pH 7.4). After centrifugation, cells were resuspended in 1 mL of 0.9% NaCl, followed by addition of 2.5 mL of ice-cold 90% ethanol. After incubation at room temperature for 30 minutes, cells were centrifuged and the supernatant was removed. Cells were resuspended in 1 mL PBS containing 50 μg/mL PI and 100 μg/mL ribonuclease A and incubated at 37°C for 30 minutes. Flow cytometric analyses were performed using the BD LSR II flow cytometer (BD Bioscience, San Jose, CA, USA).

Enzyme-linked immunosorbent assay

Measurement of human interferon-α (IFNα) was conducted by enzyme-linked immunosorbent assay (ELISA) (PBL Interferon Source, Piscataway, NJ, USA). One million MCF-7 or MCF-7:5C cells were seeded in six-well plates and allowed to acclimatize overnight. They were then treated with 250 U/mL human recombinant IFNα for 24 hours. Cells and supernatants were harvested after 24 hours and kept at −80°C until analysis. Protein was extracted by sonication in RIPA buffer supplemented with protease and phosphatase inhibitors. Supernatants and lysates were purified by centrifugation and analyzed for the presence of IFNα according to the manufacturer's instructions.

IFNAR neutralization

In order to achieve neutralization of type 1 interferon, IFNAR, MCF-7 and MCF-7:5C cells were pretreated with 5 μg/mL anti-IFNAR1/2/MMHAR2 from Millipore, Temecula, CA, USA (cat# MAB1155) for four hours and then treated overnight with 20 U/mL human recombinant IFNα (Sigma) or 1 nM E_2 (Sigma) where indicated. Cells were harvested by cell scraping for Western blot and by trypsinization for cell viability analysis with trypan blue count.

Small interfering RNA transfections

For small interfering RNA (siRNA) knockdown experiments, MCF-7:5C and MCF-7 cells were transiently transfected with PLSCR1-siRNA (h) (siPLSCR1), IFITM1-siRNA (h) (siIFITM1), STAT1-siRNA (h) (siSTAT1), STAT2-siRNA (h) (siSTAT2), IFNα2-siRNA (h) (siIFNα2), IRF-7 siRNA (h) (siIRF-7), Bax-siRNA (h) (siBax), Noxa-siRNA (h) (siNoxa), or nontarget siRNA (siCon). The siPLSCR1 (cat# sc-44028), siIFITM1 (cat# sc-44549), siSTAT1 (cat# sc-44123), siSTAT2 (cat# sc-29492), siIFNα (cat# sc-63324), siIRF-7 (cat# 38011) and siRNA negative control (cat# sc-37007) were purchased from Santa Cruz Biotechnology, and siBax and siNoxa were purchased from Thermo Fisher Scientific (Pittsburg, PA, USA). All of the siRNAs were pools of three target-specific 20 to 25 nt siRNAs. MCF-7:5C or MCF-7 cells were seeded the night before transfection at a density of 30% to 50% confluence by the time of transfection. Twenty nmol of siPLSCR1, siIFITM1, siSTAT1 and siRNA negative control were used for transfection using Lipofectamine 2000 (Invitrogen, San Diego, CA, USA) according to the manufacturer's instructions. Transfected cells were maintained in culture for two days before harvesting and

further analyses. The efficiency of the siRNA knockdown was determined by Western blot analysis.

Short hairpin RNA (shRNA) knockdown

MCF-7:5C cells were transiently transfected with IFITM1-shRNA plasmid (h) (shIFITM1, cat# sc-44549-SH) or control-shRNA (shControl, cat# sc-108060) plasmid which were purchased from Santa Cruz Biotechnology. IFITM1 shRNA plasmid is a pool of three different shRNA plasmids. sc-44549-SHA: Hairpin sequence: GATCCCA CACTTCTCAAACCTTCATTCAAG AGATGAAGGT TTGAGAAGTGTGTTTTT. Corresponding siRNA sequences (sc-44549A): Sense: CACACUUCUCAAACC UUCAtt; Antisense: UGAAGGUUUGAGAAGUGUGtt. sc-44549-SHB: Hairpin sequence: GATCCCTGTGACA GTCTACCATATTTCAAGAGAATA TGGTAGACTGT CACAGTTTTT. Corresponding siRNA sequences (sc-44549B): Sense: CUGUGACAGUCUACCAUAUtt; Antisense: AUAUGGUAGACUGUCACAGtt. sc-44549-SHC: Hairpin sequence: GATCCCTGTCTACAGTGTCATTC ATTCAAGAGATGAATGACA CTGTAGACAGTTTTT. Corresponding siRNA sequences (sc-44549C): Sense: CUGUCUACAGUGUCAUUCAtt; Antisense: UGAAUG ACACUGUAGACAGtt. MCF-7:5C cells were seeded in six-well plates and at 50% to 70% confluency were transfected with 3 μg of shIFITM1 or shControl plasmid using Lipofectamine 2000 (Invitrogen, San Diego, CA, USA) according to the manufacturer's instructions. The transfected cells were incubated for 24 or 48 hours and the efficiency of the shRNA knockdown was determined by Western blot analysis and real-time PCR. The knockdown cells were then used for additional experiments.

Cell migration and invasion assay

Cell migration was measured in a Boyden chamber using Transwell filters obtained from Corning (Cambridge, MA, USA). MCF-7:5C cells (1×10^5) in 0.5 mL serum-free medium were placed in the upper chamber, and the lower chamber was loaded with 0.8 mL medium containing 10% charcoal-stripped FBS. Cells that migrated to the lower surface of the filters were stained with Wright Giemsa solution, and five fields of each well were counted after 24 hours of incubation at 37°C with 5% CO_2. Three wells were examined for each condition and cell type, and the experiments were repeated in triplicate. Cell invasion assay was performed using a Chemicon Cell Invasion kit (Chemicon International, Temecula, CA, USA) in accordance with the manufacturer's protocol. Cells (1×10^5/mL) were seeded onto 12-well cell culture chambers using inserts with 8 μM pore size polycarbonate membrane over a thin layer of extracellular matrix (ECM). Following incubation of the plates for 24 hours at 37°C, cells that had invaded through the ECM layer and migrated to the lower surface of the membrane were stained and counted under the microscope in at least ten different fields and photographed.

RNA isolation and RT-PCR analysis

Total RNA was isolated from cultured cells using the RNeasy® Mini Kit (Qiagen, Venlo, Netherlands) according to the manufacturer's procedure. First strand cDNA synthesis was performed from 2.5 μg total RNA using Super- Script Reverse Transcriptase (Invitrogen). cDNA was amplified in a 15-μl PCR mixture containing 1 mM dNTPs, 1× PCR buffer, 2.5 mM MgCl2 and 1 U DNA Taq polymerase (Promega, Madison, WI, USA) with 25 pmol of primers specific for human PLSCR1 (sense: 5′-CATTCACCGGGCTCTCTAC-3′; antisense: 5′-GGCA GCTGGGCA ATCTTGCA-3′), IFITM1 (sense: 5′-GGA TTTCGGCTTGTCCCGAG-3′; antisense: 5′- CCATG TGGAAGGGAGGGCTC-3′), IRF-9 (sense: 5′-TTCTG TCCCTGGTGTAGAGCCT-3′, antisense: 5′- TTTCAG GACACGATTATCACGG-3′), IRF-7 sense: 5′-GAGC CCTTACCTCCC CTGTTAT-3′, antisense: 5′′-CCAC TGCAGCCCCTCATAG-3′, IFI27 (sense: 5′- GCCT CTGG CTCTGCCGTAGTT-3′, antisense: 5′-ATGGA GGACGAGGCGATTCC-3′), IFIT1 (sense 5′-TCTCA GAGGAGCCTGGCTAA-3′, antisense 5′-CCAGACTA TCCTTGACCTGATGA-3′), MX1 (sense: 5′-CTTTCC AGTCCAGCTCGGCA-3′, antisense: 5′-AGCTGCTGG CCGTACGT CTG-3′), OAS1 sense: 5′-TGAGGTCC AGGCTCCACGCT-3′, antisense: 5′-GCAGGTC GGT GCACTCCTCG-3′), STAT1 (sense: 5′-GGCACCAGA ACGAATGAGGG-3′, antisense: 5′-CCATCGTGCACA TGGTGGAG-3′, STAT2 (sense: 5′-GCAGCACAATTT GCGGAA-3′, antisense: 5′-ACAGGTGTTTCGAGAAC TGGC-3′). The condition in the logarithmic phase of PCR amplification was as follows: five minutes initial denaturation at 94°C, one minute denaturation at 94°C, 35 seconds annealing at 67°C and 1.5 min extension at 72°C for 30 cycles. The number of amplification cycles during which PCR product formation was limited by template concentration was determined in pilot experiments. PUM1 was used as the internal control (sense: 5′-TCACCGAGGCCCCTCTGAACCCTA-3′; antisense: 5′-GGCAGTAATCTCCTTCTGCATCC T-3′). The reproducibility of the quantitative measurements was evaluated by three independent cDNA syntheses and PCR amplification from each preparation of RNA. Densitometric analysis was performed using Scion Image software (Scion Corp, Frederick, MD, USA), and the relative mRNA expression level was determined as the ratio of the signal intensity of the target to that of PUM1.

Tissue microarray construction and immunohistochemistry

Paraffin-embedded de-identified human breast cancer tissue samples were collected from the Tumor Bank facility at The Research Institute of Fox Chase Cancer

Center (Philadelphia, PA, USA) and the University of Kansas Medical Center (KUMC) and the protocols were reviewed and approved by the Institutional Review Board at Fox Chase Cancer Center and KUMC. The archived tumor samples were collected from patients (N = 40) who were initially treated with Arimidex and either responded or responded but then developed recurrence disease with an average time to disease progression (TTP) of 93 months. Patients provided written informed consent for the use of their tumor samples. Tissue microarray (TMA) slides were constructed from 40 matching primary and AI-resistant tumors using duplicate cores of 0.6 mm per tumor sample. Normal mammary tissue samples (N = 10) were also included on the TMA. For immunohistochemistry assays, tissue microarray slides were incubated at room temperature for 20 minutes with antibodies against IFITM1 (Santa Cruz Biotechnology) and PLSCR1 (Chemicon Inc.) applied at 1:100 dilution in antibody diluent (Dako, Carpenteria, CA, USA). A secondary anti-mouse antibody polymer conjugated with HRP (Dako) was applied for 30 minutes and 3,3′-diaminobenzidine (DAB) was used to produce visible, localized staining viewable with light microscopy. Sections without primary antibody served as negative controls. A semi-automated quantitative image analysis system, ACIS II (ChromaVision Medical Systems, Inc., San Juan Capistrano, CA, USA), was used to quantitate the staining of the TMA slides. For immunohistochemical analysis, the scores were determined by combining the proportion of positively stained tumor cells and the intensity of staining, giving rise to a Staining Index (SI) value for each sample. The proportion of positively stained tumor cells was graded as follows: 0 (<5% positively stained tumor cells), 1 (5% to 25% positive tumor cells), 2 (25% to 50% positive tumor cells), 3 (50% to 75% positive tumor cells) and 4 (>75% positive tumor cells). The intensity of staining was recorded on a scale of 0 (no staining), 1 (weak staining, light brown), 2 (moderate staining, yellowish brown) and 3 (strong staining, brown). The SI value was calculated as follows: SI = staining intensity × proportion of positively stained tumor cells. Scores were evaluated comparatively for the expression of IFITM1 and PLSCR1 in breast tumors by SIs (scored as 0, 1, 2, 3, 4, 6 or 9). An optimal cutoff value was identified, and the SI score of ≥6 was used to define tumors with high expression and SI ≤3 as tumors with low expression of IFITM1 and PLSCR1. Immunohistochemistry (IHC) analysis was also performed on MCF-7, T47D and MCF-7:5C breast cancer cells to detect IFITM1 and PLSCR1 protein expression. Cells were cultured in their appropriate medium, harvested by cell scraper before reaching confluence, washed twice with PBS and fixed in 10% formalin for 16 hours. Each cell line was pelleted and made into a cell block. One H & E stain and two IHC stains for PLSCR1 and IFITM1 were subsequently performed for each cell line. Pretreatments consisted of enzyme digestion or other heat mediated retrieval methods. Sections were stained on a Dako Autostainer using either an Envision PlusHRP polymer (Dako) or horse anti-mouse IgG-biotin (Vector Laboratories, Inc. Burlingame, CA, USA), streptavidin-HRP (Jackson Labs) and AEC (Dako), and counterstained in hematoxylin.

Statistical analysis

At least three separate experiments were performed for each measurement. All quantitative data were expressed as mean S.D. Comparisons between two groups were analyzed using two-way analysis of variance (ANOVA), with P value of <0.05 considered to be statistically significant.

Results

IFITM1 and PLSCR1 are constitutively overexpressed in AI-resistant human breast cancer cells and AI-resistant tumors

Microarray studies previously revealed that the interferon signaling pathway was altered in AI-resistant breast cancer cells compared with AI-sensitive cells [17]. To understand better the role of the interferon signaling pathway in AI-resistant breast cancer we measured the basal expression of two well-known interferon stimulated proteins, IFITM1 and PLSCR1, in AI-resistant MCF-7:5C breast cancer cells and AI-sensitive MCF-7 and T47D cells. Our data showed that IFITM1 and PLSCR1 were constitutively overexpressed at the protein (Figure 1A) and mRNA level (Figure 1B) in AI-resistant MCF-7:5C cells but were almost undetectable at the protein and mRNA level in AI-sensitive MCF-7 and T47D cells. Notably, we also found that several other ISGs including IFI27, IFIT1, OAS1, MX1, IRF-7, IRF-9, STAT1 and STAT2 were constitutively overexpressed in AI-resistant MCF-7:5C cells compared with MCF-7 cells (Additional file 1: Figure S1). Immunocytochemistry (ICC) staining of MCF-7, T47D and MCF-7:5C cells also showed that IFITM1 and PLSCR1 were overexpressed in MCF-7:5C cells compared to MCF-7 and T47D cells (Figure 1C). Next, we investigated the clinical significance of IFITM1 and PLSCR1 expression in AI-resistant (recurrence) breast cancer by performing IHC staining on normal breast tissue, primary breast tumors (N = 40) and AI-resistant recurrence breast tumors (N = 40). We found that IFITM1 and PLSCR1 proteins were overexpressed in 90% of the AI-resistant (recurrence) tumors (36 of 40 samples) compared with only 20% of the primary tumors (8 out of 40 samples); however, in normal breast tissue PLSCR1 and IFITM1 proteins were undetectable (Figure 1D). As shown in Table 1, stained slides were scored in terms of intensity and distribution.

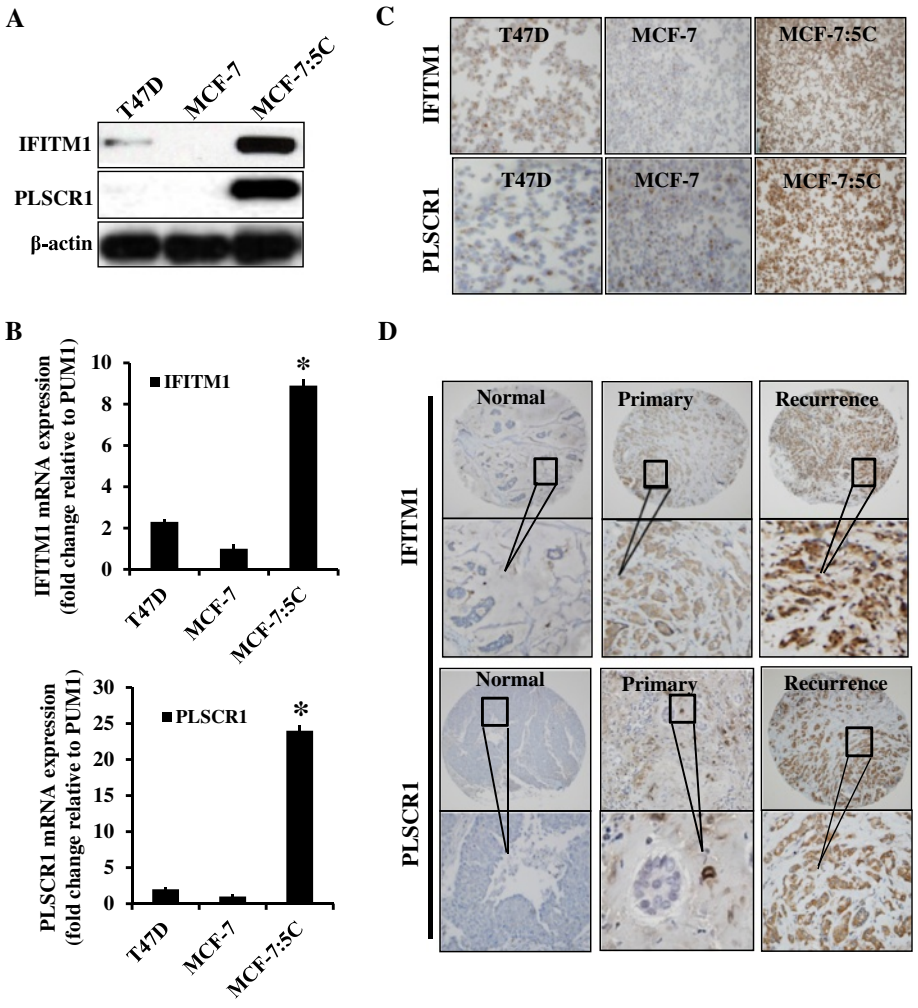

Figure 1 IFITM1 and PLSCR1 expression in endocrine-sensitive and AI-resistant breast cancer cells. (A) The cell extracts isolated from the indicated cell lines (endocrine sensitive-T47D/MCF-7, AI-resistant MCF-7:5C) were detected by Western blot analysis for PLSCR1 and IFITM1 protein and β-actin as a loading control. **(B)** Total RNA was extracted from each cell line and IFITM1 (upper panel) and PLSCR1 (lower panel) mRNA was determined by real-time PCR. Fold change was determined for each cell line relative to the internal control gene PUM1. Each value is a mean ± SD from three experiments. *P <0.05 **(C)** Relative intensity of the IFITM1 or PLSCR1 in T47D, MCF-7 and MCF-7:5C cells were determined by immunocytochemistry (ICC) staining. **(D)** Immunohistochemistry (IHC) staining for IFITM1 or PLSCR1 was performed on tissue microarrays generated from normal breast tissue (left panel), primary breast tumor tissue (middle panel) and recurrence breast tumor tissue (right panel). For immunohistochemical analysis, the scores were determined by combining the proportion of positively stained tumor cells and the intensity of staining, giving rise to a Staining Index (SI) value for each sample. The proportion of positively stained tumor cells was graded as follows: 0 (<5% positively stained tumor cells), 1 (5% to 25% positive tumor cells), 2 (25% to 50% positive tumor cells), 3 (50% to 75% positive tumor cells) and 4 (>75% positive tumor cells). Representative photomicrographs were taken using a phase-contrast microscope (original magnification, ×200). AI, aromatase inhibitor; IFITM1, interferon induced transmembrane protein1; PLSCR1, phospholipid scramblase 1; SD, standard deviation.

Normal breast tissue showed no staining for IFITM1 or PLSCR1 (SI score = 0); primary tumors showed medium staining for IFITM1 and PLSCR1 which correlated with low expression (SI score of ≤3); and AI-resistant (recurrence) tumors showed very strong staining for IFITM1 and PLSCR1 which correlated with high expression of both proteins (SI score of ≥6). Taken together, these results demonstrate that interferon regulated genes are constitutively overexpressed in AI resistant breast cancer and they suggest that interferon signaling might be deregulated in the resistant cells.

IFITM1 and PLSCR1 are localized primarily in the cytoplasm in AI-resistant cells

Previous studies have shown that IFITM1 and PLSCR1 localize primarily in the plasma membrane [38,39]; however, these proteins can also translocate to the nucleus and bind genomic DNA. We examined the cellular

Table 1 Staining intensity of IFITM1 and PLSCR1 expression in normal and breast tumor tissues

Tissue Type	Staining Intensity	IFITM1	PLSCR1
Normal tissues	No stain	10/10	9/10
	Weak	0/10	1/10
	Strong	0/10	0/10
Primary tumors	No stain	32/40	32/40
	Weak	8/40	8/40
	Strong	0/40	0/40
Recurrence tumors	No stain	0/40	0/40
	Weak	4/40	2/40
	Strong	36/40	36/40

Staining intensity was calculated for IFITM1 and PLSCR1 expression in normal breast tissue (N = 10), primary breast tumors (N = 40), and AI-resistant/recurrence breast tumors (N = 40) as described in Methods. AI, aromatase inhibitor; IFITM1, interferon induced transmembrane protein1; PLSCR1, phospholipid scramblase 1.

localization of IFITM1 and PLSCR1 in AI-resistant MCF-7:5C cells and AI-sensitive MCF-7 cells using immunofluorescence (IF). Our results showed that IFITM1 (Figure 2A) and PLSCR1 (Figure 2B) were highly expressed in resistant MCF-7:5C cells compared to parental MCF-7 cells and that both proteins localized primarily in the cytoplasm with minor nuclear localization. Western blot analysis of fractionated MCF-7 and MCF-7:5C cells confirmed that IFITM1 and PLSCR1 were overexpressed in MCF-7:5C cells compared with MCF-7 cells and that both proteins were localized primarily in the cytoplasm with some nuclear localization observed for IFITM1 (Figure 2C).

IFNα drives overexpression of IFITM1 and PLSCR1 in AI-resistant MCF-7:5C cells

Binding of interferon alpha (IFNα) to the IFN alpha Type 1 receptor (IFNAR1) complex initiates a signaling cascade comprising phosphorylation and dimerization of STAT1/2 molecules followed by their translocation to the nucleus, where they regulate the expression of ISGs. To investigate whether constitutive overexpression of IFITM1 and PLSCR1 in resistant MCF-7:5C cells is driven by the canonical IFNα signaling pathway, we first measured intracellular IFNα level in the supernatant and lysate of AI-resistant MCF-7:5C and parental MCF-7 cells using ELISA. As shown in Figure 3A, IFNα protein level was significantly higher in the supernatant and lysate of resistant MCF-7:5C cells compared to parental MCF-7 cells. IFNα mRNA expression was also significantly elevated in resistant MCF-7:5C cells compared to MCF-7 cells (Figure 3B). Next, we used a neutralizing antibody against the type 1 interferon receptor, IFNAR1/2, to see whether blocking the receptor reduces IFITM1 and PLSCR1 expression in the resistant cells. As shown in Figure 3C, the IFNAR1/2 neutralizing antibody, α-IFNAR-Ab, markedly reduced the basal expression of

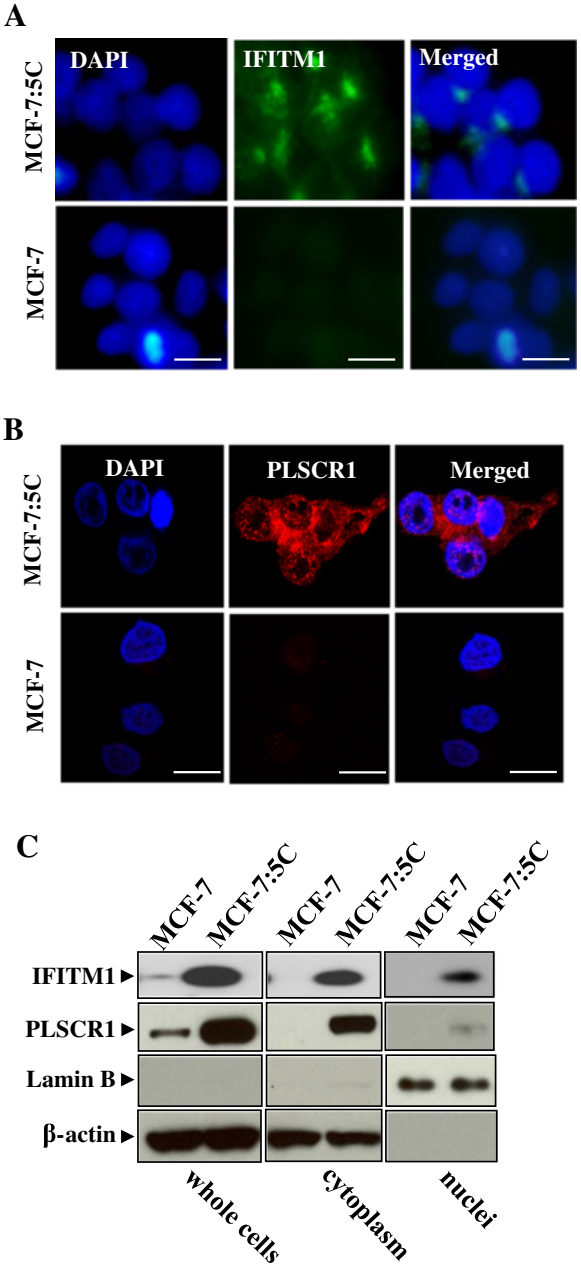

Figure 2 Subcellular localization of IFITM1 and PLSCR1 in MCF-7 and MCF-7:5C breast cancer cells. Immunofluorescence staining was performed on parental MCF-7 and AI-resistant MCF-7:5C cells to assess the subcellular localization of **(A)** IFITM1 or **(B)** PLSCR1. Cells were seeded in six-well chamber slides and after 24 hours were analyzed for immunofluorescence staining. **(C)** The whole-cell lysates, nuclear and cytoplasmic/membrane fractions of MCF-7 and MCF-7:5C cells were detected by Western blot analysis for IFITM1 or PLSCR1 protein with β-actin and lamin B as controls. AI, aromatase inhibitor; IFITM1, interferon induced transmembrane protein1; PLSCR1, phospholipid scramblase 1.

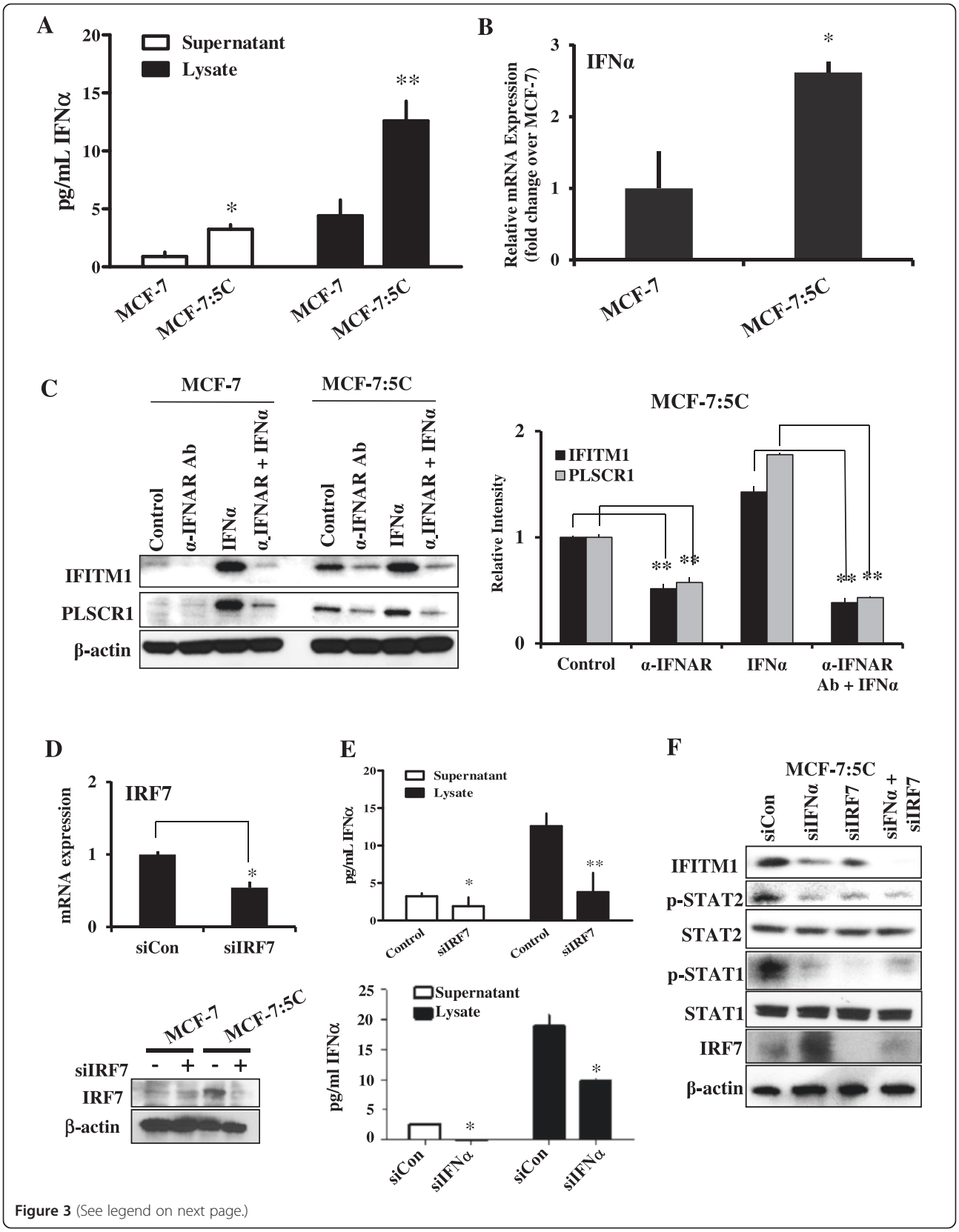

Figure 3 (See legend on next page.)

(See figure on previous page.)
Figure 3 Elevated level of intracellular IFNα drives constitutive overexpression of IFITM1. (A) ELISA analysis of baseline expression of IFNα in cell lysates and supernatant in MCF-7:5C and MCF-7 cells. Cells (1×10^6) were seeded in a six-well plate in their standard culture media and after 48 hours cells were harvested and the supernatant and pellets were collected. Cell pellets were then lysed by sonication in RIPA buffer containing protease inhibitors. IFNα was measured in the supernatants and cell lysates by ELISA as described in Methods. All the illustrated data were performed in duplicate and are expressed as mean values of three independent experiments ± SD. **(B)** Measurement of IFNα mRNA was determined by real-time PCR. Fold change was calculated by means of the ΔΔCT method using PUM1 as an internal control. Values are displayed as relative to MCF-7 cells and are means of triplicate measurements ± SD in three independent experiments. **(C)** Blockade of type 1 interferon receptor, IFNAR1, using neutralizing antibody MAB1155, in MCF-7 and MCF-7:5C cells. Cells were pretreated with 5 μg/mL anti-IFNAR1/2 for 4 hours and then treated with 20 U/mL human recombinant IFNα for 24 hours. Cells were analyzed by Western blot to assess IFITM1, PLSCR1 and β-actin protein level. Results shown are representative of three independent experiments. The protein levels were quantified using the ImageJ software (downloaded from NIH website [40]) and normalized as the ratio related to β-actin. *P <0.05 or **P <0.01 versus control. **(D)** siRNA knockdown of IRF-7 expression in MCF-7:5C cells. Cells were transiently transfected with siRNA targeting IRF-7 and after 24 hours knockdown was verified at the mRNA and protein level via RT-PCR and Western blot analyses. **(E)** Effect of IRF-7 knockdown on IFNα expression in resistant MCF-7:5C cells. Cells were transiently transfected with siRNA targeting IRF-7. After 24 hours, IFNα mRNA and IFNα protein expression were determined by real-time PCR and ELISA, respectively. Data shown for RT-PCR is expressed as fold change over cells transfected with control siRNA. Values are displayed as means ± SD of three independent experiments performed in triplicate. *P <0.05 or **P <0.01. **(F)** The effect of IFNα or IRF-7 knockdown on IFITM1, p-STAT2, STAT2, p-STAT1, STAT1, and IRF-7 protein expression in resistant MCF-7:5C cells. Cells were transiently transfected with siIFNα, siIRF-7 or siCon for 48 hours and Western blot analysis was performed on lysates. Results shown are representative of two independent experiments IFITM1, interferon induced transmembrane protein1; IFNAR1, IFN alpha Type 1 receptor; NIH, National Institutes of Health; PLSCR1, phospholipid scramblase 1; SD, standard deviation.

IFITM1 and PLSCR1 in resistant MCF-7:5C cells and it completely blocked exogenous IFNα induction of IFITM1 and PLSCR1 in parental MCF-7 cells. We further tested whether suppression of the intracellular IFNα level is capable of reducing IFITM1 and PLSCR1 expression in the resistant cells. Induction of IFNα production is primarily controlled at the transcription level by the transcription factor IRF-7, hence, we performed siRNA knockdown of IRF-7 to suppress intracellular IFNα level in the resistant cells. We should note that IRF-7 mRNA (Additional file 1: Figure S1) and IRF-7 protein (Figure 3D, bottom panel) were constitutively overexpressed in resistant MCF-7:5C cells compared to parental MCF-7 cells. As shown in Figure 3D, siIRF-7 markedly reduced IRF-7 mRNA and protein expression in resistant MCF-7:5C cells and it significantly decreased IFNα protein (Figure 3E, top) and IFNα mRNA level (data not shown) in these cells. In addition, we found that siRNA knockdown of IFNα reduced its protein level in the supernatant by 100% and in the lysate by 50% (Figure 3E, bottom). Furthermore, we found that siRNA knockdown of both IFNα and IRF-7 completely reduced IFITM1, PLSCR1, p-STAT1 and p-STAT2 protein expression in the resistant cells (Figure 3F). Taken together, these data indicate that IFNα is significantly elevated in the supernatant and lysate of AI-resistant MCF-7:5C breast cancer cells and that activation of the canonical IFNα/IFNAR signaling pathway plays a critical role in driving the constitutive overexpression of IFITM1 and other ISGs in the resistant cells.

Dysregulation of type 1 IFNα signaling in AI-resistant MCF-7:5C cells

Since IFITM1 and PLSCR1 were constitutively overexpressed in the resistant cells, we wanted to assess the functional integrity of the interferon signaling pathway in the resistant cells compared to parental MCF-7 cells. Cells were treated with 1,000 U/ml of IFNα for 0 to 24 hours and protein levels of IFITM1, PLSCR1, STAT1, p-STAT1 (Y701), STAT2, p-STAT2 (Tyr690) and IFNAR1 were determined by Western blot analysis. We found that in parental MCF-7 cells, IFNα treatment significantly increased PLSCR1, IFITM1, STAT1, p-STAT1, STAT2, p-STAT2 and IFNAR1 protein expression in a time-dependent manner with maximum induction of PLSCR1, IFITM1, STAT1, STAT2 and IFNAR1 observed at 24 hours and for p-STAT1 and p-STAT2 at 30 minutes (Figure 4A, left panel). In contrast, we found that IFITM1 and PLSCR1 were constitutively overexpressed in resistant MCF-7:5C cells and that treatment with exogenous IFNα only increased p-STAT and p-STAT2 protein; however, it did not further increase the level of IFITM1, PLSCR1 or STAT1 at any of the time points except at 24 hours where we detected a <2-fold increase in PLSCR1 and IFITM1 (Figure 4A, right panel; Additional file 2: Figure S2). A similar trend was observed at the mRNA level for IFITM1, PLSCR1 and STAT1 in resistant MCF-7:5C cells compared to parental MCF-7 cells (Additional file 3: Figure S3). In MCF-7 cells, exogenous IFNα induced IFITM1 mRNA by approximately 374-fold, PLSCR1 mRNA by approximately 9-fold and STAT1 mRNA by approximately 11-fold at 48 hours, whereas, in resistant MCF-7:5C cells, treatment with IFN-α induced IFITM1 mRNA by approximately 3-fold, PLSCR1 mRNA by approximately 2-fold, and STAT1 mRNA by approximately 2-fold (Additional file 3: Figure S3). These findings suggest that IFITM1, PLSCR1 and STAT1 are constitutively overexpressed in the resistant cells due to dysregulation of interferon signaling, whereas, in parental MCF-7 cells, the interferon signaling pathway

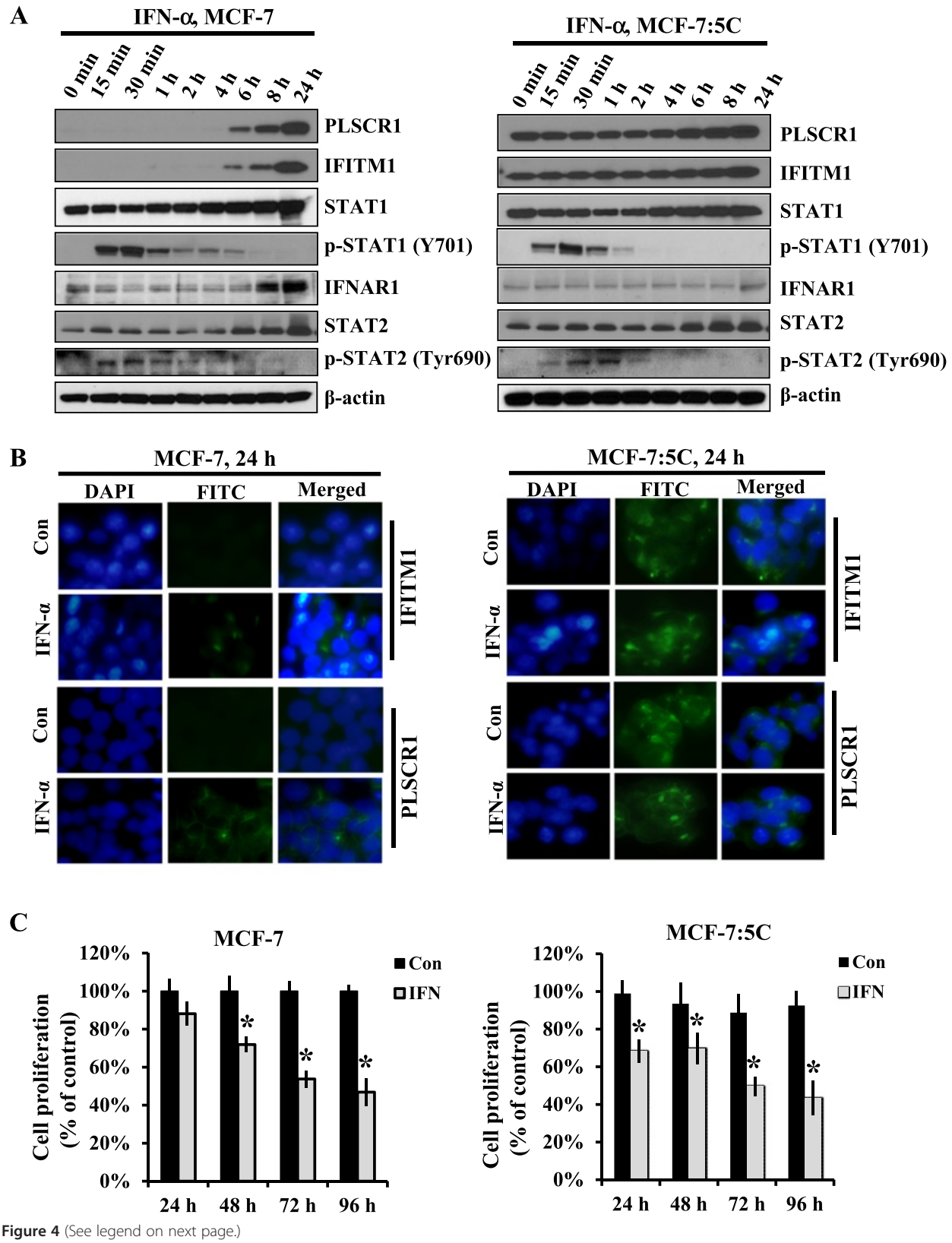

Figure 4 (See legend on next page.)

(See figure on previous page.)
Figure 4 Activation of interferon signaling pathway in parental MCF-7 and AI-resistant MCF-7:5C cells in response to INFα. (A) MCF-7 (left panel) and MCF-7:5C (right panel) cells were incubated with IFNα (1000 U/ml) for the indicated time points. The cell extracts were examined by Western blotting using anti-PLSCR1, anti-IFITM1, anti-STAT1, anti-phospho-STAT1 (Y701), anti-IFNAR1, anti-STAT2, anti-phospho-STAT2 (Tyr690) and anti-β-actin. **(B)** Cellular localization of IFITM1 and PLSCR1 in MCF-7 and MCF-7:5C cells following IFNα treatment. Cells were treated for 24 hours with IFNα (1000 U/ml) and then analyzed for immunofluorescence staining of IFITM1 and PLSCR1 (original magnification 200×). **(C)** MCF-7 and MCF-7:5C cells were treated with IFNα (1000 U/ml) for 24, 48, 72 and 96 hours and cell proliferation was measured by the MTT assay. All the illustrated data are expressed as mean values of three independent experiments. Standard deviations are shown. *P <0.05; **P <0.01. AI, aromatase inhibitor; IFITM1, interferon induced transmembrane protein1; IFNAR1, IFN alpha Type 1 receptor; MTT, 3-(4,5-dimethylthiazol-2-Yl)-2,5-diphenyltetrazolium bromide; PLSCR1, phospholipid scramblase 1; STAT1,2, Signal transducer and activator of transcription 1,2.

is functionally intact and the induction of IFITM1 and other ISGs is tightly controlled.

Next, we examined whether IFNα treatment facilitated translocation of IFITM1 and PLSCR1 from the cytoplasm to the nucleus. As shown in Figure 4B, treatment with IFNα significantly increased IFITM1 and PLSCR1 protein expression in MCF-7 cells but not in AI-resistant MCF-7:5C cells; however, it did not cause IFITM1 or PLSCR1 to translocate from the cytoplasm to the nucleus in either cell line. Interestingly, cell viability assay showed that IFNα treatment significantly inhibited the proliferation of both MCF-7 and MCF-7:5C cells in a time-dependent manner (Figure 4C) and that AI-resistant MCF-7:5C cells were slightly more sensitive to the growth inhibitory effect of IFNα than MCF-7 cells.

Knockdown of IFITM1 induces cell death in AI-resistant MCF-7:5C breast cancer cells

Previous studies have reported that IFITM1 and PLSCR1 exert both antiproliferative and proliferative effects in different types of cancer cells; however, their functional significance in AI-resistant breast cancer cells is not known. To determine the functional significance of IFITM1 and PLSCR1 in AI-resistant MCF-7:5C breast cancer cells, we transiently transfected MCF-7:5C cells with siRNA targeting IFITM1 or PLSCR1 and we assessed the effect of their knockdown on cell proliferation, cell death and cell cycle progression. Western blot analysis confirmed knockdown of IFITM1 and PLSCR1 protein in AI-resistant MCF-7:5C cells at 24, 48 and 72 hours post-transfection (Figure 5A). Cell viability assay showed that knockdown of IFITM1, but not PLSCR1, significantly inhibited the proliferation of AI-resistant MCF-7:5C cells at 72 hours relative to control cells and it markedly enhanced the inhibitory effect of E_2 in these cells (Figure 5B). The growth inhibitory effect of IFITM1-knockdown in AI-resistant MCF-7:5C cells was due to cell death, as demonstrated by annexin V-PI staining (Figure 5C). Specifically, knockdown of IFITM1 in MCF-7:5C cells increased the total number of dead cells from 10.8% (siCon) to 35.1% in the IFITM1-knockdown cells and it enhanced the apoptotic effect of E_2 from 34.6% to 57.1% (Figure 5C). We should note that the ability of E_2 to induce cell death in AI-resistant breast cancer cells has previously been reported by our laboratory [11,15,16]; however, this is the first study to show that suppression of IFITM1 enhances E_2-induced cell death in AI resistant breast cancer cells. Further analysis indicated that knockdown of IFITM1 significantly increased the expression of p21, Bax and Noxa in AI-resistant MCF-7:5C cells; however, it did not significantly alter p53 expression in these cells (Figure 5D). To validate the specificity and the biological function of IFITM1 in our resistant cells we used a second shRNA targeting IFITM1 (Additional file 4: Figure S4). We found that shRNA knockdown of IFITM1 induced poly ADP ribose polymerase (PARP) cleavage (Additional file 4: Figure S4A), reduced cell proliferation (Additional file 4: Figure S4B) and induced cell death in resistant MCF-7:5C cells which was further enhanced by the addition of E_2 (Additional file 4: Figure S4C). To confirm that IFNα was responsible for the dysregulation of IFITM1 and that blocking its function enhances E_2-induced cell death, we knockeddown IFNα expression in resistant MCF-7:5C cells and then treated the cells with E_2 for an additional 96 hours. As shown in Additional file 5: Figure S5, knockdown of IFNα significantly reduced the proliferation of MCF-7:5C cells and it significantly enhanced E_2-induced death in these cells at 96 hours. Furthermore, we found that blocking IFNAR1/2 with a neutralizing antibody also reduced the proliferation of MCF-7:5C cells and it markedly enhanced E_2-induced death in these cells at the same time point. These findings confirm that IFNα is responsible for the dysregulated expression of IFITM1 in the resistant cells and that blocking its function collaborates with E2 to enhance cell death in these cells. Furthermore, these findings suggest that IFITM1 overexpression provides a survival advantage to the resistant cells that allows them to grow in an estrogen-depleted environment and that knockdown of IFITM1 disrupts the survival pathway in these cells thus sensitizing them to cell death.

IFITM1 knockdown inhibits migration and invasion of AI-resistant MCF-7:5C cells

There is evidence that IFITM1 overexpression induces tumor resistance to natural killer (NK) cells in gastric

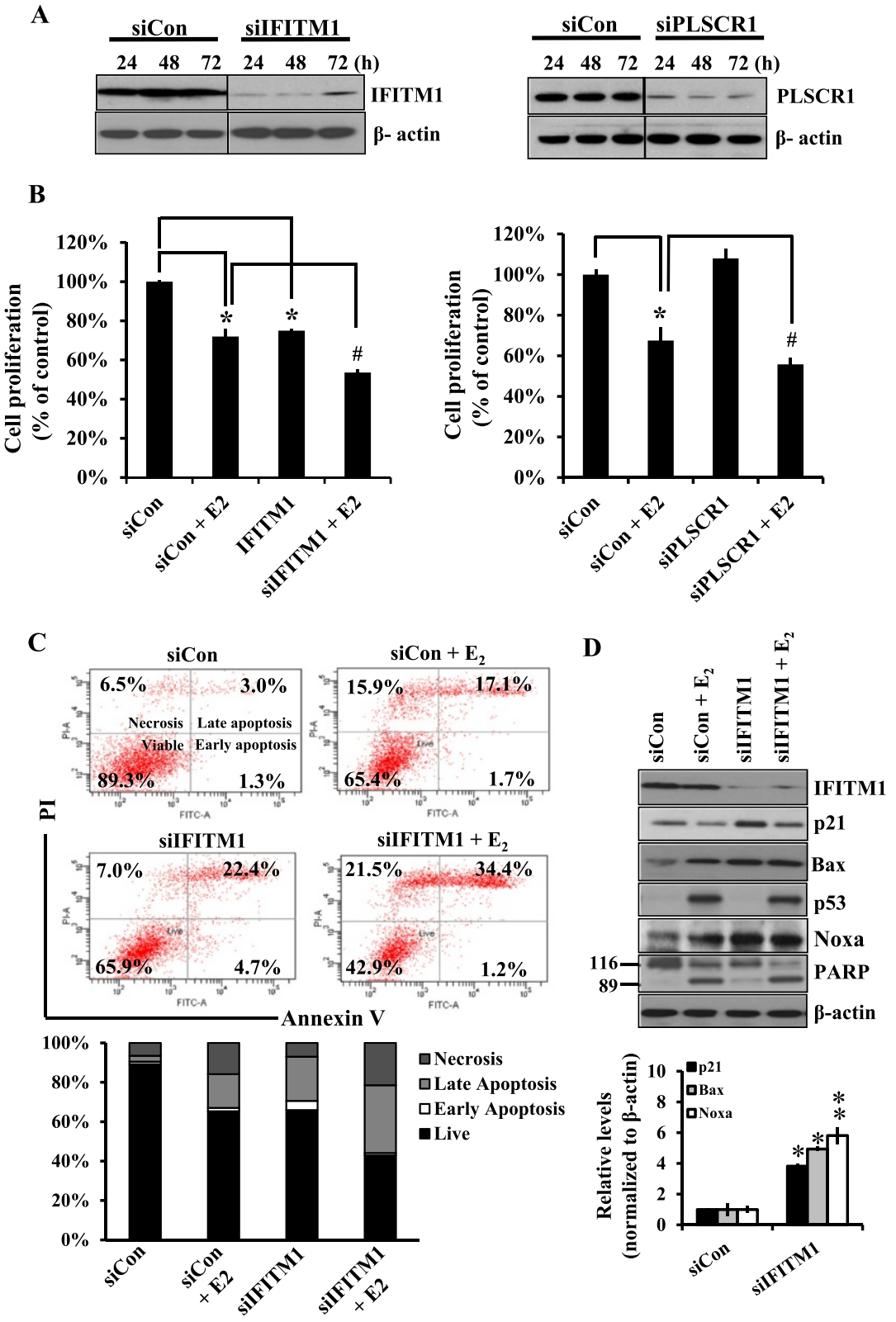

Figure 5 (See legend on next page.)

(See figure on previous page.)
Figure 5 IFITM1 knockdown increases cell death in AI-resistant breast cancer cells. (A) MCF-7:5C cells were transfected with control siRNA (siCon), IFITM1 siRNA (siIFITM1) or PLSCR1 siRNA (siPLSCR1) for 24, 48 and 72 hours and cell extracts were subject to Western blotting analysis to assess IFITM1 and PLSCR1 protein expression. **(B)** MCF-7:5C cells were transfected with siCon, siIFITM1 (left panel) or siPLSCR1 (right panel) for 24 hours and then treated with 1 nM E_2 for an additional 72 hours. Cell proliferation was measured by the MTT assay. All the illustrated data are expressed as mean values of three independent experiments. Standard deviations are shown. *P <0.05 versus control; #P <0.05 versus E_2 treatment. **(C)** MCF-7:5C cells were transfected with siCon or siIFITM1 and after 24 hours were exposed to E_2 (1 nM) for an additional 96 hours. Cells were then stained with annexin V-FITC and PI for detection of apoptosis as described in Methods. **(D)** Cells were treated as described above in **(C)** and were analyzed by Western blotting to assess IFITM1, p21, Bax, p53, Noxa and PARP protein expression. Membranes were stripped and reprobed for β-actin, which was used as a loading control. The protein levels for p21, Bax and Noxa were quantified using the ImageJ software (downloaded from the NIH website) and normalized as the ratio relate to β-actin. *P <0.05; **P <0.01. AI, aromatase inhibitor; E_2, 17β-estradiol; FITC, fluorescein isothiocyanate; IFITM1, interferon induced transmembrane protein1; IFNAR1, IFN alpha Type 1 receptor; MTT, 3-(4,5-dimethylthiazol-2-Yl)-2,5-diphenyltetrazolium bromide; NIH, National Institutes of Health; PARP, poly ADP ribose polymerase; PI, propidium iodide; PLSCR1, phospholipid scramblase 1.

tumor cells and it facilitates migration and invasion of gastric cancer cells [29]. In addition, overexpression of IFITM1 has been shown to promote head and neck tumor invasion by mediating the expression of matrix metalloproteinases 12 and 13 [32]. To investigate the role of IFITM1 in breast cancer progression, we examined the influence of IFITM1 knockdown on migration and invasion of AI-resistant MCF-7:5C breast cancer cells. Western blot and real-time PCR analysis confirmed that IFITM1 protein and mRNA expression suppressed by siRNA in MCF-7:5C cells compared with siCon-transfected cells (Figure 6A). Silencing of IFITM1 markedly reduced the migratory ability (Figure 6B) and invasion capacity (Figure 6C) of AI-resistant MCF-7:5C cells. The cell migration and invasion counted from 10 randomly selected areas per well at 24 hours showed that siRNA knockdown of IFITM1 inhibited migration by 54% (Figure 6B, bar graph) and invasion by approximately 78% (Figure 6C) compared with siCon-transfected cells. To confirm that the inhibitory effect of IFITM1 knockdown on migration and invasion was not due to cell death we measured apoptosis (via flow cytometry) and cell viability in IFITM1-knockdown MCF-7:5C cells at the same time point (24 hours) the migration and invasion assays were performed. As shown in Figure 6D, IFITM1 knockdown did not induce cell death (top panel) or reduce cell viability (bottom panel) at 24 hours; hence, its inhibitory effect on migration and invasion at 24 hours is not due to cell death. However, we should note that knockdown of IFITM1 does cause significant cell death at 72 hours; hence, migration and invasion would be inhibited at the later time points due to cell death. This result suggests that overexpression of IFITM1 enhances the ability of AI-resistant MCF-7:5C cells to migrate and invade and its suppression has the opposite effect.

STAT1 and STAT2 regulate IFITM1 and PLSCR1 expression in resistant MCF-7:5C cells

STAT1 and STAT2 are members of the signal transducers and activators of transcription family of transcription factors that play a pivotal role in regulating type I (α/β) and type II (γ) interferon signaling. In response to either IFNα or IFNβ stimulation, STAT1 and STAT2 form homodimers or heterodimers, move to the nucleus and activate the transcription of interferon response genes. Since IFITM1 and PLSCR1 are constitutively overexpressed in AI-resistant MCF-7:5C cells, we examined whether knockdown of STAT1 or STAT2 is capable of altering their expression in MCF-7:5C cells. AI-resistant MCF-7:5C cells were transiently transfected with control siRNA (siCon), STAT1 siRNA (siSTAT1) or STAT2 siRNA (siSTAT2) and the effect of knockdown on IFITM1 and PLSCR1 expression was assessed at 24 and 48 hours using Western blot analysis. As shown in Figure 7A (left panel), knockdown of STAT1 markedly reduced IFITM1 and PLSCR1 protein expression in resistant MCF-7:5C cells at 24 and 48 hours, and it significantly reduced the proliferation of MCF-7:5C cells, and it further enhanced the inhibitory effect of E_2 in these cells. STAT2 knockdown also reduced IFITM1 and PLSCR1 protein level in MCF-7:5C cells (Figure 7B, left panel), and it significantly enhanced the inhibitory effect of E_2 in these cells (Figure 7B, right panel). Furthermore, we found that knockdown of both STAT1 and STAT2 completely suppressed IFITM1 and PLSCR1 expression in resistant MCF-7:5C cells (Additional file 6: Figure S6), thereby confirming a critical role for STAT1 and STAT2 in the regulation of IFITM1 and PLSCR1 expression. Interestingly, we found that knockdown of proapoptotic Bax and Noxa enhanced IFITM1 and PLSCR1 expression in MCF-7:5C cells, however, the mechanism by which this occurs is currently not known (Figure 7C).

4-Hydroxytamoxifen inhibits IFITM1 expression in AI-resistant MCF-7:5C cells

Since knockdown of IFITM1 significantly enhanced E_2-induced cell death in AI-resistant MCF-7:5C cells, we next determined whether IFITM1 expression is regulated by the estrogen receptor (ERα). MCF-7:5C cells were treated with 1 nM E_2, 1 μM of 4-hydroxytamoxifen

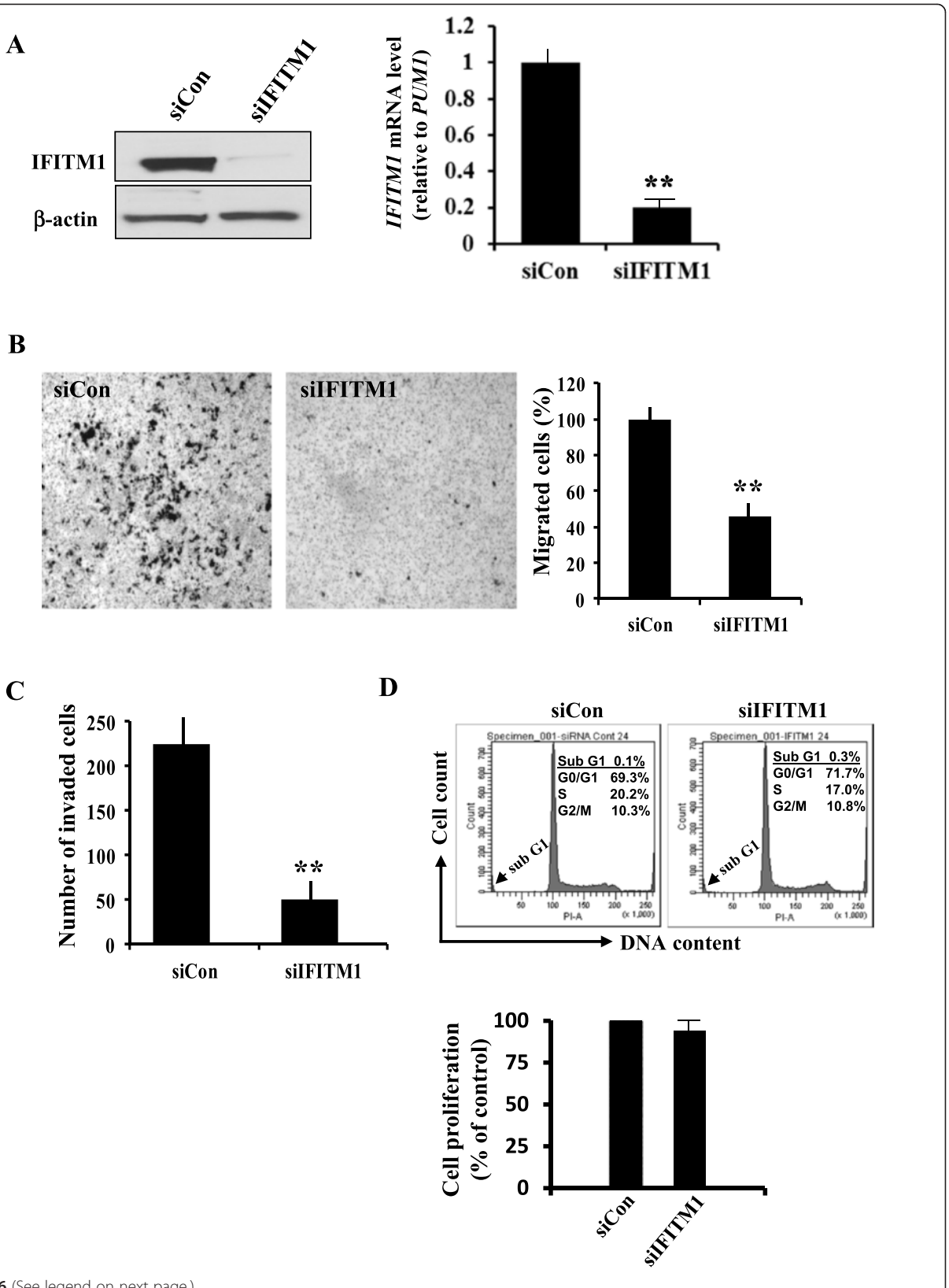

Figure 6 (See legend on next page.)

(See figure on previous page.)
Figure 6 IFITM1 knockdown decreases migration and invasion in AI-resistant MCF-7:5C breast cancer cells. (A) MCF-7:5C cells were transfected with control siRNA (siCon) or IFITM1 siRNA (siIFITM1) for 24 hours and knockdown of IFITM1 protein expression was confirmed by Western blot (right panel) and real-time PCR analyses (left panel). Standard deviations are shown. $^{**}P$ <0.01 versus siCon. **(B and C)** The effect of IFITM1 knockdown on cell migration **(B)** and invasion **(C)** was assessed by transwell migration assay and matrigel invasion assay. Cells that invaded through the Matrigel-coated transwells were fixed, stained, visualized by light microscopy and photographed. Quantitation of the Transwell assay is also shown (**B**, right panel). Ten random fields were counted per insert at 20X. $^{**}P$ <0.01. **(D)** Effect of IFITM1 knockdown on cell viability in resistant MCF-7:5C cells. Cells were transfected with siCon or siIFITM1 for 24 hours, then DNA content of cells was analyzed using flow cytometry as described in the Methods section. The arrow is sub G1 phase apoptosis. MTT assay (bottom panel) was also performed in the IFITM1-knockdown cells at 24 hours. All the illustrated data are expressed as mean values of three independent experiments. Standard deviations are shown. AI, aromatase inhibitor; IFITM1, interferon induced transmembrane protein1; MTT, 3-(4,5-dimethylthiazol-2-Yl)-2,5-diphenyltetrazolium bromide.

(4OHT), the active metabolite to tamoxifen, or 1 μM of fulvestrant (ICI 182,780), the pure antiestrogen that downregulates ERα and the expression of IFITM1, PLSCR1 and ERα were measured by Western blot analysis. As shown in Figure 8A, E_2 and fulvestrant completely down-regulated ERα protein but did not significantly alter IFITM1 or PLSCR1 expression, whereas 4OHT did not down-regulate ERα protein but it significantly reduced IFITM1 and PLSCR1 expression in the resistant cells. Interestingly, we found that 4OHT also partially blocked the cell death effect of IFITM1-knockdown in MCF-7:5C cells, as demonstrated by inhibition of PARP cleavage (Figure 8B). Thus, it is possible that IFITM1 expression might be regulated by ERα; however; we do not rule out the possibility that 4OHT might be exerting an effect on IFITM1 that is independent of ERα. Further studies are needed to understand better the mechanism by which 4OHT regulates IFITM1 and whether ERα is involved in the process.

Discussion

Estrogen deprivation by treatment with AIs is the most effective form of endocrine therapy for postmenopausal women with estrogen receptor–positive (ER+) breast cancer. Unfortunately, the majority of patients treated with AIs eventually develop resistance. While the mechanism by which endocrine resistance occurs is still not completely known, there is evidence to suggest that dysregulation in the interferon signaling pathway might play a role in the process. Indeed, studies have reported a strong correlation between constitutive expression of ISGs and resistance to radiotherapy and chemotherapy in several types of human cancers including breast cancer, ovarian cancer, lung cancer and lymphatic leukemia [41-44]. Notably, Dunbier and coworkers [45] recently reported on the poor anti-proliferative response to AI treatment in postmenopausal patients whose tumors expressed high baseline expression of immune response genes; however, these investigators did not examine interferon signaling in AI-resistant breast tumors. In the present study, we have demonstrated that interferon signaling is dysregulated in AI-resistant breast cancer cells and AI-resistant/recurrence tumors and that several interferon response genes including; *IFITM1, PLSCR1, STAT1, STAT2, IRF-7, IRF-9, IFIT1, OAS1* and *MX1* are constitutively overexpressed in AI-resistant breast cancer cells. In particular, we showed that IFITM1 and PLSCR1 were overexpressed at the mRNA and protein level in AI-resistant MCF-7:5C cells compared with AI-sensitive MCF-7 and T47D cells and that suppression of IFITM1, and to a lesser extent PLSCR1, significantly inhibits the proliferation of AI-resistant MCF-7:5C cells and blocked the ability of these cells to invade and migrate. Most interestingly, we found that silencing of IFITM1, PLSCR1 and STAT1 significantly enhanced E_2-induced cell death in AI-resistant MCF-7:5C cells which was associated with induction of p21, Bax, and Noxa. Additionally, we found that constitutive overexpression of IFITM1 and PLSCR1 was driven by IFNα signaling through the canonical IFNAR1/2/STAT1/STAT2 signaling pathway and that knockdown of STAT1 and STAT2 and blockade of IFNα function dramatically suppressed IFITM1 and PLSCR1 expression in the resistant cells. To our knowledge, this is the first study to demonstrate a link between dysregulation of the interferon signaling pathway and AI resistance and it suggests that targeting IFITM1 might be an effective strategy to block cell proliferation and enhance E_2-induced cell death in AI-resistant breast cancer cells.

Type I interferons (IFNs α and β) are known to drive the expression of ISGs that encode proteins that possess anti-viral, anti-proliferative, pro-apoptotic and pro-inflammatory functions; however, many experimental data have shown that high expression of IFN-induced genes, including STAT1 itself, promotes tumor growth, metastasis and resistance to chemotherapy and radiation [23,44,46,47]. Normally, IFNs induce rapid activation of STATs through phosphorylation on the C-terminal tyrosine residues (Y701 for STAT1 and Y690 for STAT2) which drives the expression of ISGs [19]. Several important negative feedback mechanisms collaborate to terminate the expression of these genes several hours after IFN stimulation; for example, expression of the potent negative regulator SOCS1 is rapidly induced by IFNs [48].

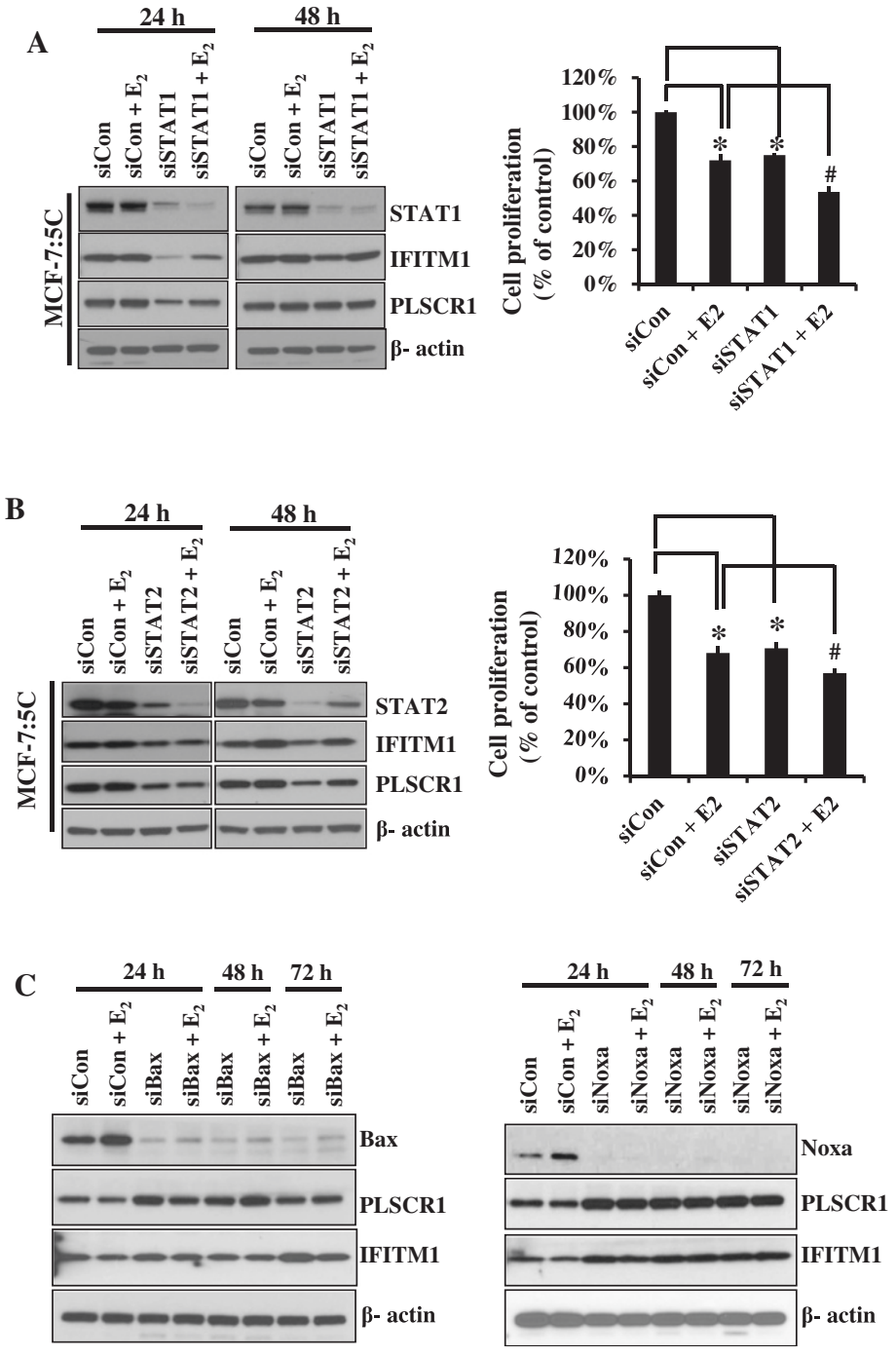

Figure 7 STAT1/STAT2 knockdown reduces IFITM1 and PLSCR1 expression. (A and B) MCF-7:5C cells were transfected with sicontrol (siCon), STAT1 siRNA (siSTAT1) or STAT2 siRNA (siSTAT2) and STAT1, STAT2, IFITM1 and PLSCR1 protein levels were assessed at 24 and 48 hours by Western blot analysis (left panels). Transfected cells were also treated with E_2 for an additional 24 and 48 hours and the above mentioned proteins were also measured (a and b, left panels). **(A, B)** Cell proliferation was measured in siSTAT1-knockdown and STAT2-knockdown cells in the presence or absence of E_2 by cell titer blue assay (right panels). Each value is a mean ± SD from three experiments. *P <0.05 or **P <0.01 versus the control; #P <0.05 versus E_2 treatment. **(C)** MCF-7:5C cells were transfected with Bax siRNA (siBax) or Noxa siRNA (siNoxa) for 24 hours and then treated with 1 nM E_2 for an additional 24, 48 or 72 hours. Cells were harvested and analyzed for Bax, PLSCR1, Noxa, and IFITM1 protein expression by Western blot. Membranes were stripped and reprobed for β-actin, which was used as a loading control. E_2, 17β-estradiol; IFITM1, interferon induced transmembrane protein1; PLSCR1, phospholipid scramblase 1; SD, standard deviation; STAT1,2, Signal transducer and activator of transcription 1,2.

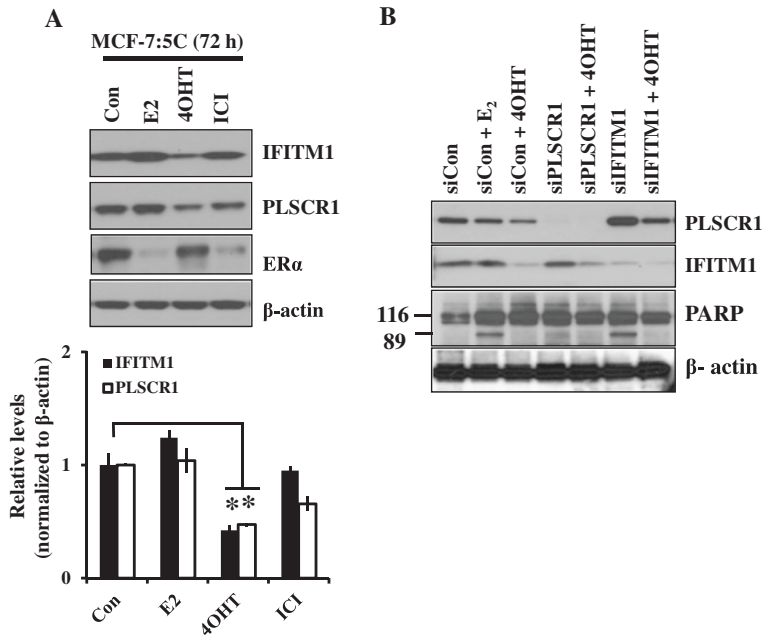

Figure 8 Tamoxifen downregulates IFITM1 and PLSCR1 expression. (**A**, upper panel) MCF-7:5C cells were treated with E_2 (1 nM), 4OHT (1 μM) or fulvestrant (1 μM) for 72 hours. The cell extracts were examined by Western blotting using anti-PLSCR1, anti-IFITM1, anti-ERα and anti-β-actin. (**A**, lower panel) IFITM1 and PLSCR1 protein levels were quantified using the ImageJ software (downloaded from the NIH website) and normalized to β-actin. **(B)** Cells were transfected with siCon, siPLSCR1 or silFITM1 for 24 hours and then treated with 1 nM E_2 or 1 μM 4-hydroxytamoxifen (4OHT) for an additional 24 hours. Cells were then harvested and analyzed by Western blotting to assess PLSCR1, IFITM1, PARP and β-actin protein levels. All the illustrated data are expressed as mean values of three independent experiments. Standard deviations are shown. *P <0.05 versus control; #P <0.05 versus 4OHT treatment. E_2, 17β-estradiol; ERα, estrogen receptor α; IFITM1, interferon induced transmembrane protein1; NIH, National Institutes of Health; PARP, poly ADP ribose polymerase; PLSCR1, phospholipid scramblase 1.

Based on our studies, we observed several ISGs including IFITM1, PLSCR1, IFIT1, IFI23, IRF-7, IRF-9, STAT1, STAT2, MX1 and OAS1 were overexpressed approximately 10- to 300-fold in AI-resistant MCF-7:5C cells compared to AI-sensitive parental MCF-7 cells (Additional file 1: Figure S1). Furthermore, we found that in parental MCF-7 cells, exogenous addition of recombinant IFNα robustly induced the expression of IFITM1, PLSCR1 and STAT1 (10- to 200-fold) within minutes to hours, whereas, in resistant MCF-7:5C cells, exogenous IFNα only increased IFITM1, PLSCR1, and STAT1 expression by 2- to 3-fold compared to basal level (Figure 4A, Fig. S2, Fig. S3). This finding suggests that in parental MCF-7 cells, IFITM1 and other ISGs, are not expressed at the basal level unless stimulated by exogenous IFNα; however, in AI-resistant MCF-7:5C cells, IFITM1, PLSCR1 and other ISGs are constitutively overexpressed possibly due to an elevated level of IFNα in the cells. Notably, we detected significantly elevated levels of IFNα in the supernatant and lysate of AI-resistant MCF-7:5C cells compared to parental MCF-7 cells and knockdown of IFNα along with neutralizing antibody blockade of the receptor (IFNAR1/2) almost completely reduced IFITM1, PLSCR1, p-STAT1 and p-STAT2 expression in the resistant cells, thus suggesting a critical role for the IFNα canonical signaling pathway in driving the constitutive expression of the ISGs in the resistant cells. Sustained expression of ISGs and their encoded proteins was previously thought to be deleterious to cell survival [19]; however, recent studies suggest that sustained expression of a subset of ISGs and their encoded proteins might provide a survival advantage to cells [49]. We should note that ER-positive breast cancer cells are dependent on estrogen for survival and growth and when they are deprived of estrogen they tend to die. Long term, however, some breast cancer cells develop strategies to allow them to survive and grow in an estrogen-depleted environment [10-12,15,16]. In our working model shown in Figure 9, we propose that in AI-resistant MCF-7:5C breast cancer cells, the transcription factor IRF-7 which is a key regulator of IFNα, is dramatically upregulated and that increased IRF-7 expression in the resistant cells stimulates the production of IFNα which is then secreted from the cells and binds to the IFNAR1/2STAT1/STAT2/IRF-9 complex to induce the expression of ISGs (that is, *IFITM1, PLSCR1, IFIT1, IFI21, OAS1, MX1, STAT, STAT2, IRF-7, IRF-9*). Thus, it is possible that the constitutive overexpression of the ISGs provides a

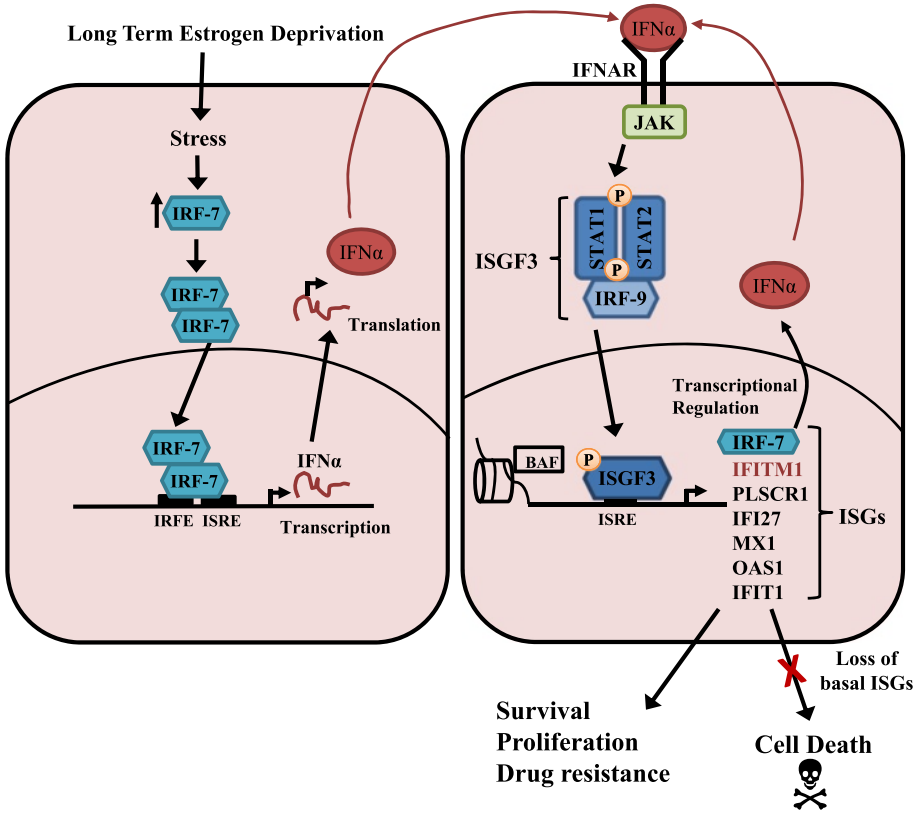

Figure 9 Schematic diagram depicting the proposed mechanism of ISG expression in AI-resistant MCF-7:5C cells. ER-positive breast cancers are dependent on estrogen for survival and growth and when these cancer cells are deprived of estrogen they tend to die. Long term, however, some breast cancer cells develop strategies to allow them to survive and grow in an estrogen-depleted environment. In our working model, we propose that long term estrogen deprivation of ERα positive breast cancer cells elicits a stress response in the cell which can possibly result in increased expression and activation of IRF-7, a known stress response gene. The activated IRF-7 enters the nucleus and binds the IFNα promoter at the IRF binding-element (IRFE) and ISRE sites, resulting in IFNα production and secretion from the cell. IFNα then binds to its cell surface receptor IFNAR1/2 which initiates JAK phosphorylation of the STAT proteins and association with IRF-9, forming the activated ISGF3 complex (p-ISGF3). The BAF complex remodels the chromatin around prospective ISGs and p-ISGF3 is imported into the nucleus where it binds to the exposed ISRE sites in ISG promoters. This results in the sustained/constitutive overexpression of numerous ISGs including IFITM1 and IRF-7, which initiates further IFNα production and thus provides autocrine cytokine signaling, reinforcing the production and accumulation of ISGs. The ISGs are pro-survival and so facilitate cell survival and proliferation under the stressful (estrogen depleted) conditions. Loss of expression of the ISGs reduces the ability of the resistant cells to survive in an estrogen-depleted environment thus causing them to die. AI, aromatase inhibitor; ER, estrogen receptor; IFITM1, interferon induced transmembrane protein1; IRF-7, IFN regulatory factor 7; ISGs, interferon stimulated genes; ISREs, IFN-stimulated response elements; JAK, Janus kinase 1 and 2; STAT, Signal transducer and activator of transcription.

survival advantage to the resistant cells that allows them to adapt and grow in an estrogen-depleted environment. The fact that knockdown of IFNα dramatically reduced IFITM1 expression in the resistant cells and its loss significantly induced cell death highlights the potential dependency of the resistant cells on elevated IFNα to maintain their resistant phenotype and to drive the constitutive overexpression of IFITM1 and the other ISGs in the cells. We should note that elevated IFN production has previously been reported in many pathological conditions, such as chronic inflammation and cancer, as well as in virus infections [50]. In cancers, IFN production is thought to be increased by infiltrating immune cells or by the cancer cells themselves [51].

While our studies identified a panel of ISGs that were constitutively overexpressed in our AI-resistant breast cancer cells, IFITM1 was the most functionally significant of the ISGs in the resistant cells. Clinical data indicated that IFITM1 was constitutively overexpressed in 36 out of 40 AI-resistant breast tumor samples and it was overexpressed in AI-resistant breast cancer cells approximately 20- to 30-fold at the mRNA and protein level. Notably, we found that knockdown of IFITM1 significantly increased cell death and it blocked invasion and migration in the resistant cells. The induction of cell death in the resistant cells following IFITM1 knockdown was associated with an increase in p21 and Bax expression; however, suppression of IFITM1 did not alter p53

expression or cause cell cycle arrest in these cells. p21 (also known as $p21^{WAF1/Cip1}$) is a multifunctional protein that belongs to the cip/kip family of cyclin-dependent kinase inhibitors and is known to promote G1/S or G2/M cell cycle arrest and survival in a p53-dependent and p53-independent manner [52]. In addition, p21 has also been shown to play a role in apoptosis and it is suggested that its ability to regulate cell cycle arrest versus apoptosis is influenced by its cellular localization; nucleus accumulation promotes cell cycle arrest whereas cytoplasmic accumulation inhibits apoptosis [53,54]. Notably, suppression of IFITM1 also induced Bax and Noxa which are important regulators of mitochondrial-mediated cell death. Interestingly, previous studies have reported that p21 counteracts mitochondrial-mediated apoptosis that relies on Bax and its upstream effector Puma [55]; however, in our study, p21 induction positively correlated with Bax and Noxa induction thus suggesting a pro-apoptotic function for p21 in the resistant cells. We should note that knockdown of IFITM1 also increased E_2-induced cell death in AI-resistant MCF-7:5C cells. The ability of E_2 to induce mitochondrial-mediated apoptosis in AI-resistant MCF-7:5C cells has previously been reported by our laboratory [11,17]; however, this is the first study to show that suppression of IFITM1 induces p21 and Bax expression and enhances E_2-induced cell death in AI-resistant breast cancer cells.

IFITM1 is a member of the IFN-inducible transmembrane (IFITM) protein family that was originally identified as Leu-13, a leukocyte antigen that is a part of a membrane complex involved in the transduction of antiproliferative and homotypic adhesion signals in lymphocytes [56,57]. IFITM1 is highly induced by type 1 interferons (IFNs α and β) and is most well-known for its ability to restrict the replication of a number of enveloped and non-enveloped viruses [30]. More recently, IFITM1 has also been implicated in tumorigenesis and there is evidence that it can positively or negatively regulate cell proliferation depending on the tumor cell type [25,27,31,32,40]. In particular, IFITM1 overexpression has been shown to inhibit proliferation in hepatoma cells [29] and its constitutive overexpression has been shown to positively correlate with improved survival in chronic myeloid leukemia patients [25]. In contrast, upregulation of IFITM1 expression has been reported to play a critical role in both the precancerous stage and carcinogenesis in patients with gastric mucosa infected with *Helicobacter pylori* and cervical cancer [33]. In addition, there is evidence that IFITM1 overexpression induces tumor resistance to natural killer (NK) cells in gastric tumor cells and it facilitates migration and invasion of gastric cancer cells [29]. More recently, investigators have reported that overexpression of IFITM1 promotes head and neck tumor invasion in the early stages of disease progression by mediating the expression of molecules downstream, including matrix metalloproteinases 12 and 13 [32].

Our data provide strong evidence that constitutive overexpression of IFITM1 is driven by IFNα through activation of the canonical signaling pathway and that STAT1 and STAT2 play a critical role. In particular, we found that p-STAT1 and p-STAT2 (Figure 3F) were constitutively overexpressed in our resistant cells and that knockdown of IFNα dramatically reduced their expression in the cells. Furthermore, we found that knockdown of STAT1 and STAT2 dramatically reduced IFITM1 expression in the resistant cells. However, we should note that knockdown of IFNα or neutralizing IFNAR1/2 did not completely suppress IFITM1 expression in the resistant cells, which suggests that IFITM1 constitutive overexpression might be regulated by other mechanisms. Indeed, recent studies suggest that IFITM1 expression is regulated by the chromatin remodeling complexes (CRCs) consisting of BRG (Brahma-related gene) and BAF (BRM-associated factor), which work in concert with histone modification enzymes such as cyclic AMP-responsive-element binding protein (CREB)-binding protein and/or p300 (CBP/p300) to bring about the regulation of IFITM1 and other IFNα-target genes [58,59]. The BAF complexes are thought to prime the IFITM1 promoter by disrupting the nucleosome that covers the ISRE which then leads to constitutive expression of IFITM1, as demonstrated in our working model in Figure 9. Future studies will be aimed at determining how IFITM1 and other ISGs are regulated by the BRG/BAF complex in the resistant cells.

Conclusions

In summary, overexpression of ISGs and their protein products are emerging as important contributors to development of clinical neoplasia and drug resistance in many types of cancers. In our study, we demonstrated that several ISGs including *IFITM1, STAT1* and *PLSCR1* and their encoded proteins are constitutively overexpressed in AI-resistant breast cancer cells and AI-resistant tumors and that their overexpression provides a survival advantage in the resistant cells. Furthermore, we showed that targeting ISGs, especially IFITM1, sensitized AI-resistant breast cancer cells to estrogen-induced cell death and it blocked the ability of these cells to migrate and invade. This finding has important clinical implications for patients with AI-resistant breast cancer because it suggests that altered interferon signaling might play a role in tumor progression and possibly the development of AI resistance. Future studies will need to address how and why interferon response genes are altered during resistance and whether an altered immune response gene profile can predict which patient will benefit from AI therapy and which patient will develop resistance following treatment.

Additional files

Additional file 1: Figure S1. Overexpression of ISGs in AI-resistant MCF-7:5C cells as compared to parental MCF-7 cells. Total RNA was extracted from each cell line and mRNA expression of the ISGs shown above was determined by real-time PCR using *PUM1* as the internal control. Primer sequences for the ISGs shown above are described in materials and methods. Fold change was calculated using the ΔΔCT method and is displayed as relative to MCF-7 cells (control). Values are means of triplicate measurements ± SD from two independent experiments.

Additional file 2: Figure S2. Activation of interferon signaling pathway in parental MCF-7 and AI-resistant MCF-7:5C cells in response to INF-a. **(A)** MCF-7 and **(B)** MCF-7:5C cells were incubated with IFN-α (1000 U/ml) for the indicated time points. The cell extracts were examined by Western blotting using anti-PLSCR1, anti-IFITM1, anti-STAT1, anti-STAT2 and anti-b-actin. The protein levels were quantified using the ImageJ software (downloaded from NIH website) and normalized as the ratio relate to β-actin. **P* <0.05 or ***P* <0.01 versus control.

Additional file 3: Figure S3. Activation of IFN signaling pathway in parental MCF-7 and AI-resistant MCF-7:5C cells in response to IFN-α. MCF-7 and MCF-7:5C cells were treated with 100 U/mL IFN-α and harvested at the indicated time points. mRNA expression of IFITM1, PLSCR1 and STAT1was measured using RT-PCR and calculated using the ΔΔCT method relative to PUM1. mRNA expression is given as fold change over control (time zero). Values shown are means of triplicate measurements ± SD from three independent experiments.

Additional file 4: Figure S4. IFITM1 knockdown increases cell death in AI-resistant breast cancer cells. (**A**, top panel) MCF-7:5C cells were transfected with control shRNA (shCon), IFITM1 shRNA (shIFITM1) for 24 hours and then treated with 1 nM E2 for an additional 72 hours. Cell extracts were subject to Western blotting for the level of IFITM1 and PARP protein (top panel). Membranes were also stripped and reprobed for β-actin, which was used as a loading control. (**A**, bottom panel) shIFITM1 mRNA level in resistant MCF-7:5C cells was determined by real-time PCR and normalized to *PUM1*. **P* <0.05 versus shcontrol (shCon). **(B)** Cell proliferation was measured in resistant MCF-7:5C cells by MTT assay. All the illustrated data were performed in triplicate and are expressed as mean values of three independent experiments. Standard deviations are shown. **P* <0.05 versus control; #*P* <0.05 versus E2 treatment. **(C)** MCF-7:5C cells were transfected with shCon or shIFITM1 and after 24 hours were exposed to E2 (1 nM) for an additional 72 hours. Cells were then stained with annexin V-FITC and PI for detection of apoptosis as described in Methods.

Additional file 5: Figure S5. Role of IFN-α in estradiol-induced cell death in resistant MCF-7:5C cells. Cells were transfected with siIFNα or siCon for 24 hours and then further treated with 1 nM estradiol (E2) for an additional 96 hours. In parallel experiments, we also pre-treated MCF-7:5C cells with 5 μg/mL α-IFNAR antibody (MAB1155) for 4 hours and then treated with 1 nM estradiol for an additional 96 hours. At the 96 hour time point cells were harvested and proliferation was determined by MTT assay (top) and apoptosis was assessed by annexin V/PI staining (bottom). Data shown are expressed as mean values of three independent experiments.

Additional file 6: Figure S6. STAT1/STAT2 knockdown reduces IFITM1 expression in MCF-7:5C cells. Cells were transfected with sicontrol (siCon), STAT1 siRNA (siSTAT1), STAT2 siRNA (siSTAT2), or siSTAT1 and siSTAT2 for 48 hours and cells were harvested and analyzed by Western blot to assess STAT1, STAT2 and IFITM1 protein expression. Membranes were stripped and reprobed for β-actin, which was used as a loading control. Blots shown are representative of three separate experiments yielding similar results.

Abbreviations

AI: aromatase inhibitor; BAF: Brahma-associated factor; BRG: Brahma-related gene; BST2: bone marrow stromal cell antigen 2; CBP/p300: CREB-binding protein 300; CRCs: chromatin remodeling complexes; CREB: cyclic AMP-responsive-element binding protein; DAB: 3,3′-diaminobenzidine; (D) MEM: (Dulbecco's) modified Eagle's medium; DMSO: dimethyl sulfoxide; E_2: 17β-estradiol; ECL: enhanced chemiluminescence; ELISA: enzyme-linked immunosorbent assay; ER: estrogen receptor; ERα: estrogen receptor alpha; ER+: estrogen receptor-positive; ERE: estrogen response element; FBS: fetal bovine serum; HRP: horseradish peroxidase; ICC: immunocytochemistry; IF: immunofluorescence; IFI27: interferon-inducible protein 27; IFIT1: Interferon-induced protein with tetratricopeptide repeats 1; IFITM1: interferon induced transmembrane protein1; IFNs: interferons; IFNR1/2: interferon receptor type 1 and 2; IgG: immunoglobulin G; IHC: immunohistochemistry; IR F-7: IFN regulatory factor 7; IRF9: IFN regulatory factor 9; ISGF3: IFN-stimulated gene factor 3; ISGs: interferon stimulated genes; ISREs: interferon stimulated response elements; JAK: Janus kinase 1 and 2; MTT: 3-(4,5-dimethylthiazol-2-Yl)-2,5-diphenyltetrazolium bromide; NK: natural killer; OAS 1,2,3: 2′-5′-oligoadenylate synthetase 1,2,3, PARP, poly ADP ribose polymerase; PBS: phosphate-buffered saline; PCR: polymerase chain reaction; PI: propidium iodide; PLSCR1: phospholipid scramblase 1; SDS-PAGE: sodium dodecyl sulfate-polyacrylamide gel electrophoresis; SI: staining index; SOCS1: suppressor of cytokine signaling 1; STAT1,2: signal transducer and activator of transcription 1,2; TTP: time to disease progression; U-ISGF3: unphosphorylated IFN-stimulated gene factor 3; 4OHT: 4-hydoxytamoxifen.

Competing interests

The authors declare that they have no competing interests.

Authors' contributions

JLW conceived the study, participated in the research design and implementation of the study, analyzed and interpreted the data, and drafted the manuscript. HJC performed the experiments, analyzed the data, and drafted the manuscript. AL performed the experiments, analyzed the data, and drafted the manuscript. JO performed some of the experiments and helped to draft the manuscript. RJ performed all of the IHC experiments. PJS provided reagents used for IF and IHC studies and helped with the discussion of the manuscript. All authors read and approved the final manuscript.

Acknowledgements

This work was supported by grants from the Department of Defense (W81XWH-12-1-0139; supporting JLW), National Cancer Institute (K01CA120051; supporting JLW), and by start-up funds from the University of Kansas Medical Center (supporting JLW, HJC, JO, AL). The funders had no role in study design, data collection and analysis, decision to publish, or preparation of the manuscript. We would like to thank the KU Cancer Center's CCSG (P30 CA168524) Biospecimen Repository Core and the Fox Chase Cancer Center Biosample Repository Core Facilities for providing the breast tumor samples used in this study. We would also like to acknowledge the Flow Cytometry Core and the Cell Imaging Core Facilities at KUMC.

Author details

[1]Department of Cancer Biology, University of Kansas Medical Center, Kansas City 66160, KS, USA. [2]Department of Physiology, University of Kansas Medical Center, Kansas City 66160, KS, USA. [3]Cancer Biology Program, Research Institute of Fox Chase Cancer Center, Philadelphia 19111, PA, USA. [4]Department of Pathology and Laboratory Medicine, University of Rochester, Rochester 14642, NY, USA.

Received: 4 April 2014 Accepted: 15 December 2014
Published online: 15 January 2015

References

1. Mouridsen H, Gershanovich M, Sun Y, Perez-Carrion R, Boni C, Monnier A, et al. Phase III study of letrozole versus tamoxifen as first-line therapy of advanced breast cancer in postmenopausal women: analysis of survival and update of efficacy from the International Letrozole Breast Cancer Group. J Clin Oncol. 2003;21:2101–9.
2. Chumsri S, Howes T, Bao T, Sabnis G, Brodie A. Aromatase, aromatase inhibitors, and breast cancer. J Steroid Biochem Mol Biol. 2011;125:13–22.
3. Goss PE, Strasser K. Aromatase inhibitors in the treatment and prevention of breast cancer. J Clin Oncol. 2001;19:881–94.
4. Jordan VC, Brodie AM. Development and evolution of therapies targeted to the estrogen receptor for the treatment and prevention of breast cancer. Steroids. 2007;72:7–25.

5. Geisler J, King N, Dowsett M, Ottestad L, Lundgren S, Walton P, et al. Influence of anastrozole (Arimidex), a selective, non-steroidal aromatase inhibitor, on in vivo aromatisation and plasma oestrogen levels in postmenopausal women with breast cancer. Br J Cancer. 1996;74:1286–91.
6. Miller WR, Larionov AA. Understanding the mechanisms of aromatase inhibitor resistance. Breast Cancer Res. 2012;14:201.
7. Ellis MJ, Gao F, Dehdashti F, Jeffe DB, Marcom PK, Carey LA, et al. Lower-dose vs high-dose oral estradiol therapy of hormone receptor-positive, aromatase inhibitor-resistant advanced breast cancer: a phase 2 randomized study. JAMA. 2009;302:774–80.
8. Iwase H, Yamamoto Y, Yamamoto-Ibusuki M, Murakami KI, Okumura Y, Tomita S, et al. Ethinylestradiol is beneficial for postmenopausal patients with heavily pre-treated metastatic breast cancer after prior aromatase inhibitor treatment: a prospective study. Br J Cancer. 2013;109:1537–42.
9. Jiang SY, Wolf DM, Yingling JM, Chang C, Jordan VC. An estrogen receptor positive MCF-7 clone that is resistant to antiestrogens and estradiol. Mol Cell Endocrinol. 1992;90:77–86.
10. Lewis JS, Cheng D, Jordan VC. Targeting oestrogen to kill the cancer but not the patient. Br J Cancer. 2004;90:944–9.
11. Lewis JS, Meeke K, Osipo C, Ross EA, Kidawi N, Li T, et al. Intrinsic mechanism of estradiol-induced apoptosis in breast cancer cells resistant to estrogen deprivation. J Natl Cancer Inst. 2005;97:1746–59.
12. Lewis JS, Osipo C, Meeke K, Jordan VC. Estrogen-induced apoptosis in a breast cancer model resistant to long-term estrogen withdrawal. J Steroid Biochem Mol Biol. 2005;94:131–41.
13. Masamura S, Santner SJ, Heitjan DF, Santen RJ. Estrogen deprivation causes estradiol hypersensitivity in human breast cancer cells. J Clin Endocrinol Metab. 1995;80:2918–25.
14. Song RX, Mor G, Naftolin F, McPherson RA, Song J, Zhang Z, et al. Effect of long-term estrogen deprivation on apoptotic responses of breast cancer cells to 17beta-estradiol. J Natl Cancer Inst. 2001;93:1714–23.
15. Lewis-Wambi JS, Jordan VC. Estrogen regulation of apoptosis: how can one hormone stimulate and inhibit? Breast Cancer Res. 2009;11:206.
16. Lewis-Wambi JS, Kim HR, Wambi C, Patel R, Pyle JR, Klein-Szanto AJ, et al. Buthionine sulfoximine sensitizes antihormone-resistant human breast cancer cells to estrogen-induced apoptosis. Breast Cancer Res. 2008;10:R104.
17. Ariazi EA, Cunliffe HE, Lewis-Wambi JS, Slifker MJ, Willis AL, Ramos P, et al. Estrogen induces apoptosis in estrogen deprivation-resistant breast cancer through stress responses as identified by global gene expression across time. Proc Natl Acad Sci U S A. 2011;108:18879–86.
18. Stark GR, Kerr IM, Williams BR, Silverman RH, Schreiber RD. How cells respond to interferons. Annu Rev Biochem. 1998;67:227–64.
19. Borden EC, Sen GC, Uze G, Silverman RH, Ransohoff RM, Foster GR, et al. Interferons at age 50: past, current and future impact on biomedicine. Nat Rev Drug Discov. 2007;6:975–90.
20. Lewin AR, Reid LE, McMahon M, Stark GR, Kerr IM. Molecular analysis of a human interferon-inducible gene family. Eur J Biochem. 1991;199:417–23.
21. Critchley-Thorne RJ, Simons DL, Yan N, Miyahira AK, Dirbas FM, Johnson DL, et al. Impaired interferon signaling is a common immune defect in human cancer. Proc Natl Acad Sci U S A. 2009;106:9010–5.
22. Schreiber RD, Old LJ, Smyth MJ. Cancer immunoediting: integrating immunity's roles in cancer suppression and promotion. Science. 2011;331:1565–70.
23. Khodarev NN, Beckett M, Labay E, Darga T, Roizman B, Weichselbaum RR. STAT1 is overexpressed in tumors selected for radioresistance and confers protection from radiation in transduced sensitive cells. Proc Natl Acad Sci U S A. 2004;101:1714–9.
24. Lewis-Wambi JS, Cunliffe HE, Kim HR, Willis AL, Jordan VC. Overexpression of CEACAM6 promotes migration and invasion of oestrogen-deprived breast cancer cells. Eur J Cancer. 2008;44:1770–9.
25. Akyerli CB, Beksac M, Holko M, Frevel M, Dalva K, Ozbek U, et al. Expression of IFITM1 in chronic myeloid leukemia patients. Leuk Res. 2005;29:283–6.
26. Deblandre GA, Marinx OP, Evans SS, Majjaj S, Leo O, Caput D, et al. Expression cloning of an interferon-inducible 17-kDa membrane protein implicated in the control of cell growth. J Biol Chem. 1995;270:23860–6.
27. Ackrill AM, Reid LE, Gilbert CS, Gewert DR, Porter AC, Lewin AR, et al. Differential response of the human 6–16 and 9–27 genes to alpha and gamma interferons. Nucleic Acids Res. 1991;19:591–8.
28. Bradbury LE, Kansas GS, Levy S, Evans RL, Tedder TF. The CD19/CD21 signal transducing complex of human B lymphocytes includes the target of antiproliferative antibody-1 and Leu-13 molecules. J Immunol. 1992;149:2841–50.
29. Yang Y, Lee JH, Kim KY, Song HK, Kim JK, Yoon SR, et al. The interferon-inducible 9–27 gene modulates the susceptibility to natural killer cells and the invasiveness of gastric cancer cells. Cancer Lett. 2005;221:191–200.
30. Huang IC, Bailey CC, Weyer JL, Radoshitzky SR, Becker MM, Chiang JJ, et al. Distinct patterns of IFITM-mediated restriction of filoviruses, SARS coronavirus, and influenza A virus. PLoS Pathog. 2011;7:e1001258.
31. Andreu P, Colnot S, Godard C, Laurent-Puig P, Lamarque D, Kahn A, et al. Identification of the IFITM family as a new molecular marker in human colorectal tumors. Cancer Res. 2006;66:1949–55.
32. Hatano H, Kudo Y, Ogawa I, Tsunematsu T, Kikuchi A, Abiko Y, et al. IFN-induced transmembrane protein 1 promotes invasion at early stage of head and neck cancer progression. Clin Cancer Res. 2008;14:6097–105.
33. Hofman VJ, Moreilhon C, Brest PD, Lassalle S, Le Brigand K, Sicard D, et al. Gene expression profiling in human gastric mucosa infected with Helicobacter pylori. Mod Pathol. 2007;20:974–89.
34. Zhou Q, Ben-Efraim I, Bigcas JL, Junqueira D, Wiedmer T, Sims PJ. Phospholipid scramblase 1 binds to the promoter region of the inositol 1,4,5-triphosphate receptor type 1 gene to enhance its expression. J Biol Chem. 2005;280:35062–8.
35. Zhou Q, Zhao J, Wiedmer T, Sims PJ. Normal hemostasis but defective hematopoietic response to growth factors in mice deficient in phospholipid scramblase 1. Blood. 2002;99:4030–8.
36. Huang Y, Zhao Q, Zhou CX, Gu ZM, Li D, Xu HZ, et al. Antileukemic roles of human phospholipid scramblase 1 gene, evidence from inducible PLSCR1-expressing leukemic cells. Oncogene. 2006;25:6618–27.
37. Silverman RH, Halloum A, Zhou A, Dong B, Al-Zoghaibi F, Kushner D, et al. Suppression of ovarian carcinoma cell growth in vivo by the interferon-inducible plasma membrane protein, phospholipid scramblase 1. Cancer Res. 2002;62:397–402.
38. Sims PJ, Wiedmer T. Induction of cellular procoagulant activity by the membrane attack complex of complement. Semin Cell Biol. 1995;6:275–82.
39. Wiedmer T, Zhou Q, Kwoh DY, Sims PJ. Identification of three new members of the phospholipid scramblase gene family. Biochim Biophys Acta. 2000;1467:244–53.
40. http://rsb.info.nih.gov/ij/download.html
41. Gongora C, Candeil L, Vezzio N, Copois V, Denis V, Breil C, et al. Altered expression of cell proliferation-related and interferon-stimulated genes in colon cancer cells resistant to SN38. Cancer Biol Ther. 2008;7:822–32.
42. Khodarev NN, Roach P, Pitroda SP, Golden DW, Bhayani M, Shao MY, et al. STAT1 pathway mediates amplification of metastatic potential and resistance to therapy. PLoS One. 2009;4:e5821.
43. Khodarev NN, Roizman B, Weichselbaum RR. Molecular pathways: interferon/stat1 pathway: role in the tumor resistance to genotoxic stress and aggressive growth. Clin Cancer Res. 2012;18:3015–21.
44. Roberts D, Schick J, Conway S, Biade S, Laub PB, Stevenson JP, et al. Identification of genes associated with platinum drug sensitivity and resistance in human ovarian cancer cells. Br J Cancer. 2005;92:1149–58.
45. Dunbier AK, Ghazoui Z, Anderson H, Salter J, Nerurkar A, Osin P, et al. Molecular profiling of aromatase inhibitor-treated postmenopausal breast tumors identifies immune-related correlates of resistance. Clin Cancer Res. 2013;19:2775–86.
46. Perou CM, Jeffrey SS, van de Rijn M, Rees CA, Eisen MB, Ross DT, et al. Distinctive gene expression patterns in human mammary epithelial cells and breast cancers. Proc Natl Acad Sci U S A. 1999;96:9212–7.
47. Rickardson L, Fryknas M, Dhar S, Lovborg H, Gullbo J, Rydaker M, et al. Identification of molecular mechanisms for cellular drug resistance by combining drug activity and gene expression profiles. Br J Cancer. 2005;93:483–92.
48. Yoshimura A, Naka T, Kubo M. SOCS proteins, cytokine signalling and immune regulation. Nat Rev Immunol. 2007;7:454–65.
49. Cheon H, Stark GR. Unphosphorylated STAT1 prolongs the expression of interferon-induced immune regulatory genes. Proc Natl Acad Sci U S A. 2009;106:9373–8.
50. de Visser KE, Eichten A, Coussens LM. Paradoxical roles of the immune system during cancer development. Nat Rev Cancer. 2006;6:24–37.
51. Leonova KI, Brodsky L, Lipchick B, Pal M, Novototskaya L, Chenchik AA, et al. p53 cooperates with DNA methylation and a suicidal interferon response to maintain epigenetic silencing of repeats and noncoding RNAs. Proc Natl Acad Sci U S A. 2013;110:E89–98.
52. el-Deiry WS, Tokino T, Velculescu VE, Levy DB, Parsons R, Trent JM, et al. WAF1, a potential mediator of p53 tumor suppression. Cell. 1993;75:817–25.

53. Asada M, Yamada T, Ichijo H, Delia D, Miyazono K, Fukumuro K, et al. Apoptosis inhibitory activity of cytoplasmic p21(Cip1/WAF1) in monocytic differentiation. EMBO J. 1999;18:1223–34.
54. Zhou BP, Liao Y, Xia W, Spohn B, Lee MH, Hung MC. Cytoplasmic localization of p21Cip1/WAF1 by Akt-induced phosphorylation in HER-2/neu-overexpressing cells. Nat Cell Biol. 2001;3:245–52.
55. Braun F, Bertin-Ciftci J, Gallouet AS, Millour J, Juin P. Serum-nutrient starvation induces cell death mediated by Bax and Puma that is counteracted by p21 and unmasked by Bcl-x(L) inhibition. PLoS One. 2011;6:e23577.
56. Chen YX, Welte K, Gebhard DH, Evans RL. Induction of T cell aggregation by antibody to a 16kd human leukocyte surface antigen. J Immunol. 1984;133:2496–501.
57. Matsumoto AK, Martin DR, Carter RH, Klickstein LB, Ahearn JM, Fearon DT. Functional dissection of the CD21/CD19/TAPA-1/Leu-13 complex of B lymphocytes. J Exp Med. 1993;178:1407–17.
58. Chi T. A BAF-centred view of the immune system. Nat Rev Immunol. 2004;4:965–77.
59. Cui K, Tailor P, Liu H, Chen X, Ozato K, Zhao K. The chromatin-remodeling BAF complex mediates cellular antiviral activities by promoter priming. Mol Cell Biol. 2004;24:4476–86.

Intrinsic Mechanism of Estradiol-Induced Apoptosis in Breast Cancer Cells Resistant to Estrogen Deprivation

Joan S. Lewis, Kathleen Meeke, Clodia Osipo, Eric A. Ross, Noman Kidawi, Tianyu Li, Eric Bell, Navdeep S. Chandel, V. Craig Jordan

Background: **We previously developed an estrogen receptor (ER)–positive breast cancer cell line (MCF-7:5C) that is resistant to long-term estrogen deprivation and undergoes rapid and complete apoptosis in the presence of physiologic concentrations of 17β-estradiol. Here, we investigated the role of the mitochondrial apoptotic pathway in this process.** ***Methods:*** **Apoptosis in MCF-7:5C cells treated with estradiol, fulvestrant, or vehicle (control) was investigated by annexin V–propidium iodide double staining and 4′,6-diamidino-2-phenylindole (DAPI) staining. Apoptosis was also analyzed in MCF-7:5C cells transiently transfected with small interfering RNAs (siRNAs) to apoptotic pathway components. Expression of apoptotic pathway intermediates was measured by western blot analysis. Mitochondrial transmembrane potential (ψ_m) was determined by rhodamine-123 retention assay. Mitochondrial pathway activity was determined by cytochrome *c* release and cleavage of poly(ADP-ribose) polymerase (PARP) protein. Tumorigenesis was studied in ovariectomized athymic mice that were injected with MCF-7:5C cells. Differences between the treatment groups and control group were determined by two-sample *t* test or one-factor analysis of variance. All statistical tests were two-sided.** ***Results:*** **MCF-7:5C cells treated with estradiol underwent apoptosis and showed increased expression of proapoptotic proteins, decreased ψ_m, enhanced cytochrome *c* release, and PARP cleavage compared with cells treated with fulvestrant or vehicle. Blockade of Bax, Bim, and p53 mRNA expression by siRNA reduced estradiol-induced apoptosis relative to control by 76% [95% confidence interval (CI) = 73% to 79%, *P*<.001], 85% [95% CI = 90% to 80%, *P*<.001], and 40% [95% CI = 45% to 35%, *P*<.001], respectively, whereas blockade of FasL by siRNA had no effect. Estradiol caused complete regression of MCF-7:5C tumors in vivo.** ***Conclusion:*** **The mitochondrial pathway of apoptosis plays a critical role in estradiol-induced apoptosis in long-term estrogen-deprived breast cancer cells. Physiologic concentrations of estradiol could potentially be used to induce apoptosis and tumor regression in tumors that have developed resistance to aromatase inhibitors. [J Natl Cancer Inst 2005;97:1746–59]**

It is generally believed that the balance between proliferation and apoptosis influences the response of tumors to treatments such as chemotherapy *(1)*, radiotherapy *(2)*, and hormonal therapy *(3)*. It has been suggested that, when these treatments fail, dysregulation of apoptosis may be the cause. Apoptosis is a form of programmed cell death that is executed by a family of proteases called caspases, which can be activated either by cell-surface death receptors (i.e., the extrinsic pathway) or by perturbation of the mitochondrial membrane (i.e., the intrinsic pathway) *(4)*. Components of the extrinsic pathway include the death receptors FasR/FasL, DR4/DR5, and tumor necrosis

Affiliations of authors: Fox Chase Cancer Center, Philadelphia, PA (JSL, VCJ, EAR, TL); Robert H. Lurie Comprehensive Cancer Center (KM, CO, NK) and Department of Medicine (EB, NSC), Northwestern University, Chicago, IL.

Correspondence to: V. Craig Jordan, OBE, PhD, DSc, Vice President and Research Director for Medical Sciences, Alfred G. Knudson Chair of Cancer Research, Fox Chase Cancer Center, 333 Cottman Ave., Philadelphia, PA 19111 (e-mail: V.Craig.Jordan@fccc.edu).

See "Notes" following "References."

DOI: 10.1093/jnci/dji400

factor (TNFR), whereas the intrinsic pathway centers on the mitochondria, which contain key apoptogenic factors such as cytochrome *c* and apoptosis-inducing factor (AIF) *(4)*. In the intrinsic pathway, the integrity of mitochondrial membranes is controlled primarily by a balance between the antagonistic actions of the proapoptotic and antiapoptotic members of the Bcl-2 family. Bcl-2 family proteins comprise three principal subfamilies: 1) antiapoptotic members, including Bcl-2/Bcl-x_L, which possess the Bcl-2 homology (BH) domains BH1, BH2, BH3, and BH4; 2) proapoptotic members, such as Bax, Bak, and Bok, which have the BH1, BH2, and BH3 domains; and 3) BH3-only proteins, such as Bid, Bim, Bad, Bik, and Puma, which generally possess only the BH3 domain *(5)*. The Bcl-2 family of proteins regulates apoptosis by altering mitochondrial membrane permeabilization and controlling the release of cytochrome *c*.

Many estrogen receptor (ERα)–positive human breast cancer cells require estrogen for their proliferation and undergo apoptotic cell death when deprived of estrogen *(6)*. As such, the current strategy for treating ERα-positive breast cancer is to block the action of estrogen on tumor cells. There are three general approaches: 1) inhibiting estrogen binding to the ERα using an antiestrogen such as tamoxifen *(7)*, 2) blocking estrogen synthesis using an aromatase inhibitor such as exemestane *(8)*, or 3) reducing ERα protein levels using a pure antiestrogen such as fulvestrant (ICI 182780 or Faslodex) *(9)*. In addition to stimulating growth of ER-positive breast cancer cells, estradiol also promotes cell survival, and it has been suggested that the ability of estradiol to act as a survival factor for breast cancer may occur, in large part, through its prevention of apoptosis via the activation of antiapoptotic proteins such as Bcl-2 and Bcl-x_L. Indeed, estradiol has been shown to inhibit apoptosis in several cell types, including neurons *(10)*, endothelial cells *(11)*, epithelial cells of the female reproductive tract *(12)*, and hormone-dependent human breast cancer MCF-7 cells *(13,14)*.

Recent evidence also suggests that estradiol is capable of inducing programmed cell death (i.e., apoptosis) in certain cell types, including bone-derived cells *(15)*, immune system cells, and breast cancer cells that have developed resistance following extensive antihormonal therapy *(16–20)*. In these models of drug resistance, our laboratory *(16–18)* and those of other investigators *(19)* have found that physiologic concentrations of estradiol induce cell death and rapid tumor regression rather than stimulate growth. These data are particularly interesting because high doses of synthetic estrogens such as diethystilbestrol (DES) or ethinyl estradiol have been used effectively to treat breast cancer patients for the last 60 years *(21)*. However, the idea that low doses of estradiol can induce cell death under appropriate circumstances is novel. Furthermore, the mechanism by which estrogen promotes apoptosis is not understood. Previous studies *(21–23)* have demonstrated a link between estradiol-induced apoptosis and activation of the FasR/FasL death-signaling pathway. Song et al. *(19)* reported that estradiol treatment statistically significantly increased the expression of FasL in a long-term estrogen-deprived (LTED) breast cancer cell model that was sensitive to estradiol-induced apoptosis, and Osipo et al. *(24)* and Liu et al. *(25)* reported an increase in FasR expression in tamoxifen-resistant tumors and raloxifene-resistant cells, respectively, during estradiol-induced apoptosis and tumor regression. More recently, however, we *(22)* have found no evidence to suggest a link between estradiol-induced apoptosis and activation of the FasR/FasL signaling pathway in MCF-7:5C, an estrogen-deprived breast cancer cell line that is resistant to estrogen withdrawal.

Therefore, in the present study, we determined the role of the mitochondrial (intrinsic) pathway in estradiol-induced apoptosis in MCF-7:5C cells. Members of the Bcl-2 family along with the tumor suppressor protein p53, which are important regulators of mitochondrion-mediated apoptosis, were examined in estradiol-treated MCF-7:5C cells. The effect of fulvestrant on the growth of MCF-7:5C cells was also examined, and its efficacy as a growth inhibitor was compared to that of estradiol. Fulvestrant was selected because it is an estrogen receptor antagonist with no agonist effects and is currently licensed in the United States for the treatment of postmenopausal women with hormone-sensitive advanced breast cancer following progression on prior antiestrogen therapy *(23)*.

Materials and Methods

Cells and Tissue Culture Conditions

The ER-positive human breast cancer MCF-7 cells were obtained from Dr. Dean Edwards (University of Texas, San Antonio), and were maintained in full serum medium (RPMI 1640 medium supplemented with 10% fetal bovine serum, 2 m*M* glutamine, 100 U/mL penicillin, 100 μg/mL streptomycin, 1× nonessential amino acids [all from Invitrogen, Carlsbad, CA], and bovine insulin at 6 ng/mL [Sigma-Aldrich, St. Louis, MO]). Estrogen-independent MCF-7:5C *(26)* cells were cloned from wild type MCF-7 cells and were also maintained in estrogen-free RPMI 1640 medium supplemented with 10% dextran-coated charcoal-stripped fetal bovine serum (SFS) and other supplements as in the full serum medium. MCF-7:5C cells stably overexpressing Bcl-x_L or the vector control pBabe were kindly provided by Dr. Navdeep Chandel (Northwestern University, Chicago, IL) and were maintained in phenol red–free RPMI 1640 medium supplemented with 10% SFS and 1-μg/mL puromycin (Sigma-Aldrich).

Cell Proliferation Assays

Wild-type MCF-7 cells were switched from phenol red RPMI 1640 medium supplemented with 10% fetal bovine serum to phenol red–free RPMI 1640 medium for 4 days prior to beginning the proliferation assay. Because MCF-7:5C cells were routinely maintained in estrogen-free RPMI 1640 medium, no medium switch was required for these cells. On the day of the experiment (day 0), MCF-7 and MCF-7:5C cells were cultured in estrogen-free RPMI containing 10% SFS at a density of 2×10^4 cells per well in 24-well plates. After 24 hours (day 1), the medium was replaced with fresh RPMI 1640 medium, and various concentrations of estradiol (10^{-14} to 10^{-8} *M*), fulvestrant (10^{-14} to 10^{-6} *M*), or <0.1% ethanol vehicle (control) were added. The compound-containing medium was replaced with fresh compound-containing medium on days 3 and 5, and the experiment was stopped on day 7. The DNA content of the cells, a measure of proliferation, was determined as previously described *(27)* using a Fluorescent DNA Quantitation kit (Bio-Rad Laboratories, Hercules, CA). In brief, cells were harvested after the appropriate treatment, sonicated in 0.1× phosphate-buffered saline (PBS) (Invitrogen) for 10 seconds, and incubated with a Hoechst dye mixture (BioRad Laboratories) for 1 hour. Total DNA was measured using a VersaFluor fluorometer (Bio-Rad Laboratories). For each

analysis, six replicate wells were used and at least three independent experiments were performed.

Annexin V Analysis of Apoptosis

The annexin V–FITC-labeled Apoptosis Detection Kit I (Pharmingen, San Diego, CA) was used to detect and quantify apoptosis by flow cytometry according to the manufacturer's instructions. In brief, MCF-7:5C cells (1×10^6 cells/mL) were seeded in 100-mm dishes and cultured overnight in estrogen-free RPMI 1640 medium containing 10% SFS. The next day, cells were treated with <0.1% ethanol vehicle (control), estradiol (1 n*M*), or fulvestrant (1 μ*M*) for 72 hours and then harvested in cold PBS (Invitrogen) and collected by centrifugation for 10 min at 500 × *g*. Cells were then resuspended at a density of 1×10^6 cells/mL in 1× binding buffer (HEPES buffer, 10 m*M*, pH 7.4, 150 m*M* NaCl, 5 m*M* KCl, 1 m*M* $MgCl_2$, and 1.8 m*M* $CaCl_2$) and stained simultaneously with FITC-labeled annexin V (25 ng/mL; green fluorescence) and propidium iodide (PI) (50 ng/mL). PI was provided as a 50-μg/mL stock (Pharmingen) and was used as a cell viability marker. Cells were analyzed using a fluorescence-activated cell sorter (FACS) flow cytometer (Becton Dickinson, San Jose, CA), and the data were analyzed with CellQuest software.

4′,6-Diamidino-2-Phenylindole Staining

MCF-7:5C cells were grown (overnight) in RPMI 1640 medium containing 10% SFS and then treated with ethanol vehicle (i.e., control), 1 n*M* estradiol alone, or 1 μ*M* fulvestrant for 96 hours. The cells were then washed in PBS, fixed with 4% paraformaldehyde for 20 minutes at room temperature, and washed again in PBS. Cells were then treated with 1 μg/mL of 4′,6-diamidino-2-phenylindole (DAPI) (Sigma Chemical Co.) for 30 minutes, washed again with PBS for 5 minutes, and treated with 50 μL of VectaShield (Vector Laboratories, Burlingame, CA). Stained nuclei were visualized and photographed using a Zeiss fluorescence microscope (Provis AX70; Olympus Optical Co., Tokyo, Japan). Apoptotic cells were morphologically defined by cytoplasmic and nuclear shrinkage and by chromatin condensation or fragmentation.

Electron Microscopy Analysis

For electron microscopic observation, MCF-7:5C cells were grown (overnight) in RPMI 1640 medium containing 10% SFS and then treated with estradiol (1 n*M*), fulvestrant (1 μ*M*), or ethanol vehicle (<0.1%) for 96 hours. Floating cells were then harvested together with adherent cells and centrifuged at 200 × *g* for 5 min. The cell pellets were fixed overnight in a 0.2 *M* sodium cacodylate buffer solution (pH 7.4) containing 2% glutaraldehyde at 4 °C. Samples were then post-fixed in cacodylate-buffered 1% osmium tetroxide, dehydrated, and embedded in Epon 812 (Structure Probe, Inc., West Chester, PA) for ultra-thin sectioning. The ultra-thin sections were stained with uranyl acetate and lead citrate and viewed with a JEOL JEM-1220 120-kV transmission electron microscope (Peabody, MA) in the Northwestern University Cell Imaging Facility.

Western Blot Analysis

After treatment with estradiol or fulvestrant, cells were washed twice with PBS and lysed in ice-cold lysis buffer (50 m*M* Tris–HCL, pH 7.5, 150 m*M* NaCl, 0.5% Nonidet P40, 1 m*M* phenylmethylsulfonyl fluoride [PMSF], 1 m*M* NaF, 1 m*M* sodium orthovanadate, 1 m*M* dithiothreitol [DTT], 10 μ*M* β-glycerophosphate, and 2-μg/μL complete protease inhibitor cocktail), as previously described *(28)*. Lysates were centrifuged at 12 000 × *g* for 30 min at 4 °C, and protein concentration was measured with the Bio-Rad Protein Assay kit (Bio-Rad Laboratories). Thirty micrograms of protein was mixed with sodium dodecyl sulfate (SDS) sample buffer, denatured by boiling, and separated on 15%, 12%, or 7.5% SDS-polyacrylamide gel gels. Proteins were then electroblotted to nitrocellulose membranes and blocked for 1 hour at room temperature in TBS-T (50 m*M* Tris–HCL, pH 7.5, 150 m*M* NaCl, 0.1% Tween-20) buffer containing 5% nonfat milk. Membranes were then incubated overnight at 4 °C with the respective primary antibodies. Antibodies against Bax (sc-493), Bak (sc-7873), Bcl-2 (sc-509), Bcl-x_L (sc-8392), Bim (sc-11425), ERα (sc-544), MDM2 (sc-5304), Noxa (sc-22764), p53 (sc-126), and Puma (sc-19187) were purchased from Santa Cruz Biotechnology (Santa Cruz, CA). Antibodies against caspase 7 (product 556541), caspase 8 (product 556466), caspase 9 (product 556510), and poly(ADP-ribose) polymerase (PARP) (product 556494) were purchased from BD Pharmingen (San Jose, CA). The antibody against β-actin (product AC-15) was obtained from Sigma-Aldrich (St. Louis, MO). Anti-mouse or anti-rabbit secondary antibody conjugated to horseradish peroxidase (Santa Cruz Biotechnology) was used to visualize the stained bands with an enhanced chemiluminescence (ECL) visualization kit (Amersham, Arlington Heights, IL).

PARP Cleavage

The intact PARP molecule (116 kDa) is activated by breaks in DNA and is cleaved by caspases to yield a p85 fragment that is a characteristic marker of apoptosis *(29)*. For detection of PARP cleavage, MCF-7:5C cells were treated with either ethanol vehicle (0.1%; control) or 1 n*M* estradiol for 24, 48, 72, and 96 hours, and lysates were analyzed by western blotting as described above. Membranes were probed with an anti-PARP monoclonal antibody from BD Pharmingen, which recognizes both the 116-kDa intact form of PARP and the 85-kDa cleavage fragment.

Real-Time Reverse Transcription–Polymerase Chain Reaction

Total RNA was reverse transcribed with TaqMan reverse transcription reagents (Applied Biosystems, Hayward, CA) and random hexamers as the primers. Primers and probes for human transforming growth factor alpha (TGF-α) and trefoil factor 1 (pS2) were designed with Primer Express TM1.5 software (Applied Biosystems) set at default parameters to select the optimal primer and probe sets for this system. Both TGF-α and pS2 are considered estrogen-responsive genes; hence, ERα activity was assessed by measuring the estrogen-responsive expression of TGF-α and pS2 mRNA in MCF-7:5C cells following estradiol or fulvestrant treatment. Eukaryotic 18S ribosomal RNA (Applied Biosystems, product 4319413E) was used as an internal control, and each total cDNA sample was normalized to the content of 18S mRNA. The sequences for all primers and probes are as follow: TGF-α forward primer, 5′-GCCTGTAACACACATG CAGTGA-3′; TGF-α reverse primer, 5′-TTTCCAAAGGACTGA

CTTGGAAG-3′; TGF- α probe, 5′-FAM-AGGCCTCACATA TACGCCTCCCTAGAAGTG-QSY7–3′; pS2 forward primer, 5′-GAGGCCCAGACAGAGACGTG-3′; pS2 reverse primer, 5′-CCCTGCAGAAGTGTCTAAAATTCA-3′; pS2 probe, 5′-FAM-CTGCTGTTTCGACGAC ACCGTTCG-QSY7–3′; p53 forward primer, 5′-CCCCAGCCAAAGAGAAACC-3′; and p53 reverse primer, 5′-TCCAAGGCCTCATTCAGCTCT-3′. All probes were labeled with 6-carboxyfluorescein (FAM) as the reporter and with QSY7 (a nonfluorescent diarylrhodamine derivative; Mega-Bases, Chicago, IL) as the quencher.

The reverse transcription–polymerase chain reaction (RT-PCR) portion of the reaction was performed with the TaqMan Universal PCR Master Mix reagent kit (Applied Biosystems, Branchburg, NJ). A 25-μL reaction mixture, containing 50 ng of total cDNA, 100 n*M* probe, and 200 n*M* primers, was prepared using 2× TaqMan Universal PCR master mix (Applied Biosystems). RT-PCR was performed with the ABI-Prism 7700 sequence detection system (Applied Biosystems). The PCR was run in a sealed 96-well optical plate, and the thermal cycler conditions were as follow: initial denaturation at 50 °C for 2 minutes and 95 °C for 10 minutes, followed by 40 cycles of a denaturation step at 95 °C for 15 seconds, and a primer annealing/extension step at 60 °C for 1 minute. RT-PCR results were quantitated by normalizing the cycle threshold (CT) values (which are proportional to mRNA copy number) of TGF-α, pS2, or p53 mRNA to the CT values of the endogenous control 185. The relative quantitation number was then calculated by subtracting the average CT for TGF-α, pS2, or p53 from the corresponding average CT for 185.

Small Interfering RNA Transfection

For transient transfections, MCF-7:5C cells were seeded at a density of 50–70% in 12-well plates in estrogen-free Opti minimal essential medium (Opti-MEM) containing 10% SFS. The following day, cells were transfected with 100 n*M* small interfering RNAs (siRNAs) for p53 (Cell Signaling, product number 6230), Bax (Dharmacon, product number M-003308–00), Bim (Dharmacon, product number M-004383–00, Noxa (Dharmacon, product number M-005275–01), Puma (Dharmacon, product number M-004380–00), or FasL (Dharmacon Research, Lafayette, CA) using Lipofectamine 2000 transfection reagent (Invitrogen, product number 116668–019), according to the manufacturer's recommended protocol. Scramble siRNA was purchased from Dharmacon and was used as a control (Silencer negative control siRNA, product number 4611). The cells were harvested 48 hours posttransfection and analyzed by western blot (as described above) and/or by RT-PCR (as described above). Transfected cells were also treated with estradiol for an additional 72 hours, and apoptotic cells were measured using annexin V staining (as described above).

Mitochondrial/Transmembrane Potential ($\Delta\psi_m$) and Cytochrome *c* Release

Mitochondrial membrane potential was measured by flow cytometry using the cationic lipophilic green fluorochrome rhodamine-123 (Rh123) (Molecular Probes). Disruption of $\Delta\Psi_m$ is associated with a lack of Rh123 retention and a decrease in fluorescence. Briefly, MCF-7:5C cells were washed twice with PBS and incubated with 1-μg/mL Rh123 at 37 °C for 30 min. Cells were then washed twice with PBS, and Rh123 intensity was determined by flow cytometry. Cells with reduced fluorescence (less Rh123) were counted as having lost some of their mitochondrial membrane potential.

For detection of cytochrome *c*, MCF-7:5C cells (1×10^7) were treated with either ethanol vehicle (<0.1%) or 1 n*M* estradiol for 48 hours and then harvested by centrifugation at 800 × *g* at 4 °C for 15 min. After washing three times with ice-cold PBS, cell pellets were resuspended in HEPES-buffer (20 m*M* HEPES, 10 m*M* KCl, 1.5 m*M* $MgCl_2$, 1 m*M* EDTA, 1 m*M* EGTA, 1 m*M* DTT, 0.1 m*M* PMSF, pH 7.5) containing 250 m*M* sucrose, homogenized with a homogenizer, and centrifuged at 800 × *g* at 4 °C for 15 min. The supernatants were centrifuged at 10 000 × *g* for 15 min at 4 °C, and the mitochondrial pellets were dissolved in SDS sample buffer (25 μL), subjected to 15% SDS- polyacrylamide gel electrophoresis, and analyzed by immunoblotting with monoclonal antibodies against cytochrome *c* (BD Biosciences; product 556433) and cytochrome oxidase subunit IV (COXIV) (Molecular Probes; product A21437). Aliquots (25 μL) of the supernatant (i.e., cytosolic fraction) were also analyzed for cytochrome *c* expression by western blotting. An anti-mouse secondary antibody conjugated to horseradish peroxidase (Santa Cruz Biotechnology) was used to visualize the stained bands with an ECL visualization kit (Amersham). COXIV, which is a mitochondrion-specific protein, was used as a control to demonstrate that mitochondrial protein fractionation was successfully achieved.

Caspase 8 Activity

A caspase 8 fluorometric assay kit (Chemicon International, Inc., Temecula, CA), which contains the caspase 8–specific substrate Acetyl-Ile-Glu-Thr-Asp-p-Nitroaniline (Ac-IETD-pNA), was used to evaluate caspase 8 enzyme activity in MCF-7:5C cells following 1 n*M* estradiol treatment (96 and 120 hours), according to the manufacturer's instructions. The broad-spectrum caspase inhibitor, benzyloxycarbonyl-Val-Ala-Asp(OMe)-fluoromethylketone (z-VAD-fmk), and the caspase 8–specific inhibitor, z-Lle-Glu(OMe)-Thr-Asp(OMe)-fluoromethyl ketone (z-IETD-FMK), were purchased from Calbiochem (La Jolla, CA).

Neutralization of the Fas Receptor and Fas Ligand

Cells (1×10^5) were seeded in 12-well plates in RPMI 1640 medium containing 10% SFS and after 24 hours were treated with an anti-FasR neutralizing antibody (ZB4) at a final concentration of 250 ng/mL for 12 hours, which we have previously determined to be the optimal treatment in terms of Fas neutralization of MCF-7:5C *(22)*. Cells were then treated with 1 n*M* estradiol for an additional 48 and 72 hours, and apoptosis was determined by annexin V staining. ZB4 is very effective at antagonizing FasR and has previously been shown to block drug-induced apoptosis in breast and cervical cancer cells *(30)*. Similar experiments were performed with the FasL neutralizing antibodies NOK1 and NOK2 at a final concentration of 500 ng/mL.

Growth of MCF-7:5C Tumors In Vivo

Approximately 1×10^7 MCF-7:5C cells suspended in saline solution (product 20012027; Invitrogen) were bilaterally inoculated into mammary fat pads of 30 ovariectomized BALB/c nu/nu

mice (Harlan Sprague Dawley, Madison, WI), as described previously *(31)*. Tumors were measured weekly with vernier calipers, and the cross-sectional tumor area was calculated by multiplying the length (l) by the width (w) by π and dividing the product by four (i.e., $lw\pi/4$). When the untreated MCF-7:5C tumors reached a mean cross-sectional area of 0.23 cm^2 (at approximately 4 weeks), groups of 10 mice were randomly assigned to the following groups: 1) 0.3-cm estradiol capsule, 2) fulvestrant (5 mg/0.1 mL of peanut oil injected subcutaneously twice a week), and 3) vehicle control. For the estradiol treatment, 0.3-cm silastic estradiol capsules (Baxter HealthCare, Mundelein, IL), were implanted subcutaneously in the mice and replaced after 8 weeks of treatment. These capsules produced a mean serum estradiol level of 83.8 pg/mL *(32)*, which is similar to postmenopausal serum levels of estradiol. For the fulvestrant treatment, fulvestrant (AstraZeneca, Cheshire, UK) was dissolved in 100% ethanol and diluted in peanut oil and injected twice a week. For the vehicle control group, the mice did not receive any treatment. All animal handling procedures were in accordance with the approved guidelines of the Animal Care and Use Committee of Northwestern University. The experiment was followed for 10 weeks (data shown for only 8 weeks), and at the end of the study, all animals were killed by CO_2 asphyxiation. For detection of apoptosis in vivo, MCF-7:5C tumors were removed from control and estradiol-treated mice on day 5, fixed in formalin, and embedded in paraffin blocks. No tumors were collected at the end of the study (week 10) because estradiol treatment caused complete tumor regression.

Terminal Deoxynucleotidyl Transferase-Mediated dUTP Nick End-Labeling Assay

The terminal deoxynucleotidyl transferase–mediated dUTP nick end–labeling (TUNEL) assay followed by tetramethylrhodamine deoxyuridine 5′-triphosphate (TMR) staining was used to detect apoptosis in vivo. An in situ cell death assay with the TMR red detection kit (Roche Diagnostic, Indianapolis, IN) was performed on paraffin-embedded MCF-7:5C tumor sections (described above), according to the manufacturer's instructions. The TUNEL assay was performed in triplicate and repeated three times with six independent tumors from each treatment group. The percentage of apoptosis was calculated by dividing the number of TMR-positive cells or TUNEL-positive cells by the total number of epithelial cells (identified by DAPI staining) and multiplying the result by 100.

Statistical Analysis

All data are expressed as the mean (with 95% confidence interval [CI]) of at least three determinations, unless otherwise stated. The differences between the treatment groups and the control group (for all analyses except tumor growth) were determined by two-sample t test or one-factor analysis of variance (ANOVA). Generalized Estimating Equation methods *(33)* were used to compare tumor growth rates among the three treatment groups using data collected in weeks 5–8. First, left and right tumor areas were averaged for each mouse at each time point. This measure was the dependent variable for subsequent analyses. Second, treatment time was log transformed to approximately linearize the growth curves. For each treatment group, slopes were estimated from the tumor growth data. Cage was included in the analysis as a clustering factor. Finally, pairwise between-group comparisons were made using robust standard errors. The type 1 error for the pairwise tests was adjusted for multiple comparisons using Bonferroni's method (i.e., $\alpha = .05/3$, or .0167). All statistical tests were two-sided.

Results

Growth of LTED Breast Cancer Cells In Vitro

Wild-type MCF-7 human breast cancer cells *(34)* are a permanent cell line that contains estrogen receptors. These cells have retained estrogen responsiveness for a sustained period of continuous cell culture and show estrogen-dependent stimulation of cell proliferation by natural estrogens or inhibition by antiestrogens *(35,36)*. Therefore, we compared the growth characteristics of wild-type MCF-7 cells with those of LTED MCF-7:5C cells in the presence of estradiol or the pure antiestrogen fulvestrant. Figure 1, A shows that estradiol treatment increased the growth of wild-type MCF-7 cells in a concentration-dependent manner, with maximum stimulation at 10^{-10} M. In contrast, fulvestrant treatment reduced the growth of MCF-7 cells, with maximum

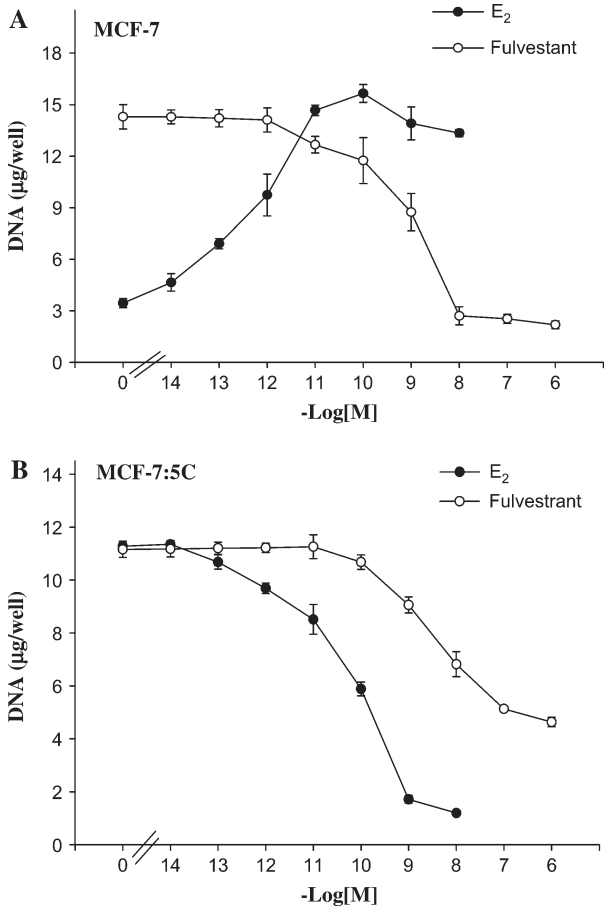

Fig. 1. Effects of estradiol (E_2) and fulvestrant (Ful) on the growth of MCF-7 cells. **A**) Wild-type MCF-7 cells. **B**) Long-term E_2-deprived MCF-7:5C cells. For growth assays, approximately 2×10^4 cells were seeded in 24-well plates and then treated with various concentrations of E_2 (10^{-14} to 10^{-8} M) or fulvestrant (10^{-14} to 10^{-6} M) for 7 days. Cells were harvested on day 7, and total DNA (micrograms/well) was quantitated. The experiment was repeated three times. The data represent the mean of three independent experiments with 95% confidence intervals.

inhibition at 10^{-6} *M*. Figure 1, B shows that estradiol at 10^{-9} *M* statistically significantly reduced the growth of MCF-7:5C cells, as measured by DNA content, from 11.5 μg [95% CI = 11 to 12 μg] in the absence of estradiol to 1.7 μg [95% CI = 1.4 to 2 μg, *P*<.001] (Fig. 1, B), whereas fulvestrant (10^{-6} *M*) reduced the growth of these cells from 11.3 μg [95% CI = 11.1 to 11.5 μg] to 4.4 μg [95% CI = 4.2 to 4.6 μg]. The difference in the inhibitory effects of fulvestrant at 10^{-6} *M* and estradiol at 10^{-9} *M* was statistically significant (*P* = .002). Overall, these results show that there are dramatic differences between MCF-7 cells and MCF-7:5C cells in their response to estradiol—specifically, that LTED altered MCF-7:5C cells in such a way that estrogen induces cell death rather than cell growth.

To assess ERα-mediated transcriptional activation in MCF-7:5C cells following estradiol or fulvestrant treatment (24 hours), the endogenous estrogen-responsive genes TGF-α and pS2 were measured by real-time PCR. Expression of TGF-α mRNA is normally induced by estradiol in MDA-MB-231 human breast cancer cells stably transfected with the wild-type ERα *(37)*. The pS2 gene is often used as a prognostic marker in breast cancer cells and has been widely used in studies of ER action, and it is suggested that estrogen regulates the expression of pS2 through an imperfect ERE in the pS2 promoter *(38)*. Our results showed that estradiol treatment increased TGF-α and pS2 mRNA expression in MCF-7:5C cells that was blocked completely by the pure antiestrogen fulvestrant (data not shown). We also found that MCF-7:5C cells expressed higher levels of ERα protein than did wild-type MCF-7 cells, as assayed by western blotting (data not shown). These results demonstrate that resistance to LTED did not alter the ability of the ER to regulate the expression of estrogen-responsive genes.

Effect of Estradiol and Fulvestrant on Apoptosis in MCF-7:5C Cells

Because a decrease in cell proliferation may result from the induction of apoptosis, we investigated whether the estradiol- or fulvestrant-induced growth inhibition of MCF-7:5C cells was due to an increase in apoptosis. MCF-7:5C cells were treated with ethanol vehicle (i.e., control), estradiol (1 n*M*), or fulvestrant (1 μ*M*) for 72 hours, and annexin V–FITC and PI fluorescence was determined by flow cytometry (Fig. 2, A). In the

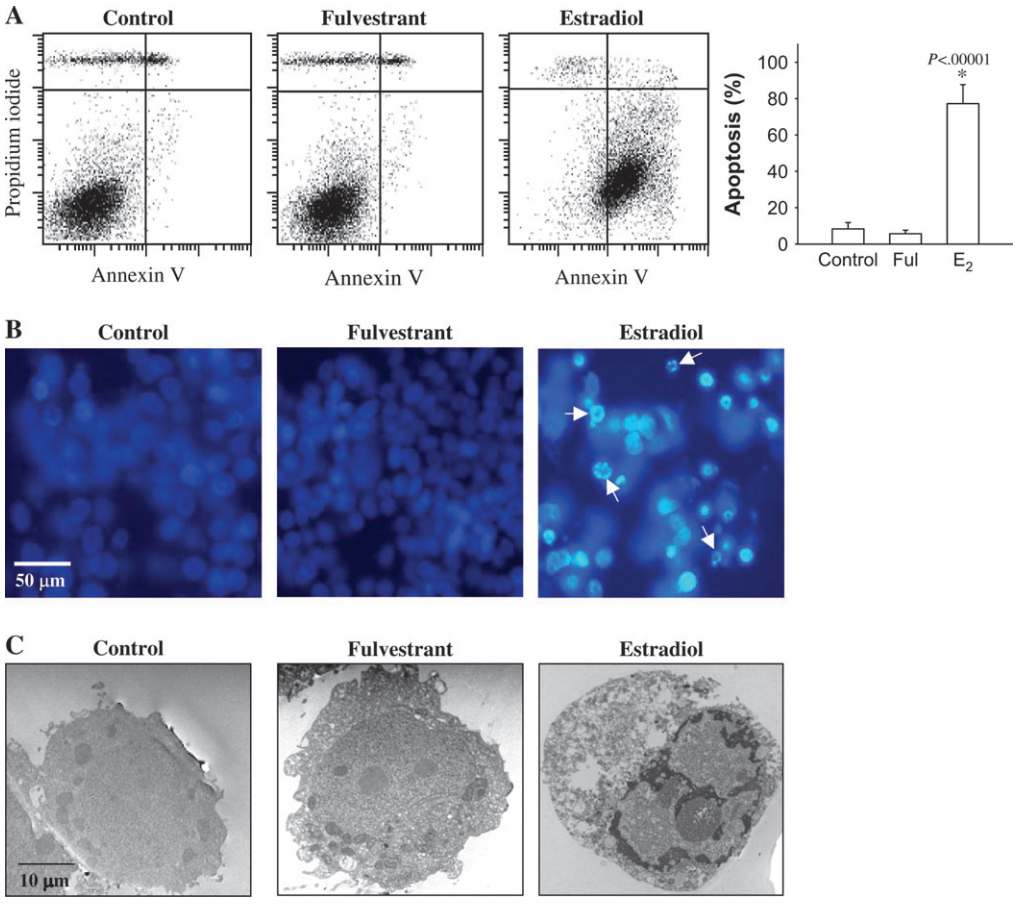

Fig. 2. Effects of estradiol and fulvestrant on apoptosis in MCF-7:5C cells. **A**) Annexin V staining for apoptosis. MCF-7:5C cells were seeded in 100-mm plates at a density of 1×10^6 per plate. After 24 hours, the cells were treated with ethanol vehicle (**control**), 1 μ*M* fulvestrant (Ful), or 1 n*M* estradiol (E_2) for 72 hours, and then cells were stained with FITC–annexin V and propidium iodide (PI) and analyzed by flow cytometry. Representative cytograms are shown for cells treated with ethanol vehicle (control), estradiol (1 n*M*), or fulvestrant (1 μ*M*). Viable cells are $FITC^-$ and PI^-, early apoptotic cells are $FITC^+$ and PI^-, and late apoptotic cells are $FITC^+$ and PI^+. **Right panel** = Quantitation of apoptosis (percentage of all cells that were apoptotic). **P*<.001 for estradiol-treated cells compared with control. The data represent the means of three independent experiments, and the error bars show upper 95% confidence intervals. **B**) Fluorescent microscopic analysis of apoptotic cells stained with 4′,6-diamidino-2-phenylindole (DAPI). Round and/or shrunken nuclei of DAPI-stained cells (**white arrows**) are hallmarks of apoptosis. Experiments were repeated three times with similar results. Representative slides are shown. **Scale bars** = 50 mm. **C**) Electron microscopic analysis of MCF-7:5C cells treated with ethanol, 1 μ*M* fulvestrant, or 1 n*M* estradiol for 96 hours. Experiments were repeated three times with similar results. Representative slides are shown. **Scale bars** = 10 μm.

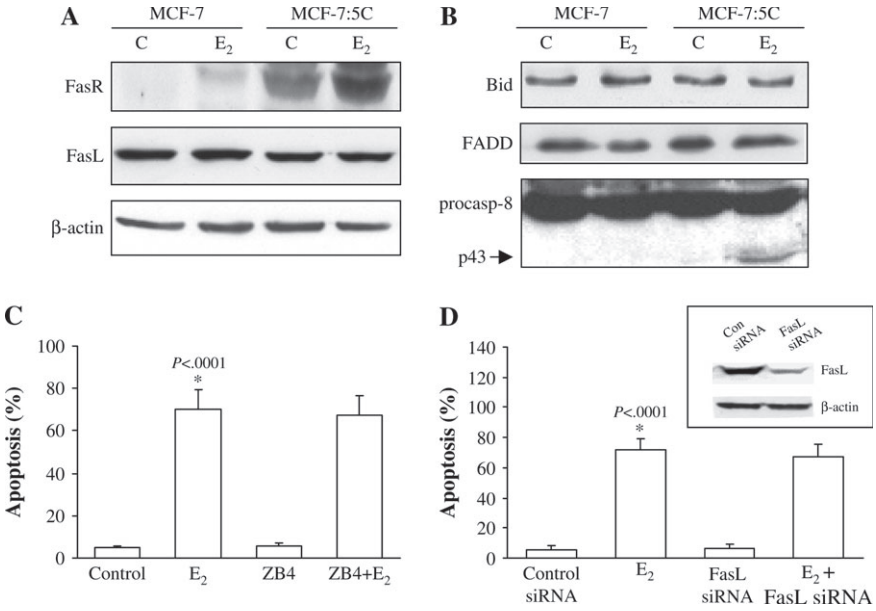

Fig. 3. Effect of estradiol on FasR/FasL signaling pathway in MCF-7 and MCF-7:5C cells. **A**) Western blot analysis for FasR and FasL protein expression in parental MCF-7 cells and MCF-7:5C cells following 96 hours of treatment with either ethanol (vehicle) (C) or 1 n*M* estradiol (E_2). FasR = 45 kDa; FasL = 38 kDa; NS = non-specific band. **B**) Western blot analysis of Bid, FADD, and caspase 8 protein expression in parental MCF-7 cells and MCF-7:5C cells following 96 hours of treatment with either 1 n*M* E_2 or ethanol. p43 is the cleaved (i.e., activated) form of caspase 8 (casp-8). **C**) Effect of Fas neutralizing antibody ZB4 on E_2-induced apoptosis in MCF-7:5C cells. Cells were preincubated with the ZB4 antibody for 12 hours and then treated with 1 n*M* E_2 for 96 hours. Percentage of cells that were apoptotic was determined by annexin V staining. Results shown are the means of three independent experiments with 95% confidence intervals. **D**) Reduction of FasL expression in MCF-7:5C cells by small interfering RNA (siRNA). Cells were transfected with a scrambled control siRNA or FasL-specific siRNA. After 48 hours, the cells were analyzed by western blotting for FasL protein expression (**insert**) or were treated with estradiol (or ethanol) for an additional 72 hours, after which apoptosis was assessed by annexin V staining.

control and fulvestrant-treated groups, only 2.8% (95% CI = 2.3% to 3.3%) and 3.8% (95% CI = 3.3% to 4.3%), respectively, of cells stained positive for annexin V, whereas, in the estradiol-treated group, 77.6% [95% CI = 71% to 84.2%] of cells stained positive for annexin V. In additional experiments (not shown), cells were treated with estradiol plus fulvestrant or estradiol plus the universal caspase inhibitor z-VAD-FMK. In both cases estradiol-induced apoptosis in MCF-7:5C cells was blocked, suggesting the involvement of the ERα and caspases in this process.

To confirm the apoptosis-inducing effect of estradiol on MCF-7:5C cells, we stained cells with DAPI. In contrast to untreated control cells and fulvestrant-treated cells, which had very little condensed or fragmented chromatin, the majority of estradiol-treated cells displayed apoptotic features, including condensed nuclei, membrane blebbing, and nuclear fragmentation (Fig. 2, B).

Electron microscopy was used to characterize the structural changes associated with estradiol-induced apoptosis in MCF-7:5C cells. Cells treated with vehicle or fulvestrant showed no signs of apoptosis (Fig. 2, C), displaying a uniform rounded shape and no condensation of chromatin. There were also very few vesicles in the cytoplasm and little debris in the extracellular space of these cells. In contrast, cells treated with estradiol displayed classic apoptotic nuclei, with completely condensed chromatin at the inner side of the nuclear envelope. Estradiol-treated cells also showed membrane blebbing and formed apoptotic bodies, which are morphologic hallmarks of apoptosis. Together, these findings suggest that estradiol induces apoptotic death in MCF-7:5C cells; by contrast, fulvestrant inhibits growth through a nonapoptotic pathway.

FasR/FasL Signaling Pathway in Estradiol-Induced Apoptosis in MCF-7:5C Cells

Song et al. *(19)* reported that estradiol-induced apoptosis in an LTED breast cancer cell line is mediated by the FasR/FasL signaling pathway. We performed several analyses to investigate whether this result was also the case in MCF-7:5C cells. First, western blot analysis was performed to measure FasR and FasL protein expression in wild-type MCF-7 cells and MCF-7:5C cells. As Fig. 3, A shows, MCF-7:5C cells expressed a higher basal level of FasR protein than did wild-type MCF-7 cells. Moreover, estradiol further increased FasR protein expression, but not FasL protein expression, to a level that was markedly higher than that of control. However, estradiol induction of FasR did not occur until after 5 days of treatment (data not shown), after apoptosis had commenced.

We next investigated whether Fas-associated death domain (FADD), caspase 8, and Bid, which are important components of the FasR/FasL death signaling pathway, are activated by estradiol. In MCF-7:5C cells, estradiol treatment increased the cleavage of caspase 8 (cleaved fragment, p43) but did not alter FADD or Bid protein levels or Bid cleavage (i.e. activation) (Fig. 3, B). Estradiol-induced cleavage of caspase 8, however, occurred after 5 days of estradiol treatment and was not associated with apoptosis induction. In addition, inhibition of caspase 8 activity using the caspase 8 inhibitory peptide z-IETD-fmk failed to block estradiol-induced apoptosis or cytochrome *c* release (data not shown), which suggests that activation of caspase 8 is not a critical event in estradiol-induced apoptosis. The ability of the universal caspase inhibitor z-VAD-FMK to completely block estradiol-induced apoptosis in MCF-7:5C cells indicates that other caspases are involved in this process.

Because the Fas protein was induced by estradiol in MCF-7:5C cells, we investigated whether this induction was required for estradiol-induced apoptosis. Treatment of cells with neutralizing antibody against FasR (ZB4) did not prevent estradiol-induced apoptosis of MCF-7:5C cells (Fig. 3, C). Finally, we reduced FasL expression in MCF-7:5C cells using siRNA. As shown in Fig. 3, D (insert), transfection of MCF-7:5C cells with FasL-specific siRNA led to a marked reduction in FasL protein levels, whereas transfection with control siRNA did not have this effect, indicating that the inhibition was sequence specific. Inhibition of FasL expression, however, did not block estradiol-induced apoptosis in MCF-7:5C cells

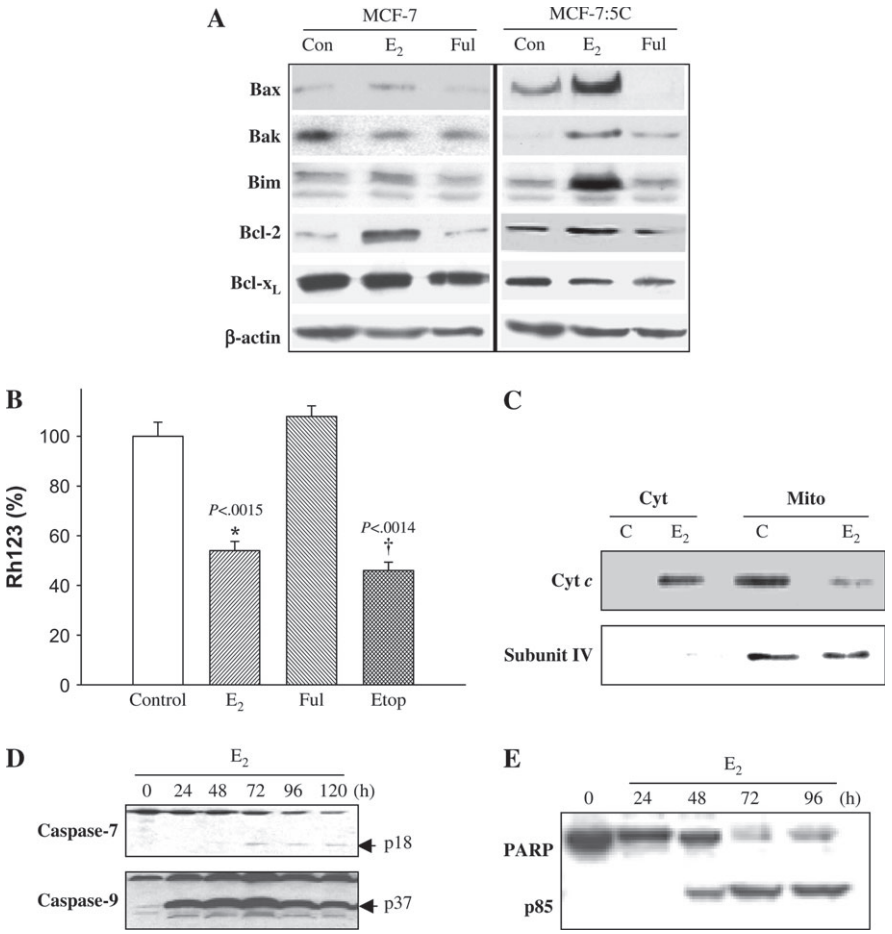

Fig. 4. Effect of estradiol on Bcl-2 family protein expression and mitochondrial function in MCF-7:5C cells. **A**) Western blot analysis for Bax, Bak, Bim, Bcl-2, and Bcl-x_L protein expression in parental MCF-7 cells and MCF-7:5C cells following 48 hours of treatment with ethanol (Con), 1 n*M* estradiol (E_2), or 1 μ*M* fulvestrant (Ful). Equal loading was confirmed by reprobing with an antibody against β-actin. **B**) Loss of mitochondrial potential (i.e., mitochondrial integrity) in MCF-7:5C cells was determined by rhodamine-123 (Rh123) retention assay. The percentage of cells retaining Rh123 in each treatment group was compared with untreated control. **P*<.001 is the E_2-treated group compared with the control group. **C**) Cytosolic and mitochondrial fractions were generated as described in "Materials and Methods." Equivalent protein loading was verified using anti-cytochrome *c* oxidase IV (subunit 4) antibody. **D**) Activation of caspase 7 (casp-7) and caspase 9 (casp-9) was assessed by Western blot using specific antibodies. The upper band of caspase 7 represents the full-length protein, and the lower band (p18) represents the cleaved activated product. **E**) PARP cleavage was determined by western blotting using a rabbit polyclonal PARP antibody. MCF-7:5C cells were treated with 1 n*M* E_2 for 24, 48, 72, and 96 hours. Full-length PARP is approximately 116 kDa; cleaved (active) PARP is 85 kDa.

(Fig. 3, D). Moreover, FasL neutralizing antibodies (NOK1/NOK2) also did not prevent estradiol-induced apoptosis (data not shown). Overall, these findings indicate that estradiol induction of apoptosis in MCF-7:5C cells did not require activation of FasR or FasL and suggest that the extrinsic death receptor pathway is not a critical mediator of estradiol-induced apoptosis.

Role of the Mitochondrial Pathway in Estradiol-Induced Apoptosis in MCF-7:5C Cells

To examine the role of the mitochondrial (i.e., intrinsic) pathway in estradiol-induced apoptosis in MCF-7:5C cells, we used Western blot analysis to measure the levels of the proapoptotic Bax, Bak, and Bim and antiapoptotic Bcl-2 and Bcl-x_L proteins, all components of the intrinsic pathway, after treatment with either estradiol or fulvestrant. Figure 4, A shows that there was a marked increase in the levels of Bax, Bak, and Bim proteins in estradiol-treated MCF-7:5C cells compared with vehicle-treated (control) cells. Estradiol treatment, however, did not increase the protein level of Bax, Bak, or Bim in wild-type MCF-7 cells (Fig. 4, A), which is consistent with its antiapoptotic activity in these cells.

A key step in the mitochondrion-dependent apoptotic pathway is the disruption of the mitochondrial membrane, leading to loss of mitochondrial transmembrane potential ($\Delta\psi_m$) *(39)*. Therefore, we examined the effect of estradiol on $\Delta\psi_m$ by Rh123 retention. Figure 4, B shows that estradiol treatment statistically significantly reduced Rh123 fluorescence in MCF-7:5C cells by 45% [95% CI = 40% to 50%, P = .002] compared with control, suggesting that the mitochondrial pathway is involved in estradiol-induced apoptosis. By contrast, fulvestrant did not have a statistically significant effect on $\Delta\psi_m$ (Fig. 4, B); however, when fulvestrant was combined with estradiol, estradiol-induced loss of $\Delta\psi_m$ was blocked completely (data not shown). This finding suggests that estradiol-induced loss of $\Delta\psi_m$ requires the estrogen receptor.

During mitochondrion-mediated apoptosis, cytochrome *c* is released from the mitochondria into the cytosol, where it promotes caspase activation *(40)*. Therefore, we examined the effects of estradiol on cytochrome *c* release in MCF-7:5C cells using western blot analysis. Figure 4, C shows that in vehicle-treated (control) cells, cytochrome *c* was detected primarily in the mitochondria and was undetectable in the cytosol; however, estradiol treatment (48 hours) led to a statistically significant increase in cytochrome *c* release from the mitochondria to the cytosol that coincided with cleavage (i.e., activation) of caspase 9 (active product p37) (Fig. 4, D) and cleavage of PARP (active product p85) (Fig. 4, E). Estradiol-induced cleavage of caspase 9 was detected as early as 24 hours after treatment. We did not detect any caspase 3 protein in MCF-7:5C cells (data not shown); however, this finding is consistent with previous reports that indicate a lack of caspase 3 in these cells *(41)*. PARP cleavage was observed 48 hours after estradiol treatment, with maximum cleavage between 72 and 96 hours. Interestingly, fulvestrant, the ER antagonist, was able to block the ability of estradiol to induce

apoptosis, cytochrome *c* release, caspase activation, and PARP cleavage (data not shown), which suggests a critical role for the ER in estradiol-induced apoptosis.

Effect of Bcl-x_L Overexpression on Estradiol-Induced Apoptosis in MCF-7:5C Cells

Overexpression of Bcl-2/Bcl-x_L has been shown to inhibit mitochondrial damage and release of cytochrome *c*, which are key events in caspase activation and apoptosis *(42)*. Therefore, to confirm the role of the mitochondrial pathway in estradiol-induced apoptosis, we investigated whether Bcl-x_L overexpression can protect MCF-7:5C cells against estradiol-induced apoptosis in MCF-7:5C cells. Western blot analysis was used to verify Bcl-x_L protein overexpression in MCF-7:5C cells stably overexpressing Bcl-x_L or the empty vector pBabe (Fig. 5, A). For the annexin V study, MCF-7:5C cells stably overexpressing Bcl-x_L or the empty vector pBabe were treated with either ethanol vehicle (control) or 1 n*M* estradiol, and apoptosis was examined by flow cytometry using annexin V–PI staining. Estradiol treatment (for 72 hours) induced marked apoptosis in the pBabe vector control cells but not in the Bcl-x_L–overexpressing cells (Fig. 5, B). The estradiol-induced reduction in $\Delta\psi_m$, as determined by Rh123 retention assay, was also partially reversed by Bcl-x_L overexpression (Fig. 5, C). These results provide further evidence that the mitochondrial pathway is required for estradiol-initiated apoptotic signaling in MCF-7:5C cells.

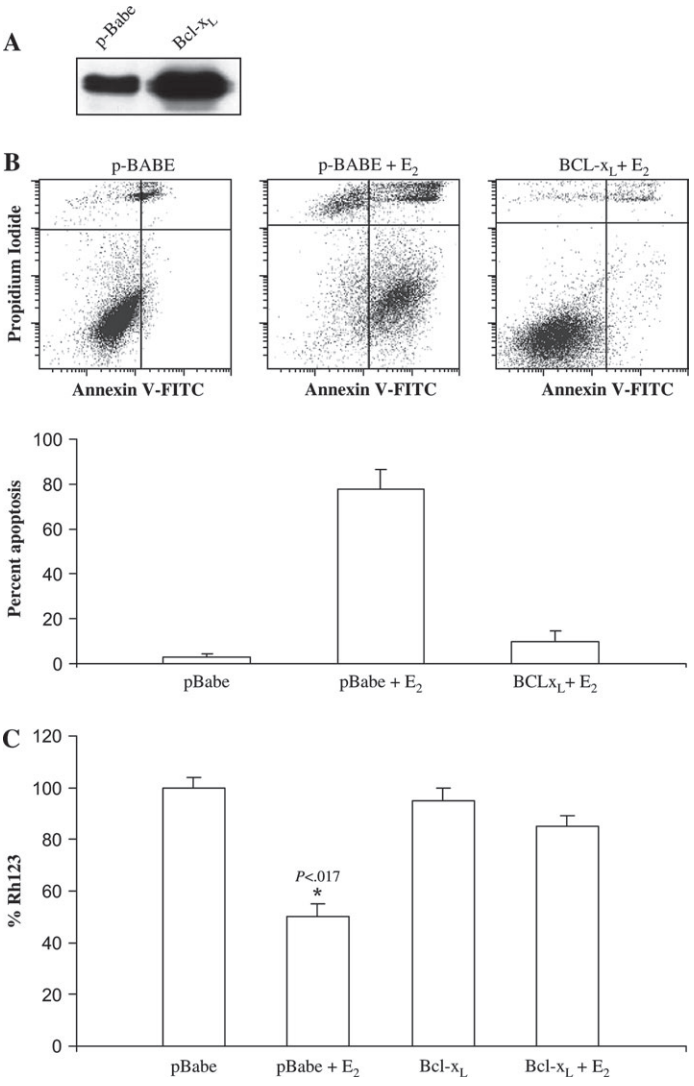

Fig. 5. Effect of overexpression of Bcl-x_L on estradiol-induced apoptosis of MCF-7:5C cells. Bcl-x_L was stably overexpressed in MCF-7:5C cells using the retroviral vector pBabe-Puro-Bcl-x_L. **A**) Western blot analysis of Bcl-x_L expression in Bcl-x_L–transfected and pBabe mock-transfected MCF-7:5C cells. **B**) Annexin V staining for apoptosis. pBabe vector control and Bcl-x_L–overexpressing MCF-7:5C cells were treated with either ethanol vehicle (control) or 1 n*M* estradiol for 72 hrs. The cells were then double stained with recombinant FITC-conjugated annexin V and propidium iodide and then analyzed by flow cytometry. The percentage of apoptotic cells in each treatment group is shown in the **bottom panel**. The experiment was repeated three times. The data represent the mean of three independent experiments, and error bars show upper 95% confidence intervals. **C**) Loss of mitochondrial transmembrane potential ($\Delta\psi_m$) was determined by rhodamine-123 (Rh123) retention assay as described in Materials and Methods.

Role of Bax and Bim in Estradiol-Induced Apoptosis in MCF-7:5C Cells

Bax and Bim are important regulators of mitochondrion-mediated apoptosis; hence, we examined the effect of blocking Bax and Bim mRNA expression (using siRNAs) on estradiol-induced apoptosis in MCF-7:5C cells. Transient transfection of MCF-7:5C cells with either Bax or Bim siRNAs almost completely abolished protein levels compared with those in cells transfected with control siRNAs (Fig. 6, A). These cells also had 65% [95% CI = 60% to 75%, *P*<.001] and 85% [95% CI = 80% to 90%, *P*<.001] reductions in estradiol-induced apoptosis, respectively, compared with cells transfected with the control siRNA (Fig. 6, B). Thus, both Bax and Bim appear to be important components of estradiol-induced apoptosis.

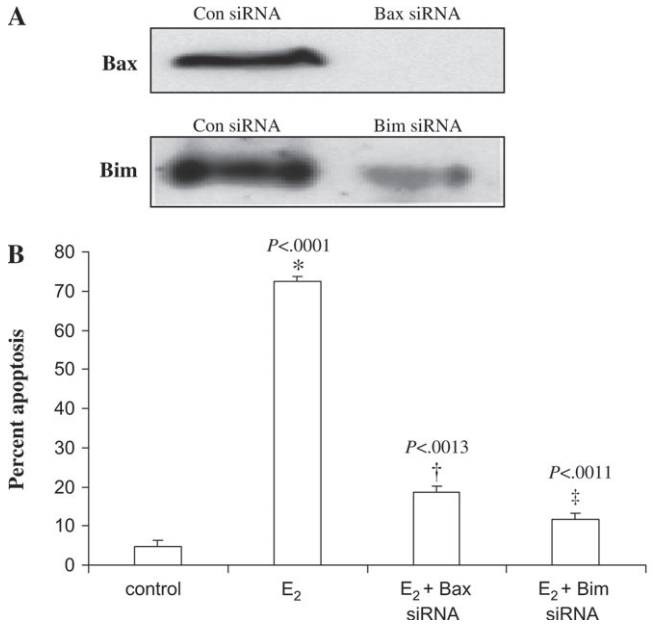

Fig. 6. RNA interference and apoptosis in MCF-7:5C cells. **A**) MCF-7:5C cells were transfected with a scrambled sequence siRNA (con), Bax siRNA, or Bim siRNA. After 48 hours, lysates were prepared and analyzed by western blotting. Representative blots are shown. **B**) Transfected MCF-7:5C cells were treated with ethanol vehicle (control) or 1 n*M* estradiol (E_2) for 72 hours, and the percentage of cells that were apoptotic was assessed by annexin V staining. **P*<.001 for the E_2 + Bax siRNA group compared with the E_2 group alone. †*P*<.001 for the E_2 + Bim siRNA group compared with the E_2 group alone.

Role of p53 in Estradiol-Induced Apoptosis in MCF-7:5C Cells

The p53 tumor suppressor protein is an important apoptosis regulator, and recent evidence suggests that p53-mediated cell death occurs primarily through the intrinsic mitochondrial pathway *(43)*. Therefore, we examined the role of p53 in estradiol-induced apoptosis in MCF-7:5C cells. Western blot analysis showed that estradiol markedly increased p53 protein level in MCF-7 cells and MCF-7:5C cells, whereas fulvestrant almost completely decreased p53 protein levels in both cell lines (Fig. 7, A). Estradiol treatment also statistically significantly increased p53 mRNA expression in MCF-7:5C cells compared with control ($P = .011$) (Fig. 7, B). To determine whether p53 was functional in MCF-7:5C cells, we also measured the expression of the p53-regulated proteins p21, Mdm2, Puma, and Noxa. Figure 7, A shows that estradiol treatment markedly increased the protein levels of Puma and Noxa in MCF-7:5C cells but did not alter the levels of p21 or MDM2.

We then examined whether p53 induction was required for estradiol-induced apoptosis by using siRNA to suppress p53 mRNA expression in MCF-7:5C cells. Cells transiently transfected with a p53-suppressing siRNA demonstrated dramatic reductions in p53 mRNA and dramatic protein levels compared with those in cells transfected with the scrambled control siRNA (Fig. 7, C and D). In addition, cells transfected with the p53 siRNA showed a strong decrease in estradiol-induced apoptosis compared with cells transfected with the control siRNA (Fig. 7, E). Overall, these results indicate that p53 induction is important for estradiol-induced apoptosis in MCF-7:5C cells.

Growth of LTED MCF-7:5C Cells In Vivo

The ability of estradiol to induce apoptosis in vitro raised the possibility that this agent might induce tumor regression in vivo. MCF-7:5C cells were bilaterally injected into the mammary fat pads of athymic mice (N = 30), and within approximately 4 weeks, measurable tumors were detected with a mean tumor cross-sectional area of 0.23 cm^2 [95% CI = 0.22 to 0.24]. The mice were then randomly assigned to a treatment group [i.e., estradiol (n = 10), fulvestrant (n = 10), and vehicle control (n = 10)] (Fig. 8, A). MCF-7:5C tumors in the vehicle control group continued to grow, reaching a mean cross-sectional area of 0.49 cm^2 [95% CI = 0.47 to 0.51] by week 8. By contrast, MCF-7:5C tumors in mice treated with postmenopausal doses of estradiol (0.3-cm silastic capsule) regressed in a time-dependent manner and were undetectable by week 8 (Fig. 8, A). Estradiol-induced tumor regression was observed as early as 1 week after treatment and became more pronounced by 2 weeks (Fig. 8, A). Fulvestrant also reduced MCF-7:5C tumor growth relative to control ($P = .007$); however, the reduction was statistically significantly less than that of estradiol ($P<.001$).

To determine whether apoptosis was involved in estradiol-induced regression of MCF-7:5C tumors, we used the TUNEL assay to quantitate apoptosis in tumor sections from control and estradiol treatment groups at day 5 after the commencement of

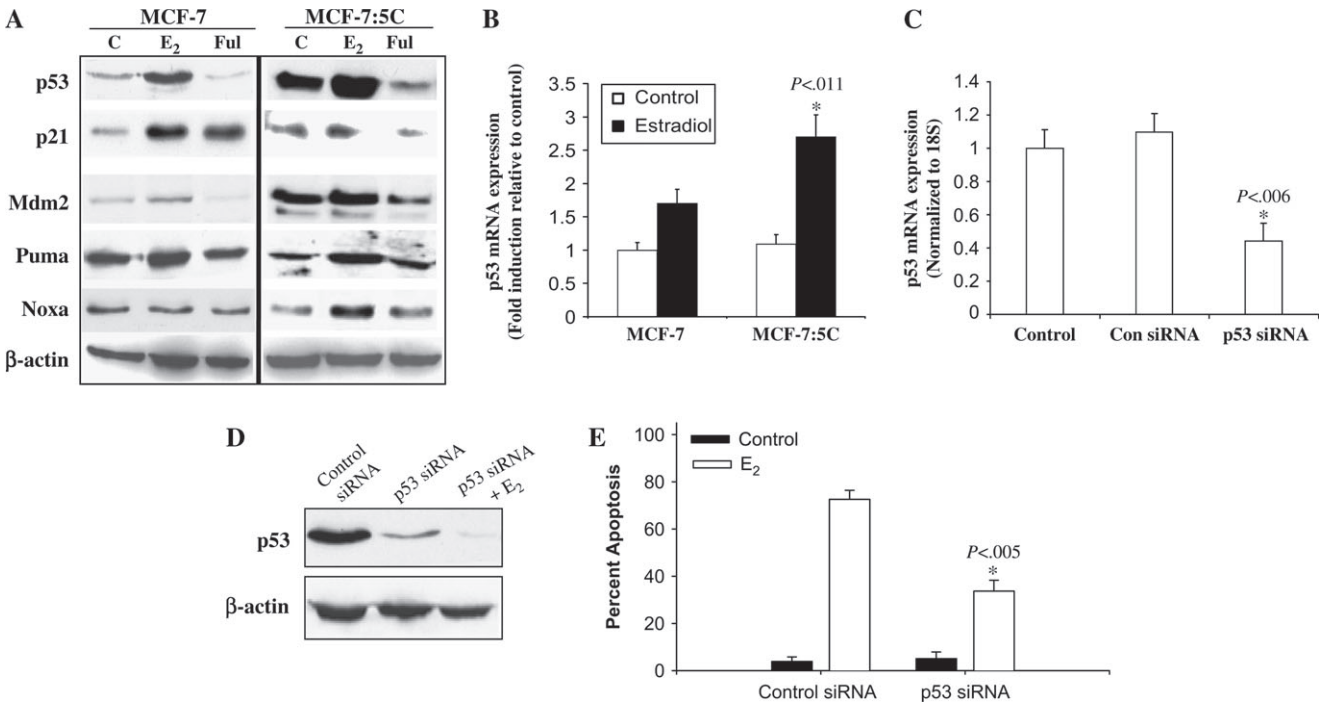

Fig. 7. Effect of estradiol and fulvestrant on expression of p53 and p53 target proteins in MCF-7 and MCF-7:5C cells. **A**) Cells were treated with ethanol vehicle (C), 1 n*M* estradiol (E_2), or 1 μ*M* fulvestrant (Ful) for 48 hours. Lysates were analyzed by western blotting with antibodies against p53, p21, MDM2, Puma, and Noxa (Santa Cruz Biotechnology). β-Actin was used as a loading control. **B**) Reverse transcriptase polymerase chain reaction (RT-PCR) of p53 expression in MCF-7 and MCF-7:5C cells following estradiol treatment for 48 hours. Ribosomal 18S mRNA was used as a loading control. **C**) Inhibition of p53 mRNA expression in MCF-7:5C cells using small siRNA. Ribosomal 18S mRNA was used as a loading control. **P* = .006 for difference in p53 expression between p53 siRNA and control siRNA. **D**) Western blot analysis of cells transfected with either control siRNA or p53 siRNA. β-Actin was used as a loading control. **E**) Percent apoptotic cells determined by annexin V staining of MCF-7:5C cells transfected with control siRNA or p53-specific siRNA and treated with 1 n*M* E_2 for 72 hours. **P* = .005 for E_2-induced apoptosis in p53-transfected cells compared with cells transfected with the control siRNA. Results are typical of three independent experiments.

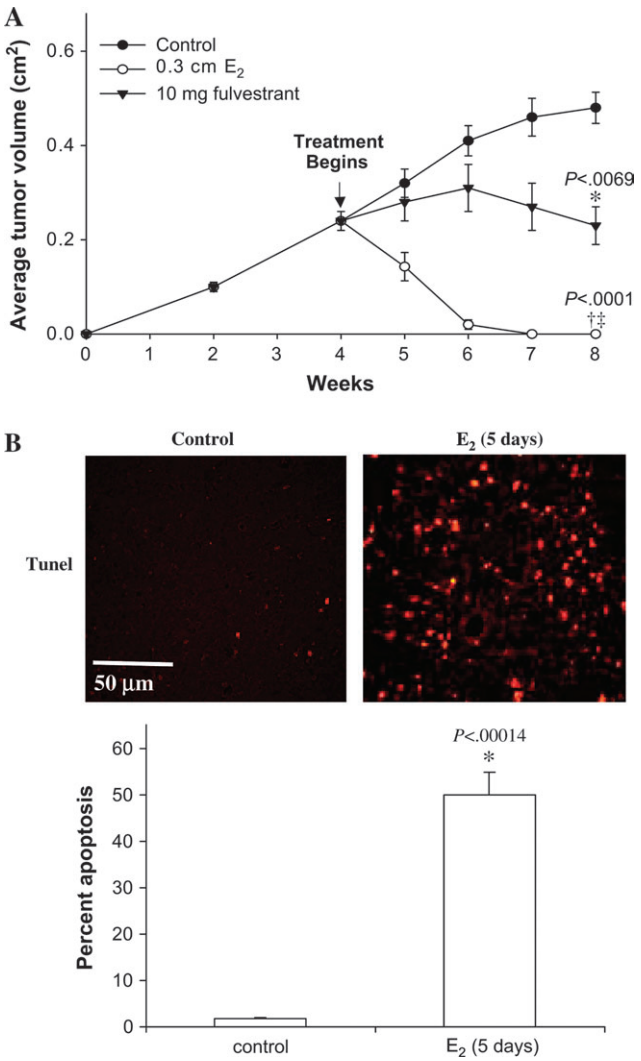

Fig. 8. Effect of estradiol and fulvestrant on the growth of MCF-7:5C tumors. **A**) Thirty ovariectomized athymic mice were injected bilaterally with MCF-7:5C cells. Tumors were grown in the absence of treatment to a mean cross-sectional area of 0.23 cm^2. Mice were then randomly assigned into three groups of 10 mice each and treated as follows: 1) vehicle (control), 2) fulvestrant, or 3) estradiol (E_2). E_2 was given as a 0.3-cm silastic capsule subcutaneously, and fulvestrant was given subcutaneously as a 5-mg dose twice a week. Tumor size was measured weekly. *Cross-sectional area at 8 weeks of fulvestrant-treated tumors was statistically significantly ($P = .007$) different from that of tumors treated with control vehicle. †Cross-sectional area of tumors at 8 weeks treated with E_2 was statistically significantly ($P<.001$) different from that of tumors treated with vehicle control. ‡Cross-sectional area of estradiol-treated tumors at 8 weeks was statistically significantly ($P<.001$) different from that of fulvestrant-treated tumors. Three separate experiments were performed (on separate occasions), yielding similar results. For each experiment, 30 mice (10 per group) were used. Data are from a representative experiment. **Error bars** = 95% confidence intervals. **B**) Terminal deoxynucleotidyl transferase–mediated deoxyuridine triphosphate nick-end labeling (TUNEL) analysis of apoptosis in tumor sections. On day 5, tumors from control and E_2-treated mice bearing MCF-7:5C tumors were fixed, sectioned, and then placed on slides for detection of apoptosis. Six independent tumors (each from a different mouse) were taken from the control group (**left panel**) or E_2-treated group (**right panel**) for apoptosis detection. Slides were examined under 40× magnification with a fluorescence microscope. The number of apoptotic cells in four random fields was measured from each tumor section, and representative fields are shown. **Scale bars** = 50 μm. **Bottom panel**, percent apoptosis was calculated by dividing the total number of TUNEL-positive cells in each field by the total number of epithelial cells and multiplying by 100. Data are the mean and 95% confidence intervals of four experiments. *$P<.001$ for the estradiol-treated group versus control group.

treatment (Fig. 8, B). We found that 49.9% [95% CI = 45.9% to 53.9%] of cells in the estradiol-treated MCF-7:5C tumors were apoptotic, whereas only 0.7% [95% CI = 1.6% to 1.8%] of cells in the vehicle control tumors were apoptotic ($P<.001$).

Discussion

In the present study, we investigated the mechanism of estradiol-induced apoptosis in MCF-7:5C cells and found that the mitochondrial (i.e., intrinsic) pathway plays a predominant role in this process. The expression of several proapoptotic proteins—including Bax, Bak, Bim, Noxa, Puma, and p53—was markedly increased with estradiol treatment, and experiments using siRNAs demonstrated that the induction of Bax, Bim, and p53 was necessary for estradiol-induced apoptosis in MCF-7:5C cells. Estradiol treatment also led to a loss of mitochondrial potential and a dramatic increase in the release of cytochrome *c* from the mitochondria, which resulted in activation of caspases and cleavage of PARP. Furthermore, overexpression of antiapoptotic Bcl-x_L was able to protect MCF-7:5C cells from estradiol-induced apoptosis. Estradiol also caused complete and rapid tumor regression in vivo, which was partially reversed by fulvestrant. To our knowledge, this study is the first to show a link between estradiol-induced cell death and activation of the mitochondrial apoptotic pathway in a breast cancer cell model resistant to estrogen withdrawal.

Song et al. *(19)* have previously reported a link between estradiol-induced apoptosis and activation of the Fas/FasL signaling pathway in LTED breast cancer cells. However, we found that activation of neither FasR nor FasL was critical for estradiol-induced apoptosis in MCF-7:5C cells. Inhibition of FasR and FasL protein expression using neutralizing antibodies and siRNAs did not prevent estradiol-induced apoptosis in MCF-7:5C cells, and estradiol treatment did not alter caspase 8 activation or Bid processing, which are important events in Fas-mediated apoptosis *(44)*. However, there is evidence indicating that Bid cleavage through caspase 8 activation plays a role in mediating cross-talk between the extrinsic and intrinsic apoptosis pathways *(45)*. For example, a recent model of Fas-induced apoptosis in breast epithelial cells suggests that proapoptotic Bid, on cleavage and activation by caspase 8, translocates from the cytosol to the mitochondria and causes a conformational change in the N terminus of Bax, resulting in mitochondrial cytochrome *c* release and amplification of apoptosis *(46)*. There is also evidence suggesting that p53 may play a linker role in connecting the Fas death receptor to the mitochondria through Bid translocation and cytochrome *c* release *(47)*. The absence of estradiol-induced caspase 8 activation and Bid cleavage in MCF-7:5C cells suggests, however, that Bid cleavage–mediated cross-talk between the extrinsic and intrinsic pathways may not be a critical factor in estradiol-induced apoptosis in MCF-7:5C cells.

We postulate that estradiol induces mitochondrion-mediated apoptosis, in part, by increasing the expression of proapoptotic Bcl-2 family proteins, disrupting mitochondrial membrane integrity, and facilitating the translocation of cytochrome *c* from the mitochondria into the cytosol. In the current study, we found that estradiol treatment markedly increased the levels of proapoptotic Bax, Bak, and Bim proteins in MCF-7:5C cells and that these increases coincided with the loss of mitochondrial membrane integrity, cytochrome *c* release, caspase 9 activation, and PARP

cleavage. Estradiol treatment also increased Bax, Bak, and Bim mRNA expression in MCF-7:5C cells (data not shown), and siRNA targeting of Bax and Bim dramatically reduced the ability of estradiol to induce apoptosis in these cells. We also found evidence of mitochondrial accumulation of Bax and Bak proteins following estradiol treatment (data not shown). Both Bax and Bak play an important role in controlling mitochondrial integrity *(48)*. Bax is normally found as a monomer in the cytosol of nonapoptotic cells, and it oligomerizes and translocates to the outer mitochondrial membrane in response to apoptotic stimuli *(49)* and induces mitochondrial membrane permeabilization *(50)* and cytochrome *c* release *(51)*. Bak resides in the mitochondrial outer membrane and has been shown to contain a homologous BH3 binding pocket critical for interactions with the Bak-activating, BH3-only protein Bid *(52)*. Once activated, Bak oligomerizes in the mitochondrial outer membrane and induces defects in membrane integrity and the release of apoptogenic factors, including cytochrome *c* *(53)*. Cytochrome *c* is normally located in the intermembrane space of the mitochondrion, loosely bound to the inner membrane. Once cytochrome *c* is released into the cytosol, it interacts with apoptotic protease activating factor-1 (Apaf-1) and procaspase 9, leading to the generation of active caspase 9, which is capable of proteolytically activating downstream caspases that then initiate the apoptotic degradation phase *(54)*. Most notably, we found substantial release of cytochrome *c* in the cytosol of estradiol-treated MCF-7:5C cells compared with vehicle-treated control, which was completely blocked by Bcl-x_L overexpression (data not shown). Activation of caspase 9 and caspase 7 and cleavage of PARP were also observed in estradiol-treated cells, and these changes were associated with the levels of cytochrome *c* in the estradiol-treated cells but not in the control cells. Overall, these findings indicate that the mitochondrion is a key target of estradiol-induced apoptosis and that the induction of proapoptotic Bax and Bak may play an important role in facilitating this process.

Although the induction of proapoptotic Bax and Bak disrupts mitochondrial membrane integrity, the overexpression of antiapoptotic proteins such as Bcl-2 and Bcl-x_L has been found to stabilize the outer mitochondrial membrane and prevent the release of cytochrome *c* following a variety of insults, including treatment with chemotherapeutic agents *(55,56)*. Heterodimers of Bcl-2/Bax have been shown to prevent pore formation and inhibit cytochrome *c* release and ultimately apoptosis *(57)*. In our study, we found that, although estradiol treatment dramatically increased the levels of proapoptotic proteins, it did not statistically significantly alter the levels of antiapoptotic Bcl-2 and Bcl-x_L proteins in MCF-7:5C cells. This finding is important because there is evidence that suggests that it is the ratio rather than the amount of antiapoptotic versus proapoptotic proteins that determines whether apoptosis will proceed *(58)*. Consistent with this notion, we have found that, in wild-type MCF-7 cells, which are resistant to estradiol-induced apoptosis, estradiol treatment dramatically increased the protein level of antiapoptotic Bcl-2 but did not alter the level of proapoptotic Bax protein. Thus, it is reasonable to suggest that the apoptotic potential of estradiol is directly related to its ability to alter the ratio between proapoptotic and antiapoptotic proteins in target cells.

The tumor suppressor protein p53 also plays a role in mitochondrion-mediated apoptotic cell death *(43)*. p53 can mediate intrinsic apoptosis by transcriptional activation of genes that encode proapoptotic proteins such as the BH3-only proteins Noxa and Puma, Bax, p53, and Apaf-1 and by transcriptional repression of Bcl-2 and IAPs *(59)*. p53 can also mediate apoptosis via transcription-independent mechanisms. In some cell types, p53-dependent apoptosis occurs in the absence of any gene transcription or translation *(60)*. Moreover, transcriptionally inactive p53 mutants have been shown to induce death in tumor cells *(61)*. In our study, estradiol treatment markedly increased p53 protein and mRNA and Puma and Noxa protein in MCF-7:5C cells. We also found that blockade of p53 mRNA expression using siRNA reduced estradiol-induced apoptosis in these cells. Although we did not sequence p53 to determine its mutational status, we did observe marked increases in the expression of the p53 target genes Noxa and Puma in estradiol-treated MCF-7:5C cells, which suggests that p53 might be functional in MCF-7:5C cells. Furthermore, blockade of p53 mRNA expression reduced estradiol-induced apoptosis in MCF-7:5C cells. Interestingly, estradiol also increased p53 protein expression in parental MCF-7 cells; however, this induction was observed in the cytosol and was not associated with apoptosis. Estradiol-induced wild-type p53 expression in MCF-7 cells has previously been reported, and it has been suggested that the induction is an ERα-mediated event and is due to ERα interaction with p53, which enhances its stability *(62)*.

A direct interaction between ERα and p53 is demonstrated by our finding that fulvestrant, which is known to degrade the ERα, was able to completely block estradiol induction of p53 and reduce the basal level of p53 in MCF-7:5C cells. Furthermore, measurable levels of p53 protein were found in the mitochondrial fraction of estradiol-treated MCF-7:5C cells. Marchenko et al. *(63)* have previously reported that the p53 protein localizes to the mitochondria in tumor cells undergoing p53-dependent apoptosis but not in cells undergoing p53-dependent growth arrest or p53-independent cell death. Although the exact mechanism by which mitochondrial p53 triggers apoptosis remains unclear, it has been proposed that p53 interacts directly with antiapoptotic Bcl-2 and Bcl-x_L, thereby liberating proapoptotic Bax and Bak to induce changes in the mitochondrial membrane that lead in turn to cytochrome *c* release, caspase activation, and cell death *(64,65)*. Overall, these results demonstrate that p53 plays an important role in estradiol-induced apoptosis in MCF-7:5C cells and that p53 acts in concert with the Bcl-2 family protein to activate the mitochondrial pathway.

Although the results in this study strongly support the involvement of the mitochondrial pathway in estradiol-induced apoptosis in MCF-7:5C cells, it is important to note that our study was essentially completed in a single MCF-7 variant. Hence, we cannot discount the importance of the FasR/FasL signaling pathway in estradiol-induced apoptosis in other breast cancer cell models that are resistant to estrogen withdrawal. As mentioned before, Song et al. *(19)* have previously reported a statistically significant link between estradiol-induced apoptosis and activation of the FasR/FasL death signaling pathway in an LTED breast cancer cell model. The LTED cells used in their study, however, were derived from a whole cell population, whereas the MCF-7:5C cells used in our study were derived from clonal selection. We chose to focus primarily on MCF-7:5C cells because they represent a pure cell model (i.e., estradiol causes rapid and complete apoptosis both in vitro and in vivo) and because doing so provided the opportunity to fully elucidate the mechanism of estradiol-induced apoptosis. Our laboratory also has developed two other LTED breast cancer cell variants, MCF-7:ED and

MCF-7:2A; however, these cells are less sensitive to estradiol-induced apoptosis than are MCF-7:5C cells.

In conclusion, our study provides a mechanistic basis for estradiol-induced apoptosis in a human breast cancer cell model resistant to LTED. Estradiol induced activation of the mitochondrial apoptotic pathway in MCF-7:5C cells by increasing proapoptotic Bax, Bak, Bim, Noxa, Puma, and p53 protein expression and increasing the loss of mitochondrial transmembrane potential and cytochrome *c* release. Of note, the pure antiestrogen fulvestrant caused growth arrest and tumor stasis but not apoptosis, whereas estradiol caused complete and rapid tumor regression. These laboratory data have important clinical implications, particularly for the use of aromatase inhibitors as long-term therapy, and they suggest that, if and when resistance to aromatase inhibition occurs, a strategy of treatment with estrogen (either exogenous estrogen or the woman's endogenous estrogen) may be sufficient to kill the cancer and control disease progression. We have previously observed that, once the estradiol-induced tumoricidal action is complete in tamoxifen-stimulated tumors, the remaining tumor tissue is again responsive to antihormonal therapy *(20)*. A clinical strategy of reducing tumor burden with low-dose, short-term estrogen therapy followed by optimal antihormonal therapy with fulvestrant or aromatase inhibitor should be tested in clinical trials.

References

(1) McKnight JJ, Gray SB, O'Kane HF, Johnston SR, Williamson KE. Apoptosis and chemotherapy for bladder cancer. J Urol 2005;173:683–90.

(2) Rupnow BA, Knox SJ. The role of radiation-induced apoptosis as a determinant of tumor responses to radiation therapy. Apoptosis 1999;4:115–43.

(3) Dowsett M, Archer C, Assersohn L, Gregory RK, Ellis PA, Salter J, et al. Clinical studies of apoptosis and proliferation in breast cancer. Endocr Relat Cancer 1999;6:25–8.

(4) Peter ME, Krammer PH. The CD95(APO-1/Fas) DISC and beyond. Cell Death Differ 2003;10:26–35.

(5) Tsujimoto Y. Bcl-2 family of proteins: life-or-death switch in mitochondria. Biosci Rep 2002;22:47–58.

(6) Thiantanawat A, Long BJ, Brodie AM. Signaling pathways of apoptosis activated by aromatase inhibitors and antiestrogens. Cancer Res 2003;63:8037–50.

(7) Fisher B, Costantino JP, Wickerham DL, Redmond CK, Kavanah M, Cronin WM, et al. Tamoxifen for prevention of breast cancer: report of the National Surgical Adjuvant Breast and Bowel Project P-1 Study. J Natl Cancer Inst 1998;90:1371–88.

(8) Coombes RC, Hall E, Gibson LJ, Paridaens R, Jassem J, Delozier T, et al. A randomized trial of exemestane after two to three years of tamoxifen therapy in postmenopausal women with primary breast cancer. N Engl J Med 2004;350:1081–92.

(9) Johnston S. Fulvestrant and the sequential endocrine cascade for advanced breast cancer. Br J Cancer 2004;90(Suppl 1):S15–8.

(10) Zhang W, Couldwell WT, Song H, Takano T, Lin JH, Nedergaard M. Tamoxifen-induced enhancement of calcium signaling in glioma and MCF-7 breast cancer cells. Cancer Res 2000;60:5395–400.

(11) Haynes MP, Sinha D, Russell KS, Collinge M, Fulton D, Morales-Ruiz M, et al. Membrane estrogen receptor engagement activates endothelial nitric oxide synthase via the PI3-kinase-Akt pathway in human endothelial cells. Circ Res 2000;87:677–82.

(12) Choi KC, Kang SK, Tai CJ, Auersperg N, Leung PC. Estradiol up-regulates antiapoptotic Bcl-2 messenger ribonucleic acid and protein in tumorigenic ovarian surface epithelium cells. Endocrinology 2001;142:2351–60.

(13) Kyprianou N, English HF, Davidson NE, Isaacs JT. Programmed cell death during regression of the MCF-7 human breast cancer following estrogen ablation. Cancer Res 1991;51:162–6.

(14) Teixeira C, Reed JC, Pratt MA. Estrogen promotes chemotherapeutic drug resistance by a mechanism involving Bcl-2 proto-oncogene expression in human breast cancer cells. Cancer Res 1995;55:3902–7.

(15) Hughes DE, Dai A, Tiffee JC, Li HH, Mundy GR, Boyce BF. Estrogen promotes apoptosis of murine osteoclasts mediated by TGF-beta. Nat Med 1996;2:1132–6.

(16) Jordan VC. Selective estrogen receptor modulation: concept and consequences in cancer. Cancer Cell 2004;5:207–13.

(17) Lewis JS, Cheng D, Jordan VC. Targeting oestrogen to kill the cancer but not the patient. Br J Cancer 2004;90:944–9.

(18) Osipo C, Liu H, Meeke K, Jordan VC. The consequences of exhaustive antiestrogen therapy in breast cancer: estrogen-induced tumor cell death. Exp Biol Med (Maywood) 2004;229:722–31.

(19) Song RX, Mor G, Naftolin F, McPherson RA, Song J, Zhang Z, et al. Effect of long-term estrogen deprivation on apoptotic responses of breast cancer cells to 17beta-estradiol. J Natl Cancer Inst 2001;93:1714–23.

(20) Yao K, Lee ES, Bentrem DJ, England G, Schafer JI, O'Regan RM, et al. Antitumor action of physiological estradiol on tamoxifen-stimulated breast tumors grown in athymic mice. Clin Cancer Res 2000;6:2028–36.

(21) Haddow A, Watkinson JM, Paterson E. Influence of synthetic oestrogens upon advanced malignant disease. Br Med J 1944;2:393–8.

(22) Lewis JS, Osipo C, Meeke K, Jordan VC. Estrogen-induced apoptosis in a breast cancer cell model resistant to long-term estrogen withdrawal. J Ster Biochem Mol Biol 2005;94:131–41.

(23) Dodwell D, Vergote I. A comparison of fulvestrant and the third-generation aromatase inhibitors in the second-line treatment of postmenopausal women with advanced breast cancer. Cancer Treat Rev 2005;31:274–82.

(24) Osipo C, Gajdos C, Liu H, Chen B, Jordan VC. Paradoxical action of fulvestrant in estradiol-induced regression of tamoxifen-stimulated breast cancer. J Natl Cancer Inst 2003;95:1597–608.

(25) Liu H, Lee ES, Gajdos C, Pearce ST, Chen B, Osipo C, et al. Apoptotic action of 17beta-estradiol in raloxifene-resistant MCF-7 cells in vitro and in vivo. J Natl Cancer Inst 2003;95:1586–97.

(26) Jiang SY, Wolf DM, Yingling JM, Chang C, Jordan VC. An estrogen receptor positive MCF-7 clone that is resistant to antiestrogens and estradiol. Mol Cell Endocrinol 1992;90:77–86.

(27) Labarca C, Paigen K. A simple, rapid, and sensitive DNA assay procedure. Anal Biochem 1980;102:344–52.

(28) MacGregor Schafer J, Liu H, Bentrem DJ, Zapf JW, Jordan VC. Allosteric silencing of activating function 1 in the 4-hydroxytamoxifen estrogen receptor complex is induced by substituting glycine for aspartate at amino acid 351. Cancer Res 2000;60:5097–105.

(29) Patel T, Gores GJ, Kaufmann SH. The role of proteases during apoptosis. FASEB J 1996;10:587–97.

(30) Park IC, Woo SH, Park MJ, Lee HC, Lee SJ, Hong YJ, et al. Ionizing radiation and nitric oxide donor sensitize Fas-induced apoptosis via up-regulation of Fas in human cervical cancer cells. Oncol Rep 2003;10:629–33.

(31) Gottardis MM, Jordan VC. Development of tamoxifen-stimulated growth of MCF-7 tumors in athymic mice after long-term antiestrogen administration. Cancer Res 1988;48:5183–7.

(32) O'Regan RM, Cisneros A, England GM, MacGregor JI, Muenzner HD, Assikis VJ, et al. Effects of the antiestrogens tamoxifen, toremifene, and ICI 182 780 on endometrial cancer growth. J Natl Cancer Inst 1998;90:1552–8.

(33) Zeger SL, Liang KY. Longitudinal data analysis for discrete and continuous outcomes. Biometrics 1986;42:121–30.

(34) Soule HD, Vazguez J, Long A, Albert S, Brennan M. A human cell line from a pleural effusion derived from a breast carcinoma. J Natl Cancer Inst 1973;51:1409–16.

(35) Lippman M, Bolan G, Huff K. The effects of estrogens and antiestrogens on hormone-responsive human breast cancer in long-term tissue culture. Cancer Res 1976;36:4595–601.

(36) Lippman ME, Bolan G. Oestrogen-responsive human breast cancer in long term tissue culture. Nature 1975;256:592–3.

(37) Jiang SY, Jordan VC. Growth regulation of estrogen receptor-negative breast cancer cells transfected with complementary DNAs for estrogen receptor. J Natl Cancer Inst 1992;84:580–91.

(38) Berry M, Nunez AM, Chambon P. Estrogen-responsive element of the human pS2 gene is an imperfectly palindromic sequence. Proc Natl Acad Sci U S A 1989;86:1218–22.

(39) Green DR, Reed JC. Mitochondria and apoptosis. Science 1998;281: 1309–12.
(40) Nunez G, Benedict MA, Hu Y, Inohara N. Caspases: the proteases of the apoptotic pathway. Oncogene 1998;17:3237–45.
(41) Hadjiloucas I, Gilmore AP, Bundred NJ, Streuli CH. Assessment of apoptosis in human breast tissue using an antibody against the active form of caspase 3: relation to tumour histopathological characteristics. Br J Cancer 2001;85:1522–6.
(42) Vander Heiden MG, Chandel NS, Williamson EK, Schumacker PT, Thompson CB. Bcl-xL regulates the membrane potential and volume homeostasis of mitochondria. Cell 1997;91:627–37.
(43) Schuler M, Green DR. Mechanisms of p53-dependent apoptosis. Biochem Soc Trans 2001;29:684–8.
(44) Hengartner MO. The biochemistry of apoptosis. Nature 2000;407:770–6.
(45) Gross A, Yin XM, Wang K, Wei MC, Jockel J, Milliman C, et al. Caspase cleaved BID targets mitochondria and is required for cytochrome c release, while BCL-XL prevents this release but not tumor necrosis factor-R1/Fas death. J Biol Chem 1999;274:1156–63.
(46) Murphy KM, Streips UN, Lock RB. Bax membrane insertion during Fas(CD95)-induced apoptosis precedes cytochrome c release and is inhibited by Bcl-2. Oncogene 1999;18:5991–9.
(47) Thiery J, Abouzahr S, Dorothee G, Jalil A, Richon C, Vergnon I, et al. p53 potentiation of tumor cell susceptibility to CTL involves Fas and mitochondrial pathways. J Immunol 2005;174:871–8.
(48) Korsmeyer SJ. BCL-2 gene family and the regulation of programmed cell death. Cancer Res 1999;59(7 Suppl):1693s–1700s.
(49) Goping IS, Gross A, Lavoie JN, Nguyen M, Jemmerson R, Roth K, et al. Regulated targeting of BAX to mitochondria. J Cell Biol 1998;143:207–15.
(50) Kuwana T, Newmeyer DD. Bcl-2-family proteins and the role of mitochondria in apoptosis. Curr Opin Cell Biol 2003;15:691–9.
(51) Wei MC, Zong WX, Cheng EH, Lindsten T, Panoutsakopoulou V, Ross AJ, et al. Proapoptotic BAX and BAK: a requisite gateway to mitochondrial dysfunction and death. Science 2001;292:727–30.
(52) Korsmeyer SJ, Wei MC, Saito M, Weiler S, Oh KJ, Schlesinger PH. Pro-apoptotic cascade activates BID, which oligomerizes BAK or BAX into pores that result in the release of cytochrome c. Cell Death Differ 2000;7:1166–73.
(53) Wei MC, Lindsten T, Mootha VK, Weiler S, Gross A, Ashiya M, et al. tBID, a membrane-targeted death ligand, oligomerizes BAK to release cytochrome c. Genes Dev 2000;14:2060–71.
(54) Green D, Kroemer G. The central executioners of apoptosis: caspases or mitochondria? Trends Cell Biol 1998;8:267–71.
(55) Nunez G, Clarke MF. The Bcl-2 family of proteins: regulators of cell death and survival. Trends Cell Biol 1994;4:399–403.
(56) Reed JC. Bcl-2 and the regulation of programmed cell death. J Cell Biol 1994;124:1–6.
(57) Oltvai ZN, Milliman CL, Korsmeyer SJ. Bcl-2 heterodimerizes in vivo with a conserved homolog, Bax, that accelerates programmed cell death. Cell 1993;74:609–19.
(58) Chao DT, Korsmeyer SJ. BCL-2 family: regulators of cell death. Annu Rev Immunol 1998;16:395–419.
(59) Johnstone RW, Ruefli AA, Lowe SW. Apoptosis: a link between cancer genetics and chemotherapy. Cell 2002;108:153–64.
(60) Gao C, Tsuchida N. Activation of caspases in p53-induced transactivation-independent apoptosis. Jpn J Cancer Res 1999;90:180–7.
(61) Kokontis JM, Wagner AJ, O'Leary M, Liao S, Hay N. A transcriptional activation function of p53 is dispensable for and inhibitory of its apoptotic function. Oncogene 2001;20:659–68.
(62) Okumura N, Saji S, Eguchi H, Hayashi S, Nakashima S. Estradiol stabilizes p53 protein in breast cancer cell line, MCF-7. Jpn J Cancer Res 2002;93:867–73.
(63) Marchenko ND, Zaika A, Moll UM. Death signal-induced localization of p53 protein to mitochondria. A potential role in apoptotic signaling. J Biol Chem 2000;275:16202–12.
(64) Mihara M, Moll UM. Detection of mitochondrial localization of p53. Methods Mol Biol 2003;234:203–9.
(65) Mihara M, Erster S, Zaika A, Petrenko O, Chittenden T, Pancoska P, et al. p53 has a direct apoptogenic role at the mitochondria. Mol Cell 2003;11: 577–90.

Notes

Supported by the Avon Foundation, a Specialized Programs of Research Excellence (SPORE) grant CA89018 in breast cancer research (to V. C. Jordan) from the National Cancer Institute, National Institutes of Health, Department of Health and Human Services, and the Lynn Sage Breast Cancer Research Foundation. J. S. Lewis was funded by a Department of Defense Training Grant in Breast Neoplasia DAMD17–00–5671–0386 and Signal Transduction Training Grant #T32 CA70085–06. C. Osipo was funded by a Judy Dlugie Memorial Fund Fellowship for Breast Cancer Research. The sponsors were not involved in the design, conduct, or reporting of the study.

Manuscript received March 16, 2005; revised September 2, 2005; accepted September 28, 2005.

Hayes and Lewis-Wambi *Breast Cancer Research* (2015) 17:40
DOI 10.1186/s13058-015-0542-y

Breast Cancer RESEARCH

REVIEW

Mechanisms of endocrine resistance in breast cancer: an overview of the proposed roles of noncoding RNA

Erin L Hayes[1,2] and Joan S Lewis-Wambi[1,2*]

Abstract

Endocrine therapies such as tamoxifen and aromatase inhibitors are the standard treatment options for estrogen receptor-positive breast cancer patients. However, resistance to these agents has become a major clinical obstacle. Potential mechanisms of resistance to endocrine therapies have been identified, often involving enhanced growth factor signaling and changes in the expression or action of the estrogen receptor, but few studies have addressed the role of noncoding RNA (ncRNA). Two important types of ncRNA include microRNA (miRNA) and long noncoding RNA (lncRNA). miRNAs are small RNA molecules that regulate gene expression via translational inhibition or degradation of mRNA transcripts, while lncRNAs are larger RNA molecules that have been shown to play a role in multiple cellular maintenance functions such as protein scaffolding, chromatin looping, and regulation of mRNA stability. Both miRNA and lncRNA have recently impacted the field of breast cancer research as important pieces in the mechanistic puzzle of the genes and pathways involved in breast cancer development and progression. This review serves as an overview of the roles of miRNA and lncRNA in breast cancer progression and the development of endocrine resistance. Ideally, future experiments in the field should include identification of ncRNAs that could be potential therapeutic targets in endocrine-resistant tumors, as well as ncRNA biomarkers that facilitate more tumor-specific treatment options for endocrine-resistant breast cancer patients.

Introduction

Breast cancer is the most commonly diagnosed cancer in the United States and is the second leading cause of cancer death. Approximately one out of every eight US women will develop invasive breast cancer over the course of her lifetime [1]. About 70% of all breast cancers express estrogen receptor (ER) alpha and belong to the molecular subtypes luminal A or luminal B [1,2]. While the exact etiology of breast cancer is not known, there is strong evidence that estrogen plays a critical role in the development and progression of the disease. ERα-positive breast cancers rely on estrogen signaling for proliferation, and hence the most effective strategy to stop or slow the growth of these hormone-sensitive tumors is to block estrogen action in the tumor using endocrine therapy. Current endocrine therapies for ERα breast cancer include: tamoxifen, the selective ER modulator that antagonizes ERα function; fulvestrant, the pure anti-estrogen that degrades/downregulates ERα; and aromatase inhibitors (AIs) (letrozole, anastrozole, and exemestane), which suppress estrogen production in peripheral tissues by blocking the aromatase enzyme. Unfortunately, the majority of patients treated with endocrine therapy eventually develop resistance, leading to disease progression and death. The mechanism by which resistance occurs is still not completely known and thus represents a major clinical problem. This review will offer information regarding the recently studied roles of noncoding RNAs (ncRNAs) in acquired endocrine resistance.

Estrogen mediates its biological effects by binding to ERα and ERβ, which are members of the nuclear receptor superfamily of ligand-inducible transcription factors [3,4]. ERα is encoded by *ESR1*, a 300 kb gene located on chromosome 6, and has six functional domains, A to F, which include both ligand-binding and DNA-binding

* Correspondence: jlewis-wambi@kumc.edu
[1]Department of Cancer Biology, University of Kansas Medical Center, 3901 Rainbow Blvd, Wahl Hall East 1031, Kansas City, KS 66160, USA
[2]Department of Physiology, University of Kansas Medical Center, Kansas City, KS 66160, USA

domains, as described by Kumar and coworkers [5]. It is also important to note that there are multiple sites of phosphorylation on ERα. For instance, Ser118 phosphorylation by a mitogen-activated protein kinase (MAPK) leads to ligand-independent activation of ERα activity, and Ser167 phosphorylation by protein kinase B (Akt) can also lead to ligand-independent activation of ERα [6,7].

When estrogen binds ERα, the receptor dimerizes and translocates to the nucleus where it binds estrogen response elements in the DNA, stimulating transcription of target genes involved in cell proliferation [8]. The estrogen-activated ERα is also able to bind other transcription factors, such as Ap-1 and Sp-1, independent of estrogen response elements, where it may recruit coactivators to stimulate transcription of additional growth and survival genes [9]. Much of the molecular signaling mediated by ERα involves the MAPK and phosphoinositide 3-kinase (PI3K) pathways, the primary facilitators of cell growth and proliferation [10].

Endocrine therapies

Estrogen receptor antagonists

Targeting ERα using selective ER modulators and selective ER downregulators has been an effective treatment strategy for patients with ERα-positive hormone-dependent breast cancer. For the past few decades, the selective ER modulator tamoxifen has been the most widely used drug for the treatment of breast cancer, with success both as a long-term adjuvant therapy and as a preventative agent for women at increased risk for breast cancer [11,12]. Normally, estrogen-bound ERα is in a conformation that favors the recruitment of coactivators to promote transcription of target genes. However, when tamoxifen binds to the ligand-binding domain of ERα in mammary epithelium, it induces a conformation that recruits corepressors, which blocks estrogen from binding its receptor and prevents the proliferative action of ERα signaling [13]. In addition to tamoxifen, the use of selective ER downregulators, which act as pure anti-estrogens, has also been under investigation. Only one selective ER downregulator, fulvestrant, has thus far been approved for clinical use [14].

Aromatase inhibitors

While ER antagonists have played an important role in combating ERα-positive breast cancers for the past few decades, another class of therapies has emerged – AIs. The aromatase enzyme (a cytochrome P450 heme-containing protein) is required for the synthesis of estrogen via aromatization of androgens such as testosterone [15]. Circulating levels of estrogen decrease as a woman enters menopause, since there is no longer production of estrogen by the ovaries. Thus, the local synthesis of estrogen by breast adipose tissue plays a large role in the growth and survival of ERα-positive breast tumors [16]. Inhibition of aromatase activity in these tumors is a rational treatment strategy to suppress estrogen production in peripheral tissues, thus inhibiting tumor growth.

Currently, there are three US Food and Drug Administration-approved oral AIs in clinical use for the treatment of postmenopausal women with hormone receptor-positive breast cancer. These AIs can be divided into two categories: steroidal AIs (exemestane) and nonsteroidal AIs (anastrozole, letrozole). There has been great interest in the development of AIs since it has been observed in clinical trials that they can be more tolerable than tamoxifen, and are usually more effective or equivalently effective in clinical response rate and median time to progression [17]. Indeed, the third-generation AIs have all been shown to suppress circulating estrogen levels in postmenopausal breast cancer patients by more than 97% [18,19].

Resistance to endocrine therapies

Mechanisms of tamoxifen resistance

Many of the key pathways involved in tamoxifen resistance involve growth factors, such as human epidermal growth factor receptor 2 (HER2) (Figure 1A). The growth of the tamoxifen-resistant cell model MCF-7/HER2-18 (HER2 overexpressing) is increased with treatment of tamoxifen, revealing a crosstalk between HER2 and ERα [20]. Likewise, early *in vivo* studies of breast tumors by Gottardis and Jordan revealed that, in the process of acquiring tamoxifen resistance, tumors may gain the ability to grow in a tamoxifen-stimulated manner [21]. There is strong evidence that the ability of tamoxifen to function as an agonist or an antagonist is dependent on whether it recruits coactivators or corepressors to the ERα transcription complex [22]. Perhaps the most studied coregulator of ERα is the amplified in breast cancer 1 (AIB1) protein. Increased expression of AIB1 correlates with tamoxifen resistance since AIB1 expression contributes to the agonistic activity of tamoxifen – especially in the presence of HER2 (Figure 1A) [23].

In addition to HER2 signaling, the growth factor receptors insulin-like growth factor receptor 1 and fibroblast growth factor receptor 1 can activate the MAPK and PI3K pathways, which have been shown to confer tamoxifen unresponsiveness [24,25]. Altered expression of ERα also contributes to the development of tamoxifen resistance. Since ERα is the target of tamoxifen treatment, lack of ERα expression is known to result in resistance. Hypermethylation of CpG islands and histone deacetylase activity in the *ESR1* promoter (Figure 1A) are similar to the absence of ERα because these can inactivate the gene so the cells express much less ERα [26].

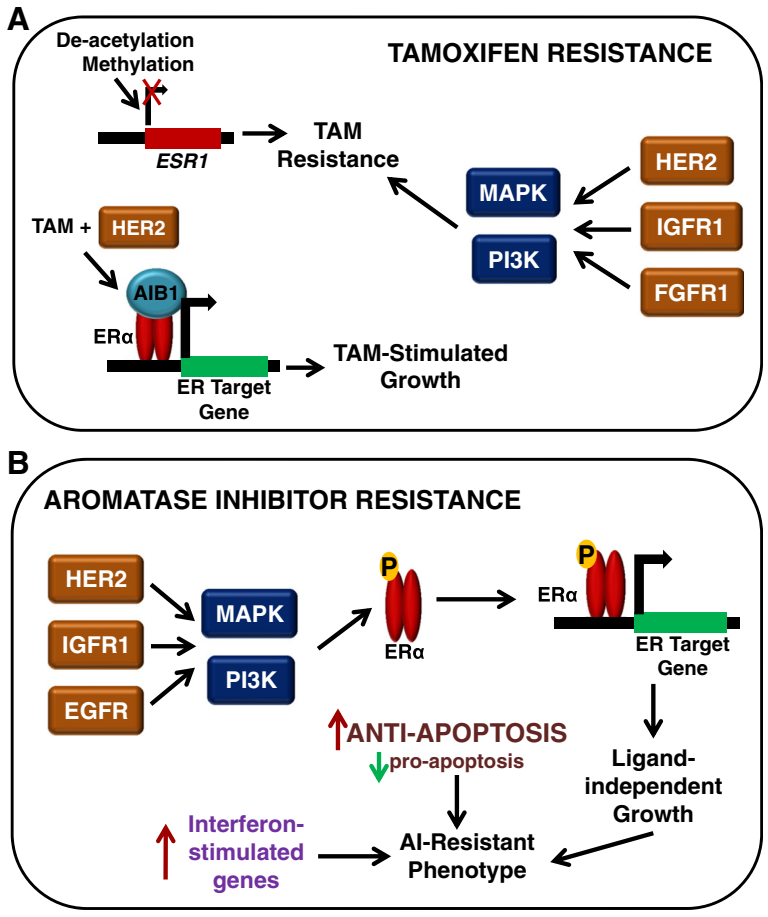

Figure 1 Mechanisms of endocrine resistance in breast cancer cells. (A) Mechanisms of tamoxifen (TAM) resistance may involve the loss of estrogen receptor (ER) alpha expression, which can be achieved by methylation of CpG islands or histone deacetylase activity in the *ESR1* promoter. Tamoxifen-resistant growth is also stimulated by the upregulation of growth factor signaling pathways (HER2, IGFR1, and FGFR1) and subsequent activation of the mitogen-activated protein kinase (MAPK) cascade or phosphoinositide 3-kinase (PI3K) pathway. Finally, tamoxifen has even been shown to stimulate the growth of breast cancer cells when bound to certain coactivators, such as AIB1, and this is especially true in HER2-expressing cells. **(B)** The mechanisms of aromatase inhibitor (AI) resistance share similarities with tamoxifen resistance, especially in terms of growth factor pathway upregulation. The enhanced activity of growth factors such as MAPK can result in estrogen-independent phosphorylation and activation of ERα. In addition to growth factor signaling, interferon response genes and anti-apoptotic proteins have also been shown to have increased expression in AI-resistant cells. AIB1, amplified in breast cancer 1; FGFR1, fibroblast growth factor receptor 1; HER2, human epidermal growth factor receptor 2; IGFR1, insulin-like growth factor receptor 1.

Resistance to tamoxifen can also arise from dysregulated metabolism of the drug. In the liver, cytochrome P450 enzymes CYP2D6 and CYP3A4 convert tamoxifen to its active metabolites 4-hydroxytamoxifen and endoxifen, which both have 30-fold to 100-fold higher potency to inhibit estrogen-dependent proliferation than tamoxifen [27]. Polymorphisms in the cytochrome P450 proteins, especially CYP2D6, have been associated with poor metabolic activity, and are associated with worse clinical outcome after tamoxifen treatment [28,29]. In addition, it is also possible that altered cellular accumulation of tamoxifen and its metabolites – potentially through the induction of efflux transporters such as P-glycoprotein/multi-drug resistance protein 1 (MDR1) – might influence a patient's response to tamoxifen [30]. Notably, P-glycoprotein expression has been associated with a shorter overall survival for tamoxifen-treated patients, but its use as a prognostic marker is still under investigation [31,32].

Mechanisms of aromatase inhibitor resistance

There are several pathways implicated in the acquired AI-resistant phenotype. These include the MAPK [33], epidermal growth factor receptor [34], and PI3K pathways (Figure 1B) [35]. ERα has also been shown to play a role in AI resistance, in the form of a constitutively

active ligand-independent mutant ERα [36], via different genome binding patterns [37], or simply by modified expression levels [38]. In fact, one study reveals that ligand-independent ERα activation is required for the development of an AI-resistant phenotype in the aromatase-overexpressing MCF-7aro cell line [39]. The phosphorylation of ERα by MAPK (Ser118) and Akt (Ser167) is often essential for the ligand-independent action of ERα, as discussed previously (Figure 1B) [6,7].

Since the mechanism by which AIs induce death of ER-positive breast cancer cells often involves apoptosis, a disturbance in the balance of pro-apoptotic and anti-apoptotic genes could also play a role in resistance to AI treatment (Figure 1B) [40]. Indeed, this imbalance has been shown in an aromatase-expressing MCF-7 cell line with a mutant ERα gene (K303R) [41]. The K303R mutation was shown to cause resistance to both tamoxifen and the AI anastrozole, and these K303R MCF-7/Aro cells have an increase in the Bcl-2 (anti-apoptotic)/Bax (pro-apoptotic) ratio, which is further exacerbated upon treatment with anastrozole [41].

The clonally selected long-term estrogen-deprived (LTED) models MCF-7:5C [42,43] and MCF-7:2A [44,45], used in our laboratory, have revealed some of the significant genetic reprogramming that occurs when the breast tumor cells are deprived of estrogen in the long term (>1 year) [46]. Notably, recent findings from our laboratory have identified a critical role for interferon-stimulated genes, in particular interferon-induced transmembrane protein 1 (*IFITM1*), which has been shown to be markedly overexpressed (>25-fold) in AI-resistant MCF-7:5C breast cancer cells and AI-resistant breast tumors. Interestingly, we have found that overexpression of IFITM1 is strongly associated with enhanced cell survival, proliferation, and invasiveness of AI-resistant cells and that knockdown of IFITM1 induces cell death and blocks the ability of the resistant cells to migrate and invade [47].

Noncoding RNAs and breast cancer

The development and progression of breast cancer are affected by many factors, most of which involve a change in expression of certain genes. Of the mechanisms for regulating gene expression, ncRNAs have proven to be integral to the cell in recent studies [48]. ncRNAs include microRNA (miRNA), long noncoding RNA (lncRNA), transfer RNA, ribosomal RNA, and small nucleolar RNA. Two forms of ncRNA that are especially important for regulation of gene expression in cells are miRNA and lncRNA.

microRNAs and breast cancer

miRNAs are small RNA molecules of 18 to 22 base pairs that regulate the expression of target mRNAs by inhibiting translation or degrading the transcripts [49]. After miRNA genes are initially transcribed by RNA polymerase II, a process regulated by transcription factors and nuclear receptors, the transcripts undergo significant processing both in the nucleus and cytoplasm (Figure 2) [50]. First, the pri-miRNA sequence is cleaved in the nucleus by Drosha, a class 2 RNase III enzyme that works in conjunction with DiGeorge syndrome chromosomal region 8 (DGCR8). The resulting pre-miRNA hairpin is exported from the nucleus to the cytoplasm via Exportin 5 where it is further cleaved by Dicer, another member of the RNase III family, resulting in a short double-strand piece of RNA. The two strands of the RNA then separate into the passenger strand, which often gets degraded, and the mature miRNA strand, which binds to argonaute (Ago) proteins to form the RNA-induced silencing complex [49]. The miRNA of the RNA-induced silencing complex guides the complex to a complementary mRNA 3′ untranslated region. Complementarity of the miRNA seed sequence (base pairs 2 to 7) to the target mRNA stimulates Ago2 in the RNA-induced silencing complex to degrade the mRNA [51]. However, if there is only partial complementarity, the translation of the mRNA will be inhibited.

Expression profiles of miRNA in breast tumor samples have been correlated with biopathologic features such as hormone receptor status and proliferation index, and are used to distinguish between basal and luminal subtypes [52,53]. For example, miRNAs overexpressed in basal, ERα-negative primary breast cancers include miR-150, which has been shown to promote breast cancer growth [54], and miR-135b, which correlates with early metastasis of breast cancer cells [55]. miRNAs overexpressed in luminal, ERα-positive breast cancers include miR-126 and miR-10a, which are associated with an increase in patients' relapse-free time after tamoxifen treatment [56].

Beyond the use of expression profiles, specific miRNAs have been associated with regulation of genes involved in breast cancer. The let-7 miRNA family has been shown to regulate the self-renewal capacity of breast tumor-initiating cells derived from cell lines and primary patient tumors by inhibition of *HRAS* and high mobility group AT-hook2 (*HMGA2*) – genes involved in self-renewal and differentiation, respectively [57]. miR-21, which targets phosphatase and tensin homolog (*PTEN*), was identified to be upregulated in primary patient samples of invasive breast cancer compared with normal breast tissue by miRNA *in situ* hybridization staining [58]. miR-373 and miR-520c are considered metastasis-promoting miRNAs and are shown to be upregulated in lymph node metastases compared with primary tumor samples [59]. Promotion of tumor invasion and metastasis by miR-373 and miR-520c is probably achieved via suppression of the *CD44* gene, which codes for a hyaluronan receptor and has been identified as a metastasis suppressor in breast cancer [60].

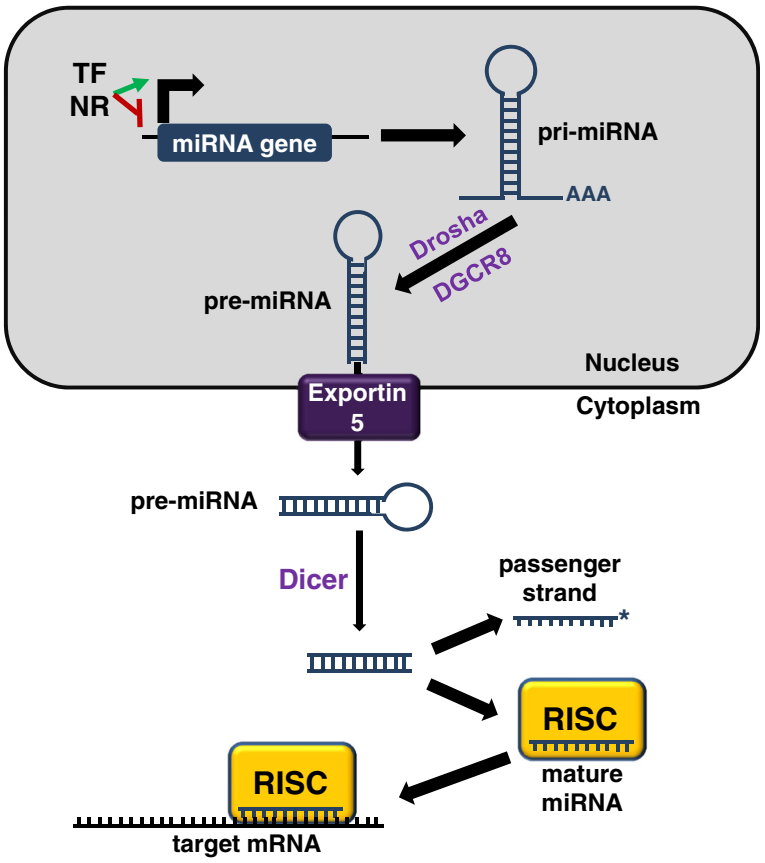

Figure 2 Standard pathway by which microRNAs are processed and loaded onto RISC to regulate gene expression. Regulation of microRNA (miRNA) expression is controlled at the miRNA promoter by transcription factors (TF) and nuclear receptors (NR). After transcription, the pri-miRNA is processed inside the nucleus by Drosha and DGCR8 to form pre-miRNA – a hairpin miRNA. Exportin 5 exports the pre-miRNA from the nucleus into the cytoplasm where it gets cleaved further by Dicer, resulting in a short double-strand piece of RNA. These strands are separated into the passenger strand, which often gets degraded, and the mature strand, which is loaded onto RNA-induced silencing complex (RISC) for action on target mRNA. If the seed sequence (base pairs 2 to 7) of the mature miRNA is complementary to the mRNA, the transcript is degraded. However, if there is not perfect complementarity between the miRNA seed sequence and its target mRNA, the result is inhibition of translation. DGCR8, DiGeorge syndrome chromosomal region 8.

For a more comprehensive look at the miRNAs involved in breast cancer, the reader should refer to reviews by O'Day and Lal and by Singh and Mo [61,62].

Long noncoding RNAs and breast cancer

lncRNAs are ncRNA transcripts longer than 200 base pairs that are transcribed from various genomic locations, such as in the promoters, enhancers, introns, or antisense coding regions of genes, or in their own stand-alone position in the genome (Figure 3A) [63]. Unlike miRNAs whose primary role is to repress the translation of their mRNA targets, lncRNAs have been shown to act as protein–DNA or protein–protein scaffolds, miRNA sponges, and protein decoys, as well as regulators of translation (Figure 3B) [64]. While previously thought of as junk DNA, lncRNAs are now regarded as an important part of the cell's gene regulation machinery, controlling cell cycle, apoptosis, and differentiation [65-67].

Some investigators have begun to identify lncRNAs whose expression is associated with aberrant signaling or unregulated survival of cancer cells. According to the lncRNADisease Database [68], there are 16 lncRNAs known to play a role in breast cancer including H19, growth arrest-specific 5 (GAS5), homeobox antisense intergenic RNA (HOTAIR), and breast cancer anti-estrogen resistance 4 (BCAR4) [69-72].

The lncRNA H19, present on the maternal allele, normally plays a role in imprinted regions of the genome to silence insulin-like growth factor 2 (*IGF2*) [73]. H19 was said to have an oncogenic role in breast cancer cells in 2002, but has since been found to exhibit tumor suppressive action *in vivo* [69,74]. Hormonal regulation of H19 is important, as estradiol is able to stimulate H19

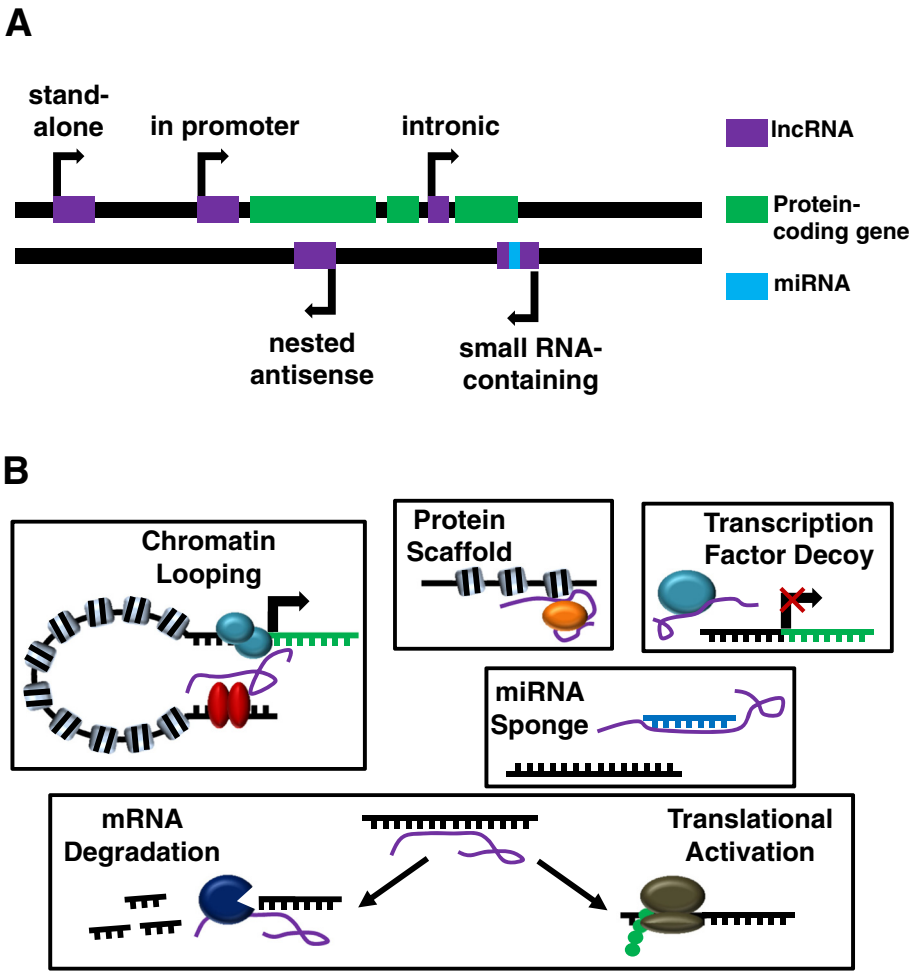

Figure 3 Location of long noncoding RNAs in the genome and roles of long noncoding RNAs in regulation of cellular processes. (A) Long noncoding RNA (lncRNA) genes reside in various genomic locations, such as in the promoters, enhancers, introns, or anti-sense coding regions of genes, and can also be in their own stand-alone position in the genome. These lncRNA genes sometimes contain small RNA genes, like microRNA (miRNA), that are spliced out of the lncRNA after transcription. **(B)** The actions of lncRNAs affect many cellular processes. lncRNAs may serve as scaffolds to bring nuclear receptors in contact with promoters of their target genes via chromatin looping, or they may recruit an epigenetic modifier to the chromatin. They can also bind proteins, such as transcription factors, to prevent their binding to DNA – similar to their mechanism of miRNA inhibition. Among the effects lncRNAs have on mRNA, translational activation and maintenance of mRNA stability are also important.

transcription in MCF-7 breast cancer cells, while tamoxifen inhibits this transcription [75].

GAS5 expression is downregulated in breast cancer samples relative to adjacent unaffected normal breast tissue, and has a distinct tumor suppressive role in breast cancer by inducing apoptosis and suppressing cell proliferation [70]. GAS5 acts primarily by preventing the glucocorticoid receptor from binding target DNA. Despite additional interactions with the androgen receptor and progesterone receptor, results show that GAS5 does not bind the ER [76].

HOTAIR was first identified as an lncRNA that regulates the homeobox D (*HOXD*) cluster by tethering the polycomb repressor complex 2 (PRC2) protein to the DNA at this site. PRC2 is able to promote histone H3K27 trimethylation and subsequent repression of transcription at the *HOXD* cluster, thereby preventing differentiation and leading to an invasive cellular phenotype [77]. Overexpression of HOTAIR has been associated with enhanced metastasis and invasion of breast cancer cells and can be used as a predictor of overall survival and progression-free survival [71]. A potential explanation for HOTAIR overexpression in breast cancer could be related to the presence of estrogen response elements in the HOTAIR promoter, leading to estradiol-induced HOTAIR expression [78].

Of the known lncRNAs associated with breast cancer, BCAR4 is most noteworthy for its role in endocrine resistance (see Long noncoding RNAs and tamoxifen resistance).

Noncoding RNAs and endocrine resistance

microRNAs and tamoxifen resistance

The miRNAs associated with endocrine resistance have been explored, and this effort has primarily focused on the differential expression of miRNAs in tamoxifen-resistant cells. miRNAs that inhibit ERα, such as miR-221/222, are implicated in resistance to anti-ERα therapies. One study showed that ectopic expression of miR-221 or miR-222 was enough to decrease ERα protein expression in MCF-7 and T47D breast cancer cells, and this led to the cells acquiring resistance to tamoxifen (Figure 4A) [79]. In addition, silencing of miR-221 and miR-222 in ERα-negative, endocrine-resistant MDA-MB-468 breast cancer cells has been shown to increase ERα expression and sensitize cells to tamoxifen-induced apoptosis [79].

In addition to targeting ERα, miRNAs associated with tamoxifen resistance have been shown to regulate genes related to cell survival and metastasis. Following *in vitro* treatment of MCF-7 cells with tamoxifen there is an increase in cell survival factor 14-3-3ζ [80]. miR-451, which normally targets the anti-apoptotic factors PI3K/Akt and 14-3-3ζ, has very low expression in tamoxifen-resistant MCF-7 cells, which could contribute to the survival of these cells after tamoxifen treatment (Figure 4A). In fact, re-expression of miR-451 has been shown to decrease cell proliferation and colony formation, as well as reduce HER2, epidermal growth factor receptor, and

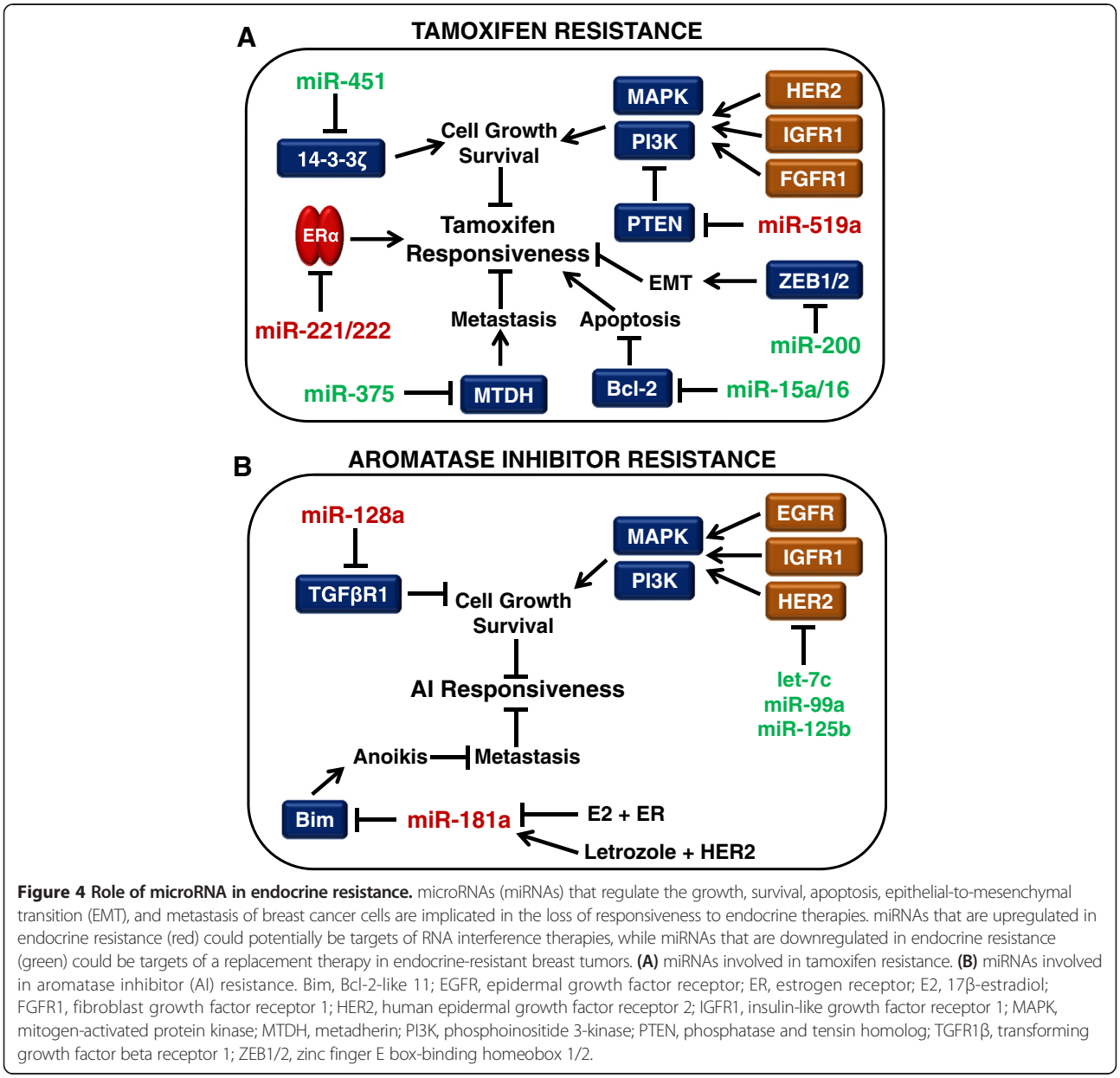

Figure 4 Role of microRNA in endocrine resistance. microRNAs (miRNAs) that regulate the growth, survival, apoptosis, epithelial-to-mesenchymal transition (EMT), and metastasis of breast cancer cells are implicated in the loss of responsiveness to endocrine therapies. miRNAs that are upregulated in endocrine resistance (red) could potentially be targets of RNA interference therapies, while miRNAs that are downregulated in endocrine resistance (green) could be targets of a replacement therapy in endocrine-resistant breast tumors. **(A)** miRNAs involved in tamoxifen resistance. **(B)** miRNAs involved in aromatase inhibitor (AI) resistance. Bim, Bcl-2-like 11; EGFR, epidermal growth factor receptor; ER, estrogen receptor; E2, 17β-estradiol; FGFR1, fibroblast growth factor receptor 1; HER2, human epidermal growth factor receptor 2; IGFR1, insulin-like growth factor receptor 1; MAPK, mitogen-activated protein kinase; MTDH, metadherin; PI3K, phosphoinositide 3-kinase; PTEN, phosphatase and tensin homolog; TGFR1β, transforming growth factor beta receptor 1; ZEB1/2, zinc finger E box-binding homeobox 1/2.

MAPK levels, followed by a restored sensitivity to tamoxifen in resistant MCF-7 cells [80]. There is also evidence that miR-451 expression is reduced in doxorubicin-resistant MCF-7 breast cancer cells and that it regulates the drug transporter P-glycoprotein/MDR1 in these cells [81]. Both tamoxifen and 4-hydroxytamoxifen are known to bind to P-glycoprotein, and endoxifen has been shown to be a substrate of this transporter, thus suggesting the importance of this efflux transporter to tamoxifen therapy [82,83].

In another tamoxifen-resistant cell model (MCF-7/TAMR), miR-375 was identified as one of the top downregulated miRNAs. Re-expression of miR-375 was enough to reverse the tamoxifen-resistant phenotype via repression of metadherin (*MTDH*), a metastasis-promoting cell surface protein (Figure 4A) [84]. Expression of MTDH and miR-375 were inversely correlated in primary breast cancer samples, and survival data from tamoxifen-treated patients revealed that higher expression of MTDH was associated with a shorter disease-free survival and higher risk of relapse [84]. Another recent study of miRNA in the tamoxifen-resistant MCF-7 TamR cells has revealed upregulation of the C19MC cluster, a primate-specific cluster of 19 miRNAs, with miR-519a being most highly overexpressed [85]. miR-519a was shown to directly target the tumor suppressor genes *CDKN1A* (P21), *PTEN*, and *RB1*, allowing for the enhanced signaling of the PI3K growth and survival pathway in tamoxifen-resistant cells (Figure 4A).

MCF-7 cells expressing an oncogenic isoform of HER2 (MCF-7/HER2Δ16) evade tamoxifen treatment by upregulating the expression of the anti-apoptotic factor Bcl-2 and downregulating the expression of miR-15a/16, which inhibit expression of Bcl-2 [86]. Treatment of the MCF-7/HER2Δ16 cells with exogenous miR-15a/16 decreased tamoxifen-induced Bcl-2 levels and re-sensitized the cells to tamoxifen-induced cell death [86]. These MCF-7/HER2Δ16 cells also present decreased expression of miR-342, which was shown to regulate expression of genes involved in breast tumor cell cycle progression, such as cyclin B1, p53, and breast cancer 1 (BRCA1) [87]. miR-342 expression was also shown to be downregulated in tamoxifen refractory human breast tumors, which confirms its clinical relevance [87].

Other miRNAs that play a role in tamoxifen resistance include members of the miR-200 family – miR-200a, miR-200b, and miR-200c, all of which inhibit the expression of zinc finger Ebox-binding homeobox 1/2 (*ZEB1/2*) [88]. The miR-200 family has been shown to be expressed at low levels in tamoxifen-resistant LY2 breast cancer cells compared with tamoxifen-sensitive MCF-7 parental cells (Figure 4A). ZEB1/2-mediated transcriptional repression of E-cadherin is necessary for epithelial-to-mesenchymal transition, so the upregulation of ZEB1/2 could contribute to the invasiveness of tamoxifen-resistant breast cancer cells. Overexpression of the miR-200 family members has been shown to inhibit cell migration and reverse epithelial-to-mesenchymal transition [88].

In a study of 235 ERα-positive breast cancer specimens, high expression of miR-26a was significantly associated with clinical benefit and prolonged time to progression. A combination of high miR-26a expression and low expression of the miR-26a targets cyclin-dependent kinase 1 (*CDC2*) and cyclin E1 (*CCNE1*) was associated with favorable outcome after tamoxifen treatment [89]. Another study measured the expression of five miRNAs in 246 ERα-positive primary breast cancer tumors from patients treated with tamoxifen for advanced disease and found that high expression of miR-30a, miR-30c, and miR-182 was significantly associated with tamoxifen sensitivity and longer progression-free survival [90]. miR-30c was the most significant and independent predictor of clinical benefit, and correlated positively with ERα and inversely with epidermal growth factor receptor [90]. Lastly, analysis of miRNA expression in matched samples from ERα-positive breast cancer patients treated with tamoxifen indicated that high expression of miR-126 and miR-10a were associated with an increase in patients' relapse-free time after tamoxifen treatment [56]. Additionally, miR-126 has been shown to suppress metastasis of breast cancers in subtype-specific mechanisms that involve inhibiting infiltration of mesenchymal stem cells and inflammatory monocytes [91].

Long noncoding RNAs and tamoxifen resistance

The lncRNA BCAR4 was discovered in a functional screen of ZR-75-1 breast cancer cells to identify mechanisms of anti-estrogen resistance [92]. Overexpression of BCAR4 in tamoxifen-sensitive ZR-75-1 cells blocked the anti-proliferative effects of tamoxifen, and BCAR4 has since been shown to be a clinically relevant biomarker for increased invasiveness and tamoxifen resistance [72,92]. The role of BCAR4 in tamoxifen resistance relies on the coexpression of HER2, but is independent of ERα [93,94]. A HER2 inhibitor may thus be ideal for those patients whose tumors are resistant to traditional endocrine therapy due to high levels of BCAR4, and are accompanied by HER2 overexpression. However, if a method of RNA interference is developed to diminish levels of BCAR4 in breast cancer patients, this could also be a rational therapy. When it is not present at high levels in breast tumors, BCAR4 is normally found only in the human placenta and oocyte, diminishing the side effects of such a therapy [93].

microRNAs and aromatase inhibitor resistance

The topic of miRNAs involved in AI resistance is newer than that of miRNAs in tamoxifen resistance, but recent studies have started to shed light on the field. Masri and

colleagues conducted a miRNA expression analysis for four AI-resistant cell models, all derived from aromatase-overexpressing MCF-7aro cells [95]. MCF-7aro cells were treated with testosterone and each of three AIs until they acquired resistance. An LTED cell line (LTEDaro) was also derived from the MCF-7aro cells for comparison. When compared with LTEDaro cells and cells treated only with testosterone, letrozole-resistant cells overexpressed miR-128a – suggesting miR-128a plays a role in AI resistance. miR-128a is associated with breast cancer aggressiveness, and is involved in regulation of transforming growth factor beta receptor 1 (Figure 4B) [96]. Inhibition of miR-128a in the letrozole-resistant cells led to resensitization to transforming growth factor beta growth-inhibitory effects [95]. It is also interesting to note that the expression profiles for the cells resistant to the steroidal AI (exemestane) and the nonsteroidal AIs (letrozole, anastrozole) were distinct from one another, and the AI-resistant cells were distinct from the LTEDaro model of AI resistance, which supports the idea that multiple mechanisms of acquired resistance to AIs may exist [95].

Unpublished data from our laboratory have given additional insight into the miRNAs that may be involved in the AI-resistant phenotype. Next-generation sequencing of miRNA in MCF-7 cells, MCF-7:5C (LTED) cells, and MCF-7:2A (LTED) cells has revealed over 120 miRNAs whose expression levels are altered in both the MCF-7:5C and MCF-7:2A cells compared with the parental MCF-7 cells. One of the most interesting results is that both MCF-7:5C and MCF-7:2A cells show an increase in miR-181a, which targets Bcl-2-like 11 (Bim), a pro-apoptotic protein involved in anoikis (cell death) after breast cancer cells detach from the basement membrane in preparation for metastasis (Figure 4B) [97]. Recent work from Angela Brodie's laboratory indicates a HER2-dependent upregulation of miR-181a in letrozole-resistant ERα-negative/HER2-positive breast cancer cells, and indicates that miR-181a expression is increased in ERα-negative/HER2-positive and ERα-positive/HER2-positive clinical samples [98]. Several miRNAs have been described as estrogen responsive, and this information is important when studying estrogen-deprived cells in these AI-resistant tumors [99]. Thus, it is worth noting that miR-181a is downregulated upon estrogen treatment, which might explain its overexpression in the LTED cells [100].

In addition to the confirmed role of miR-128a, Masri and colleagues also briefly mentioned the downregulation of miR-125b in the letrozole-resistant, anastrozole-resistant, and exemestane-resistant cells compared with the LTEDaro cells [95]. A recent study in MCF-7:2A (LTED) cells confirms downregulation of miR-125b in this AI-resistant LTED model and also indicates relevance of the other members of its miRNA cluster [101]. The let-7c/miR-99a/miR-125b miRNA cluster encoded within the *LINC00487* gene was shown to be downregulated in MCF-7:2A cells compared with MCF-7 parental cells. A luciferase reporter assay confirmed that let-7c and miR-125b bind the HER2 3′ untranslated region, but it was revealed that while miR-125b directly regulates HER2 expression via the binding of HER2 3′ untranslated region, let-7c regulation of HER2 is indirect via the inhibition of Dicer, one of the proteins involved in miRNA function [101]. Upon analysis of clinical data from The Cancer Genome Atlas, it was clear that let-7c and HER2 were inversely correlated in luminal A breast tumors and that low expression of the let-7c/miR-99a/miR-125b cluster was associated with worse overall survival compared with patients who had high expression of this cluster [101].

Proposed roles of miRNA in AI resistance can be also determined by focusing on miRNAs that have shown importance in estrogen-independent growth and survival or are differentially expressed following anti-estrogen therapy. An *in vivo* selection process using a miRNA library revealed six miRNAs that were shown to confer estrogen-independent growth and increased phosphorylated-Akt in MCF-7 breast cancer cells [102]. Of these six, miR-101 was capable of promoting estrogen-independent growth, while the other five were not. Further characterization of miR-101 revealed that it inhibits expression of membrane-associated guanylate kinase (MAGI-2), a protein necessary for PTEN activity [102]. Expression of miR-101 is thus important for estrogen-independent growth mediated by the PI3K/Akt pathway, which could be important for resistance to both tamoxifen and AIs.

In a study to identify estrogen-regulated miRNAs, a group of miRNAs was shown to have elevated expression upon combined treatment of tamoxifen and exemestane, including miR-21, miR-181b, miR-26a/b, miR-27b, and miR-23b [100]. As discussed earlier, miR-21 is upregulated in primary patient samples of invasive breast cancer compared with normal breast tissue, and miR-26a is associated with favorable outcome after tamoxifen treatment [58,89]. While these miRNAs have not been directly implicated in AI resistance, their overexpression after treatment makes them candidates for a role in survival of AI-resistant cells. Likewise, a study of miRNA expression in MCF-7 cells revealed several miRNAs that are increased following letrozole treatment [103]. Perhaps the most interesting result was the upregulation of let-7f upon treatment with letrozole, as it inhibits the expression of the aromatase gene (*CYP19A1*) [103]. This study may reveal a mechanism of resistance similar to that of tamoxifen resistance – loss of the inhibitor's target. Just as tamoxifen resistance occurs in conjunction with absence of ERα, resistance to AIs may eventually develop due to pronounced loss of aromatase

expression due to upregulation of certain miRNAs upon treatment.

Long noncoding RNAs and aromatase inhibitor resistance

There have been few studies that have focused specifically on the role of lncRNA in AI resistance. Nevertheless, there is some evidence that the lncRNAs regulating steroid receptors such as ERα may play a role in resistance. It has been shown that the lncRNA steroid receptor RNA activator 1 (SRA1) acts as a coactivator of ERα, and this action depends on the phosphorylation of ERα at Ser118 [104]. When this phosphorylation event occurs via the kinase action of MAPK (a protein that is often upregulated in AI-resistant cells), it is associated with estrogen-independent activation of ERα [6]. This putative mechanism of resistance is similar to that of AIB1 and tamoxifen resistance – just as AIB1 coactivates ERα in the presence of tamoxifen and this is enhanced by the presence of HER2, SRA1 could potentially coactivate ERα in an AI-induced estrogen-deprived environment, and this requires MAPK activity.

The scaffolding lncRNAs prostate cancer associated noncoding RNA 1 (PRNCR1) and prostate-specific transcript 1 (PCGEM1) have previously been reported to play a role in transcription of androgen receptor target genes in the androgen-resistant prostate cancer cell lines CWR22Rv1 and LNCaP-cds1/2 via a chromatin-looping mechanism involving the androgen receptor [105]. A more recent study by Prensner and colleagues, however, refutes that PCGEM1 and PRNCR1 interact with the androgen receptor and that either gene is a component of androgen receptor signaling or is involved in castration-resistant prostate cancer [106]. There were differences between the two studies, which might partially explain the conflicting observations reported. Prensner and coworkers analyzed castration-resistant prostate tumor samples that were collected from high-risk prostate cancer patients but they did not evaluate castration-resistant prostate cancer cell lines, whereas the study by Yang and coworkers evaluated castration-resistant prostate tumor samples as well as castration-resistant prostate cancer cell lines. Overall, despite the inconclusive results from these two studies, they still offer insight into a possible chromatin-looping mechanism by which lncRNAs could facilitate the transcription of ERα target genes in the absence of estrogen in breast cancer cells that have acquired AI resistance.

Conclusions

In summary, there are numerous ncRNAs shown to be involved in acquired resistance to endocrine therapies. ncRNAs provide an exciting avenue of gene regulation that has not yet been fully explored. As we uncover the miRNAs and lncRNAs involved in specific disease states, such as resistance to breast cancer treatments, it will be possible to use these RNAs as both therapeutic targets and biomarkers.

Regarding therapeutic approaches, oncogenic ncRNAs that contribute to the progression of disease would need to be eliminated via RNA interference, while tumor-suppressive ncRNAs may be part of replacement therapies. There are over 20 RNA interference-based therapies employing various methods of small interfering RNA delivery currently in phase I clinical trials for the treatment of diseases such as viral infections, hereditary disorders, and cancer [107]. The only RNA replacement clinical trial to date began in April 2013 as a strategy to deliver miR-34, a tumor-suppressive miRNA that regulates expression of *BCL-2* and *MYC*, to patients with liver-based cancers [108]. Although there are not yet published results on this MRX34 treatment, a recent update revealed that MRX34 has a manageable safety profile with only one incidence of a dose-limiting toxicity [109].

With the use of innovative technologies, it is now possible to use ncRNAs as biomarkers and compile biomarker panels for diagnosis and prognosis of diseases, including cancer. Circulating miRNAs are ideal for clinical use, since they are highly stable and can be detected by a non-invasive manner in a blood sample. Circulating miRNA levels in breast cancer patients have been studied at diagnosis, in early stage tumors, after surgical resection, following chemotherapy/radiation treatments, and following metastatic relapse – all to understand the unique miRNA profiles throughout the progression of breast cancer [110-112]. Because of the low abundance of miRNAs in the blood, the use of powerful detection methods such as high-throughput sequencing will need to be employed in clinical settings. A more complete picture of the differentially expressed regulatory RNAs is crucial for the development of these therapeutic strategies and biomarker signatures, especially in a disease as complex as breast cancer.

Abbreviations

Ago: Argonaute; AI: Aromatase inhibitor; AIB1: Amplified in breast cancer 1; Akt: Protein kinase B; BCAR4: Breast cancer anti-estrogen resistance 4; ER: Estrogen receptor; GAS5: Growth arrest-specific 5; HER2: Human epidermal growth factor receptor 2; HOTAIR: Homeobox antisense intergenic RNA; HOXD: Homeobox D; IFITM1: Interferon-induced transmembrane protein 1; lncRNA: Long noncoding RNA; LTED: Long-term estrogen-deprived; MAPK: Mitogen-activated protein kinase; MDR1: Multi-drug resistance protein 1; miRNA: microRNA; MTDH: Metadherin; ncRNA: Noncoding RNA; PCGEM1: Prostate-specific transcript 1; PI3K: Phosphoinositide 3-kinase; PRC2: Polycomb repressor complex 2; PRNCR1: Prostate cancer associated noncoding RNA 1; PTEN: Phosphatase and tensin homolog; SRA1: Steroid receptor RNA activator 1; ZEB1/2: Zinc finger E box-binding homeobox 1/2.

Competing interests

The authors declare that they have no competing interests.

Acknowledgements

This work was supported by grants from the Department of Defense (W81XWH-12-1-0139; supporting JSL-W), the National Cancer Institute

(K01CA120051; supporting JSL-W), the National Science Foundation Graduate Research Fellowship (QH866640; supporting ELH) and by start-up funds from the University of Kansas Medical Center (supporting JSL-W and ELH).

Received: 12 September 2014 Accepted: 19 February 2015
Published online: 17 March 2015

References

1. American Cancer Society. Cancer Facts & Figures 2014. Atlanta: American Cancer Society; 2014.
2. Stanford JL, Szklo M, Brinton LA. Estrogen receptors and breast cancer. Epidemiol Rev. 1986;8:42–59.
3. Beato M, Herrlich P, Schutz G. Steroid hormone receptors: many actors in search of a plot. Cell. 1995;83:851–7.
4. Tsai MJ, O'Malley BW. Molecular mechanisms of action of steroid/thyroid receptor superfamily members. Annu Rev Biochem. 1994;63:451–86.
5. Kumar V, Green S, Stack G, Berry M, Jin JR, Chambon P. Functional domains of the human estrogen receptor. Cell. 1987;51:941–51.
6. Kato S, Endoh H, Masuhiro Y, Kitamoto T, Uchiyama S, Sasaki H, et al. Activation of the estrogen receptor through phosphorylation by mitogen-activated protein kinase. Science. 1995;270:1491–4.
7. Vilgelm A, Lian Z, Wang H, Beauparlant SL, Klein-Szanto A, Ellenson LH, et al. Akt-mediated phosphorylation and activation of estrogen receptor alpha is required for endometrial neoplastic transformation in Pten+/– mice. Cancer Res. 2006;66:3375–80.
8. Hall JM, Couse JF, Korach KS. The multifaceted mechanisms of estradiol and estrogen receptor signaling. J Biol Chem. 2001;276:36869–72.
9. Nilsson S, Makela S, Treuter E, Tujague M, Thomsen J, Andersson G, et al. Mechanisms of estrogen action. Physiol Rev. 2001;81:1535–65.
10. Levin ER. Integration of the extranuclear and nuclear actions of estrogen. Mol Endocrinol. 2005;19:1951–9.
11. Davies C, Pan H, Godwin J, Gray R, Arriagada R, Raina V, et al. Long-term effects of continuing adjuvant tamoxifen to 10 years versus stopping at 5 years after diagnosis of oestrogen receptor-positive breast cancer: ATLAS, a randomised trial. Lancet. 2013;381:805–16.
12. Fisher B, Costantino JP, Wickerham DL, Redmond CK, Kavanah M, Cronin WM, et al. Tamoxifen for prevention of breast cancer: report of the National Surgical Adjuvant Breast and Bowel Project P-1 Study. J Natl Cancer Inst. 1998;90:1371–88.
13. Tate AC, Greene GL, DeSombre ER, Jensen EV, Jordan VC. Differences between estrogen- and antiestrogen-estrogen receptor complexes from human breast tumors identified with an antibody raised against the estrogen receptor. Cancer Res. 1984;44:1012–8.
14. Bross PF, Cohen MH, Williams GA, Pazdur R. FDA drug approval summaries: fulvestrant. Oncologist. 2002;7:477–80.
15. Simpson ER, Mahendroo MS, Means GD, Kilgore MW, Hinshelwood MM, Graham-Lorence S, et al. Aromatase cytochrome P450, the enzyme responsible for estrogen biosynthesis. Endocrine Rev. 1994;15:342–55.
16. Simpson ER. Sources of estrogen and their importance. J Steroid Biochem Mol Biol. 2003;86:225–30.
17. Chumsri S, Howes T, Bao T, Sabnis G, Brodie A. Aromatase, aromatase inhibitors, and breast cancer. J Steroid Biochem Mol Biol. 2011;125:13–22.
18. Geisler J, Haynes B, Anker G, Dowsett M, Lonning PE. Influence of letrozole and anastrozole on total body aromatization and plasma estrogen levels in postmenopausal breast cancer patients evaluated in a randomized, cross-over study. J Clin Oncol. 2002;20:751–7.
19. Geisler J, King N, Anker G, Ornati G, Di Salle E, Lonning PE, et al. In vivo inhibition of aromatization by exemestane, a novel irreversible aromatase inhibitor, in postmenopausal breast cancer patients. Clin Cancer Res. 1998;4:2089–93.
20. Shou J, Massarweh S, Osborne CK, Wakeling AE, Ali S, Weiss H, et al. Mechanisms of tamoxifen resistance: increased estrogen receptor-HER2/neu cross-talk in ER/HER2-positive breast cancer. J Natl Cancer Inst. 2004;96:926–35.
21. Gottardis MM, Jordan VC. Development of tamoxifen-stimulated growth of MCF-7 tumors in athymic mice after long-term antiestrogen administration. Cancer Res. 1988;48:5183–7.
22. Smith CL, Nawaz Z, O'Malley BW. Coactivator and corepressor regulation of the agonist/antagonist activity of the mixed antiestrogen, 4-hydroxytamoxifen. Mol Endocrinol. 1997;11:657–66.
23. Osborne CK, Bardou V, Hopp TA, Chamness GC, Hilsenbeck SG, Fuqua SA, et al. Role of the estrogen receptor coactivator AIB1 (SRC-3) and HER-2/neu in tamoxifen resistance in breast cancer. J Natl Cancer Inst. 2003;95:353–61.
24. Zhang Y, Moerkens M, Ramaiahgari S, de Bont H, Price L, Meerman J, et al. Elevated insulin-like growth factor 1 receptor signaling induces antiestrogen resistance through the MAPK/ERK and PI3K/Akt signaling routes. Breast Cancer Res. 2011;13:R52.
25. Turner N, Pearson A, Sharpe R, Lambros M, Geyer F, Lopez-Garcia MA, et al. FGFR1 amplification drives endocrine therapy resistance and is a therapeutic target in breast cancer. Cancer Res. 2010;70:2085–94.
26. Sharma D, Blum J, Yang X, Beaulieu N, Macleod AR, Davidson NE. Release of methyl CpG binding proteins and histone deacetylase 1 from the estrogen receptor alpha (ER) promoter upon reactivation in ER-negative human breast cancer cells. Mol Endocrinol. 2005;19:1740–51.
27. Desta Z, Ward BA, Soukhova NV, Flockhart DA. Comprehensive evaluation of tamoxifen sequential biotransformation by the human cytochrome P450 system in vitro: prominent roles for CYP3A and CYP2D6. J Pharmacol Exp Ther. 2004;310:1062–75.
28. Xu Y, Sun Y, Yao L, Shi L, Wu Y, Ouyang T, et al. Association between CYP2D6 *10 genotype and survival of breast cancer patients receiving tamoxifen treatment. Ann Oncol. 2008;19:1423–9.
29. Goetz MP, Rae JM, Suman VJ, Safgren SL, Ames MM, Visscher DW, et al. Pharmacogenetics of tamoxifen biotransformation is associated with clinical outcomes of efficacy and hot flashes. J Clin Oncol. 2005;23:9312–8.
30. Clarke R, Skaar TC, Bouker KB, Davis N, Lee YR, Welch JN, et al. Molecular and pharmacological aspects of antiestrogen resistance. J Steroid Biochem Mol Biol. 2001;76:71–84.
31. Tsukamoto F, Shiba E, Taguchi T, Sugimoto T, Watanabe T, Kim SJ, et al. Immunohistochemical detection of P-glycoprotein in breast cancer and its significance as a prognostic factor. Breast Cancer. 1997;4:259–63.
32. Larkin A, O'Driscoll L, Kennedy S, Purcell R, Moran E, Crown J, et al. Investigation of MRP-1 protein and MDR-1 P-glycoprotein expression in invasive breast cancer: a prognostic study. Int J Cancer. 2004;112:286–94.
33. Jelovac D, Sabnis G, Long BJ, Macedo L, Goloubeva OG, Brodie AM. Activation of mitogen-activated protein kinase in xenografts and cells during prolonged treatment with aromatase inhibitor letrozole. Cancer Res. 2005;65:5380–9.
34. Gilani RA, Kazi AA, Shah P, Schech AJ, Chumsri S, Sabnis G, et al. The importance of HER2 signaling in the tumor-initiating cell population in aromatase inhibitor-resistant breast cancer. Breast Cancer Res Treat. 2012;135:681–92.
35. Burris 3rd HA. Overcoming acquired resistance to anticancer therapy: focus on the PI3K/AKT/mTOR pathway. Cancer Chemother Pharmacol. 2013;71:829–42.
36. Robinson DR, Wu YM, Vats P, Su F, Lonigro RJ, Cao X, et al. Activating ESR1 mutations in hormone-resistant metastatic breast cancer. Nat Genet. 2013;45:1446–51.
37. Jansen MP, Knijnenburg T, Reijm EA, Simon I, Kerkhoven R, Droog M, et al. Hallmarks of aromatase inhibitor drug resistance revealed by epigenetic profiling in breast cancer. Cancer Res. 2013;73:6632–41.
38. Garcia-Becerra R, Santos N, Diaz L, Camacho J. Mechanisms of resistance to endocrine therapy in breast cancer: focus on signaling pathways, miRNAs and genetically based resistance. Int J Mol Sci. 2012;14:108–45.
39. Chen S. An 'omics' approach to determine the mechanisms of acquired aromatase inhibitor resistance. Omics. 2011;15:347–52.
40. Thiantanawat A, Long BJ, Brodie AM. Signaling pathways of apoptosis activated by aromatase inhibitors and antiestrogens. Cancer Res. 2003;63:8037–50.
41. Barone I, Cui Y, Herynk MH, Corona-Rodriguez A, Giordano C, Selever J, et al. Expression of the K303R estrogen receptor-alpha breast cancer mutation induces resistance to an aromatase inhibitor via addiction to the PI3K/Akt kinase pathway. Cancer Res. 2009;69:4724–32.
42. Jiang SY, Wolf DM, Yingling JM, Chang C, Jordan VC. An estrogen receptor positive MCF-7 clone that is resistant to antiestrogens and estradiol. Mol Cell Endocrinol. 1992;90:77–86.
43. Lewis JS, Meeke K, Osipo C, Ross EA, Kidawi N, Li T, et al. Intrinsic mechanism of estradiol-induced apoptosis in breast cancer cells resistant to estrogen deprivation. J Natl Cancer Inst. 2005;97:1746–59.
44. Pink JJ, Jiang SY, Fritsch M, Jordan VC. An estrogen-independent MCF-7 breast cancer cell line which contains a novel 80-kilodalton estrogen receptor-related protein. Cancer Res. 1995;55:2583–90.
45. Lewis-Wambi JS, Swaby R, Kim H, Jordan VC. Potential of L-buthionine sulfoximine to enhance the apoptotic action of estradiol to reverse acquired antihormonal resistance in metastatic breast cancer. J Steroid Biochem Mol Biol. 2009;114:33–9.

46. Ariazi EA, Cunliffe HE, Lewis-Wambi JS, Slifker MJ, Willis AL, Ramos P, et al. Estrogen induces apoptosis in estrogen deprivation-resistant breast cancer through stress responses as identified by global gene expression across time. Proc Natl Acad Sci U S A. 2011;108:18879–86.
47. Choi HJ, Lui A, Ogony J, Jan R, Sims PJ, Lewis-Wambi J. Targeting interferon response genes sensitizes aromatase inhibitor resistant breast cancer cells to estrogen-induced cell death. Breast Cancer Res. 2015;17:6 [Epub ahead of print].
48. Morris KV, Mattick JS. The rise of regulatory RNA. Nat Rev Genet. 2014;15:423–37.
49. He L, Hannon GJ. MicroRNAs: small RNAs with a big role in gene regulation. Nat Rev Genet. 2004;5:522–31.
50. Krol J, Loedige I, Filipowicz W. The widespread regulation of microRNA biogenesis, function and decay. Nat Rev Genet. 2010;11:597–610.
51. Meister G, Landthaler M, Patkaniowska A, Dorsett Y, Teng G, Tuschl T. Human Argonaute2 mediates RNA cleavage targeted by miRNAs and siRNAs. Mol Cell. 2004;15:185–97.
52. Blenkiron C, Goldstein LD, Thorne NP, Spiteri I, Chin SF, Dunning MJ, et al. MicroRNA expression profiling of human breast cancer identifies new markers of tumor subtype. Genome Biol. 2007;8:R214.
53. Iorio MV, Ferracin M, Liu CG, Veronese A, Spizzo R, Sabbioni S, et al. MicroRNA gene expression deregulation in human breast cancer. Cancer Res. 2005;65:7065–70.
54. Huang S, Chen Y, Wu W, Ouyang N, Chen J, Li H, et al. miR-150 promotes human breast cancer growth and malignant behavior by targeting the pro-apoptotic purinergic P2X7 receptor. PLoS One. 2013;8:e80707.
55. Arigoni M, Barutello G, Riccardo F, Ercole E, Cantarella D, Orso F, et al. miR-135b coordinates progression of ErbB2-driven mammary carcinomas through suppression of MID1 and MTCH2. Am J Pathol. 2013;182:2058–70.
56. Hoppe R, Achinger-Kawecka J, Winter S, Fritz P, Lo WY, Schroth W, et al. Increased expression of miR-126 and miR-10a predict prolonged relapse-free time of primary oestrogen receptor-positive breast cancer following tamoxifen treatment. Eur J Cancer. 2013;49:3598–608.
57. Yu F, Yao H, Zhu P, Zhang X, Pan Q, Gong C, et al. let-7 regulates self renewal and tumorigenicity of breast cancer cells. Cell. 2007;131:1109–23.
58. Qi L, Bart J, Tan LP, Platteel I, Sluis T, Huitema S, et al. Expression of miR-21 and its targets (PTEN, PDCD4, TM1) in flat epithelial atypia of the breast in relation to ductal carcinoma in situ and invasive carcinoma. BMC Cancer. 2009;9:163.
59. Huang Q, Gumireddy K, Schrier M, le Sage C, Nagel R, Nair S, et al. The microRNAs miR-373 and miR-520c promote tumour invasion and metastasis. Nat Cell Biol. 2008;10:202–10.
60. Lopez JI, Camenisch TD, Stevens MV, Sands BJ, McDonald J, Schroeder JA. CD44 attenuates metastatic invasion during breast cancer progression. Cancer Res. 2005;65:6755–63.
61. O'Day E, Lal A. MicroRNAs and their target gene networks in breast cancer. Breast Cancer Res. 2010;12:201.
62. Singh R, Mo YY. Role of microRNAs in breast cancer. Cancer Biol Ther. 2013;14:201–12.
63. Kung JT, Colognori D, Lee JT. Long noncoding RNAs: past, present, and future. Genetics. 2013;193:651–69.
64. Hu W, Alvarez-Dominguez JR, Lodish HF. Regulation of mammalian cell differentiation by long non-coding RNAs. EMBO Rep. 2012;13:971–83.
65. Kitagawa M, Kitagawa K, Kotake Y, Niida H, Ohhata T. Cell cycle regulation by long non-coding RNAs. Cell Mol Life Sci. 2013;70:4785–94.
66. Rossi MN, Antonangeli F. LncRNAs: new players in apoptosis control. Int J Cell Biol. 2014;2014:473857.
67. Iyengar BR, Choudhary A, Sarangdhar MA, Venkatesh KV, Gadgil CJ, Pillai B. Non-coding RNA interact to regulate neuronal development and function. Front Cell Neurosci. 2014;8:47.
68. Chen G, Wang Z, Wang D, Qiu C, Liu M, Chen X, et al. LncRNADisease: a database for long-non-coding RNA-associated diseases. Nucleic Acids Res. 2013;41:D983–6.
69. Lottin S, Adriaenssens E, Dupressoir T, Berteaux N, Montpellier C, Coll J, et al. Overexpression of an ectopic H19 gene enhances the tumorigenic properties of breast cancer cells. Carcinogenesis. 2002;23:1885–95.
70. Mourtada-Maarabouni M, Pickard MR, Hedge VL, Farzaneh F, Williams GT. GAS5, a non-protein-coding RNA, controls apoptosis and is downregulated in breast cancer. Oncogene. 2009;28:195–208.
71. Gupta RA, Shah N, Wang KC, Kim J, Horlings HM, Wong DJ, et al. Long non-coding RNA HOTAIR reprograms chromatin state to promote cancer metastasis. Nature. 2010;464:1071–6.
72. Godinho MF, Sieuwerts AM, Look MP, Meijer D, Foekens JA, Dorssers LC, et al. Relevance of BCAR4 in tamoxifen resistance and tumour aggressiveness of human breast cancer. Br J Cancer. 2010;103:1284–91.
73. Weksberg R, Nishikawa J, Caluseriu O, Fei YL, Shuman C, Wei C, et al. Tumor development in the Beckwith-Wiedemann syndrome is associated with a variety of constitutional molecular 11p15 alterations including imprinting defects of KCNQ1OT1. Hum Mol Genet. 2001;10:2989–3000.
74. Yoshimizu T, Miroglio A, Ripoche MA, Gabory A, Vernucci M, Riccio A, et al. The H19 locus acts in vivo as a tumor suppressor. Proc Natl Acad Sci U S A. 2008;105:12417–22.
75. Adriaenssens E, Lottin S, Dugimont T, Fauquette W, Coll J, Dupouy JP, et al. Steroid hormones modulate H19 gene expression in both mammary gland and uterus. Oncogene. 1999;18:4460–73.
76. Kino T, Hurt DE, Ichijo T, Nader N, Chrousos GP. Noncoding RNA gas5 is a growth arrest- and starvation-associated repressor of the glucocorticoid receptor. Sci Signal. 2010;3:ra8.
77. Tsai MC, Manor O, Wan Y, Mosammaparast N, Wang JK, Lan F, et al. Long noncoding RNA as modular scaffold of histone modification complexes. Science. 2010;329:689–93.
78. Bhan A, Hussain I, Ansari KI, Kasiri S, Bashyal A, Mandal SS. Antisense transcript long noncoding RNA (lncRNA) HOTAIR is transcriptionally induced by estradiol. J Mol Biol. 2013;425:3707–22.
79. Zhao JJ, Lin J, Yang H, Kong W, He L, Ma X, et al. MicroRNA-221/222 negatively regulates estrogen receptor alpha and is associated with tamoxifen resistance in breast cancer. J Biol Chem. 2008;283:31079–86.
80. Bergamaschi A, Katzenellenbogen BS. Tamoxifen downregulation of miR-451 increases 14-3-3zeta and promotes breast cancer cell survival and endocrine resistance. Oncogene. 2012;31:39–47.
81. Kovalchuk O, Filkowski J, Meservy J, Ilnytskyy Y, Tryndyak VP, Chekhun VF, et al. Involvement of microRNA-451 in resistance of the MCF-7 breast cancer cells to chemotherapeutic drug doxorubicin. Mol Cancer Ther. 2008;7:2152–9.
82. Bekaii-Saab TS, Perloff MD, Weemhoff JL, Greenblatt DJ, von Moltke LL. Interactions of tamoxifen, N-desmethyltamoxifen and 4-hydroxytamoxifen with P-glycoprotein and CYP3A. Biopharm Drug Dispos. 2004;25:283–9.
83. Teft WA, Mansell SE, Kim RB. Endoxifen, the active metabolite of tamoxifen, is a substrate of the efflux transporter P-glycoprotein (multidrug resistance 1). Drug Metab Dispos. 2011;39:558–62.
84. Ward A, Balwierz A, Zhang JD, Kublbeck M, Pawitan Y, Hielscher T, et al. Re-expression of microRNA-375 reverses both tamoxifen resistance and accompanying EMT-like properties in breast cancer. Oncogene. 2013;32:1173–82.
85. Ward A, Shukla K, Balwierz A, Soons Z, Konig R, Sahin O, et al. microRNA-519a is a novel oncomir conferring tamoxifen resistance by targeting a network of tumor-suppressor genes in ER+ breast cancer. J Pathol. 2014;233:368–79.
86. Cittelly DM, Das PM, Salvo VA, Fonseca JP, Burow ME, Jones FE. Oncogenic HER2Δ16 suppresses miR-15a/16 and deregulates BCL-2 to promote endocrine resistance of breast tumors. Carcinogenesis. 2010;31:2049–57.
87. Cittelly DM, Das PM, Spoelstra NS, Edgerton SM, Richer JK, Thor AD, et al. Downregulation of miR-342 is associated with tamoxifen resistant breast tumors. Mol Cancer. 2010;9:317.
88. Manavalan TT, Teng Y, Litchfield LM, Muluhngwi P, Al-Rayyan N, Klinge CM. Reduced expression of miR-200 family members contributes to antiestrogen resistance in LY2 human breast cancer cells. PLoS One. 2013;8:e62334.
89. Jansen MP, Reijm EA, Sieuwerts AM, Ruigrok-Ritstier K, Look MP, Rodriguez-Gonzalez FG, et al. High miR-26a and low CDC2 levels associate with decreased EZH2 expression and with favorable outcome on tamoxifen in metastatic breast cancer. Breast Cancer Res Treat. 2012;133:937–47.
90. Rodriguez-Gonzalez FG, Sieuwerts AM, Smid M, Look MP, Meijer-van Gelder ME, de Weerd V, et al. MicroRNA-30c expression level is an independent predictor of clinical benefit of endocrine therapy in advanced estrogen receptor positive breast cancer. Breast Cancer Res Treat. 2011;127:43–51.
91. Zhang Y, Yang P, Sun T, Li D, Xu X, Rui Y, et al. miR-126 and miR-126* repress recruitment of mesenchymal stem cells and inflammatory monocytes to inhibit breast cancer metastasis. Nat Cell Biol. 2013;15:284–94.
92. Meijer D, van Agthoven T, Bosma PT, Nooter K, Dorssers LC. Functional screen for genes responsible for tamoxifen resistance in human breast cancer cells. Mol Cancer Res. 2006;4:379–86.
93. Godinho M, Meijer D, Setyono-Han B, Dorssers LC, van Agthoven T. Characterization of BCAR4, a novel oncogene causing endocrine resistance in human breast cancer cells. J Cell Physiol. 2011;226:1741–9.

94. Godinho MF, Wulfkuhle JD, Look MP, Sieuwerts AM, Sleijfer S, Foekens JA, et al. BCAR4 induces antioestrogen resistance but sensitises breast cancer to lapatinib. Br J Cancer. 2012;107:947–55.
95. Masri S, Liu Z, Phung S, Wang E, Yuan YC, Chen S. The role of microRNA-128a in regulating TGFbeta signaling in letrozole-resistant breast cancer cells. Breast Cancer Res Treat. 2010;124:89–99.
96. Foekens JA, Sieuwerts AM, Smid M, Look MP, de Weerd V, Boersma AW, et al. Four miRNAs associated with aggressiveness of lymph node-negative, estrogen receptor-positive human breast cancer. Proc Natl Acad Sci U S A. 2008;105:13021–6.
97. Taylor MA, Sossey-Alaoui K, Thompson CL, Danielpour D, Schiemann WP. TGF-beta upregulates miR-181a expression to promote breast cancer metastasis. J Clin Invest. 2013;123:150–63.
98. Kazi AA, Sabnis G, Zhou Q, Chumsri S, Schech A, Shah P, et al. HER2 regulated miRNA expression in letrozole resistant breast cancer [abstract]. In Proceedings of the 105th Annual Meeting of the American Association for Cancer Research; 2014 Apr 5-9; San Diego, CA. Philadelphia (PA): AACR; Cancer Res. 2014;74:Abstract nr 1471. doi:10.1158/1538-7445.AM2014-1471
99. Klinge CM. miRNAs and estrogen action. Trends Endocrinol Metab. 2012;23:223–33.
100. Maillot G, Lacroix-Triki M, Pierredon S, Gratadou L, Schmidt S, Benes V, et al. Widespread estrogen-dependent repression of micrornas involved in breast tumor cell growth. Cancer Res. 2009;69:8332–340.
101. Bailey ST, Westerling T, Brown M. Loss of estrogen-regulated microRNA expression increases HER2 signaling and is prognostic of poor outcome in luminal breast cancer. Cancer Res. 2014;75:436–45.
102. Sachdeva M, Wu H, Ru P, Hwang L, Trieu V, Mo YY. MicroRNA-101-mediated Akt activation and estrogen-independent growth. Oncogene. 2011;30:822–31.
103. Shibahara Y, Miki Y, Onodera Y, Hata S, Chan MS, Yiu CC, et al. Aromatase inhibitor treatment of breast cancer cells increases the expression of let-7f, a microRNA targeting CYP19A1. J Pathol. 2012;227:357–66.
104. Deblois G, Giguere V. Ligand-independent coactivation of ERalpha AF-1 by steroid receptor RNA activator (SRA) via MAPK activation. J Steroid Biochem Mol Biol. 2003;85:123–31.
105. Yang L, Lin C, Jin C, Yang JC, Tanasa B, Li W, et al. lncRNA-dependent mechanisms of androgen-receptor-regulated gene activation programs. Nature. 2013;500:598–602.
106. Prensner JR, Sahu A, Iyer MK, Malik R, Chandler B, Asangani IA, et al. The lncRNAs PCGEM1 and PRNCR1 are not implicated in castration resistant prostate cancer. Oncotarget. 2014;5:1434–8.
107. Kanasty R, Dorkin JR, Vegas A, Anderson D. Delivery materials for siRNA therapeutics. Nat Mater. 2013;12:967–77.
108. Bader AG. miR-34 – a microRNA replacement therapy is headed to the clinic. Front Genet. 2012;3:120.
109. Beg MS, Borad M, Sachdev J, Hong DS, Smith S, Bader A, et al. Multicenter phase I study of MRX34, a first-in-class microRNA miR-34 mimic liposomal injection [abstract]. In Proceedings of the 105th Annual Meeting of the American Association for Cancer Research; 2014 Apr 5-9; San Diego, CA. Philadelphia (PA): AACR; Cancer Res. 2014;74:Abstract nr CT327. doi:10.1158/1538-7445.AM2014-CT327
110. Sochor M, Basova P, Pesta M, Dusilkova N, Bartos J, Burda P, et al. Oncogenic microRNAs: miR-155, miR-19a, miR-181b, and miR-24 enable monitoring of early breast cancer in serum. BMC Cancer. 2014;14:448.
111. Kodahl AR, Lyng MB, Binder H, Cold S, Gravgaard K, Knoop AS, et al. Novel circulating microRNA signature as a potential non-invasive multi-marker test in ER-positive early-stage breast cancer: a case control study. Mol Oncol. 2014;8:874–83.
112. Wu X, Somlo G, Yu Y, Palomares MR, Li AX, Zhou W, et al. De novo sequencing of circulating miRNAs identifies novel markers predicting clinical outcome of locally advanced breast cancer. J Transl Med. 2012;10:42.